

BRUNEL UNIVERSITY

EngD Environmental Technology Dissertation

DAVID WARWICK

Integrating Active Thermal Mass Strategies in Responsive Buildings

July 2010

Dissertation Submitted in Fulfilment for the Degree of Engineering
Doctorate in Environmental Technology

Supervisors:

Andrew Cripps

Maria Kolokotroni

ABSTRACT

Thermal mass can be used in buildings to reduce the need for and dependence on mechanical heating and cooling systems whilst maintaining environmental comfort. Active thermal mass strategies further enhance the performance of thermal mass through integration with the Heating, Ventilation and Air Conditioning (HVAC) systems. For the design of new buildings to include active thermal mass strategies, experience from operational projects and design guidelines are normally used by engineers. However, dynamic thermal modelling is required in most cases to accurately determine the performance of its integration with the environmental systems of the building. Design decisions made in the preliminary stages of the design of a building often determine its final thermal characteristics. At this stage, reasons for not integrating active thermal mass strategies include the lack of knowledge about the performance of previous buildings and the time and resources required to carry out detailed modelling.

In this research project a commercially available dynamic building thermal program has been used to construct models for active thermal mass strategies and compare the results with monitored temperatures in buildings incorporating the strategies in the UK. Four active thermal mass strategies are considered (a) hollow core slabs (HCS), (b) floor void with mass, (FVWM) (c) earth-to-air heat exchanger (ETAHE) and (d) thermal labyrinth (TL). The operational strategies and monitoring are presented and their modelling is described in terms of geometrical configuration and input parameters. The modelling results are compared with the measured parameters successfully.

Using the calibrated model, an excel based tool (TMAir) was then developed that can be used at the concept design stages of a typical office building to determine the benefits of integrating an active thermal mass strategy. Key design parameters were identified for each system. These parameters can be split into two categories; fixed parameters and user selected parameters. The fixed parameters are pre-selected for the design tool and have to be a fair representation of the projects that the tool will be used for. The user selected parameters are chosen by the user to represent the way the building will be used, and to look at the effect of key design decisions on the performance of the building.

The tool has an easy-to-use interface which allows direct comparison of the different active thermal mass strategies together with the effects of changing key design parameters. Results are presented in terms of thermal comfort and energy consumption.

TMAir has then been used to carry out a series of parametric analyses. These have concluded the following:

- There is only a benefit in integrating a HCS strategy when night cooling is introduced
- There is no benefit in integrating a FVWM strategy when only one parameter is improved
- An ETAHE and TL strategy will always provide a benefit, although the benefits are greater when night cooling is introduced, solar and internal gains are reduced and when the air change rate is increased

When all of the parametric improvements are applied to the test room the results show that all of the active thermal mass strategies can provide a reduction in annual overheating hours when compared to the Standard Strategy.

Only a small benefit is found for the FVWM Strategy, however around a 25% reduction is found for the HCS Strategy, over a 50% reduction for the TL Strategy and nearly a 75% reduction for the ETAHE Strategy. This demonstrates the importance of applying a low energy, passive approach when considering the application of active thermal mass strategie.

The key results have shown that when comfort cooling is provided, adding a HCS or FVWM strategy always results in an increase in the annual cooling load. This is as a result of the temperature of the air being supplied into the cores or floor void being higher than that of the internal surface temperatures of the cores or void. This results in the supply air being heated, and less cooling provided to the test room per cooling energy delivered. Due to the pre cooling effect of the ETAHE and TL strategies, these strategies always result in a reduction in the annual cooling load.

The key results have shown that the annual heating load is reduced by a small amount for the HCS and FVWM strategies unless the solar gains or internal gains are reduced, whereas the ETAHE and TL strategies always result in a around a 10% reduction in annual heating load as a result of the preheating effect these strategies have on the supply air.

CONTENTS

1.0	EXECUTIVE SUMMARY	1
1.1	Background information.....	1
1.2	Introduction to the Research Topic and Objectives.....	4
1.3	Research methods and main results.....	5
2.0	INTRODUCTION	10
2.1	Energy in Buildings	10
2.2	Active Thermal Mass Strategies.....	11
2.3	Concept Design Tools	13
2.4	Offices	13
2.5	Objectives of the Research	14
2.6	Structure of the Thesis.....	15
3.0	LITERATURE REVIEW	17
3.1	Introduction	17
3.2	Active Thermal Mass Strategies.....	17
3.3	Designing Active Thermal Mass Strategies	29
3.4	The Role of Simplified Design Tools.....	32
3.5	Simulation of Active Thermal Mass Strategies.....	37
3.6	IES Virtual Environment.....	39
3.7	Summary.....	47
4.0	MONITORING & SIMULATION	49
4.1	Introduction	49
4.2	Description of the buildings and active thermal mass strategies.....	49
4.3	Description of the models.....	53
4.4	Comparison of simulation results with monitoring and discussion.....	68
4.5	Summary.....	76
5.0	DEVELOPMENT OF A CONCEPT DESIGN TOOL	77
5.1	Introduction	77
5.2	Selection of Parameters	78
5.3	Simulation Settings.....	103
5.4	Description Of Output Results	104

5.5	Summary.....	107
6.0	HOLLOW CORE SLAB MODEL: RESULTS AND ANALYSIS.....	109
6.1	Introduction.....	109
6.2	Overheating Hours.....	109
6.3	Annual Cooling Load	118
6.4	Annual Heating Load.....	125
6.5	Chapter Summary	129
7.0	FLOOR VOID WITH MASS: RESULTS AND ANALYSIS.....	130
7.1	Introduction.....	130
7.2	Overheating Hours.....	130
7.3	Annual Cooling Load	138
7.4	Annual Heating Load.....	145
7.5	Chapter Summary	149
8.0	EARTH TO AIR HEAT EXCHANGER MODEL: RESULTS AND ANALYSIS ...	150
8.1	Introduction.....	150
8.2	Overheating Hours.....	150
8.3	Annual Cooling Load	155
8.4	Annual Heating Load.....	160
8.5	Chapter Summary	163
9.0	THERMAL LABYRINTH MODEL: RESULTS AND ANALYSIS.....	165
9.1	Introduction.....	165
9.2	Overheating Hours.....	165
9.3	Annual Cooling Load	170
9.4	Annual Heating Load.....	175
9.5	Chapter Summary	179
10.0	DISCUSSION.....	181
10.1	Introduction	181
10.2	Base Case	181
10.3	Thermal Mass	184
10.4	Thermal Mass with Night Cooling.....	187
10.5	Solar Gains	190
10.6	Internal Gains	193

10.7	Air Change Rate	196
10.8	Combinations of Parameters	199
10.9	Summary	201
11.0	CONCLUSION	204
11.1	Introduction	204
11.2	Building Monitoring & Simulation	205
11.3	Development of a Concept Design Tool	207
11.4	Main Findings	209
12.0	REFERENCES	215

APPENDIX A: Parametric Analysis Results

APPENDIX B: International Energy Agency (IES) Annex 44 Brochure

APPENDIX C: Peer Reviewed Paper

APPENDIX D: Conference Papers

LIST OF FIGURES

Figure 1—1 Nature of the Brunel/Surrey Engineering Doctorate Programme	1
Figure 3—1 Building parameter groups for a building integrating an active thermal mass strategy	33
Figure 3—2 Graphical representation of building weights	35
Figure 3—3 Element represented by a finite number of discrete slices	45
Figure 3—4 Conduction heat transfer of an internal slice.....	45
Figure 4—1 Booths' Case-study: Plan of Director's office with the location of temperature sensors	50
Figure 4—2 Booths' Case-study: Schematic representation of Director's office ventilation strategy with the location of temperature sensors	50
Figure 4—3 Longley Park Case-study: Plan of Computer room with the location of temperature sensors	51
Figure 4—4 Longley Park Case-study: Schematic representation of Computer room ventilation strategy. The location of temperature sensors is marked.....	51
Figure 4—5 Lowry Case-study: Schematic Plan of the theatre. The location of temperature sensors is marked.....	52
Figure 4—6 Lowry Case-study: Schematic representation of theatre ventilation strategy	52
Figure 4—7 Longley Park cross section of actual hollow core slab	57
Figure 4—8 Longley Park cross section of simplified slab modelled.....	57
Figure 4—9 Plan of the Lowry showing dimensions of the ETAHE and the plenum under the theatre	59
Figure 4—10 The Lowry cross section of actual ETAHE	60
Figure 4—11 The Lowry cross section of simplified ETAHE modelled.....	60
Figure 4—12 Booths HQ - Mid Season 2006 – Input data	63
Figure 4—13 Booths HQ - Summer 2007 – Input data.....	63
Figure 4—14 Longley Park - Mid season 2006 – Input data	65
Figure 4—15 Longley Park - Summer 2006 – Input data	65
Figure 4—16 The Lowry – summer 2006 – input data	67

Figure 4—17 The Lowry – Winter 2007 – input data	67
Figure 4—18 Comparison of monitored and simulated results for Booth’s HQ summer 2006..	68
Figure 4—19 Comparison of monitored and simulated results for Booth’s HQ Mid Season 2007	69
Figure 4—20 Comparison of monitored and simulated results for Longley Park in mid season 2006	70
Figure 4—21 Comparison of monitored and simulated results for Longley Park in summer 2006	71
Figure 4—22 Comparison of monitored and simulated results for the ETAHE in Lowry in summer 2006	73
Figure 4—23 Comparison of monitored and simulated results for the ETAHE in Lowry in winter 2007	73
Figure 4—24 Comparison of monitored and simulated results for the labyrinth in Lowry in summer 2006	75
Figure 4—25 Comparison of monitored and simulated results for the labyrinth in Lowry in winter 2007	75
Figure 5—1 Process diagram for TMAir.....	78
Figure 5—2 Plan and elevation of office blocks with test rooms highlighted	79
Figure 5—3 Opening tab of TMAir – input parameter selection	81
Figure 5—4 Layout of hollow core slabs in test room.	82
Figure 5—5 Layout of thermal labyrinth beneath each office block.....	86
Figure 5—6 Office occupancy profile	90
Figure 5—7 Office lighting profile.....	91
Figure 5—8 Office equipment profile	91
Figure 5—9 Constructions to be used in the development of TMAir	100
Figure 5—10 Additional options within TMAir	102
Figure 5—11 TMAir Summary Results single page printout	105
Figure 6—1 HCS vs Standard Strategy Annual Overheating Hours – Thermal Mass.....	110
Figure 6—2 HCS vs Standard Strategy T_{res} on a peak summer day – Thermal Mass	110
Figure 6—3 HCS vs Standard Strategy Ceiling Surface Temperature – Thermal Mass.....	111

Figure 6—4 HCS vs Standard Strategy Internal Wall Surface Temperature – Thermal Mass ...	111
Figure 6—5 HCS vs Standard Strategy Annual Overheating Hours – Thermal Mass with Night Cooling	112
Figure 6—6 HCS vs Standard Strategy T_{res} on a peak summer day – Thermal Mass with Night	112
Figure 6—7 HCS vs Standard Strategy Ceiling Surface Temperature – Thermal Mass with Night Cooling	113
Figure 6—8 HCS vs Standard Strategy Annual Overheating Hours – Solar Gain	114
Figure 6—9 HCS vs Standard Strategy T_{res} on a peak summer day – Solar Gain	114
Figure 6—10 HCS vs Standard Strategy Ceiling Surface Temperature – Solar Gain	114
Figure 6—11 HCS vs Standard Strategy Annual Overheating Hours – Internal Gain	115
Figure 6—12 HCS vs Standard Strategy T_{res} on a peak summer day – Internal Gain	115
Figure 6—13 HCS vs Standard Strategy Ceiling Surface Temperature – Internal Gain	116
Figure 6—14 HCS vs Standard Strategy Annual Overheating Hours – Air Change Rate.....	117
Figure 6—15 HCS vs Standard Strategy T_{res} on a peak summer day – Air Change Rate.....	117
Figure 6—16 HCS vs Standard Strategy Ceiling Surface Temperature – Air Change Rate.....	117
Figure 6—17 HCS vs Standard Strategy Annual Cooling Load– Thermal Mass.....	118
Figure 6—18 HCS vs Standard Strategy with cooling T_{res} on a peak summer day – Thermal Mass.....	118
Figure 6—19 HCS vs Standard Strategy with Cooling Ceiling Surface Temperature – Thermal Mass.....	119
Figure 6—20 HCS vs Standard Strategy Annual Cooling Load– Thermal Mass with Night Cooling	120
Figure 6—21 HCS vs Standard Strategy with cooling T_{res} on a peak summer day – Thermal Mass with Night Cooling.....	120
Figure 6—22 HCS vs Standard Strategy with Cooling Ceiling Surface Temperature – Thermal Mass with Night Cooling.....	120
Figure 6—23 HCS vs Standard Strategy Annual Cooling Load– Solar Gain.....	121
Figure 6—24 HCS vs Standard Strategy with cooling T_{res} on a peak summer day – Solar Gain	121

Figure 6—25 HCS vs Standard Strategy with Cooling Ceiling Surface Temperature – Solar Gain	122
Figure 6—26 HCS vs Standard Strategy Annual Cooling Load– Internal Gain.....	123
Figure 6—27 HCS vs Standard Strategy with cooling T_{res} on a peak summer day – Internal Gain	123
Figure 6—28 HCS vs Standard Strategy with Cooling Ceiling Surface Temperature – Internal Gain.....	123
Figure 6—29 HCS vs Standard Strategy Annual Cooling Load– Air Change Rate	124
Figure 6—30 HCS vs Standard Strategy with cooling T_{res} on a peak summer day – Air Change Rate	124
Figure 6—31 HCS vs Standard Strategy with Cooling Ceiling Surface Temperature – Air Change Rate.....	125
Figure 6—32 HCS vs Standard Strategy Annual Heating Load – Thermal Mass	126
Figure 6—33 HCS vs Standard Strategy Annual Heating Load – Solar Gain	127
Figure 6—34 HCS vs Standard Strategy Annual Heating Load – Internal Gain	128
Figure 6—35 HCS vs Standard Strategy Annual Heating Load – Air Change Rate	128
Figure 7—1 FVWM vs Standard Strategy Annual Overheating Hours – Thermal Mass.....	131
Figure 7—2 FVWM vs Standard Strategy T_{res} on a peak summer day – Thermal Mass.....	131
Figure 7—3 FVWM vs Standard Strategy Floor Surface Temperature – Thermal Mass.....	131
Figure 7—4 FVWM vs Standard Strategy Annual Overheating Hours – Thermal Mass with Night Cooling	132
Figure 7—5 FVWM vs Standard Strategy T_{res} on a peak summer day – Thermal Mass with Night Cooling	132
Figure 7—6 FVWM vs Standard Strategy Floor Surface Temperature – Thermal Mass with Night Cooling	133
Figure 7—7 FVWM vs Standard Strategy Annual Overheating Hours – Solar Gain.....	134
Figure 7—8 FVWM vs Standard Strategy T_{res} on a peak summer day – Solar Gains	134
Figure 7—9 FVWM vs Standard Strategy Floor Surface Temperature – Solar Gain.....	134
Figure 7—10 FVWM vs Standard Strategy Annual Overheating Hours – Internal Gain.....	135
Figure 7—11 FVWM vs Standard Strategy T_{res} on a peak summer day – Internal Gains	135

Figure 7—12 FVWM vs Standard Strategy Floor Surface Temperature – Internal Gain.....	136
Figure 7—13 FVWM vs Standard Strategy Annual Overheating Hours – Air Change Rate	137
Figure 7—14 FVWM vs Standard Strategy T_{res} on a peak summer day – Air Change Rate	137
Figure 7—15 FVWM vs Standard Strategy Floor Surface Temperature – Air Change Rate	137
Figure 7—16 FVWM vs Standard Strategy Annual Cooling Load– Thermal Mass	138
Figure 7—17 FVWM vs Standard Strategy with cooling T_{res} on a peak summer day – Thermal Mass.....	138
Figure 7—18 FVWM with Standard Strategy with Cooling Floor Surface Temperature – Thermal Mass	139
Figure 7—19 FVWM vs Standard Strategy Annual Cooling Load– Thermal Mass with Night Cooling	140
Figure 7—20 FVWM vs Standard Strategy with cooling T_{res} on a peak summer day – Thermal Mass with Night Cooling.....	140
Figure 7—21 FVWM vs Standard Strategy with Cooling Floor Surface Temperature – Thermal Mass with Night Cooling.....	140
Figure 7—22 FVWM vs Standard Strategy Annual Cooling Load– Solar Gain	141
Figure 7—23 FVWM vs Standard Strategy with cooling T_{res} on a peak summer day – Solar Gain	141
Figure 7—24 FVWM vs Standard Strategy with Cooling Floor Surface Temperature – Solar Gain	142
Figure 7—25 FVWM vs Standard Strategy Annual Cooling Load– Internal Gain	143
Figure 7—26 FVWM vs Standard Strategy with cooling T_{res} on a peak summer day – Internal Gain	143
Figure 7—27 FVWM vs Standard Strategy with Cooling Floor Surface Temperature – Internal Gain	143
Figure 7—28 FVWM vs Standard Strategy Annual Cooling Load– Air Change Rate	144
Figure 7—29 FVWM vs Standard Strategy with cooling T_{res} on a peak summer day – Air Change Rate.....	144
Figure 7—30 FVWM vs Standard Strategy with Cooling Floor Surface Temperature – Air Change Rate.....	145
Figure 7—31 FVWM vs Standard Strategy Annual Heating Load – Thermal Mass.....	146
Figure 7—32 FVWM vs Standard Strategy Annual Heating Load – Solar Gain	147

Figure 7—33 FVWM vs Standard Strategy Annual Heating Load – Internal Gain	148
Figure 7—34 FVWM vs Standard Strategy Annual Heating Load – Air Change Rate	148
Figure 8—1 ETAHE vs Standard Strategy Annual Overheating Hours – Thermal Mass	151
Figure 8—2 ETAHE vs Standard Strategy T_{res} on a peak summer day – Thermal Mass	151
Figure 8—3 ETAHE vs Standard Strategy Annual Overheating Hours – Thermal Mass with Night Cooling	152
Figure 8—4 ETAHE vs Standard Strategy T_{res} on a peak summer day – Thermal Mass with Night Cooling	152
Figure 8—5 ETAHE vs Standard Strategy Annual Overheating Hours – Solar Gain	153
Figure 8—6 ETAHE vs Standard Strategy T_{res} on a peak summer day – Solar Gain	153
Figure 8—7 ETAHE vs Standard Strategy Annual Overheating Hours – Internal Gain	154
Figure 8—8 ETAHE vs Standard Strategy T_{res} on a peak summer day – Internal Gain	154
Figure 8—9 ETAHE vs Standard Strategy Annual Overheating Hours – Air Change Rate	155
Figure 8—10 ETAHE vs Standard Strategy T_{res} on a peak summer day – Air Change Rate	155
Figure 8—11 ETAHE vs Standard Strategy Annual Cooling Load– Thermal Mass	156
Figure 8—12 ETAHE vs Standard Strategy Annual Cooling Load– Thermal Mass with Night Cooling	157
Figure 8—13 ETAHE vs Standard Strategy Annual Cooling Load– Solar Gain	158
Figure 8—14 ETAHE vs Standard Strategy Annual Cooling Load– Internal Gain	159
Figure 8—15 ETAHE vs Standard Strategy Annual Cooling Load– Air Change Rate	160
Figure 8—16 ETAHE vs Standard Strategy Annual Heating Load – Thermal Mass	161
Figure 8—17 ETAHE vs Standard Strategy Annual Heating Load – Solar Gain	161
Figure 8—18 ETAHE vs Standard Strategy Annual Heating Load – Internal Gain	162
Figure 8—19 ETAHE vs Standard Strategy Annual Heating Load – Air Change Rate	163
Figure 9—1 TL vs Standard Strategy Annual Overheating Hours – Thermal Mass	166
Figure 9—2 TL vs Standard Strategy T_{res} on a peak summer day – Thermal Mass	166
Figure 9—3 TL vs Standard Strategy Annual Overheating Hours – Thermal Mass with Night Cooling	167

Figure 9—4 TL vs Standard Strategy T_{res} on a peak summer day – Thermal Mass with Night Cooling	167
Figure 9—5 TL vs Standard Strategy Annual Overheating Hours – Solar Gain	168
Figure 9—6 TL vs Standard Strategy T_{res} on a peak summer day – Solar Gain	168
Figure 9—7 TL vs Standard Strategy Annual Overheating Hours – Internal Gain	169
Figure 9—8 TL vs Standard Strategy T_{res} on a peak summer day – Internal Gain	169
Figure 9—9 TL vs Standard Strategy Annual Overheating Hours – Air Change Rate	170
Figure 9—10 TL vs Standard Strategy T_{res} on a peak summer day – Air Change Rate.....	170
Figure 9—11 TL vs Standard Strategy Annual Cooling Load– Thermal Mass.....	171
Figure 9—12 TL vs Standard Strategy Annual Cooling Load– Thermal Mass with Night Cooling	172
Figure 9—13 TL vs Standard Strategy Annual Cooling Load– Solar Gain.....	173
Figure 9—14 TL vs Standard Strategy Annual Cooling Load– Internal Gain.....	174
Figure 9—15 TL vs Standard Strategy Annual Cooling Load– Air Change Rate	175
Figure 9—16 TL vs Standard Strategy Annual Heating Load – Thermal Mass	176
Figure 9—17 TL vs Standard Strategy Annual Heating Load – Solar Gain.....	177
Figure 9—18 TL vs Standard Strategy Annual Heating Load – Internal Gain.....	178
Figure 9—19 TL vs Standard Strategy Annual Heating Load – Air Change Rate	179
Figure 10—1 Comparison of Strategies Annual Overheating Hours – Base Case	182
Figure 10—2 Comparison of Strategies T_{res} on a peak summer day – Base Case	182
Figure 10—3 Comparison of Strategies Annual Cooling Load – Base Case.....	183
Figure 10—4 Comparison of Strategies T_{res} on a peak summer day with Cooling – Base Case	183
Figure 10—5 Comparison of Strategies Annual Heating Load – Base Case	184
Figure 10—6 Comparison of Strategies Annual Overheating Hours – Thermal Mass.....	185
Figure 10—7 Comparison of Strategies T_{res} on a peak summer day – Thermal Mass	185
Figure 10—8 Comparison of Strategies Annual Cooling Load – Thermal Mass	186
Figure 10—9 Comparison of Strategies T_{res} on a peak summer day with Cooling – Thermal Mass.....	186

Figure 10—10 Comparison of Strategies Annual Heating Load – Thermal Mass.....	187
Figure 10—11 Comparison of Strategies Annual Overheating Hours – Thermal Mass with Night Cooling	188
Figure 10—12 Comparison of Strategies Tres on a peak summer day – Thermal Mass with Night Cooling	188
Figure 10—13 Comparison of Strategies Annual Cooling Load – Thermal Mass with Night Cooling	189
Figure 10—14 Comparison of Strategies Tres on a peak summer day with Cooling – Thermal Mass with Night Cooling.....	189
Figure 10—15 Comparison of Strategies Annual Heating Load – Thermal Mass with Night Cooling	190
Figure 10—16 Comparison of Strategies Annual Overheating Hours – Solar Gains	191
Figure 10—17 Comparison of Strategies Tres on a peak summer day – Solar Gains	191
Figure 10—18 Comparison of Strategies Annual Cooling Load – Solar Gain	192
Figure 10—19 Comparison of Strategies Tres on a peak summer day with Cooling – Solar Gain	192
Figure 10—20 Comparison of Strategies Annual Heating Load – Solar Gain	193
Figure 10—21 Comparison of Strategies Annual Overheating Hours – Internal Gains	194
Figure 10—22 Comparison of Strategies Tres on a peak summer day – Internal Gains	194
Figure 10—23 Comparison of Strategies Annual Cooling Load – Internal Gain	195
Figure 10—24 Comparison of Strategies Tres on a peak summer day with Cooling – Internal Gain.....	195
Figure 10—25 Comparison of Strategies Annual Heating Load – Internal Gain	196
Figure 10—26 Comparison of Strategies Annual Overheating Hours – Air Change rate	197
Figure 10—27 Comparison of Strategies Tres on a peak summer day – Air Change rate.....	197
Figure 10—28 Comparison of Strategies Annual Cooling Load – Air Change rate.....	198
Figure 10—29 Comparison of Strategies Tres on a peak summer day with Cooling – Air Change rate	198
Figure 10—30 Comparison of Strategies Annual Heating Load – Air Change rate	199
Figure 10—31 Comparison of Strategies Annual Overheating Hours – Combinations of Parameters.....	200

Figure 10—32 Comparison of Strategies Annual Cooling Load – Combinations of Parameters	200
Figure 10—33 Comparison of Strategies Annual Heating Load – Combinations of Parameters	201
Figure A—1 Standard Strategy Annual Overheating Hours – Thermal Mass	1
Figure A—2 Standard Strategy T_{res} on a peak summer day – Thermal Mass	1
Figure A—3 Standard Strategy Floor Surface Temperature – Thermal Mass	2
Figure A—4 Standard Strategy Ceiling Surface Temperature – Thermal Mass	2
Figure A—5 Standard Strategy Internal Wall Surface Temperature – Thermal Mass	3
Figure A—6 Standard Strategy Annual Overheating Hours – Thermal Mass with Night Cooling	4
Figure A—7 Standard Strategy T_{res} on a peak summer day – Thermal Mass with Night Cooling.	4
Figure A—8 Standard Strategy Floor Surface Temperature – Thermal Mass with Night Cooling	5
Figure A—9 Standard Strategy Ceiling Surface Temperature – Thermal Mass with Night Cooling	5
Figure A—10 Standard Strategy Internal Wall Surface Temperature – Thermal Mass with Night Cooling	5
Figure A—11 Standard Strategy Annual Overheating Hours – Solar Gain	6
Figure A—12 Standard Strategy Annual Overheating Hours – Internal Gain	7
Figure A—13 Standard Strategy Annual Overheating Hours – Air Change Rate	8
Figure A—14 Standard Strategy Annual Cooling Load– Thermal Mass	9
Figure A—15 Standard Strategy with cooling T_{res} on a peak summer day – Thermal Mass	9
Figure A—16 Comparison of T_{air} and T_{res} for Standard Strategy Base Case test room	10
Figure A—17 Standard Strategy with Cooling Floor Surface Temperature – Thermal Mass	11
Figure A—18 Standard Strategy with Cooling Ceiling Surface Temperature – Thermal Mass ...	11
Figure A—19 Standard Strategy with Cooling Internal Wall Surface Temperature – Thermal Mass	11
Figure A—20 Standard Strategy Annual Cooling Load– Thermal Mass with Night Cooling	12
Figure A—21 Standard Strategy with cooling T_{res} on a peak summer day – Thermal Mass with Night Cooling	12

Figure A—22 Standard Strategy with Cooling Ceiling Surface Temperature – Thermal Mass with Night Cooling	13
Figure A—23 Standard Strategy with Cooling Internal Wall Surface Temperature – Thermal Mass with Night Cooling.....	13
Figure A—24 Standard Strategy Annual Cooling Load – Solar Gain	14
Figure A—25 Standard Strategy Annual Cooling Load – Internal Gain	15
Figure A—26 Standard Strategy Annual Cooling Load – Air Change Rate.....	16
Figure A—27 Standard Strategy Annual Heating Load – Thermal Mass.....	17
Figure A—28 Standard Strategy Annual Heating Load – Solar Gain.....	18
Figure A—29 Standard Strategy Annual Heating Load – Internal Gain.....	19
Figure A—30 Standard Strategy Annual Heating Load – Air Change Rate.....	20
Figure A—31 HCS Strategy core and supply air temperatures.....	21
Figure A—32 HCS Strategy Annual Overheating Hours – Thermal Mass.....	23
Figure A—33 HCS Strategy T_{res} on a peak summer day – Thermal Mass	23
Figure A—34 HCS Strategy Floor Surface Temperature – Thermal Mass.....	24
Figure A—35 HCS Strategy Ceiling Surface Temperature – Thermal Mass	24
Figure A—36 HCS Strategy Internal Wall Surface Temperature – Thermal Mass	25
Figure A—37 HCS Strategy core and supply air temperatures – Thermal Mass.....	25
Figure A—38 HCS Strategy Annual Overheating Hours – Thermal Mass with Night Cooling .	26
Figure A—39 HCS Strategy T_{res} on a peak summer day – Thermal Mass with Night Cooling ..	26
Figure A—40 HCS Strategy Ceiling Surface Temperature – Thermal Mass with Night Cooling	27
Figure A—41 HCS Strategy core and supply air temperatures – Thermal Mass with Night Cooling	27
Figure A—42 HCS Strategy Annual Overheating Hours – Solar Gain	29
Figure A—43 HCS Strategy Ceiling Surface Temperature – Solar Gain	29
Figure A—44 HCS Strategy core and supply air temperatures – Solar Gain	30
Figure A—45 HCS Strategy Annual Overheating Hours – Internal Gain	32
Figure A—46 HCS Strategy Ceiling Surface Temperature – Internal Gain	32

Figure A—47 HCS Strategy core and supply air temperatures – Internal Gain	32
Figure A—48 HCS Strategy Annual Overheating Hours – Air Change Rate	34
Figure A—49 HCS Strategy Ceiling Surface Temperature – Air Change Rate	34
Figure A—50 HCS Strategy core and supply air temperatures – Air Change Rate.....	34
Figure A—51 HCS Strategy with Cooling core and supply air temperatures	35
Figure A—52 HCS Strategy Annual Cooling Load– Thermal Mass.....	36
Figure A—53 HCS Strategy with cooling T_{res} on a peak summer day – Thermal Mass	36
Figure A—54 HCS Strategy with Cooling Floor Surface Temperature – Thermal Mass	38
Figure A—55 HCS Strategy with Cooling Ceiling Surface Temperature – Thermal Mass	38
Figure A—56 HCS Strategy with Cooling Internal Wall Surface Temperature – Thermal Mass	38
Figure A—57 HCS Strategy with Cooling core and supply air temperatures – Thermal Mass ...	38
Figure A—58 HCS Strategy Annual Cooling Load– Thermal Mass with Night Cooling.....	40
Figure A—59 HCS Strategy with cooling T_{res} on a peak summer day – Thermal Mass with Night Cooling	40
Figure A—60 HCS Strategy with Cooling Ceiling Surface Temperature – Thermal Mass with Night Cooling	41
Figure A—61 HCS Strategy with Cooling core and supply air temperatures – Thermal Mass with Night Cooling	41
Figure A—62 HCS Strategy Annual Cooling Load– Solar Gain.....	43
Figure A—63 HCS Strategy with Cooling Ceiling Surface Temperature – Solar Gain	43
Figure A—64 HCS Strategy with Cooling core and supply air temperatures – Solar Gain	44
Figure A—65 HCS Strategy Annual Cooling Load– Internal Gain.....	45
Figure A—66 HCS Strategy with Cooling Ceiling Surface Temperature – Internal Gain	45
Figure A—67 HCS Strategy with Cooling core and supply air temperatures – Internal Gain	46
Figure A—68 HCS Strategy Annual Cooling Load– Air Change Rate	47
Figure A—69 HCS Strategy with Cooling Ceiling Surface Temperature – Air Change Rate	47
Figure A—70 HCS Strategy with Cooling core and supply air temperatures – Air Change Rate	48
Figure A—71 HCS Strategy Annual Heating Load – Thermal Mass	49

Figure A—72 HCS Strategy Annual Heating Load – Solar Gain	50
Figure A—73 HCS Strategy Annual Heating Load – Internal Gain	51
Figure A—74 HCS Strategy Annual Heating Load – Air Change Rate	52
Figure A—75 FVWM Strategy void and supply air temperatures	53
Figure A—76 FVWM Strategy void and supply air temperatures	54
Figure A—77 FVWM Strategy Annual Overheating Hours – Thermal Mass	55
Figure A—78 FVWM Strategy T_{res} on a peak summer day – Thermal Mass	55
Figure A—79 FVWM Strategy Floor Surface Temperature – Thermal Mass	56
Figure A—80 FVWM Strategy Ceiling Surface Temperature – Thermal Mass	56
Figure A—81 FVWM Strategy Internal Wall Surface Temperature – Thermal Mass	57
Figure A—82 FVWM Strategy void and supply air temperatures – Thermal Mass	57
Figure A—83 FVWM Strategy Annual Overheating Hours – Thermal Mass with Night Cooling	58
Figure A—84 FVWM Strategy T_{res} on a peak summer day – Thermal Mass with Night Cooling	58
Figure A—85 FVWM Strategy Floor Surface Temperature – Thermal Mass with Night Cooling	59
Figure A—86 FVWM Strategy void and supply air temperatures – Thermal Mass with Night Cooling	59
Figure A—87 FVWM Strategy Annual Overheating Hours – Solar Gain	60
Figure A—88 FVWM Strategy Floor Surface Temperature – Solar Gain	60
Figure A—89 FVWM Strategy void and supply air temperatures – Solar Gain	61
Figure A—90 FVWM Strategy Annual Overheating Hours – Internal Gain	62
Figure A—91 FVWM Strategy Floor Surface Temperature – Internal Gain	62
Figure A—92 FVWM Strategy void and supply air temperatures – Internal Gain	63
Figure A—93 FVWM Strategy Annual Overheating Hours – Air Change Rate	64
Figure A—94 FVWM Strategy Floor Surface Temperature – Air Change Rate	64
Figure A—95 FVWM Strategy void and supply air temperatures – Air Change Rate	65
Figure A—96 FVWM Strategy with Cooling void and supply air temperatures	66

Figure A—97 FVWM Strategy Annual Cooling Load– Thermal Mass	67
Figure A—98 FVWM Strategy with cooling T_{res} on a peak summer day – Thermal Mass	67
Figure A—99 FVWM Strategy with Cooling Floor Surface Temperature – Thermal Mass	68
Figure A—100 FVWM Strategy with Cooling void and supply air temperatures – Thermal Mass	68
Figure A—101 FVWM Strategy Annual Cooling Load– Thermal Mass with Night Cooling	69
Figure A—102 FVWM Strategy with cooling T_{res} on a peak summer day – Thermal Mass with Night Cooling	69
Figure A—103 FVWM Strategy with Cooling Floor Surface Temperature – Thermal Mass with Night Cooling	69
Figure A—104 FVWM Strategy with Cooling void and supply air temperatures – Thermal Mass with Night Cooling	69
Figure A—105 FVWM Strategy Annual Cooling Load– Solar Gain	70
Figure A—106 FVWM Strategy with Cooling Floor Surface Temperature – Solar Gain	70
Figure A—107 FVWM Strategy with Cooling void and supply air temperatures – Solar Gain ..	71
Figure A—108 FVWM Strategy Annual Cooling Load– Internal Gain	72
Figure A—109 FVWM Strategy with Cooling Floor Surface Temperature – Internal Gain	72
Figure A—110 FVWM Strategy with Cooling void and supply air temperatures – Internal Gain	72
Figure A—111 FVWM Strategy Annual Cooling Load– Air Change Rate	73
Figure A—112 FVWM Strategy with Cooling Floor Surface Temperature – Air Change Rate ..	73
Figure A—113 FVWM Strategy with Cooling void and supply air temperatures – Air Change Rate	74
Figure A—114 FVWM Strategy Annual Heating Load – Thermal Mass	75
Figure A—115 FVWM Strategy Annual Heating Load – Solar Gain	76
Figure A—116 FVWM Strategy Annual Heating Load – Internal Gain	77
Figure A—117 FVWM Strategy Annual Heating Load – Air Change Rate	78
Figure A—118 ETAHE Strategy surface and supply air temperatures	79
Figure A—119 ETAHE Strategy Annual Overheating Hours – Thermal Mass	80
Figure A—120 ETAHE Strategy T_{res} on a peak summer day – Thermal Mass	80

Figure A—121 ETAHE Strategy Annual Overheating Hours – Thermal Mass with Night Cooling	81
Figure A—122 ETAHE Strategy T_{res} on a peak summer day – Thermal Mass with Night Cooling	81
Figure A—123 ETAHE Strategy Annual Overheating Hours – Solar Gain	82
Figure A—124 ETAHE Strategy Annual Overheating Hours – Internal Gain	83
Figure A—125 ETAHE Strategy Annual Overheating Hours – Air Change Rate	84
Figure A—126 ETAHE Strategy Annual Cooling Load– Thermal Mass.....	85
Figure A—127 ETAHE Strategy with cooling T_{res} on a peak summer day – Thermal Mass.....	85
Figure A—128 ETAHE Strategy Annual Cooling Load– Thermal Mass with Night Cooling....	86
Figure A—129 ETAHE Strategy with cooling T_{res} on a peak summer day – Thermal Mass with Night Cooling	86
Figure A—130 ETAHE Strategy Annual Cooling Load– Solar Gain	87
Figure A—131 ETAHE Strategy Annual Cooling Load– Internal Gain	88
Figure A—132 ETAHE Strategy Annual Cooling Load– Air Change Rate.....	89
Figure A—133 ETAHE Strategy Annual Heating Load – Thermal Mass	90
Figure A—134 ETAHE Strategy Annual Heating Load – Solar Gain.....	91
Figure A—135 ETAHE Strategy Annual Heating Load – Internal Gain.....	92
Figure A—136 ETAHE Strategy Annual Heating Load – Air Change Rate	93
Figure A—137 TL Strategy surface and supply air temperatures	94
Figure A—138 TL Strategy Annual Overheating Hours – Thermal Mass	95
Figure A—139 TL Strategy T_{res} on a peak summer day – Thermal Mass	95
Figure A—140 TL Strategy Annual Overheating Hours – Thermal Mass with Night Cooling ..	96
Figure A—141 TL Strategy T_{res} on a peak summer day – Thermal Mass with Night Cooling ...	96
Figure A—142 TL Strategy Annual Overheating Hours – Solar Gain	97
Figure A—143 TL Strategy Annual Overheating Hours – Internal Gain	98
Figure A—144 TL Strategy Annual Overheating Hours – Air Change Rate.....	99
Figure A—145 TL Strategy Annual Cooling Load– Thermal Mass	100

Figure A—146 TL Strategy with cooling T_{res} on a peak summer day – Thermal Mass	100
Figure A—147 TL Strategy Annual Cooling Load– Thermal Mass with Night Cooling.....	101
Figure A—148 TL Strategy with cooling T_{res} on a peak summer day – Thermal Mass with Night Cooling	101
Figure A—149 TL Strategy Annual Cooling Load– Solar Gain	102
Figure A—150 TL Strategy Annual Cooling Load– Internal Gain.....	103
Figure A—151 TL Strategy Annual Cooling Load– Air Change Rate.....	104
Figure A—152 TL Strategy Annual Heating Load – Thermal Mass	105
Figure A—153 TL Strategy Annual Heating Load – Solar Gain.....	106
Figure A—154 TL Strategy Annual Heating Load – Internal Gain.....	107
Figure A—155 TL Strategy Annual Heating Load – Air Change Rate	108

LIST OF TABLES

Table 3—1 Traditional CIBSE surface convective heat transfer coefficients.....	20
Table 3—2 Surface radiative heat transfer coefficients	20
Table 3—3 Design guidance on active thermal mass strategies.....	30
Table 3—4 Concept design tools available for active thermal mass strategies in offices.....	31
Table 4—1 Materials and properties of floor void modelling for Booths HQ	56
Table 4—2 Materials and properties of hollow core modelling for Longley Park	58
Table 4—3 Materials and properties of ETAHE modelling for Lowry.	61
Table 4—4 Materials and properties for labyrinth modelling for the Lowry.....	62
Table 5—1 TMAir BASE Case Default Values.....	81
Table 5—2 Materials and properties of Hollow Core Slab for TMAir	83
Table 5—3 Hollow Core Slab air flow rate, air velocity and heat transfer coefficient.....	83
Table 5—4 Materials and properties of Floor Void with Mass for TMAir.....	84
Table 5—5 Air flow rate and the number of earth tubes required for each test room.....	84
Table 5—6 Materials and properties of Earth to Air Heat Exchanger for TMAir	85
Table 5—7 Materials and properties of Thermal Labyrinth for TMAir.....	86
Table 5—8 TMAir internal heat gains.....	89
Table 5—9 Solar load per unit floor area for different combinations of g_{eff} and window area – North Facing Facade.....	94
Table 5—10 Solar load per unit floor area for different combinations of g_{eff} and window area – East/West Facing Facade.....	94
Table 5—11 Solar load per unit floor area for different combinations of g_{eff} and window area – South Facing Facade.....	95
Table 5—12 Glazing areas and g_{eff} to achieve solar categories for each orientation	96
Table 5—13 g-values for different solar gains and orientations	96
Table 5—14 Glazing configurations used within calculations for TMAir.....	97
Table 5—15 Glazing constructions used within IES for TMAir.....	97
Table 5—16 Admittance values to be used in the development of TMAir.....	98

Table 5—17 Material properties to be used in the development of the TMAir	101
Table 5—18 Construction properties to be used in the development of the TMAir	101
Table 5—19 Simulation settings	103
Table 10—1 Annual Overheating Hours	202
Table 10—2 Annual Cooling	202
Table 10—3 Annual Heating	203
Table A—1 HCS Efficiency	22
Table A—2 HCS Heat Exchange Efficiency – HW Thermal Mass	25
Table A—3 HCS Heat Exchange Efficiency – HW Thermal Mass with Night Cooling	28
Table A—4 HCS Heat Exchange Efficiency - Low Solar Gain	30
Table A—5 HCS Heat Exchange Efficiency - Low Internal Gain	33
Table A—6 HCS Heat Exchange Efficiency – 10achr ⁻¹	35
Table A—7 HCS with Cooling Heat Exchange Efficiency – HW Thermal Mass	39
Table A—8 HCS with Cooling Heat Exchange Efficiency – HW Thermal Mass with Night Cooling	42
Table A—9 HCS with Cooling Heat Exchange Efficiency – Low Solar Gain	44
Table A—10 HCS with Cooling Heat Exchange Efficiency – Low Internal Gains	46
Table A—11 HCS with Cooling Heat Exchange Efficiency – 10achr ⁻¹	48

GLOSSARY OF TERMS

AHU	Air Handling Unit
BMS	Building Management System
BRE	Building Research Establishment
BSRIA	The Building Services Research and Information Association
CFD	Computational Fluid Dynamics
CIBSE	Chartered Institute of Building Services Engineers
DRT	Dry Resultant Temperature
DSY	Design Summer Year
DTM	Dynamic Thermal Model
ETAHE	Earth to Air Heat Exchanger
EWY	Example Weather Year
FVWM	Floor Void with Mass
HCS	Hollow Core Slab
HVAC	Heating Ventilation and Air Conditioning
HW	Heavyweight
LW	Lightweight
MRT	Mean Radiant Temperature

NC	Night Cooling
POE	Post Occupancy Evaluation
RIBA	Royal Institute of British Architects.
SFP	Specific Fan Power
TL	Thermal Labyrinth
TMAir	Thermal Mass Activation Air medium
TRV	Thermostatic Radiator Valve
TRY	Test Reference Year
VHW	Very Heavyweight
VLW	Very Lightweight –

1.0 EXECUTIVE SUMMARY

1.1 Background information

The Engineering Doctorate Programme (EngD) is a four-year research degree, awarded for industrially relevant research, based in industry and supported by a programme of professional development courses. The EngD Programme is sponsored by the Engineering and Physical Science Research Council (EPSRC) and was set up in response to industry needs for more industrially orientated research.

The industrial perspective of the work included in this thesis was instigated by Buro Happold, who also provided additional funding to the EPSRC sponsorship, as required by the EngD Programme.

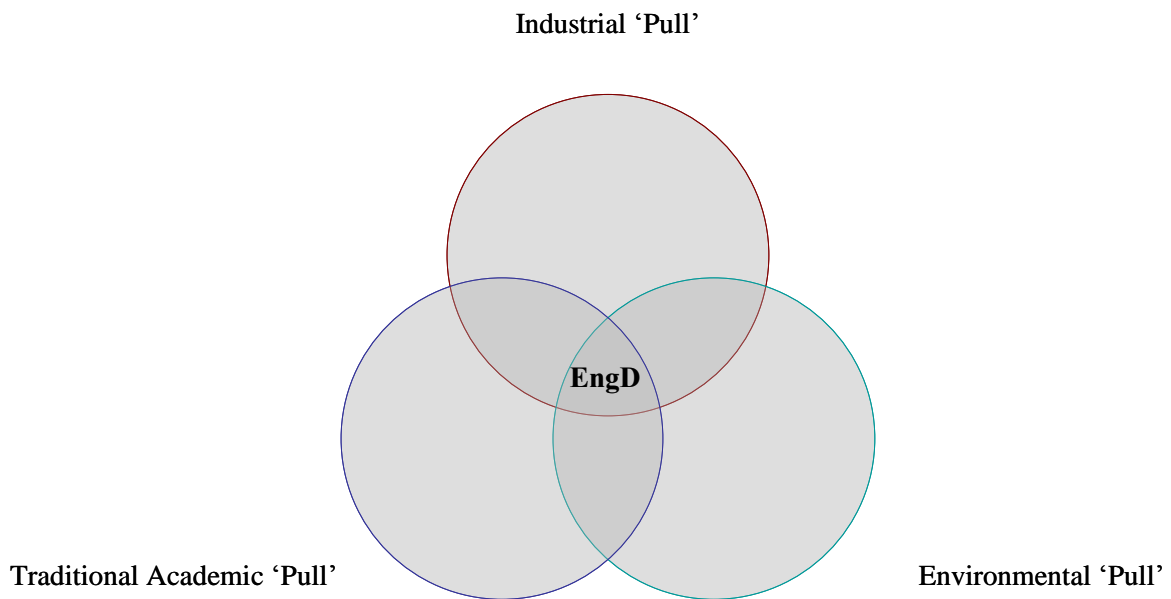


Figure 1—1 Nature of the Brunel/Surrey Engineering Doctorate Programme

The work included in this thesis was carried out within an EngD managed jointly by Brunel and Surrey Universities. All research projects undertaken at the Brunel/Surrey EngD centre follow the theme of “Environmental Technology” and aim to ‘provide graduates with the necessary skills to balance environmental risks with all of the traditional variables of cost, quality, shareholder value and legislative compliance’.

The Brunel/Surrey EngD programme aims to balance a number of competing interests. The research engineer must reconcile both academic and industrial requirements of the research while considering the environmental issues inherent in the project undertaken. Figure 1—1 sums up the three elements of an EngD research project.

The EngD programme includes complementary courses that must be completed by the EngD candidates. These courses have the following aims:

- To present a view of the relationship between engineering and the environment including sociological aspects.
- To provide professional development in key business skills and competencies.
- To close any gaps in the knowledge required in undertaking the research project.

The programme of courses is comprised of compulsory and elective modules and the completion of a relevant assignment is usually required after each course. The modules taken and successfully completed during this research are outlined below:

- Project Management
- Sustainable Development
- Research Methods
- Life Cycle Approaches
- Social Research
- Environmental Risk Assessment

- Hands on Environmental Audit
- Environmental Law
- Environmental Management for Developing Countries
- Finance
- Environmental Economics
- Integrated Assessment
- Talking to the Media

The EngD Candidates are also given the opportunity to present their research either orally or through poster presentations, at the annual EngD Conference. The conferences are attended by all EngD Candidates, supervisors and invited delegates. Papers written for the conference by the Research Engineer are included in published proceedings.

From the research conducted in this thesis, the following papers were written and published for the EngD conferences:

- Warwick, D.J, Cripps, A, and Kolokotroni, M, 2007, Integrating active thermal mass strategies with HVAC systems: dynamic thermal modelling, Brunel and Surrey EngD Conference, Summer 2006
- Warwick, D.J, Cripps, A, and Kolokotroni, M, 2008, Integrating active thermal mass strategies with HVAC systems: dynamic thermal modelling, Brunel and Surrey EngD Conference, Summer 2008

In addition to attending courses, submitting assignments and presenting the results of the research to the EngD Conferences, EngD candidates are also expected to complete a progress report every six months. The aim of these progress reports is to inform the EngD Programme Management Committee and supervisors of the progress made towards the completion of research projects at given stages during the programme.

This section gave a brief introduction to the EngD Programme in order to describe the overall framework of the research work included in this thesis.

1.2 Introduction to the Research Topic and Objectives

Thermal mass can be used to reduce the need and dependence on mechanical heating and cooling systems, whilst maintaining environmental comfort in the building. Active methods enhance the performance of thermal mass by passing air or fluid across or through the materials with high thermal mass.

Such systems have been applied to buildings but there is still uncertainty on how to incorporate them in new designs and how to carry out accurate (but as simple as possible) modelling during the detailed design of a building. Therefore the solution can be provided in two parts. The first must deal with simplified guidelines on how activated thermal mass would reduce energy consumption (and by how much) and possibly improve environmental conditions. The second must deal with building up confidence in dynamic thermal models used by building services engineers to accurately predict environmental conditions in a building incorporating active thermal mass strategies.

The aim of this research project has been to improve the understanding of architects, building services engineers and building physicists of the performance of active thermal mass strategies in operational buildings, and also to provide guidance for their use in suitable future buildings. The active thermal mass strategies included within this research project are: Hollow Core Slabs, Floor Void with Mass, Earth-to-Air Heat Exchangers and Thermal Labyrinths.

The research objectives can be simplified to the following:

- Develop a profile of the performance of active thermal mass strategies in operational buildings
- Determine the accuracy of commercially available dynamic thermal models
- Create simple design guidance for the use at the concept design stages of a project

1.3 Research methods and main results

This section summarizes the research methods and main results from the project carried out as part of this EngD Programme and are presented in detail in the following chapters of this research thesis.

Building Monitoring & Simulation

To develop a profile of the performance of active thermal mass strategies, buildings recently designed by the design organisation, and subsequently constructed, that integrated active thermal mass strategies were selected for post occupancy monitoring.

Three buildings, incorporating different active thermal mass strategies, were selected for monitoring:

- Building 1: Booth's HQ Office - Floor Void with Thermal Mass (FVWM)
- Building 2: Longley Park School - Hollow Core Slabs (HCS)
- Building 3: The Lowry – Earth to Air Heat Exchanger (ETAHE) and Thermal Labyrinth (TL)

Each building was monitored for a minimum of two periods in different weather periods (winter, mid season or summer).

Models of each building, focusing on the active thermal mass strategies, were constructed within the commercially available dynamic building thermal program IES Virtual Environment (IES, 2008). Record drawings and on site measurements were used to determine the geometry and construction types.

Simplifications for ease of modelling were made; including changes in physical representation.

It was possible to isolate the performance of the thermal mass by using measurements of the adjacent space temperatures, supply air temperatures into the thermal mass, ambient air temperatures and fan running times as input data into the simulation models.

Simulation results of the air temperatures within the active thermal mass strategies showed good comparison with the monitored data.

Development of a Concept Design Tool

To develop a simplified design tool that can be used by designers at the concept stages of a project to quickly analyse the effects of integrating active thermal mass strategies into UK office buildings the calibrated modelling methods were then used to construct a model of a standard office space coupled with each of the active thermal mass strategies.

Key design parameters were identified for each system and parametric analysis carried out to determine the resulting environmental conditions and energy consumption in the office.

All of the possible combinations of the user selected parameters were then simulated and the results fed into the excel based tool TMAir (Thermal Mass Activation – Air Medium).

The tool has been developed to have easy-to-use interface which allows direct comparison of the different active thermal mass strategies together with the effects of changing key design parameters. Results are presented in terms of thermal comfort and energy consumption.

Using TMAir a parametric analysis was then performed for the Standard strategy model and each of the four active thermal mass strategies to investigate the effect of (a) thermal mass (b) night cooling, (c) solar gain (d) internal gain and (e) air change rate on the performance of each strategy. The performance was analysed in terms of (a) number of overheating hours (b) annual cooling load and (c) annual heating load.

These results were then further analysed to identify the benefit that adding the active thermal mass strategies have compared to a Standard strategy.

The key results have shown that when only mechanical ventilation is provided (i.e. no cooling) the performance of the Hollow Core Slab (HCS) and Floor Void with Mass (FVWM) strategies are dependent on the performance of the test room and will only result in a reduction in annual overheating hours when the performance of the test room is optimised (i.e. solar gains reduced, night cooling introduced, etc), whereas the Earth to Air Heat Exchanger (ETAHE) and Thermal

Labyrinth (TL) strategies will always provide a reduction in annual overheating hours. When only one parameter is improved from the BASE Case Option:

- There is only a benefit in integrating a HCS strategy when night cooling is introduced
- There is no benefit in integrating a FVWM strategy when only one parameter is improved
- An ETAHE and TL strategy will always provide a benefit, although the benefits are greater when night cooling is introduced, solar and internal gains are reduced and when the air change rate is increased

When all of the parametric improvements are applied to the test room the results show that all of the active thermal mass strategies can provide a reduction in annual overheating hours when compared to the Standard Strategy.

Only a small benefit is found for the FVWM Strategy, however around a 25% reduction is found for the HCS Strategy, over a 50% reduction for the TL Strategy and nearly a 75% reduction for the ETAHE Strategy. This demonstrates the importance of applying a low energy, passive approach when considering the application of active thermal mass strategy.

The key results have shown that when comfort cooling is provided, adding a HCS or FVWM strategy always results in an increase in the annual cooling load. This is as a result of the temperature of the air being supplied into the cores or floor void being higher than that of the internal surface temperatures of the cores or void. This results in the supply air being heated, and less cooling provided to the test room per cooling energy delivered. Due to the pre cooling effect of the ETAHE and TL strategies, these strategies always result in a reduction in the annual cooling load.

The key results have shown that the annual heating load is reduced by a small amount for the HCS and FVWM strategies unless the solar gains or internal gains are reduced, whereas the ETAHE and TL strategies always result in a around a 10% reduction in annual heating load as a result of the preheating effect these strategies have on the supply air.

Originality and Contribution to Knowledge

The project makes contributions to the field of building engineering in three distinct ways:

- i) Developed a profile of four active thermal mass strategies in three operational buildings

The monitored data provides real data on the actual performance of operational buildings integrating active thermal mass strategies in the UK.

- ii) The validation of the application of commercially available software to simulate the performance of four active thermal mass strategies

Previous research has shown the validation of simulation methods when applied to active thermal mass strategies, however this has not previously been done using commercially available software commonly used with building services design consultancies.

- iii) The creation of a simplified design tool that can be used by designers at the concept stages of a project to quickly analyse the effects of integrating active thermal mass strategies into UK office buildings

There is currently limited design guidance on the performance of active thermal mass strategies, other than for Night Cooling or Earth-to-Air Heat Exchangers (ETAHE). The concept design tool TMAir presents results in terms of thermal comfort and energy consumption and allows the direct comparison of the four active thermal mass strategies; Hollow Core Slabs (HCS), Floor Void with Mass (FVWM), Earth to Air Heat Exchangers (ETAHE) and Thermal Labyrinth (TL), and a Standard Strategy, together with the effects of changing key design parameters.

Contribution to IEA-ECBCS Annex 44

This research project was part of the UK contribution to the IEA-ECBCS Annex 44

“Integrating Environmentally Responsive Elements in Buildings”. A description of Annex 44 is included in Appendix B and more details can be found in its website.

It was beneficial to participate in the project and the 6-monthly meeting where progress by all participating countries was presented. The interaction with international researchers working on similar technologies was invaluable.

Publications

It is a requirement of the EngD to publish one peer-reviewed journal paper. The following have been published by the researcher during the course of the doctorate.

Peer reviewed journal papers (Appendix C):

- Warwick, DJ, Cripps, AJ, and Kolokotroni, M, 2009, Integrating Active Thermal Mass Strategies with HVAC Systems: Dynamic Thermal Modelling. The International Journal of Ventilation Vol. 7 N. 4 pp345-367

Conference papers (Appendix D):

- Warwick, DJ, Cripps, AJ and Kolokotroni, M, 2006, Monitoring and analysis of a building incorporating actively controlled thermal mass strategies, Proc The World Renewable Energy Congress IX, 19-25 August 2006, Florence, Italy (invited paper)
- Warwick, DJ, Cripps, AJ and Kolokotroni, M, 2007, Monitoring and modelling of the performance of activated thermal mass in two operational building, Proc AIVC/PALENC, Crete, Greece, September 2007
- Warwick, DJ, Cripps, AJ and Kolokotroni, M, 2008. Integrating active thermal mass strategies with HVAC systems in office buildings: development of a concept design tool, AIVC Conference, Kyoto, Japan, 16-18 October 2008.

2.0 INTRODUCTION

2.1 Energy in Buildings

Climate change is a key issue worldwide and in response to the Royal Commission for Environmental Pollution (RCEP, 2000) the UK government have committed to putting themselves on the path to a 60% reduction in the UK's carbon emissions by 2050.

The energy used in buildings accounts for around 50% of the carbon dioxide emissions in the UK (BRE, 2006). In non-domestic UK buildings 41% of the carbon dioxide emissions are attributed to heating and 5% to cooling and ventilation (CIBSE, 2004a). In hotter and more humid climates the use of air conditioning is much higher with refrigeration and air conditioning consuming around 15% of all electricity consumed worldwide (JRAIA, 2002). The use of air conditioning is also increasing due to the increased living standards in the developed world (Santamouris, 2006) with a survey in Japan showing a 28% increase of sales of air conditioning units between 1998 and 2002 (JRAIA, 2002).

Using air conditioning not only increases the absolute energy use in buildings, but also increases the peak electricity load and creates indoor air quality issues (Santamouris, 2006).

Although air conditioned buildings maintain an objectively better climate they are subjectively rated lower than naturally ventilated working conditions (Voss *et al.*, 2007). However, to ensure that summer comfort can be maintained without actively cooling or dehumidifying the supply air, passive cooling measures must be integrated (Santamouris and Asimakopoulos, 1997).

There are a number of methods by which the need for air conditioning can be reduced in buildings (CIBSE, 2005b). Suitable design and construction of a building can be used to reduce the energy burden a building imposes by using passive technologies to eliminate the problem at the source instead of considering 'end of pipe' technologies (Russell & Surendran, 2001). There are a number of passive technologies that can be used in a building which have been investigated extensively in the past; most of these technologies include utilisation of thermal mass usually incorporated in the building envelope.

However, recently the notion of controlling the incorporated thermal mass using active methods is gaining momentum as a suitable low carbon technology. There is still relatively less knowledge about the performance of activated thermal mass and in particular its integration with other environmental systems in buildings.

2.2 Active Thermal Mass Strategies

Thermal mass can be included in the outer envelope or the interior mass of a building and can be used to improve the environmental comfort in a building whilst reducing the need and dependence on mechanical heating and cooling systems (Barnard and Jaunzens, 2001; Li and Xu, 2006)).

Outer envelopes (walls and roof) with high thermal mass store a proportion of the energy from high solar gains during the day, dampening fluctuations in ambient air temperatures (Fernandez *et al.*, 2005; Cheng *et al.*, 2005), and then slowly release them through to the indoor environment delaying the occurrence of peak indoor temperatures by up to several hours (Becker & Paciuk, 2002).

Including interior mass within a building's internal structure (floors, partitions, etc) creates a heat sink into which internally generated heat can be absorbed and stored during the occupied period (Russell & Surendran, 2001). During the unoccupied period the mass is then cooled using night cooling (Kolokotroni *et al.*, 1999).

The potential benefits of fabric energy storage include (Barnard, 1994):

- Cooling available from low night time ambient air temperatures can be stored for use the following day
- Heating and cooling plant sizes may be reduced
- Plant is able to operate at full load for extended periods, increasing efficiency
- Advantage can be taken of low electricity charge rates

The performance of thermal mass depends on: building material properties; building location and orientation; thermal insulation; ventilation; climatic conditions; occupancy patterns and the use of auxiliary cooling and heating systems (Balaras, 1996; Seamen *et al.*, 2000; Cheng *et al.*, 2005; Yohanis & Norton, 2002; Mohammad *et al.*, 2005).

The density, thermal conductivity and specific heat capacity of the building's materials determine the heat that can be stored (Seamen *et al.*, 2000). The thermal diffusivity determines the depth that the diurnal heat wave reaches within the storage material (Balaras, 1996).

Active methods enhance the performance of thermal mass by passing air or fluid across the surfaces with high thermal mass (Barnard, 1994; Russell & Surendran, 2001). The potential of internal thermal mass can also be better exploited if mechanical ventilation is used to control the internal air change rate and enhance the heat transfer rates to the structure (Braham *et al.*, 2001b). A number of various active thermal mass methods have been developed and used in buildings; these are:

- **Hollow Core Slabs:** Hollow core pre-cast concrete slabs are used as a path for supply air thus increasing the coupling between the thermal mass and the supply air (Ren and Wright, 1997) and attenuating variations in ambient air temperatures (Barton *et al.*, 2002).
- **Floor Void with Thermal Mass:** A void created between a raised floor and a structural concrete slab as a supply air plenum, again increasing the coupling with the thermal mass and supply air (Nagano *et al.*, 2006).
- **Earth to Air Heat Exchanger :** An earth-to-air heat exchanger draws ventilation air through ducts buried underground (Zimmerman and Remund, 2001; Grosso and Raimondo, 2008).
- **Thermal Labyrinth:** A thermal labyrinth decouples the thermal mass from the occupied space by creating a concrete undercroft, increasing the surface area of thermal mass, beneath the building. The benefits of decoupling the mass are that it can be cooled lower than if it was in the occupied space and the stored 'coolth' can

be used to condition the occupied space for up to 3 or 4 days in hot periods (Evans, 1998).

2.3 Concept Design Tools

Building simulation, simplified guidelines and expert advice based on experience can be used to support building design (deWit & Augenbroe, 2002). Building simulation programs require the building geometry, the comfort criteria and the specification of the HVAC systems (Ghiaus *et al.*, 2006) making them more suitable for evaluation at the detailed design stage rather than at the concept design stages (Shaviv, 1998; Al-Homoud, 2001; Olsen *et al.*, 2003; Clarke *et al.*, 2004). Investing in thermal analysis during the initial design stages of a building would make architects less competitive, because of this thermal analysis is usually carried out by engineers after the building is designed to estimate the heating and cooling loads (deWit & Augenbroe, 2002).

Building services engineers therefore frequently have to design their services and strategies around relatively finalised buildings, not having an input into the orientation, form or layout of the building, making the building services an ‘add-on’ to the building instead of an integrated part of the building (Lovins, 1992). The decisions made on the building fabric, form and orientation will determine the buildings performance throughout its lifetime (Sorell, 2003). Design tools for analysing the energy and carbon consequences of design decisions, that can be used by architects and engineers and require the minimum amount of input whilst providing moderately accurate results are therefore required at the concept design stage of a building (Ellis *et al.*, 2002; Sorrell, 2003).

Lack of information is also a common obstacle to improved efficiency in new construction and will create an incentive to stick with familiar designs (Golove *et al.*, 1996). There is therefore a need to demonstrate the performance of new strategies and technologies.

2.4 Offices

Since the 1980s office buildings have been designed to isolate the internal conditions from the outdoor climate through the extensive use of energy to support building services for heating, ventilation and air conditioning (HVAC) systems (Voss *et al.*, 2006). Through the

use of suspended ceilings, raised floors and lightweight walls the room air is decoupled from the buildings thermal mass, this together with the requirement to maintain constant indoor conditions throughout the year means that there are few days when neither heating or cooling is required (Voss *et al.*, 2006). Commercial office buildings, in the UK, are estimated to account for 11% of the total energy consumed within the public and commercial sectors (Pout *et al.*, 2002), this equates to 2.4 MtC per year.

The active thermal mass strategies considered in this research project all work on a 24 hour energy cycle, with 'coolth' being stored in the thermal mass throughout the night, cooling the supply ventilation air the following day. With offices not usually being occupied throughout the night they are suited to strategies that utilise night cooling (Kolokotroni *et al.*, 1999).

2.5 Objectives of the Research

This chapter 2 has examined the drivers for the research project and has highlighted that the reduction of energy use in buildings will play a major part in reducing climate change and global warming. The use of active thermal mass strategies has been identified as a method that can be used to reduce the use of energy in buildings.

Evidence has been presented showing current reasons for not incorporating active thermal mass strategies in buildings include the lack of knowledge about the performance of previous buildings and the time and resources required to carry out detailed modelling.

Design tools, for analysing the energy and carbon consequences of design decisions, which can be used by architects and engineers and require the minimum amount of input whilst providing moderately accurate results, are therefore required at the concept design stage of a building.

Office buildings have been highlighted as a building type well suited to active thermal mass strategies and the need for energy and carbon savings in offices has been shown.

This thesis aims to improve the understanding of architects, building services engineers and building physicists of the performance of active thermal mass strategies in operational buildings, and also to provide guidance for their use in suitable future buildings. This

This will be achieved by the following objectives:

- Develop a profile of the performance of active thermal mass strategies in operational
- Determine the accuracy of commercially available dynamic thermal models
- Create simple design guidance for the use at the concept design stages of a project

2.6 Structure of the Thesis

Chapter 1 sought to provide an overview of the work carried out, and present a background to the Brunel/Surrey Engineering Doctorate Programme.

Chapter 2 begins to introduce the context for the study, looking at the importance of energy in buildings, in the context of reducing the need for air conditioning through passive design, followed by the integration of active thermal mass strategies, the role of design tools at the concept stages of a project and the importance in terms of office buildings.

Chapter 3 is a literature review of active thermal mass strategies, exploring the heat transfer processes and benefits of the different strategies, current design tools available to design active thermal mass strategies, the role of simplified design tools and the simulation of active thermal mass strategies.

Chapter 4 uses a commercially available dynamic building thermal model to construct models for four active thermal mass strategies and compare the results with monitored temperatures in buildings incorporating the strategies.

Chapter 5 outlines the development of a simplified design tool, TMAir (Thermal Mass Activation – Air Medium), that can be used by designers at the concept stages of a project

to quickly analyse the effects, in terms of energy and comfort, of integrating active thermal mass strategies into UK office buildings based in South East England for a range of design parameters.

Chapter 6 presents the analysis of the results to identify the benefit that adding a Hollow Core Slab (HCS) Strategy has compared to the standard strategy.

Chapter 7 presents the analysis of the results to identify the benefit that adding a Floor Void With Mass (FVWM) Strategy has compared to the standard strategy.

Chapter 8 presents the analysis of the results to identify the benefit that adding a Earth to Air Heat Exchanger (ETAHE) Strategy has compared to the standard strategy.

Chapter 9 presents the analysis of the results to identify the benefit that adding a Thermal Labyrinth (TL) Strategy has compared to the standard strategy.

Chapter 10 uses the concept design tool, TMAir (Thermal Mass Activation – Air Medium), to compare the performance of the different active thermal mass strategies against one another

Chapter 11 brings out the general conclusions from the work and highlights potential future work

3.0 LITERATURE REVIEW

3.1 Introduction

This chapter 3 provides a background to the relevant literature that has shaped this thesis.

The first part of the review examines Active Thermal Mass Strategies looking at what thermal mass is and how heat is transferred to and from this mass. Active strategies are then introduced and the enhanced heat transferred presented before the previous monitoring and simulation is reviewed.

The second part of the review looks at currently available design tools that can be used when designing Active Thermal Mass Strategies, this then leads on to a review of the role of simplified design tools at the concept design stages of a building.

Finally, the simulation of Active Thermal Mass Strategies is reviewed and the commercially available dynamic thermal simulation program IES-Virtual Environment is introduced.

3.2 Active Thermal Mass Strategies

Li and Xu (2006) classify thermal mass in the building according to its location as external and internal thermal mass. The external thermal mass such as walls and roofs are directly exposed to ambient temperature variation while the internal thermal mass such as furniture and purpose-built internal concrete partitions are exposed to indoor air temperature.

This research focuses on the use of internal thermal mass as a method to improve the environmental comfort in a building whilst reducing the need and dependence on mechanical heating and cooling systems.

Kolarik and Yang (2009) classify thermal mass activation components into two main categories, accordingly to the “activation principles”: Surface Thermal Mass Activation (SA) and Core Thermal Mass Activation (CA).

- Surface Thermal Mass Activation (SA) - involves only the surface of the element.
- Core Thermal Mass Activation (CA) - heating and cooling systems that are integrated with a building construction (floor, ceiling, walls, etc) with high thermal capacity. The thermal mass is “equipped” with ducts for circulation of air or embedded pipes for the circulation of a heat carrier (usually water) (Kolarik and Yang, 2009).

This thesis focuses on core thermal mass activation systems that are integrated (or thermally coupled) with a building construction having high thermal capacity (floor/ceiling slab, walls etc.). The International standard EN 15377 (2008) uses the term “Thermo Active Building System” (TABS). The systems are also called “Thermally Activated Building System” in some literature. Moreover, the new REHVA Guidebook by Babiak et al. (2007) uses the term “Thermally Active Building System”. This thesis focuses on air-based systems.

3.2.1 Defining Thermal Mass

Thermal mass describes the ability of a material to store and release heat when subject to variations in temperature. All materials have some thermal mass, however for a material to provide a useful level of thermal mass, a combination of three basic properties is required (The Concrete Centre, 2009, Seaman et al, 2000):

- High specific heat capacity
- High density
- Moderate thermal conductivity

The specific heat capacity and the density determine how much heat the material can store per m³ (volumetric heat capacity). The thermal conductivity then describes the ability of the material to absorb and emit heat. If the thermal conductivity is too high then the material will heat up and cool down very quickly and remain at around the room temperature, alternatively if the thermal conductivity is too low the material will not absorb heat well.

False ceilings and surface finishes can insulate the thermal mass from the occupied space, although thin layers of relatively conductive material (such as plaster) should not have a significant effect (Barnard *et al.*, 2001; CIBSE, 2005a).

A practical method of comparing the thermal mass of a building construction is to measure the rate at which its surface can absorb heat from the air (Rennie and Parand, 1998). Thermal admittance describes the ability of a material or construction to exchange heat with the environment when subject to a simple cyclic variation in temperature, which for buildings is 24 hours (CIBSE, 2007). Thermal admittance takes account of both the surface resistance and thermal properties of the element and provides a measure of the dynamic thermal storage performance of an element. This allows direct comparison of different constructions. High values indicate high thermal mass and can provide a useful means of assessing the likely performance of different constructions. The thermal mass of a whole room can also be determined by totalling the thermal admittance of each room's surfaces and dividing this by its floor area.

3.2.2 Heat Transfer

Heat is transferred to and from a material by convection, radiation and conduction. Thermal mass exchanges heat with the room air via convection and heat with the occupants and the other materials within the room via radiation. Heat is transferred through the material or to other materials or occupants in contact with the surface via conduction.

The heat transfer by convection is determined as function of the convective heat transfer coefficient and the heat transfer by radiation as a function of the radiative heat transfer coefficient. The heat transfer through a material is determined by the U-value of the material.

The direction of heat flow determines the heat transfer coefficient. Thermal mass will absorb heat when the material is at a temperature lower than the air in contact with it and release it when it is at a higher temperature. If the heat is flowing in the same direction ...

Heat transfer by convection is characterised by a heat transfer coefficient, h_c . This depends upon the temperature difference between the surface and the air, the surface roughness, the air velocity and the direction of heat flow (CIBSE, 2007).

The traditional CIBSE (CIBSE, 2007) values for buoyancy driven flow are presented in Table 3—1:

Table 3—1 Traditional CIBSE surface convective heat transfer coefficients

Surface	Direction of heat flow	Surface coefficient, h_c ($\text{W}\cdot\text{m}^2\cdot\text{K}^{-1}$)
Floor	Upwards	4.3
	Downwards	1.5
Wall	Horizontal	3.0
Ceiling	Upwards	4.3
	Downwards	1.5

The radiative heat transfer coefficient depends upon the absolute temperatures of both the radiating surface and the surface or environment receiving the radiation. High surface emissivity is required to achieve good radiant heat transfer, however most building materials have values of around 0.9 so this is not a problem. The following is an adequate approximation for most building services applications:

$$h_r = 4 \cdot \sigma \cdot T_s^3 \cdot (3.5)$$

Equation 3-1

where h_r is the radiative heat transfer coefficient ($\text{W}\cdot\text{m}^{-2}\cdot\text{K}^{-1}$), σ is the Stefan-Boltzmann constant ($5.67 \times 10^{-8} \text{W}\cdot\text{m}^{-2}\cdot\text{K}^{-4}$) and T_s is the surface temperature (K).

Table 3—2 Surface radiative heat transfer coefficients

Mean temperature of surfaces ($^{\circ}\text{C}$)	Radiative heat transfer coefficient, h_r ($\text{W}\cdot\text{m}^2\cdot\text{K}^{-1}$)
-10	4.1
0	4.6
10	5.1
20	5.7

For most floor construction types the ability of the floor slab to conduct and store the thermal energy is superior to the rate of surface heat transfer (Barnard *et al.*, 2001, CIBSE,

2005a) it is therefore the surface heat transfer characteristics that determines or limits the performance of the slab.

One method to increase the convective heat transfer coefficient is through the formation of coffers, troughs or profiling the surface. This can be used to double the surface area and therefore the convective heat transfer coefficient (Barnard *et al.*, 2001), although this results in little benefit to the radiant heat transfer coefficient because a coffered surface will have an overall geometric exposure similar to a flat surface when viewed from the occupant.

3.2.3 Thermal Mass Activation

Convective heat transfer coefficients can also be further increased by using mechanical means to create forced convective heat transfer rather than relying on natural buoyancy forces (CIBSE, 2005a; Braham *et al.*, 2001b).

Active methods enhance the performance of thermal mass by passing air or fluid across the surfaces with high thermal mass (Barnard, 1994; Russell & Surendran, 2001).

Air is forced (using a mechanical fan) into a void with exposed thermal mass. This mass is in contact with the void exchanging heat to and from the air dominantly via convection (Barnard, 1994) due to the air being turbulent.

3.2.3.1 Strategies

A number of active thermal mass methods have been developed and used in buildings; four Active Thermal Mass Strategies that use air as the transfer medium are listed below:

Active Hollow Core Slabs: Hollow core pre-cast concrete slabs are used as a path for supply air thus increasing the coupling between the thermal mass and the supply air (Ren and Wright, 1997) and attenuating variations in ambient air temperatures (Barton *et al.*, 2002).

The Termodeck® system is an example of a hollow core slab strategy. Prefabricated hollow core concrete slabs are used to create an air path. The standard slabs are 1.2m wide with a span up to 18m. The thickness of the slabs vary with the span.

Each slab has five hollow cores. Typically, the three central cores are used for air distribution. The ends of the cores are capped and cores are connected by bends to form a serpentine air path. Ventilation air is supplied to each slab through holes in the bottom of the slab via a main supply duct that is usually run in a central corridor above a suspended ceiling. Air is then extracted from the room close to ceiling level and collected via a main extract duct, again running within the central corridor ceiling void. As the air passes through the cores it exchanges heat with the concrete. The underside of the slab is exposed to the occupied space below, also adding thermal mass to the room.

Floor Void with Thermal Mass: A void created between a raised floor and a structural concrete slab as a supply air plenum, again increasing the coupling with the thermal mass and supply air (Nagano et al, 2006; Lin et al., 2005).

Supply air is ducted into the false floor void where it comes into thermal contact with the exposed surface of the concrete slab (Barnard, 1994). Heat exchange takes place between the air and the slab before the air is supplied to the occupied space via floor diffusers. The air is then extracted at high level.

Earth to Air Heat Exchanger : In many cases thermal mass has been installed in the form of an earth-to-air heat exchanger (ETAHE) to further exploit contact with the ground. An earth-to-air heat exchanger draws ventilation air through ducts buried underground (Zimmerman and Remund, 2001; Grosso and Raimondo, 2008). ETAHEs are suitable for moderate climates that have a large temperature difference between night and day as well as between summer and winter (Breesch et al, 2005; Gan, 2001; Cook and Rees, 2006) and can only be used to satisfy a low or moderate cooling demand or can be used in combination with air conditioning to satisfy higher cooling demand

The temperature fluctuation of the ground below a depth of 3 m is small compared with temperature fluctuations in the ambient air; with temperature being practically constant throughout the year at a depth of about 10 m. This temperature is usually higher than the

average ambient air temperature during the winter and lower than the average ambient air temperature during the summer, providing space conditioning throughout the year, with the air being heated in the winter and cooled in the summer period (Ghosal et al, 2005). It was found that the performance of coupling a building with the earth is dependent upon (Santamouris et al, 1996; Mihalakakou et al, 1996a; Mihalakakou et al, 1996b; Santamouris, 2006:

- The depth below the earth;
- Length and cross sectional area of the air path;
- Soil properties;
- Velocity of the air

Thermal Labyrinth: A thermal labyrinth decouples the thermal mass from the occupied space by creating a concrete undercroft, increasing the surface area of thermal mass, beneath the building. The benefits of decoupling the mass are that it can be cooled lower than if it was in the occupied space and the stored ‘coolth’ can be used to condition the occupied space for up to 3 or 4 days in hot periods (Evans, 1998).

3.2.3.2 Heat Transfer

All of the active thermal mass systems described use air as the medium to activate the thermal mass.

Flow in tubes is considered to be turbulent when the Reynolds Number (Re) > 3000 (CIBSE 2007):

$$\text{Re} = \frac{\rho \cdot v \cdot d_e}{\mu} \quad \text{Equation 3-2}$$

Where:

ρ air density (kg.m⁻³)

v air velocity (m.s⁻¹)

d_e effective tube diameter (m)

μ air dynamic viscosity (Pa.s)

$$d_e = \frac{4A_c}{P}$$

Equation 3-3

Where:

A_c Cross sectional area (m²)

P Perimeter (m)

For turbulent flow in circular and non-circular ducts the following correlation can then be used (CIBSE 2007):

$$Nu = 0.023 Re^{0.8} Pr^{0.33}$$

Equation 3-4

Where:

Re Reynolds Number

Pr Prandtl Number

$$Pr = \frac{c_p \cdot \mu}{k}$$

Equation 3-5

Where:

c_p specific heat capacity (J.kg⁻¹.K⁻¹)

μ dynamic viscosity

k thermal conductivity (W.m⁻¹.K⁻¹)

The heat transfer coefficient has then been calculated using Equation 3-6:

$$Nu = \frac{h_c \cdot d_e}{k} \quad \text{Equation 3-6}$$

However, as Barnard (1994) discussed this relationship is based on the surface roughness of the air path being smooth. The Reynolds-Colburn analogy (Holman, 1990) relates heat transfer and fluid friction and leads to an expression in terms of the Stanton Number (St):

$$St \cdot Pr^{2/3} = f/2 \quad \text{Equation 3-7}$$

Where:

$$St = \frac{h_c}{\rho \cdot u \cdot c_p} \quad \text{Equation 3-8}$$

Therefore:

$$h_c = \frac{\rho \cdot u \cdot c_p \cdot f}{2Pr^{2/3}} \quad \text{Equation 3-9}$$

Where:

f friction coefficient

$$f = \frac{k_s}{d_e} \quad \text{Equation 3-10}$$

Where:

k_s Surface roughness (m)

d_e effective tube diameter (m)

For the ground temperature the temperature of the ground at 10m below the surface has been used, this is because at this depth the undisturbed ground temperature is almost equal to the average annual ambient air temperature (Carslaw and Jaeger 1959).

The undisturbed ground temperature becomes:

$$T(z,t) = T_m - A_s \exp\left[-z(\pi/365\alpha)^{1/2}\right] \cos\left\{2\pi/365\left[t - t_0 - z/2(365/\pi\alpha)^{1/2}\right]\right\} \quad \text{Equation 3-11}$$

Where:

$T(z,t)$ undisturbed ground temperature ($^{\circ}\text{C}$)

T_m mean annual temperature at the grounds surface ($^{\circ}\text{C}$)

A_s amplitude of the temperature fluctuation at the grounds surface ($^{\circ}\text{C}$)

z depth in the ground (m)

α soil thermal diffusivity ($\text{m}^2 \cdot \text{day}^{-1}$)

t time

t_0 phase lag

3.2.3.3 Previous Monitoring & Simulation

There has been a large amount of research into the benefits of thermal mass and night cooling for offices. Night cooling in combination with a thermally heavyweight building is increasingly being used as a means of avoiding or minimising the need for mechanical cooling in buildings whilst maintaining thermal comfort (Barnard *et al.*, 2001). Through the summer months cool outdoor air is circulated through the building, cooling the building fabric. The cooled fabric then absorbs heat from the space the following day, offsetting some of the heat gains and reducing the temperature of the space or the amount of mechanical cooling required. Artmann *et al.* (2007) found that there is a very significant potential for passive cooling of buildings by night time ventilation in the British Isles.

Monitored data has shown that night cooling can be used to reduce and delay the peak indoor air temperature and reduce the average indoor temperature the following day (Blondeau *et al.*, 1997; Pfafferott *et al.*, 2004; Geros *et al.*, 1999). Specific thermal conditions cannot be maintained and some deviation from nominal design conditions must

be accepted by the occupants (Blondeau *et al.*, 1997). Night cooling can still be used to reduce the daytime cooling requirements of the building and thus the periods in which active cooling is needed..

Further, simulation has demonstrated that the main parameters affecting the performance of night time ventilation are: the diurnal temperature range, the interior planning of the building, method of ventilation, amount and surface area of thermal mass, air flow rate, internal heat gains, minimum temperature required for comfort, orientation, glazing, solar protection and amount of air infiltration (Shaviv *et al.*, 2001; Pfafferott *et al.*, 2004; Birtles *et al.*, 1996; Geros *et al.*, 1999; Kolokotroni *et al.*, 1998; Kolokotroni *et al.*, 1999; La Roche & Milne, 2004; Fletcher & Martin, 1996) carried out a detailed study into night cooling control strategies to optimise the amount of cooling provided, whilst avoiding overcooling and the need for subsequent reheating. Eicker *et al.* (2006) evaluated the influence of air change rate and heat transfer coefficient on the room temperature drop. It was concluded that complete discharging of internal surfaces during longer hot periods in summer can only be achieved with very high air change rates and high heat transfer coefficients.

Thermal mass also has an influence on the amount of energy required to heat a building. Barnard *et al.* (2001) found increasing the thermal mass of a typical open plan, naturally ventilated, office space resulted in an 16% increase in the annual heating demand. This increase was attributed to the thermal mass acting as a store for unwanted infiltration and conduction heat losses at night. There are only a few studies that both assess the potential heating and cooling load benefits of exposed thermal mass in office buildings (Høseggen *et al.*, 2009).

The performance of earth-to-air heat exchangers has also been the topic of a large amount of research. Monitoring of earth-to-air heat exchangers coupled with low energy office buildings in mild climatic regions has demonstrated that they can be used for preheating the supply air in the winter and cooling in the summer (Breesch *et al.*, 2005; Eicker *et al.*, 2006; Wagner *et al.*, 2000). The performance of an earth-to-air heat exchanger is dependent on the system design parameters: duct length, duct radius, air velocity inside the duct, span between ducts, length of duct beneath foundations, length of duct beneath undeveloped ground, and the duct depth below the earth (Mihalakakou *et al.*, 1995,

Mihalakakou *et al.*; 1996a, Stevens, 2004; Kurpaska and Slipek, 2000; Santamouris *et al.*, 1996; Wagner *et al.*, 2000; and De Paepe and Janssens, 2003). And also the local conditions; ambient air temperature and ground cover (Mihalakakou *et al.*, 1996b).

The thermal performance of a hollow core slab has been studied by Barton *et al.* (2002). A two-dimensional finite difference model was used to simulate variations in temperature at incremental slab lengths and time periods. A cyclic 24 hour sinusoidal air temperature for the inlet air temperature and the adjacent room temperature were used. The output from the model is the supply air temperature and the results have proved consistent with previous research. It was also found that the bend sections have a minimal effect on the overall heat transfer and that the adjacent room air temperatures have a strong influence on the core air temperature. Ren *et al.* (1998) reviewed the previous literature on modelling the performance of hollow core slabs and summarised that the existing models were either limited in their modelling of the heat transfer along the slab air path or were unable to represent the effect of time variant disturbances on the room and the ventilated slab. This led to the development of lumped parameter thermal network model of a hollow core concrete slab thermal storage system and associated room. Using comparison with measured data an increase in convective heat transfer coefficient around the corners of the air cores was 50 times higher than for a plain duct.

Buildings that incorporate active hollow core strategies have been monitored as a whole and have demonstrated an energy consumption of less than half that for a good practice air conditioned office building (Standeven *et al.*, 1998) whilst also been perceived to be comfortable buildings (Bordass *et al.*, 1999), although the whole benefit cannot only be attributed to the hollow core slab strategy.

Evans (1998) presented information on the performance of a thermal labyrinth coupled with 1800m² of exhibition gallery and retail area for a proposed building using computer modelling. To reduce the amount of concrete required, a honeycomb slab was created by a labyrinth of walls between two flat concrete plates. A 1.1m deep labyrinth was calculated to be adequate, but 1.6m was required for health and safety for maintenance access. The air flow is regulated by an air handling unit and dampers that allows the labyrinth to be bypassed when free cooling from ambient air is available. To allow the labyrinth to be cooled lower than the room heating set-point during the night, to around 16°C (below 15°C

there is a risk of condensation), night cooling can be applied to only the labyrinth. It was found that the viability of using a labyrinth system required the use of displacement ventilation (Butler, 2002). Carbon dioxide emissions of around half that of a good ‘standard CIBSE building’ were calculated for the building.

3.3 Designing Active Thermal Mass Strategies

Garde-Bentaleb *et al.* (2002) distinguished three types of design tool available to the architect and the thermal engineer:

- the expert rules and design guides
- the simplified or adapted computer programs
- specialised computer programs

At the early stages of a building’s design a knowledge and appreciation of the interrelations between the buildings form, climate, HVAC systems and the buildings performance is required (Shaviv, 1999). Experience from previous projects and design guidelines can be used, but because the interrelations between the different design parameters and the energy characteristics of buildings are complex it is difficult to define general and simple design rules (Shaviv, 1999) and therefore they are not often used (Garde-Bentaleb *et al.*, 2002).

Table 3—3 presents a summary of the guidance available for active thermal mass strategies.

Table 3—3 Design guidance on active thermal mass strategies

Reference	Active thermal mass strategy					Description
	NC	HCS	FVWM	ETAHE	TL	
Barnard and Jaunzens (2001)	☆		☆	☆		Early design guidance on applications, benefits, typical cost indicators, performance, spatial considerations and combinations with other technologies.
BRE (1995)	☆	☆				General guidance with case study buildings.
ODPM (2005)				☆		General guidance with calculation for carbon emissions saving.
Braham <i>et al.</i> (2001a)	☆					General guidance.
Braham <i>et al.</i> (2001b)		☆				General guidance.
Parsloe (2005)	☆	☆		☆		General guidance.
Fletcher and Martin (1996)	☆					General guidance with case study buildings.
Kolokotroni (1998)	☆					Early design guidance on weather suitability, building type suitability, predicted cooling potential and performance, control strategies and suitability to new and refurbished buildings.
Barnard <i>et al.</i> (2001)	☆					Guidance on modelling.
The Concrete Centre (2005)	☆	☆	☆			Early design guidance on typical applications, cooling capacity, key benefits and referenced case study buildings.
Santamouris (2006)				☆		Early design guidance with examples and performance data.
BRESCU (2002)	☆	☆		☆		Early design guidance on favourable design factors, application limitations, design aims and design requirements/concerns.
Barnard (1994)	☆	☆	☆			Early design guidance with monitored and modelled examples.
Seaman <i>et al.</i> (2000)	☆	☆	☆	☆		General guidance with case study examples.

NC = Night Cooling

ETAHE = Earth-to-air Heat Exchanger

HCS = Hollow Core Slab

FVWM = Floor Void with Mass

TL = Thermal Labyrinth

Simplified or adapted computer programs are mathematically and numerically simplified to increase the speed, although they give more than adequate precision for the concept stages of a project (Ellis & Matthews, 2002). They can generally be divided into two categories (Kolokotroni *et al.*, 2004) parametric analysis based and built in simplified or fast-to-run algorithms. The concept design tools available for active thermal mass strategies in offices are summarised in Table 3—4.

Table 3—4 Concept design tools available for active thermal mass strategies in offices

Reference	Active thermal mass strategy					Description
	NC	HCS	FVWM	ETAHE	TL	
Zimmermann and Remund (2001)				☆		Series of charts and correction factors to determine the effects of depth, size, climate, air flow rate and duct material on the outlet air temperature. Based on parametric studies.
Gratia and De Herde (2002)	☆					Parametric studies, using TRNSYS, were used to establish formulas to calculate estimated overheating hours, necessary ventilation and energy consumption for a standard office building.
Kolokotroni <i>et al.</i> (1997)	☆					Single zone ventilation model using a lumped parameter simulation method to analyse the effect of changing key parameters on the dry resultant temperature, energy savings and cooling capacity saving for a standard office space
Rennie and Parand (1998)	☆					Design tables, calculated using the admittance procedure, as a simple method for architects and engineers to check their sketch designs for overheating.

Dynamic thermal models can be used in the design of active thermal mass strategies, but they require detailed building information requiring the architect to have finalised the design, at which time it is too late for the thermal analysis to be optimising the buildings thermal characteristics (Ellis & Mathews, 2002).

It is often difficult to fully quantify the benefits due to thermal mass strategies as there are other influences on the building operation including solar shading, window opening and the benefit of mechanical ventilation (Seaman *et al.*, 2000) and as a result architects and engineers continue to be hesitant to apply low-energy techniques (Breech *et al.*, 2005).

3.4 The Role of Simplified Design Tools

The design decisions made by architects in the preliminary design stages of a building often determine the building's final thermal characteristics (Ellis & Mathews, 2002). Simplified tools for use at the concept stage of a building need to suit architectural use by:

- Simplifying input complexity by identifying and focusing on critical parameters.
- Defining input parameters in architectural terms.
- Verifying that the tool provides results of suitable accuracy.
- Developing a simple means of comparing and rating design efficiency.
- Evaluation of design tool by practising designers.

3.4.1 Simplifying Input Complexity

Designers can be overwhelmed by the amount of information or knowledge required by design tools, especially during the early design stages when certain aspects are yet unknown (Ellis *et al.*, 2001). It is therefore important to limit the number of parameters that need to be changed by the user, and where this is not possible specify default values.

The main parameters that determine the efficiency of night ventilation can be classified into three broad groups (Blondeau *et al.*, 1997):

- Climatic parameters
- Building parameters
- Technical parameters

Givoni (1992) showed that diurnal temperature range could be considered as a good climatic potential index. Blondeau *et al* (1997) also found that the average outdoor temperature seemed to better represent the climatic potential.

The technical parameters relate to the way night ventilation is achieved and the general operation of the building.

The building parameters relate to the building type, envelope openings such as windows and doors, building material and building structure (Zhou *et al.*, 2008).

Active thermal mass strategies share a number of key parameters, whereas other parameters are dependent on the selected strategy. Translating this for active thermal mass strategies the parameters can be split into climatic, building, technical and active thermal mass strategy (Figure 3—1).

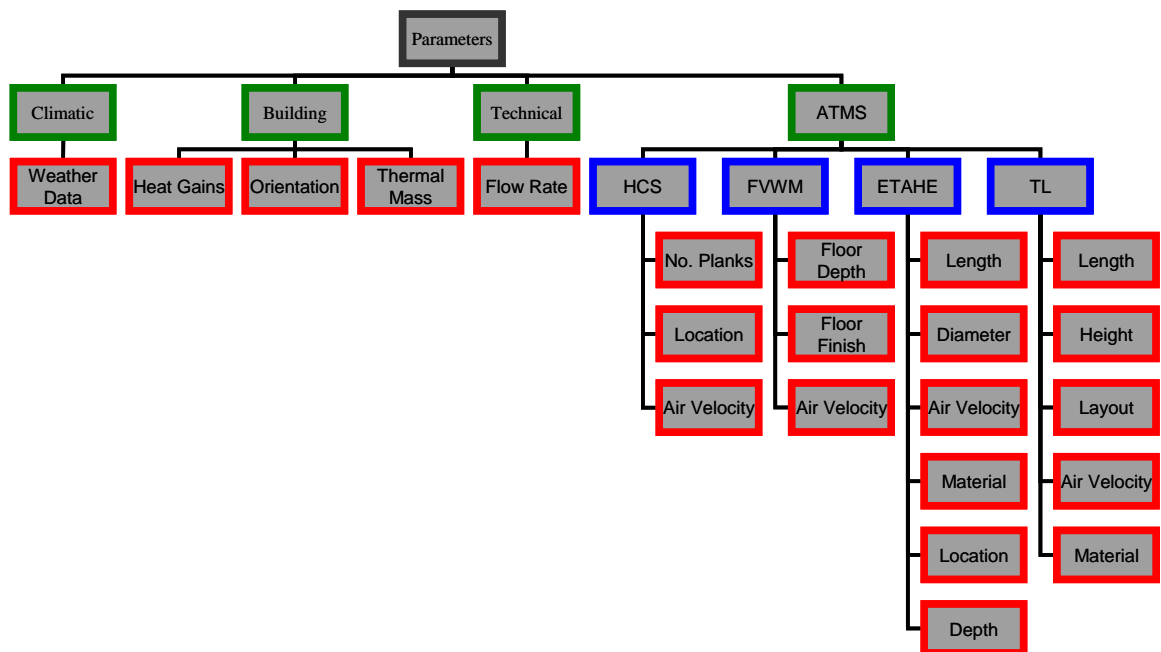


Figure 3—1 Building parameter groups for a building integrating an active thermal mass strategy

When considering the performance of an office building the performance can be based on a whole office building (Gratia & De Herde, 2002) or on a typical office space (Rennie and Parand, 1998, Kolokotroni *et al.*, 1997 and Kolokotroni *et al.*, 2004).

Rennie and Parand (1998) presented their tool based on a typical room in a building, providing results for different room depths and heights with a series of correction factors to determine the maximum internal air temperature.

Basing a tool on a typical cellular office allows a number of the building parameters to be fixed to be 'standard' or 'typical' values, although this must be made clear to the users of the tool (Ellis & Mathews, 2001).

Kolokotroni *et al.* (1997) and Kolokotroni *et al.* (2004) based their tools on a typical cellular office with dimensions 10m width, 6m depth and 3m floor-to-ceiling height, positioned in the middle of a row of offices on the middle floor of a 3-storey office. This cellular office has been derived as suitable for night cooling by Tindale *et al.* (1995) and has been used in various energy simulation research in the UK (e.g. CIBSE, 2002a).

The impact of changing one design parameter on the building's performance can vary from beneficial to unbeneficial depending on the values of the other parameters (Shaviv, 1999).

Zimmermann and Remund (2001) presented their design tool as a series of graphs and correction factors to allow the exit air temperature from an earth-to-air heat exchanger, allowing the effect of changing more than one parameter using parametric analyses to be determined without having to perform simulations for all parameter permutations.

Design tools can also be used to calculate only the performance of one system alone, Zimmermann and Remund (2001) looked at the performance of an earth-to-air heat exchanger alone

3.4.2 Defining Input Parameters in Architectural Terms

The design and construction of a building is a very fragmented process with a large number of participants interacting in complex ways over a prolonged period (Kalay *et al.*, 1998). Green buildings require an integrated design team, combining a wide range of different specialisms (Sorrell, 2003). The input parameters need to be understood by all the users of the tool.

Rennie and Parand (1998) considered four building weights from very lightweight to very heavyweight and identified graphically the properties of the floor and ceiling, internal partition and external wall allowing easier understanding for the users of the tool (Figure 3—2).

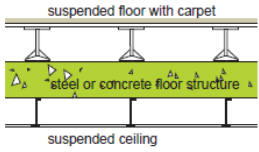

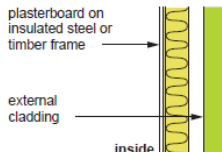
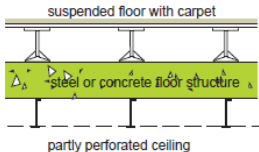
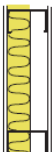
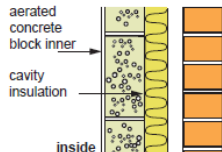
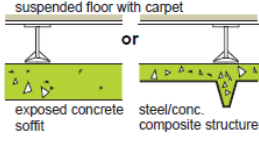

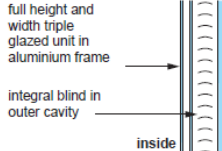
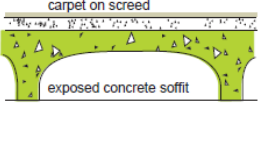

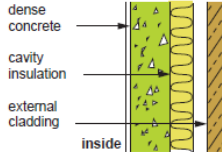
Fig	Thermal mass (Room admittance per m ² floor area ^{**})	Floor and ceiling (In order of increasing thermal mass)	Internal partition (In order of increasing thermal mass)	External wall <i>*(Not all in order of increasing thermal mass – see fig. 24)*</i>	Notes
22	Very light (6–8W/m ² K)				The false floor and ceiling prevent the cooling air from reaching the structure. Similarly, insulation prevents the cooling air from reaching the external wall. The internal partitions are lightweight, providing little thermal mass.
23	Light (8–10W/m ² K)				False floor and ceiling. The lightweight blockwork of the traditional external cavity walls provide a little thermal mass. The open-cell false ceiling allows some access to the thermal mass of the structure.
24	Heavy (14–18W/m ² K)				* False floor for services. The exposed concrete ceiling and the blockwork partitions compensate for the low thermal mass of the all-glazed external wall. Mid-pane blinds give good solar control, and allow less heat in than internal blinds.
25	Very heavy (18–24W/m ² K) ^{**} (The typical room assumed for calculating this admittance is 6m square and 2.7m high.)				No false floor or ceiling for services. The exposed concrete ceiling, floor, partitions, and external wall have high thermal mass – the largest contribution coming from the coffered ceiling.

Figure 3—2 Graphical representation of building weights

3.4.3 Verification

There is growing gap between the design tools offered by scientists and researchers and what is really used in practice, with the more technically orientated scientists and researchers requiring powerful and accurate models that adequately represent real-world complexity, compared with designers who are more interested in simple, straightforward and intuitive tools (Hong *et al.*, 1997). Computational building evaluation tools provide an effective means to support informed design decisions, however this comes with a cost not only in software acquisition but also the time needed for learning and using the software (Mahdavi and El-Bellahy, 2005). Of key importance to designers is the amount of time required to prepare and run calculations and to interpret the results. An accuracy of 80%

for calculations is still within design limits considering the influence that workmanship during construction and the actual use of the building have on the final performance of the building (Ellis & Mathews, 2002; Gratia & De Herde, 2002). Errors of up to 20% will also be acceptable if the tool answers ‘what if’ questions in minutes rather than hours (Richards, 1992), allowing the design team to take into account the impact of different options (Gratia & De Herde, 2002).

During the detailed design stage of a building, appropriate detailed simulation tools can be used to verify the results and optimise the design of the active thermal mass strategies.

3.4.4 Comparing & Rating Design Efficiency

Performance simulation tools are usually partial since they have a very specific and technical scope and require more than one tool to supply the design information required, with crossovers in information, leaving the user to evaluate which results are taken forward (Mahdavi and El-Bellahy, 2005).

At the early design stages of a building simple design tools are very useful to facilitate discussions about the feasibility of different design options between clients, designers and engineers. This is very important for active thermal mass strategies because they need to be included at this stage, because once the building fabric and form have been chosen it is very difficult to integrate them. The results therefore need to be aimed at all the stakeholders of the building design, allowing quick evaluation of their designs without the need for detailed processing of the analysis results (Ellis *et al.*, 2001).

Energy analysis of buildings is carried out to achieve one or all of the following (Al-Homoud, 2001):

- Evaluation of alternative designs, systems, subsystems, components.
- Allocation of annual energy budgets.
- Compliance with energy standards.
- Economic optimization.

The Zimmermann and Remund (2001) tool for the performance of an earth-to-air heat exchanger presented the output as tables, graphs and correction factors that can be used to calculate the exit air temperature and the amount of cooling that this provides. This requires the information to be used by the energy engineer or building services engineer to determine how the strategy will be performed when coupled with a building. Rennie and Parand (1998) again presented the output as a series of tables and correction factors to determine the maximum internal air temperature for a typical room in a building. This allows all users of the tool to understand the results easily and an evaluation of alternative designs to be made, but this cannot be used to understand the benefits in terms of savings of energy and carbon emissions. Other tools have presented the results of the dry resultant air temperature within an individual office space and the energy required for heating and cooling (Gratia & De Herde, 2002; Kolokotroni *et al.*, 1997; Kolokotroni *et al.*, 2004).

Tools that can be used to impress clients are more likely to be used by designers (Stevens, 1991). Currently the main method to do this is to show the economic benefits (Sorrell, 2003). Other methods that are developing interest are the demonstration of the environmental impact and the influence of Building Policy and Regulation.

3.4.5 Evaluation of Design Tool

To ensure greater confidence in the use of design tools the socio-economic aspects must be taken into consideration and practical verification carried out (Ellis *et al.*, 2001).

For new tools to be truly effective they need to be developed in close co-operation with the designers they are intended for (Holm, 1993). Designers must also be educated about the benefits and limitations of design tools (Batty and Swann, 1997).

3.5 Simulation of Active Thermal Mass Strategies

Due to the complex and dynamic nature of the heat exchange between the thermal mass, external air, internal air and heat gains to the space dynamic thermal modelling is required to analyse the performance (CIBSE, 2005a).

A dynamic thermal model is a model in which a number of parameters vary with time and calculations represent behaviour over a chosen time period, e.g. of one hour or less. This allows temporal variations in thermal storage, weather, occupancy etc., to be represented (CIBSE, 2006a).

CIBSE recognises two levels of dynamic modelling (CIBSE, 2006a):

- Cyclic- the analysis is carried out using a sequence of identical days for which the external conditions vary on a 24-hour cyclical basis, of which the CIBSE admittance method and ASHRAE transfer function method are good examples.
- Transient - the state of the building and its components changes with time during the period of interest and do not go through a repeated cycle. Transient models can provide a realistic simulation of the performance of a building.

Weather data for analysing the performance of systems using thermal mass to store night cooling should incorporate day to day variations in temperature. Analysing the performance for a single repeated design day can result in significant under estimate of performance as the residual cooling stored from a preceeding cool period will not be taken into account (Barnard *et al.*, 2001). Cyclic models are therefore better suited to applications, such as cooling load calculations, that require an assessment of the conditions after a long period of identical days. To analyse the performance of thermal mass accurately therefore requires detailed dynamic thermal modelling using real weather data.

Detailed modelling of thermal storage elements can be very complex and time consuming. Simplification of coffered, waffled or hollow core type ceilings can be made by representing them with horizontal and vertical surfaces with equivalent surface area and volume (Barnard *et al.*, 2001).

For systems where the air is passed through cores or under sheeting, it is important that the variation of the air temperature as it passes through this theoretical 'heat exchanger' is reflected in the model, as assuming a single air temperature along the air path can significantly underestimate performance (Barnard *et al.*, 2001).

3.6 IES Virtual Environment

The Apache dynamic thermal simulation program of IES-Virtual Environment is used extensively by building consultancies. Apache originated as a three-dimensional finite element program for steady-state or transient heat conduction analysis. It is now a fully integrated environmental simulation program which includes many features and has been included in a recent study of twenty major building energy simulation programs (Crawley et al, 2008). The following is an extract from Crawley et al, 2008 which has been provided by IES Virtual Environment.

“The IES /VES is an integrated suite of applications linked by a common user interface and a single integrated data model. Virtual Environment modules include:

- ModelIT—geometry creation and editing
- ApacheCalc—loads analysis
- ApacheSim—thermal
- MacroFlo—natural ventilation
- Apache HVAC—component-based HVAC
- SunCast—shading visualisation and analysis
- MicroFlo—3D computational fluid dynamics
- FlucsPro/Radiance—lighting design
- DEFT—model optimisation
- LifeCycle—life-cycle energy and cost analysis
- Simulex—building evacuation

The program provides an environment for the detailed evaluation of building and system designs, allowing them to be optimized with regard to comfort criteria and energy use”.

IES Virtual Environment is extensively used in both research activities and within industry and has been validated to be in accordance with ANSI/ASHRAE 140 Standard and CIBSE AM 11 (CIBSE, 1998).

The thermal simulation software within IES is ApacheSim. Apachesim performs calculations based on the concept of bulk air temperature and humidity, which are assumed to be uniform within each cell. The thermal conditions are calculated by balancing the sensible and latent heat flows entering and leaving each air mass and each surface.

The main interest of the research project is the heat transfer by air movement and the interior convection heat gain together with the conduction and storage of heat. The origin, derivation and application of the equations used to simulate these in IES Virtual Environment will now be reviewed.

NOTATION

C	= surface orientation coefficient	c_p	= specific heat capacity of air (kJ/KgK)
Q	= heat transfer (kW)	f	= mean air speed coefficient
R	= thermal resistance of the air gap (m ² K/W)	g	= moisture content of room air (kg/kg)
T	= temperature (°C)	g_i	= moisture content of supply air (kg/kg)
T_a	= air temperature (°C)	h_c	= convective heat transfer coefficient (W/m ² K)
T_i	= supply air temperature (°C)	m	= air mass flow rate (kg/s)
T_r	= mean room air temperature (°C)	n	= flow exponent
T_s	= mean surface temperature (°C)	w	= moisture added (kg/s)
V	= air volume (m ³)	ρ	= density (kg/m ³)
W	= heat flux (W/m ²)	ρ_a	= density of air (kg/m ³)
c	= specific heat capacity (J/kgK)	λ	= conductivity (W/m ² K)

3.6.1 Heat Transfer By Air Movement

The heat transfer associated with a body of air entering a cell is defined by:

$$Q = mc_p (T_i - T_r) \quad \text{Equation 3-12}$$

The moisture gain associated with the supply air is calculated using:

$$w = m(g_i - g) \quad \text{Equation 3-13}$$

3.6.2 Convection Heat Transfer

The rate of convective heat transfer at a surface can be described by:

$$W = h_c (T_r - T_s) \quad \text{Equation 3-14}$$

The rate of convection heat transfer between air masses inside the building and the adjacent building elements is calculated using CIBSE variable convection coefficients (CIBSE, 1986).

The heat transfer coefficient is calculated as a function of surface orientation, air-surface temperature difference and mean room air velocity:

$$h_c = fC\Delta T^{n-1} \quad \text{Equation 3-15}$$

Values for C , n and f are obtained from CIBSE Guide C (1986) Tables C3.12 and C3.13.

3.6.3 Heat Conduction And Storage

3.6.3.1 Fundamentals

The following partial differential equations (PDEs) govern the time-evolution of the spatial temperature distribution in a solid without internal heat sources:

$$W = -\lambda \nabla T \quad \text{Equation 3-16}$$

$$\nabla \cdot W = -\rho c \frac{\partial T}{\partial t} \quad \text{Equation 3-17}$$

Equation 3-16 is the expression of the principle of conduction heat transfer and equation 6 is the expression of the principle of heat storage.

The heat transfer through a homogenous material is derived by accounting for (Underwood & Yik, 2004):

- (i) The rate of heat transfer across each boundary surface of an elemental control volume within the material that would arise corresponding to the temperature gradient that exists at the surface;
- (ii) The rate of heat generation or removal by internal heat sources or sinks present within the control volume; and
- (iii) The change in internal energy of the material in the control volume, which is reflected by the change in temperature of the material.

Therefore:

$$\rho c \frac{\partial T}{\partial t} - \nabla \lambda \nabla T - \dot{W} = 0 \quad \text{Equation 3-18}$$

Equation 3-18 can be simplified for the analysis of the heat transfer through walls and slabs in buildings by making the following assumptions (Underwood & Yik, 2004):

- (i) Only the heat transfer in the direction across the thickness of each wall or slab (assumed to be in the x -direction) needs to be modelled whereas heat transfer in the other two directions (the y - and z -directions) can be ignored;
- (ii) Heat transfer in the material is isotropic;
- (iii) Properties of the material (ρ , c and k) are independent of temperature; and
- (iv) No internal heat source or sink exists within the material ($\dot{W} = 0$).

$$\frac{\partial^2 T}{\partial x^2} = \frac{\rho c}{\lambda} \frac{\partial T}{\partial t} \quad \text{Equation 3-19}$$

The air masses contained within the building also have heat storage:

$$Q = c_p \rho_a V \frac{\partial T_a}{\partial t} \quad \text{Equation 3-20}$$

3.6.3.2 Discretisation

A finite difference approach is adopted to solve the heat diffusion equation. The element is replaced with a finite number of discrete slices and the temporal domain is divided into finite time steps (Figure 3—3). The temperature within each slice is then represented by the state at the mid point within the slice, referred to as a node. The variation in temperature between each pair of adjoining nodes is assumed to be linear. The energy balance approach is adopted to derive the finite difference equations for describing the time evolution of the nodal temperatures.

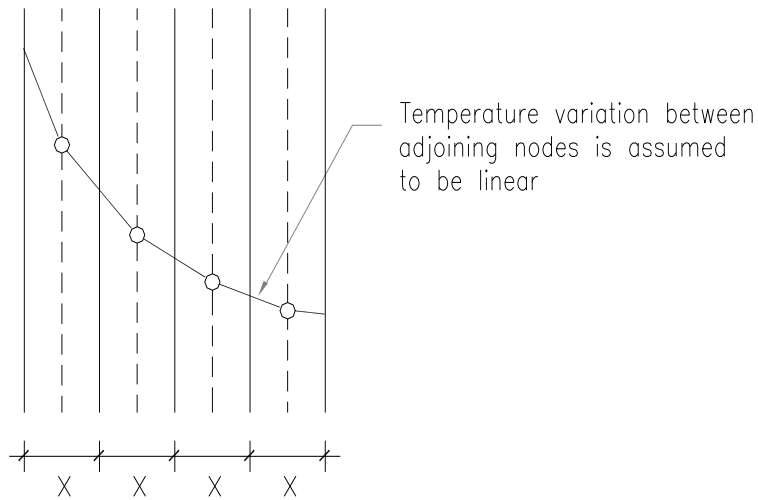


Figure 3—3 Element represented by a finite number of discrete slices

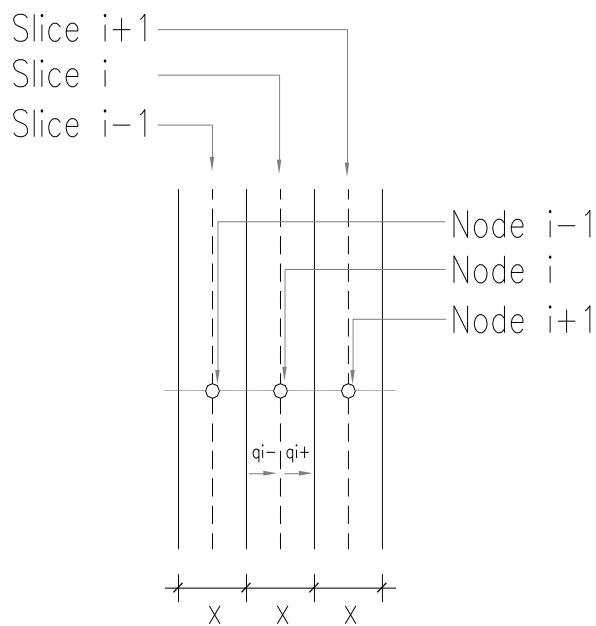


Figure 3—4 Conduction heat transfer of an internal slice

The temperature gradient between the $(i - 1)^{\text{th}}$ and the i^{th} nodes and between the i^{th} and the $(i + 1)^{\text{th}}$ slices (Figure 3—4) are:

$$\frac{T_i - T_{i-1}}{\Delta x} \quad \text{and} \quad \frac{T_{i+1} - T_i}{\Delta x}$$

The rate of conduction heat transfer through a plane is proportional to the temperature gradient at the plane, therefore the heat flux through the interface between $(i - 1)^{\text{th}}$ and i^{th} slices (q_{i-}) and between the i^{th} and the $(i + a)^{\text{th}}$ slices (q_{i+}) are:

$$W_{i-} = -k \frac{T_i - T_{i-1}}{\Delta x} \quad \text{and} \quad W_{i+} = -k \frac{T_{i+1} - T_i}{\Delta x}$$

Assuming there are no internal heat sources or sinks the rate of change in the internal energy of the i^{th} slice of the slab will equal the net heat gain of the i^{th} slice due to conduction heat transfer between the slice and each of the two adjoining slices:

$$\rho c \Delta x \frac{\Delta T_i}{\Delta t} = -k \frac{T_i - T_{i-1}}{\Delta x} + k \frac{T_{i+1} - T_i}{\Delta x} \quad \text{Equation 3-21}$$

Re-arranging this to describe the rise in temperature ΔT_i at node i over the time interval Δt gives:

$$\frac{\Delta T_i}{\Delta t} = \alpha \frac{T_{i-1} - 2T_i + T_{i+1}}{\Delta x^2} \quad \text{Equation 3-22}$$

Recalling Equation 3-15 $\left[\frac{\partial^2 T}{\partial x^2} = \frac{\rho c}{\lambda} \frac{\partial T}{\partial t} \right]$

Rearranging to describe the change in temperature over the change in time gives:

$$\frac{\partial T}{\partial t} = \frac{\lambda}{\rho c} \frac{\partial^2 T}{\partial x^2} \quad \text{Equation 3-23}$$

$$\frac{\partial T}{\partial t} \approx \frac{\Delta T_i}{\Delta t} \quad \text{Equation 3-24}$$

Therefore:

$$\frac{T_{i-1} - 2T_i + T_{i+1}}{\Delta x^2} = \frac{\rho c}{\lambda} \frac{\partial T}{\partial t} \quad \text{Equation 3-25}$$

The time step is discretised using the ‘hopscotch’ method (Myers, 1971). This method applies explicit and implicit time-stepping to alternative nodes of the construction, this gives the advantage of a high level of accuracy combined with very efficient computation.

3.6.4 Air Gaps

Air gaps in opaque and transparent constructions are modelled as pure resistances:

$$W = \frac{(T_1 - T_2)}{R} \quad \text{Equation 3-26}$$

Where:

T_1 & T_2 = adjacent surface temperatures (°C)

3.7 Summary

The literature review has shown that recently there is interest both in activate thermal mass strategies where air is forced across surfaces with high thermal mass and ETAHE systems. Such systems have been applied to buildings but there is still uncertainty on how to incorporate them in new designs and how to carry out accurate (but as simple as possible) modelling during the detailed design of a building. Therefore the solution can be provided in two parts. The first must deal with simplified guidelines on how activated thermal mass would reduce energy consumption (and by how much) and possibly improve environmental conditions. The second must deal with building up confidence in dynamic thermal models used by building services engineers to accurately predict environmental conditions in a building incorporating active thermal mass strategies.

The requirements of a concept design tool have also been reviewed, highlighting the need for future tools to be suitable for architectural use by:

- Simplifying input complexity by identifying and focusing on critical parameters.
- Defining input parameters in architectural terms.
- Verifying that the tool provides results of suitable accuracy.
- Developing a simple means of comparing and rating design efficiency.
- Evaluation of design tool by practising designers.

The literature has also highlighted the need for dynamic thermal modelling when simulating the performance of active thermal mass strategies, and the commercially available dynamic thermal simulation program IES-Virtual Environment is introduced.

The next chapter 4 describes the monitoring and simulation of three operation buildings integrating four different active thermal mass strategies.

4.0 MONITORING & SIMULATION

4.1 Introduction

The previous chapter 3 has demonstrated that active thermal mass strategies have been applied to buildings, but there is still uncertainty on how to incorporate them in new designs and how to carry out accurate (but as simple as possible) modelling during the detailed design of a building. Therefore the solution can be provided in two parts. The first must deal with simplified guidelines on how activated thermal mass would reduce energy consumption (and by how much) and possibly improve environmental conditions. The second must deal with building up confidence in dynamic thermal models used by building services engineers to accurately predict environmental conditions in a building incorporating active thermal mass strategies.

This chapter 4 addresses the second point by using a commercially available dynamic building thermal model (IES, 2008) to construct models for four active thermal mass strategies and compare the results with monitored temperatures in buildings incorporating the strategies. Four active thermal mass strategies were studied using air as the transfer medium:

Three buildings were chosen as case studies and monitoring (temperature at discrete points within the thermal mass structure) was carried out during short periods of time. Models of the buildings focusing on the active thermal mass strategy were constructed within the commercially available dynamic building thermal program IES and the simulation results were compared with measured temperatures.

4.2 Description of the buildings and active thermal mass strategies

4.2.1 Building 1: Booth's HQ Office - floor void with thermal mass

Booth's Headquarters Office is the head office of Booth's supermarket chain and is located in Preston in the North of the UK.

The meeting rooms, training rooms and directors' offices utilize an underfloor displacement ventilation system - one of the director's offices has been monitored in this study.

Air is drawn, via supply fan, directly from outside, ducted through the building (approx. 4m) and into the floor void plenum created by a raised floor and an exposed concrete slab base (see Figure 4—1 and Figure 4—2).

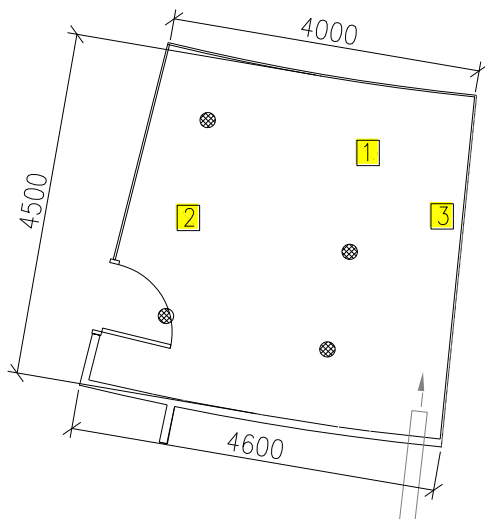


Figure 4—1 Booths' Case-study: Plan of Director's office with the location of temperature sensors

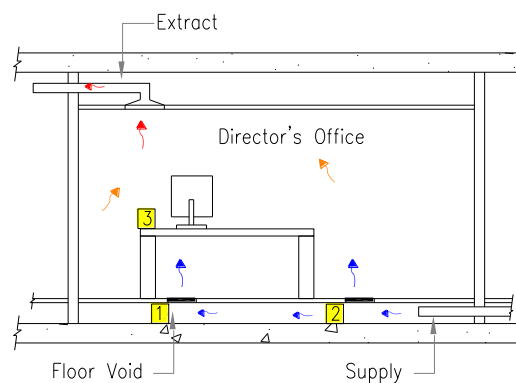


Figure 4—2 Booths' Case-study: Schematic representation of Director's office ventilation strategy with the location of temperature sensors

Diffusers in the raised floor transfer the air to the office space, which is then extracted at high level, via extract fan. The fans are controlled in the room by the user, with a normal occupancy of 0900 to 1700 hours, and have a flow rate of $0.025\text{m}\cdot\text{s}^{-1}$ (1.7ach^{-1}). The office is 4.3m (L) x 4.5m (W) x 2.7m (H) and is an internal room with lightweight partition walls (admittance $1.4\text{W}\cdot\text{m}^{-2}\cdot\text{K}^{-1}$). The floor void is 0.2m deep with a suspended floor with carpet finish. There is 1 computer in the office, with a normal occupancy of 1. The maximum internal heat gain is 0.56kW ($29\text{W}\cdot\text{m}^{-2}$).

4.2.2 Building 2: Longley Park School - Hollow Core Slabs

Longley Park College is a secondary education school located in Sheffield in the North of the UK. Two thirds of the building utilizes a hollow core slab ventilation system - one of the computer rooms has been monitored in this study.

Supply air is ducted to the hollow core slabs from an air handling unit located on the roof. The air is then ducted down the building and along the ceiling void in the corridor (approx. 40m) to the hollow core slabs. Six hollow core slabs with three 0.185m active cores supply a total of $0.3\text{m}\cdot\text{s}^{-1}$ (6.2 ach^{-1}) to the room at high level, which is then extracted via a bulkhead at high level (see Figure 4—3 and Figure 4—4). The air supply is controlled via the BMS supplying air during the occupied hours of 0900 and 1600 hours with night cooling during unoccupied hours dependent on internal and external conditions. Comfort cooling on the supply air operates between 0900 and 1600 hours, cooling the supply air to a minimum of 16°C with the aim to maintain a 23°C setpoint within the occupied space.

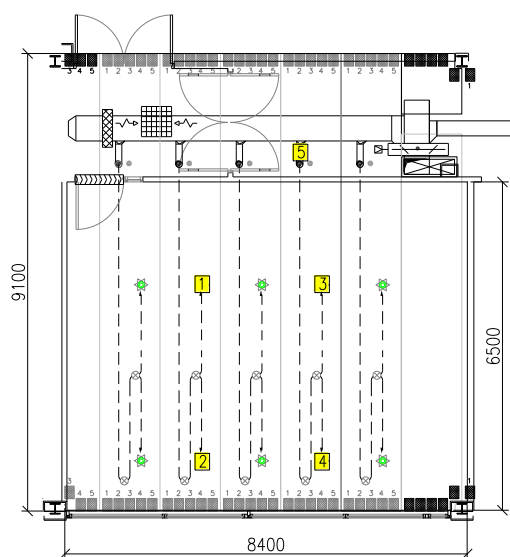


Figure 4—3 Longley Park Case-study: Plan of Computer room with the location of temperature sensors

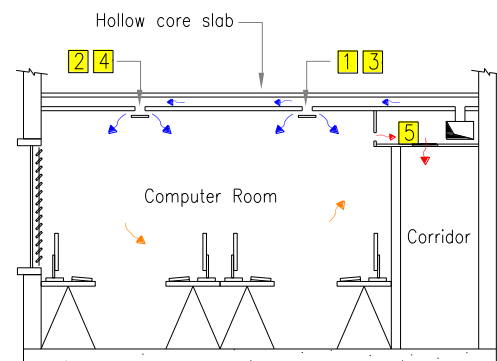


Figure 4—4 Longley Park Case-study: Schematic representation of Computer room ventilation strategy. The location of temperature sensors is marked

The room is 8.4m (L) x 6.5m (W) x 3.2m (H) and has one external wall (west facing) of a lightweight construction (admittance $2.4\text{W}\cdot\text{m}^{-2}\cdot\text{K}^{-1}$). The internal walls are of a medium weight construction (admittance $3.3\text{W}\cdot\text{m}^{-2}\cdot\text{K}^{-1}$). There are 26 computers in the room, with a maximum occupancy of 27. The maximum internal heat gain is 3.7kW ($68\text{W}\cdot\text{m}^{-2}$)

4.2.3 Building 3: The Lowry – earth to air heat exchanger and thermal labyrinth

The Lowry (see Figure 4—5 and Figure 4—6) is a large building incorporating two theatres, an art gallery, corporate hospitality and storage. It is located adjacent to the Manchester ship canal at Salford Quays, Salford, Greater Manchester, UK and has a high level of exposure.

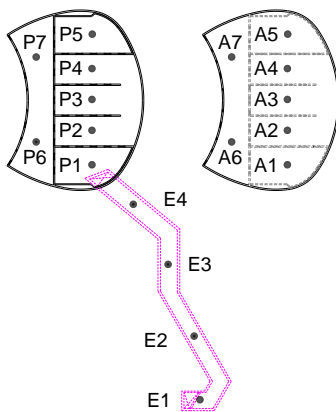


Figure 4—5 Lowry Case-study: Schematic Plan of the theatre. The location of temperature sensors is marked

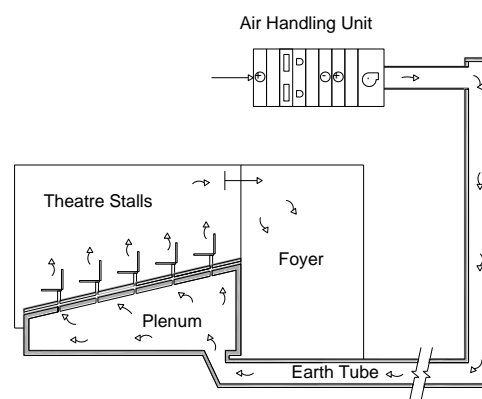


Figure 4—6 Lowry Case-study: Schematic representation of theatre ventilation strategy

One of the theatres is ventilated using a low velocity displacement system, supplying air through pedestal diffusers in the stalls and step diffusers in the tiers above. There are three levels of seating, each served by dedicated air handling units (AHUs) supplying full fresh air and providing supplementary heating and cooling.

To supply air to the theatre stalls a 44.4m long earth-to-air heat exchanger (2.4m x 2.0m) was constructed (see Figure 4—5 and Figure 4—6). This provides a supply air path

between the AHU and the large air plenum created by the stalls raked seating concrete structure. This structure can be approximated to an earth to air heat exchanger and was studied in this project.

For coordination of holes through the plenum with the theatre seats a secondary 50mm plenum was created above by a 50mm plywood layer. 100mm diameter holes through the plenum ceiling supply air into the secondary plenum. 100mm diameter holes through the plywood layer supply air to the pedestal diffusers of the theatre seats (see Figure 4—6). This can be approximated to a thermal labyrinth.

The air from the whole theatre is then extracted at high level. This air passes over a run around coil (recovering heat for the other theatre AHUs). The air is then either supplied to the Foyer at high level, when there is a heating demand, or discharged to atmosphere.

The approximate dimensions of the theatre are 25 m (L) x 18 m (W) x 15 m (H) and has all walls internal with only the ceiling exposed to external variations. The internal walls are of a medium weight construction.

4.3 Description of the models

4.3.1 Monitoring

To develop an understanding of the thermal performance of each of the active thermal mass strategies each building was monitored for a minimum of two periods in different weather periods (winter, mid season or summer). This allowed two sets of data to calibrate the dynamic thermal models against.

Building Management Systems (BMS) have been used at each building to log the ambient air temperature, supply air temperatures, adjacent room temperatures and fan running times, where available, at 15 minute intervals. Supplementary Gemini tiny talk data loggers have been placed within the active thermal mass strategies to measure air temperatures at 20 minute intervals.

- Gemini Tinytalk data loggers have been chosen because;
 - They are small and discrete and can be placed in tight spaces.
 - Each logger is independent, removing the need for intrusive wiring.
 - They have a memory that can log for over a 4 week period at a 30 minute interval.
 - They have an accuracy of 0.2°C when monitoring temperatures between 0 and 50°C

To simulate the performance of the different Active Thermal Mass strategies a number of different input parameters need to be fed into the models. Because the strategies are being monitored in real operational buildings, and not test cells, it is not possible to fix these parameters.

All of the buildings have varying levels of internal and solar gains that would be difficult to monitor accurately without severely disrupting the running of the buildings and at a cost that could not be justified. It has therefore been chosen to monitor the temperatures adjacent to the thermal mass, which will vary with the internal and solar gains, and set these with the simulation models. The room air temperature is an input to the model; the temperature of the air as it leaves the duct is simulated.

For this reason and for each of the strategies the temperature of the air before it enters the thermal mass should be known and the air temperature of the spaces adjacent to the thermal mass should be known. For further confidence in the models the surface temperatures of the internal surfaces of the thermal mass also need to be known.

In Booth's HQ building, supplementary Gemini tiny talk data loggers were placed in the floor void (sensors 1 and 2, Figure 4—2), and in the room (sensor 3).

In Longley Park, supplementary Gemini tiny talk data loggers were placed at the supply diffusers to measure the temperature of the air leaving the hollow core slabs (sensors 1 to 4, see Figure 4—3 and Figure 4—4). It was intended to monitor the air temperature just before it entered the hollow core slab (sensor 5), but due to technical restrictions on site

this was not possible. The temperature of the room above and below were monitored via the BMS.

In the Lowry, supplementary Gemini tiny talk data loggers were placed throughout the ETAHE, plenum and airspace. The monitoring sensors are labelled as follows (see Figure 4—5): E1 to E4 are temperature sensors placed in the ETAHE about 300mm away from the walls, P1 to P7 are temperature sensors in the plenum (labyrinth), halfway between the top and the bottom of the plenum and A1-A7 are temperature sensors within the air space between the seating and the plenum (Figure 4—6).

4.3.2 Simulation models

To simulate the performance of each of the active thermal mass strategies a computer model of each has been created using IES Virtual Environment (IES, 2008). Record drawings and on site measurements were used to determine the geometry and construction types.

To isolate the performance of the active thermal mass strategy in each model, monitored data has been used as input data into the model. All three buildings employ different active thermal mass strategies, but the way in which they operate is the same in principle. Air is forced (using a mechanical fan) into a void with exposed thermal mass. This mass is in contact with the void exchanging heat to and from the air dominantly via convection (Barnard, 1994) due to the air being turbulent.

The mass is also in contact with the adjoining spaces through conduction. For Booth's HQ and Longley Park case studies these are the rooms above and below the floor void or hollow core slab. For the Lowry ETAHE, this is the surrounding ground temperature and the ambient air temperature and for the Lowry Plenum, this is the theatre above and the ground below.

The monitored data for the adjacent rooms and the ambient air temperature has been taken from the monitored data and the adjacent temperatures in the model set to these. For the ground temperature the temperature of the ground at 10m below the surface has been used,

this is because at this depth the undisturbed ground temperature is almost equal to the average annual temperature (Carslaw and Jaeger 1959).

This depth of soil has also been included within the model to allow the dynamic effect of the ground temperature on the ETAHE to be simulated and also the effect of the ETAHE on the ground.

The flow rates from the monitored data have also been used as input into the model.

4.3.3 Booths HQ

The floor void has been added into the model with the same geometry as the actual building. The floor void is 200mm in depth with a suspended floor above and a concrete slab below.

Table 4—1 Materials and properties of floor void modelling for Booths HQ

	Thickness (m)	Conductivity (W.m ⁻¹ .K ⁻¹)	Density (kg.m ⁻³)	Specific Heat Capacity (J.kg ⁻¹ .K ⁻¹)
Suspended Floor				
- Carpet	0.005	0.600	200.0	1300.0
- Chipboard	0.028	0.120	630.0	2260.0
Bottom of Floor void				
- Pre-cast Concrete	0.200	1.900	2300.0	840.0
- Ceiling Void	0.500			
- Ceiling Tiles	0.015	0.380	1120.0	840.0

Due to the low air flow rate into the floor void the turbulence in the floor void is low, therefore the CIBSE variable heat transfer coefficients (CIBSE, 2007) have been used for the surfaces in the floor void. They are controlled according to the ventilation air flow and they are the same for a given ventilation rate.

4.3.4 Longley Park

Figure 4—7 shows the cross section of the slab with its dimensions. The slab cores have been simplified as two parallel plates with air passing between them, one in contact with the room above and one in contact with the room below (Ren & Wright, 1998) as shown in Figure 4—8.

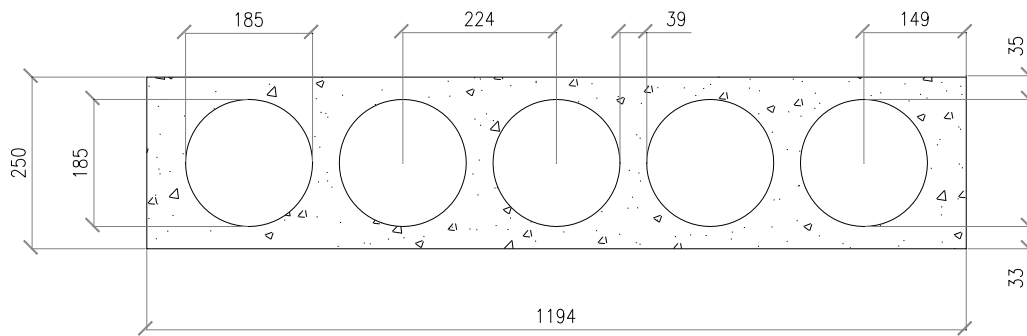


Figure 4—7 Longley Park cross section of actual hollow core slab

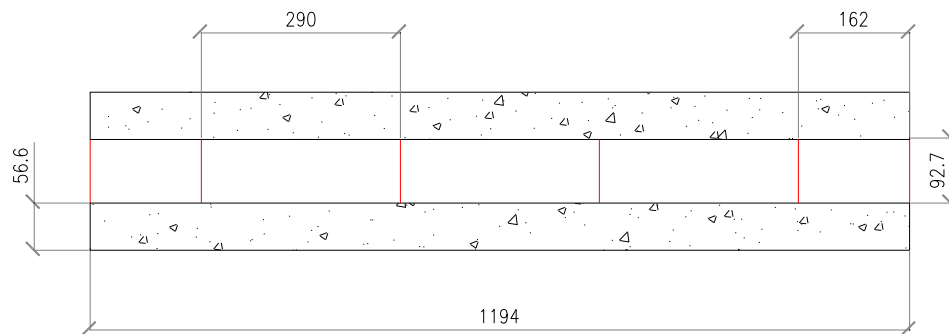


Figure 4—8 Longley Park cross section of simplified slab modelled

The following calculations were made to achieve equivalence:

$$\text{Cross sectional area of concrete} = (1.194 \times 0.250) - (5 \times \pi \times 0.09252) = 0.1641\text{m}^2$$

Splitting this between two plates there is 0.082m^2 of concrete in contact with the room above and 0.082m^2 in contact with the room below. Splitting this between the 5 cores there is 0.0164m^2 in contact with each core.

The internal surface area of the hollow core slab is used to determine the width and depth of concrete for each core:

$$\text{Circumference} = \pi d = 3.142 \times 0.185 = 0.58127\text{m}$$

Therefore 0.29m is in contact with the room above and 0.29m in contact with the room below.

$$\text{Depth} = 0.0164 / 0.29 = 0.0566\text{m}$$

Each hollow core is modelled separately and because the temperature in the cores is similar it is assumed to be no heat transfer between cores.

To keep the cross sectional area of the air path through the slab the same the depth of the air void is determined by this.

$$\text{Cross section of 1 core} = \pi \times 0.09252 = 0.02688\text{m}^2$$

The depth of the air void between the parallel plates is therefore:

$$\text{Depth of air void} = 0.02688 / 0.29 = 0.0927\text{m}$$

Table 4—2 shows the materials and their properties used for the hollow core modelling (CIBSE 2006a).

Table 4—2 Materials and properties of hollow core modelling for Longley Park

	Thickness (m)	Conductivity (W.m ⁻¹ .K ⁻¹)	Density (kg.m ⁻³)	Specific Heat Capacity (J.kg ⁻¹ .K ⁻¹)
Top of Hollow Core Slab				
- Carpet	0.005	0.600	200.0	1300.0
- Screed	0.075	0.410	1200.0	840.0
- Pre-cast Concrete	0.0565	1.900	2300.0	840.0
Bottom of Hollow Core Slab				
- Pre-cast Concrete	0.0565	1.900	2300.0	840.0

Using Equation 3-6 the heat transfer coefficient has been calculated to be 8.609W.m⁻².K⁻¹ and using Equation 3-9 is 9.386W.m⁻².K⁻¹. In trial test it was found that this had a minimum influence on the results (see section 4.4.2). The value of 8.609 W.m⁻².K⁻¹ was used for the simulations.

4.3.5 The Lowry

Earth Tube (ETAHE)

The earth to air heat exchanger (ETAHE) starts 2.0m x 2.4m transferring to 2.4 x 2.0m after 30m (Figure 4—9).

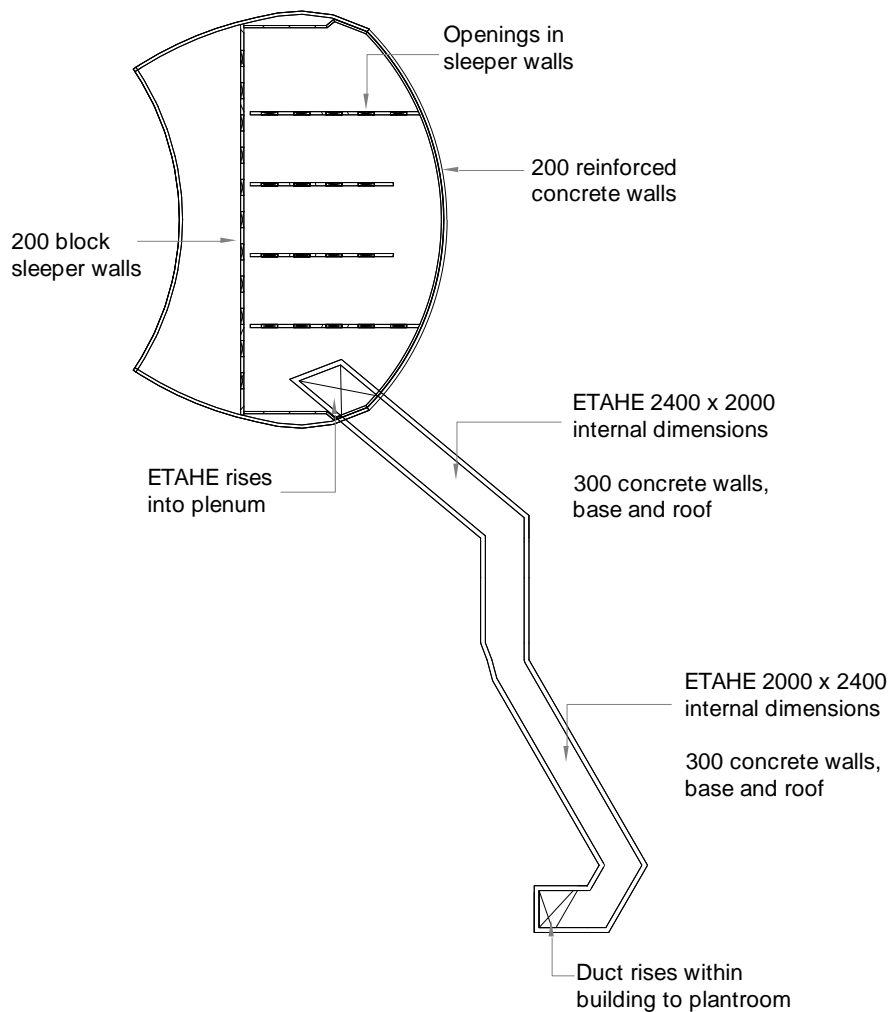


Figure 4—9 Plan of the Lowry showing dimensions of the ETAHE and the plenum under the theatre

This has been simplified as two parallel plates with air passing between them, one in contact with the ambient air temperature/room above and one in contact with the undisturbed ground temperature (Figure 4—10 and Figure 4—11).

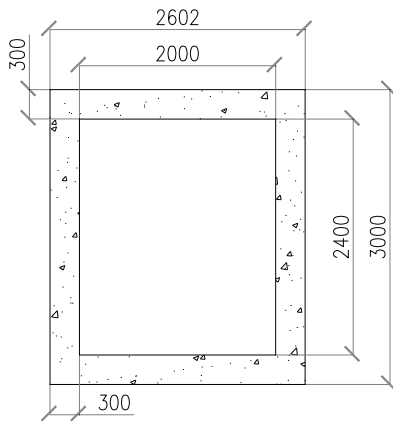


Figure 4—10 The Lowry cross section of actual ETAHE

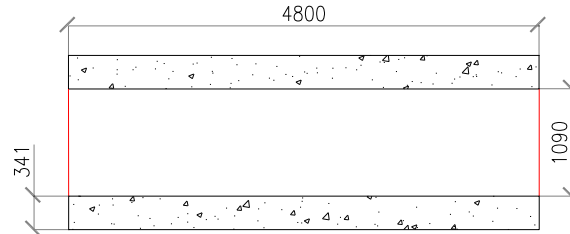


Figure 4—11 The Lowry cross section of simplified ETAHE modelled

$$\text{Cross sectional area of concrete} = (2.6 \times 3.0) - (2.0 \times 2.4) = 3.0 \text{ m}^2$$

The depth of concrete is determined by keeping the internal surface area the same, therefore:

$$\text{Depth of concrete} = 3.0 / 8.8 = 0.341 \text{ m}$$

To keep the cross sectional area of the air path through the ETAHE the same, the depth of the air void is determined by this.

$$\text{Cross section of ETAHE} = 2.0 \times 2.4 = 4.8 \text{ m}$$

The depth of the air void between the parallel plates is therefore:

$$\text{Depth of air void} = 4.8 / 4.4 = 1.09 \text{ m}$$

Table 4—3 shows the materials and their properties used for the ETAHE model (CIBSE 2006a).

Table 4—3 Materials and properties of ETAHE modelling for Lowry.

	Thickness (m)	Conductivity ($\text{W}\cdot\text{m}^{-1}\cdot\text{K}^{-1}$)	Density ($\text{kg}\cdot\text{m}^{-3}$)	Specific Heat Capacity ($\text{J}\cdot\text{kg}^{-1}\cdot\text{K}^{-1}$)
ETAHE Roof with soil				
- Cast Concrete	0.20	1.330	2000.0	1000.0
- Soil	0.89	1.210	1960.0	840.0
Pre-cast Concrete	0.30	1.900	2300.0	840.0
- ETAHE Roof				
- Pre-cast Concrete	0.30	1.900	2300.0	840.0
ETAHE Ceiling below foyer				
- Pre-cast concrete	0.50	1.900	2300.0	840.0
ETAHE Floor				
- Soil	4.40	1.210	1960.0	840.0
- Pre-cast concrete	0.50	1.900	2300.0	840.0

Using Equation 3-6 the heat transfer coefficient has been calculated to be $5.729\text{W}\cdot\text{m}^{-2}\cdot\text{K}^{-1}$ and using Equation 3-9 is $7.284\text{W}\cdot\text{m}^{-2}\cdot\text{K}^{-1}$. Here again trial tests indicated that the effect on the results was minimal. The value of $5.729\text{W}\cdot\text{m}^{-2}\cdot\text{K}^{-1}$ was used for the simulations.

Plenum

The theatre plenum has a floor area of 291.3m^2 and an internal volume of 410.154m^3 . The geometry of the plenum is complex as it is formed beneath the raked theatre stalls. To represent the amount of mass that the plenum has, in the model a rectangular room (16m wide x 18m long x 1.425m high) with the same surface area and air volume has been constructed. The internal sleeper walls have also been included within the model.

Table 4—4 shows the materials and their properties used for the labyrinth model (CIBSE 2006a).

Table 4—4 Materials and properties for labyrinth modelling for the Lowry

	Thickness (m)	Conductivity (W.m ⁻¹ .K ⁻¹)	Density (kg.m ⁻³)	Specific Heat Capacity (J.kg ⁻¹ .K ⁻¹)
Plenum roof				
- Pre-cast concrete	0.25	1.900	2300.0	840.0
Plenum floor				
- Soil	4.40	0.610	1680.0	880.0
- Cast concrete	0.40	1.330	2000.0	1000.0
Plenum Walls				
- Pre-cast concrete	0.20	1.900	2300.0	840.0
Sleeper Walls				
- Concrete Block	0.20	0.600	1350.0	840.0

Due to the low air flow rate into theatre plenum the turbulence in the theatre plenum is low, therefore the CIBSE Variable heat transfer coefficients (CIBSE, 2007) have been used for the surfaces in the theatre plenum.

4.3.6 Input data

4.3.6.1 Booth's HQ

From the monitored data the input data for the model are:

- Ambient Air Temperature – the heat gain from the supply fan and through the ductwork is then included within the model.
- Room temperatures above and below the hollow core slab.
- Fan running times

These are shown in Figure 4—12 and Figure 4—13 for the mid-season and summer monitored periods.

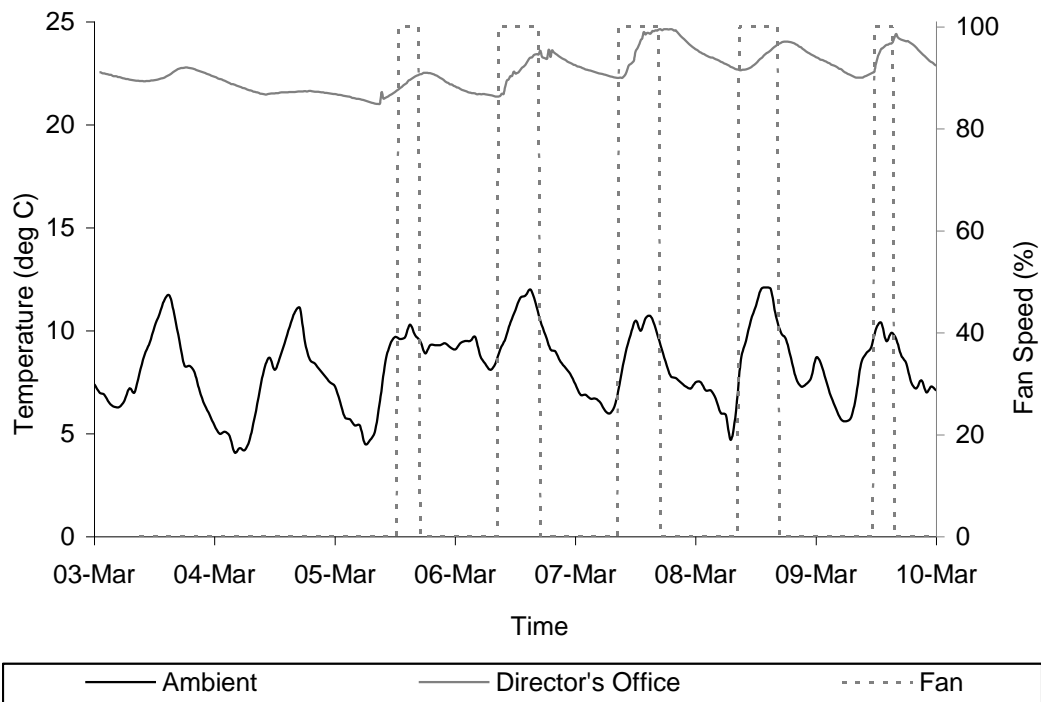


Figure 4—12 Booths HQ - Mid Season 2006 – Input data

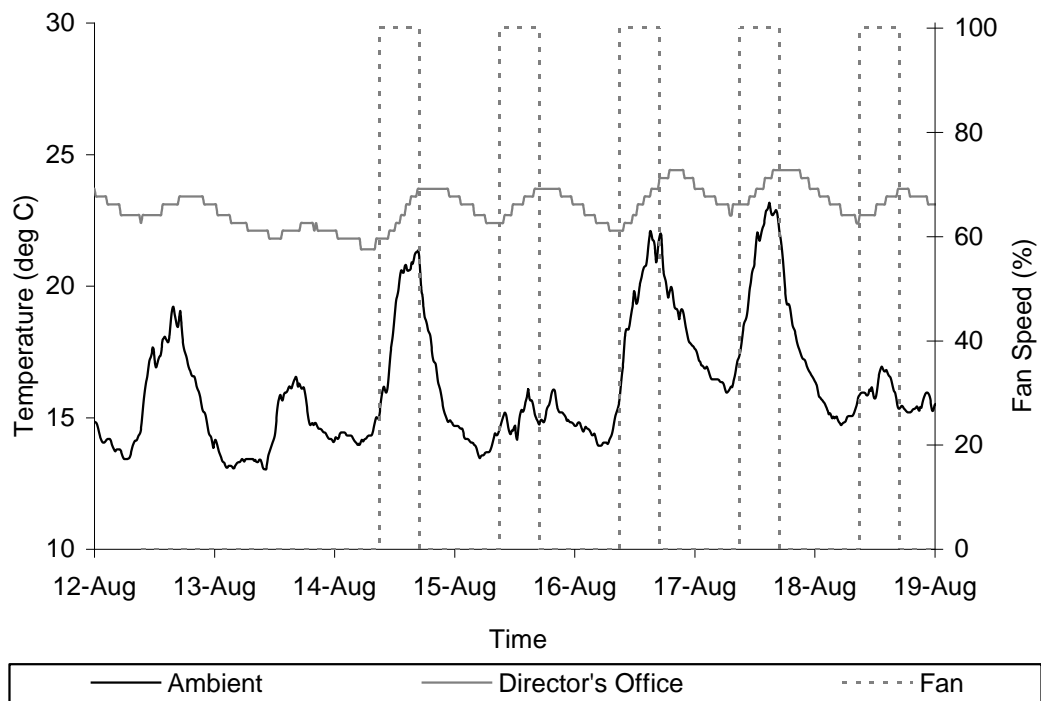


Figure 4—13 Booths HQ - Summer 2007 – Input data

4.3.6.2 Longley Park

From the monitored data the input data for the model are:

- Air temperature leaving the Air Handling Unit (AHU) – the heat gain through the ductwork is then included within the model.
- Room temperatures above and below the hollow core slab. During the summer monitoring period the temperature in the room below the hollow core slab did not log correctly. The room temperature below the hollow core slab has been assumed to be the same as the temperature of the room above the hollow core slab.
- During both monitoring periods no air was being supplied to one of the monitored hollow core slabs. Only data from one slab was therefore useful.
- Fan running times.

These are shown in Figure 4—14 and Figure 4—15 for the summer and winter monitored periods.

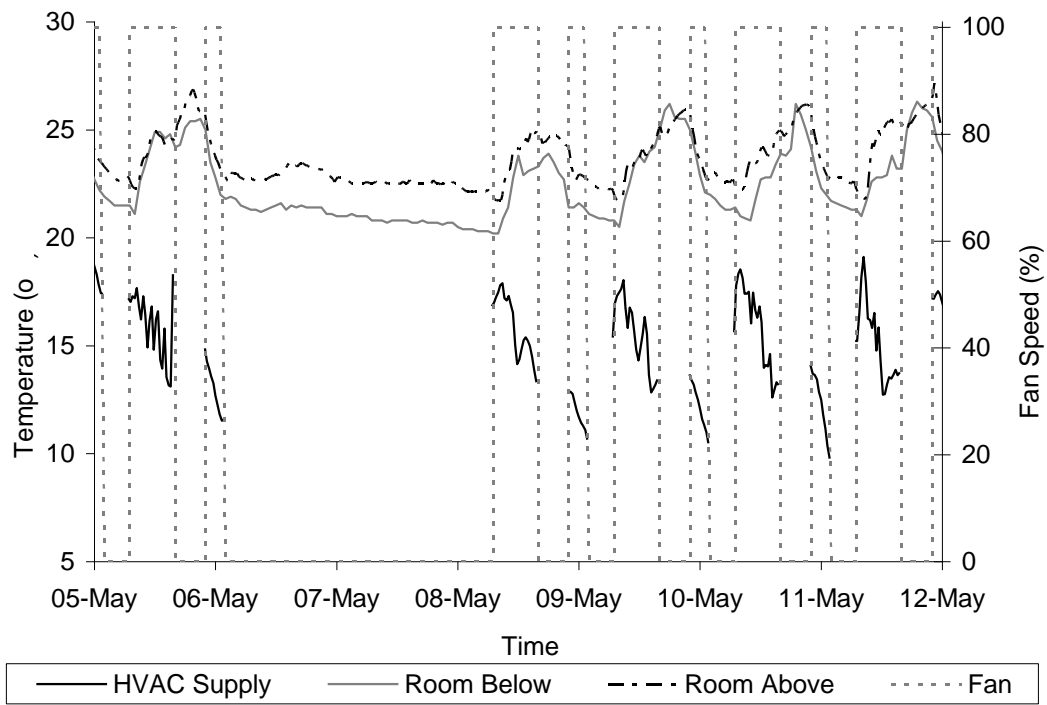


Figure 4—14 Longley Park - Mid season 2006 – Input data

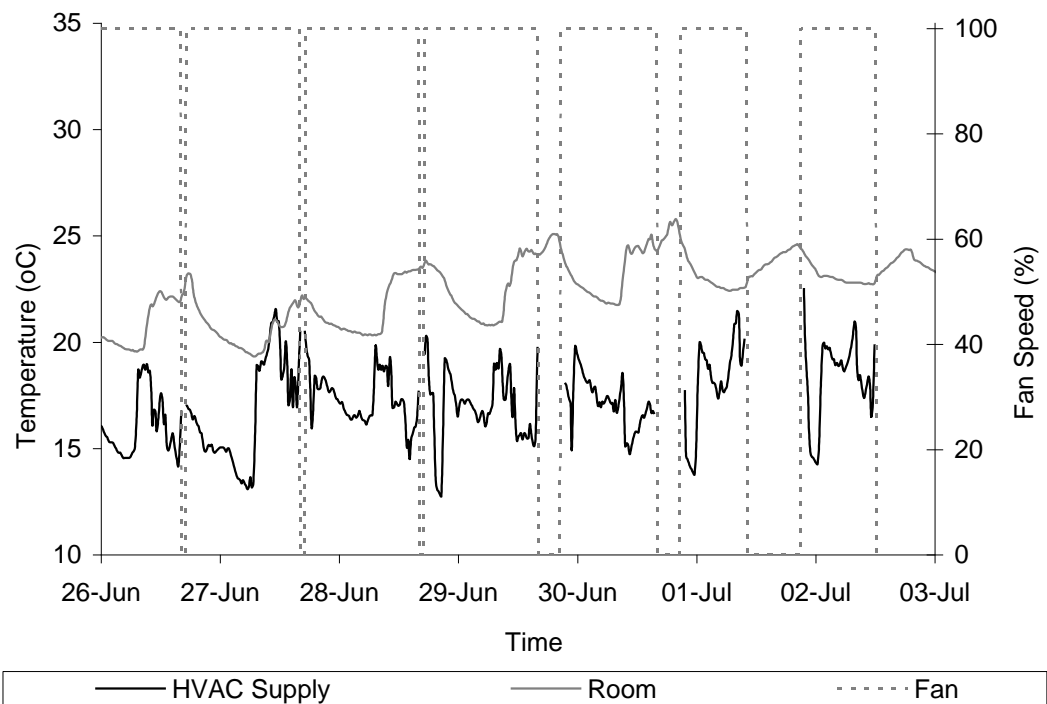


Figure 4—15 Longley Park - Summer 2006 – Input data

4.3.6.3 The Lowry

From the monitored data the input data for the model are:

- Air temperature entering the ETAHE (ET01) (see Figure 4—6).
- Foyer temperature – the foyer temperature was monitored using the BMS, and records the extract air temperature from the space. In the model it has been assumed in the winter the temperature is 20°C and in the summer the temperature is the same as the ambient air temperature (limited to a minimum of 20°C during the night).
- Air space temperature (A2 and A4 in the winter, and A3 and A5 in the summer). (see Figure 4—6).
- Ground temperature above ETAHE – the depth of soil has been added to the construction of ETAHE roof (0.89m). The ambient air temperature is then set as the adjacent temperature.
- Ground temperature below ETAHE – 4.5m (limited by the model as this is the maximum it will allow) of soil has been added to the construction of the ETAHE floor. This reaches (1.39 + 1.09 +4.5) almost 8 m below ground and can be considered a good approximation to constant ground temperature which should have been at 10m ideally. Equation 3-11 has been used with the ambient air temperature from the design summer year (DSY) for London 2005 together with the soil properties in Table 4—4 to calculate the average temperature at a depth of .
- The rooms adjacent to the theatre plenum were not monitored, but have been set to be 21°C in the winter and 22°C in the summer.

The input data are shown in Figure 4—16 and Figure 4—17 for the summer and winter monitored periods.

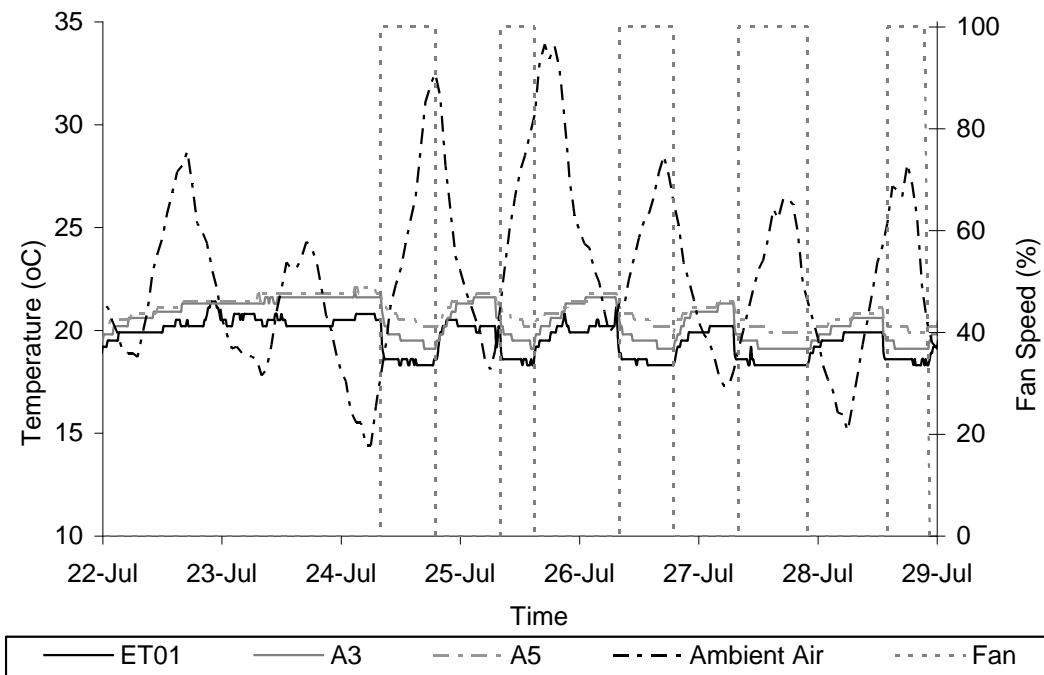


Figure 4—16 The Lowry – summer 2006 – input data

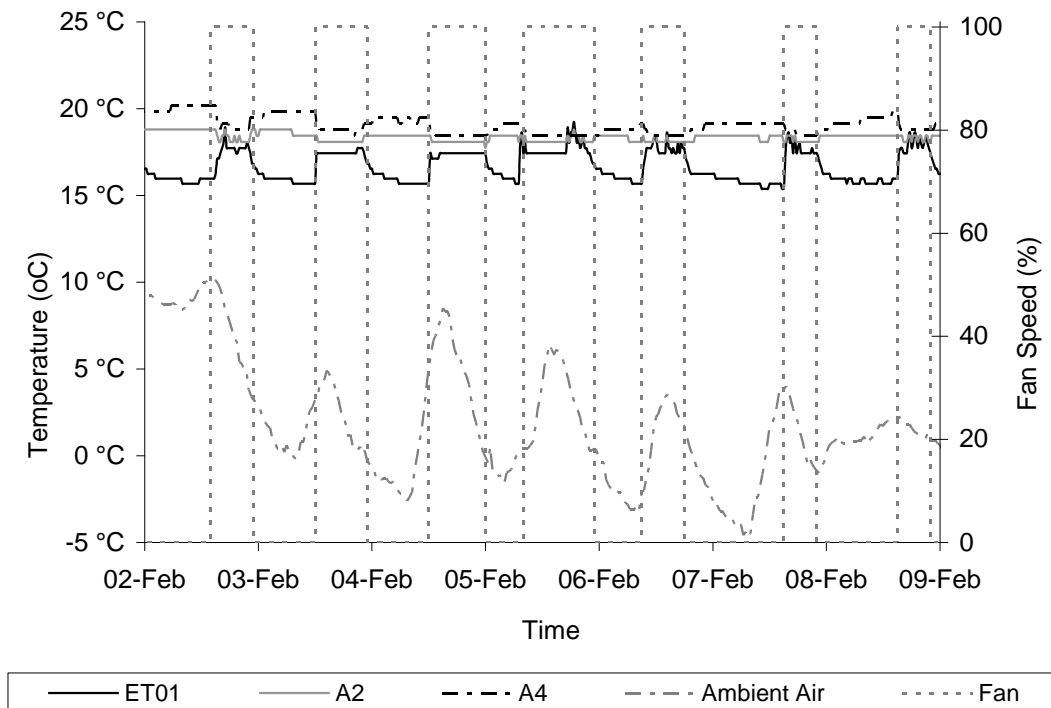


Figure 4—17 The Lowry – Winter 2007 – input data

4.4 Comparison of simulation results with monitoring and discussion

4.4.1 Booth's HQ

Figure 4—18 and Figure 4—19 show the measured and simulated temperatures in the concrete void under the director's office. The plotted monitored air temperature is the average of the two points monitored. The simulation model treated the floor void as one space and the plotted simulated air temperature is the temperature in this space. The temperature of the air before entering the floor void is also shown (into void). The fan speed indicates the operation times of the fan (100% on, 0% off).

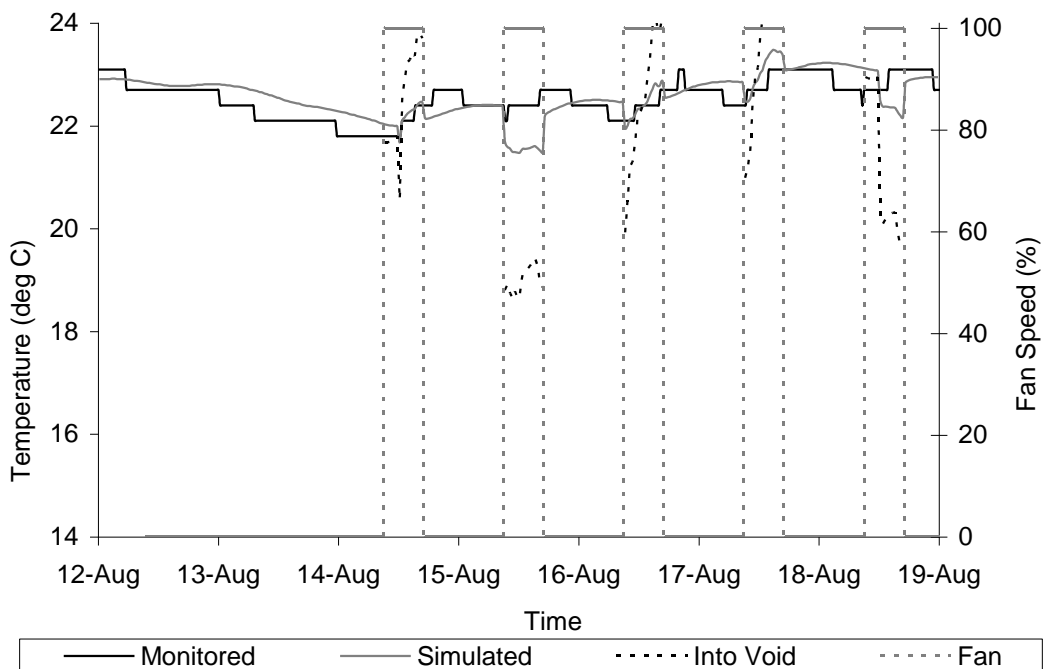


Figure 4—18 Comparison of monitored and simulated results for Booth's HQ summer 2006

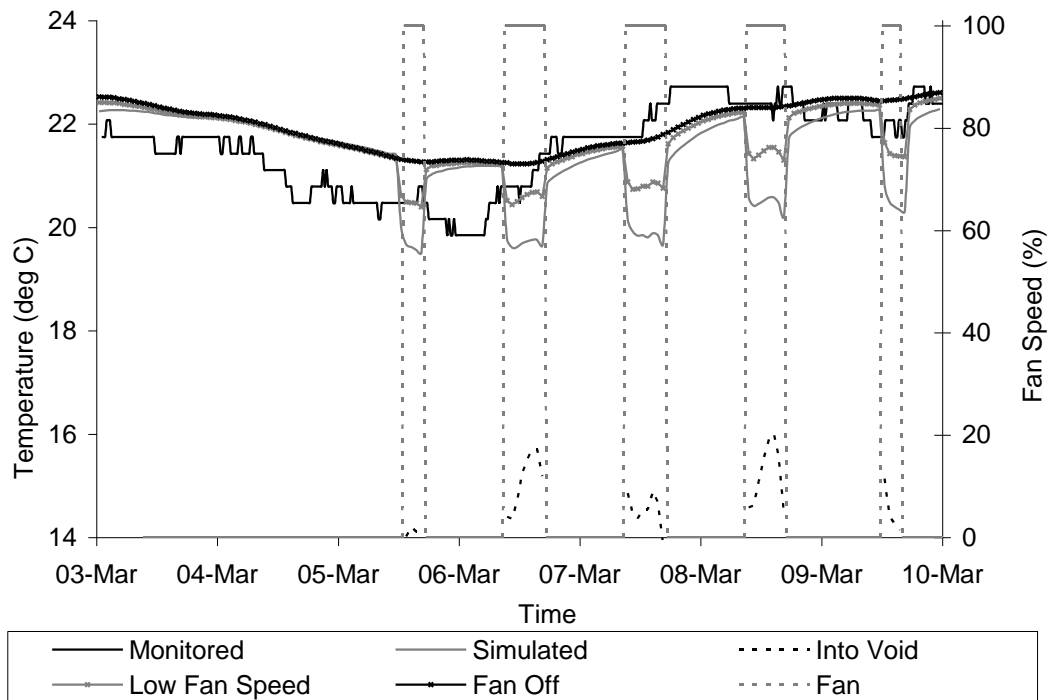


Figure 4—19 Comparison of monitored and simulated results for Booth's HQ Mid Season 2007

The simulated temperatures in the void in the summer (Figure 4—18) show a very good comparison with the monitored temperatures. The simulated results in the winter (Figure 4—19) show the air supplied to the floor void is only heated in the floor void to around 75% of what is shown in the monitored data.

The fan is controlled within the office by the occupant and has three choices of setting low, medium or high. The system has been designed on (and is normally run at) the medium speed. However, in the winter due to there not being a need for cooling the occupant may not have turned the fan on or only ran the fan at the low speed. This has been investigated by running additional simulations with the fan off and at low speed during winter. The simulated results are indicated in Figure 4—19 and indicate better agreement with monitored temperatures.

4.4.2 Longley Park

Figure 4—20 and Figure 4—21 show the measured and simulated temperatures in the hollow core concrete floor under the computer room. The plotted monitored average air temperature is the average of the two sensors positioned at the exit of the operational hollow core slab. The air temperature and mean radiant temperature are the simulated temperatures just before the air leaves the hollow core slab. The temperature of the air before it enters the hollow core slab is also shown (into slab). The fan speed indicates the operation times of the fan (100% on, 0% off).

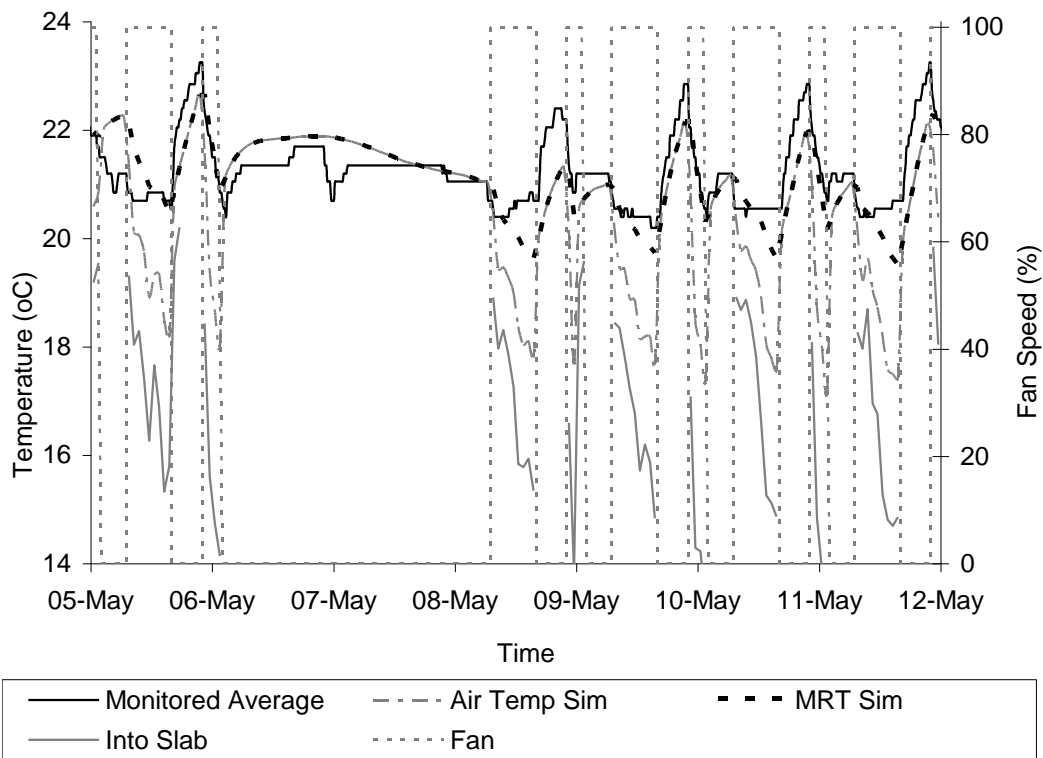


Figure 4—20 Comparison of monitored and simulated results for Longley Park in mid season 2006

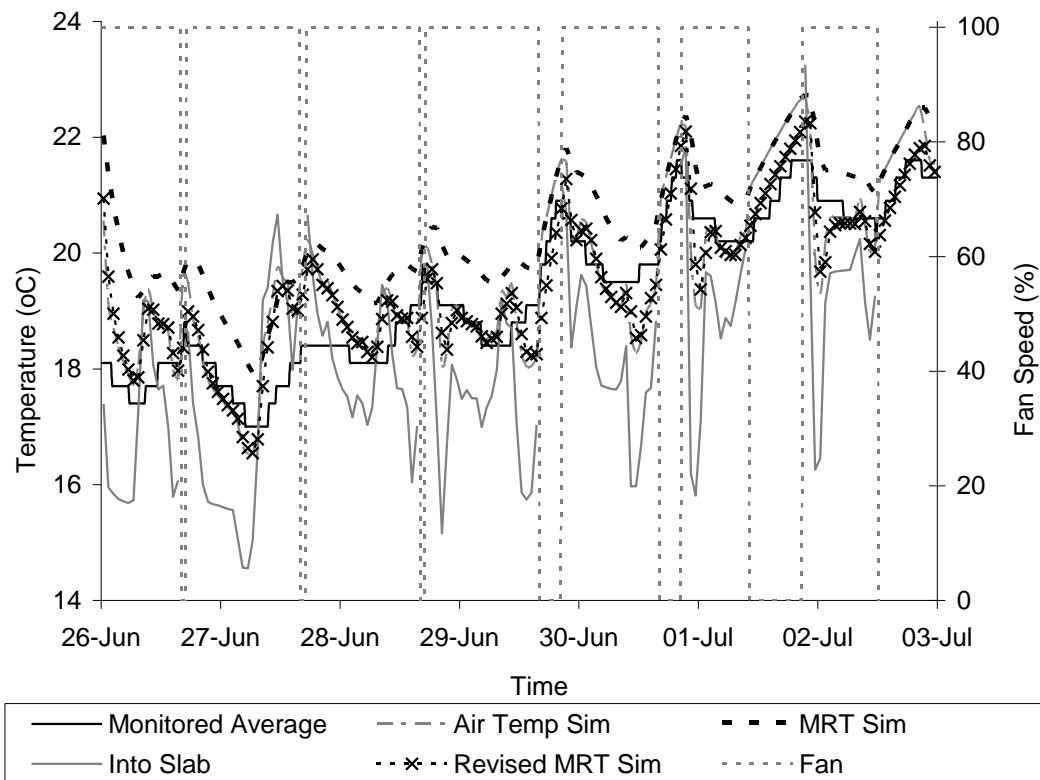


Figure 4—21 Comparison of monitored and simulated results for Longley Park in summer 2006

The simulated air temperature in the mid season (Figure 4—20) show that the air temperature leaving the hollow core slab is only heated to around 50% of what is shown in the monitored data. The temperature sensors were positioned within the hollow core slab at the end of the final core. The diameter of each core is 185mm, so the sensor is very close to the walls of the core. To consider the radiant effect of the core concrete surfaces on the temperature the mean radiant temperature (MRT) of the surfaces (Gan, 2001) has been looked at (Figure 4—20). The mean radiant temperature shows very good comparison with the monitored data.

The simulated results in the summer (Figure 4—21) show the air temperature leaving the hollow core slab is in good agreement with the monitored data. The mean radiant temperature is higher than the monitored data, but does remove the sharp variations shown in the simulated air temperature that are not shown in the monitored temperature.

Because only the air temperature for the room above the hollow core slab was logged during the summer monitoring period (see section 4.3.6.2) it was assumed the room below temperature was the same. However, when looking at the mid season monitored data the average room temperature in the room above is around 1°C higher than the room below. This results in the simulated air temperature and mean radiant temperature being higher. This was investigated for the summer period with additional simulations and it was found that the change in the temperature of the room below does shift the predicted air and mean radiant temperature to give a better comparison with the monitored data.

To explore the effects of the heat transfer coefficient within the hollow core slabs the effect of the surface roughness and the corners have been simulated. Barnard (1994) considered the surface roughness to increase the heat transfer coefficient within the cores. Ren and Wright (1997) found that the heat transfer on the bends is 50 times that of a straight section of hollow core, whereas Barton et al (2002) demonstrated that the bend sections have a minimal effect on the overall heat transfer within the hollow core slab. The effect on the temperature of the air leaving the slab (air temperature and mean radiant temperature) was found to be minimal for both the surface roughness and the bends.

4.4.3 The Lowry

4.4.3.1 Earth Tube (ETAHE)

Figure 4—22 and Figure 4—23 show the measured and simulated temperatures in the earth-to-air heat exchanger. The plotted E_{av} is the average of the temperatures monitored in the earth-to-air heat exchanger. Simulated E_{av} is also the average of the simulated temperatures. The fan speed indicates the operation times of the fan (100% on, 0% off).

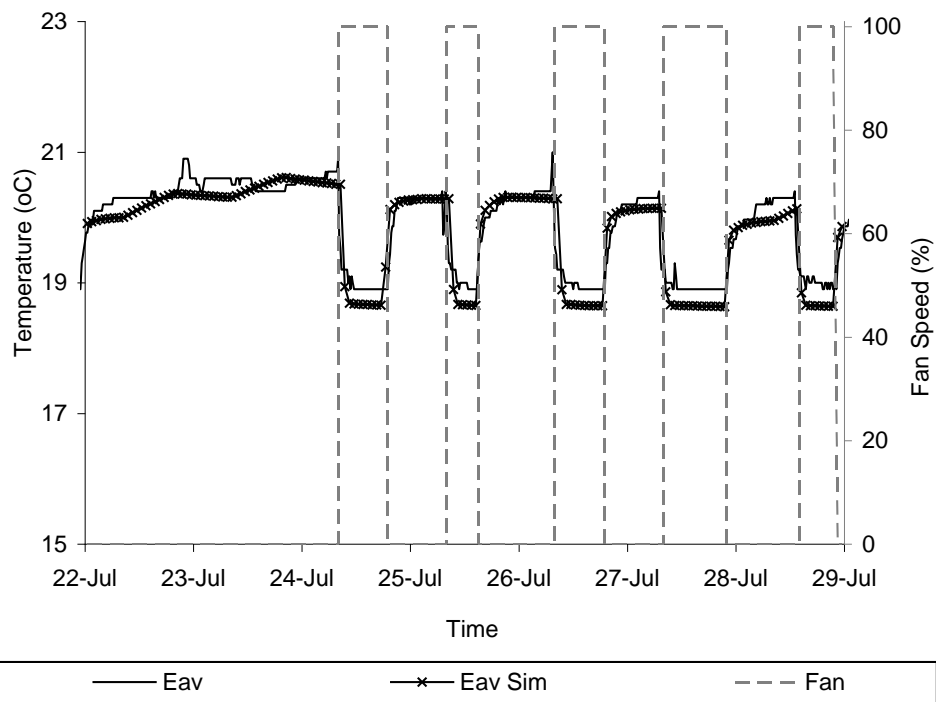


Figure 4—22 Comparison of monitored and simulated results for the ETAHE in Lowry in summer 2006

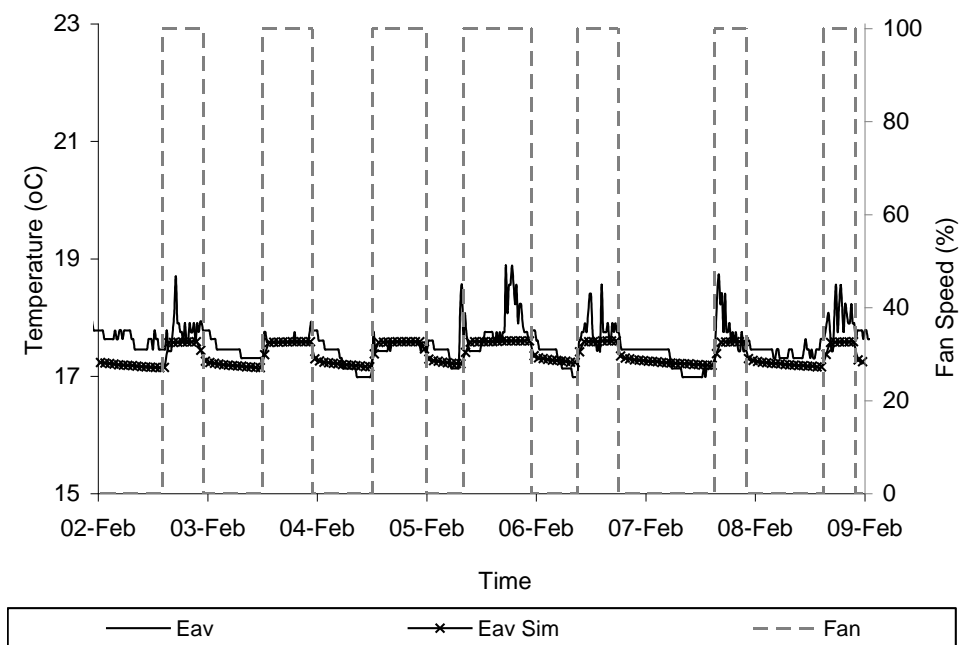


Figure 4—23 Comparison of monitored and simulated results for the ETAHE in Lowry in winter 2007

The simulated temperatures in the void in the summer (Figure 4—22) and in the winter (Figure 4—23) show a very good comparison with the monitored temperatures. The static difference between measured and simulated E_{av} can be explained by the influence of the building on the ground temperature; as the ground around the ETAHE is partly below the building, this would have affected the earth temperature but it was too complicated and beyond the scope of this study to investigate fully. However, a simulation was run with earth temperature 18 °C in summer and 24 °C in winter which resulted in an even better matching between measurement and simulation. It was felt that as the influence of the building on the ground temperature was not studied fully to present the original simulation results without the building's effect.

4.4.3.2 Labyrinth

Figure 4—24 and Figure 4—25 show the measured and simulated temperatures in the theatre plenum. The plotted $Plenum_{Av}$ is the average of the air temperatures monitored in the theatre plenum. The plenum was treated as one space, plotted plenum sim is the air temperature in this space. The fan speed indicates the operation times of the fan (100% on, 0% off).

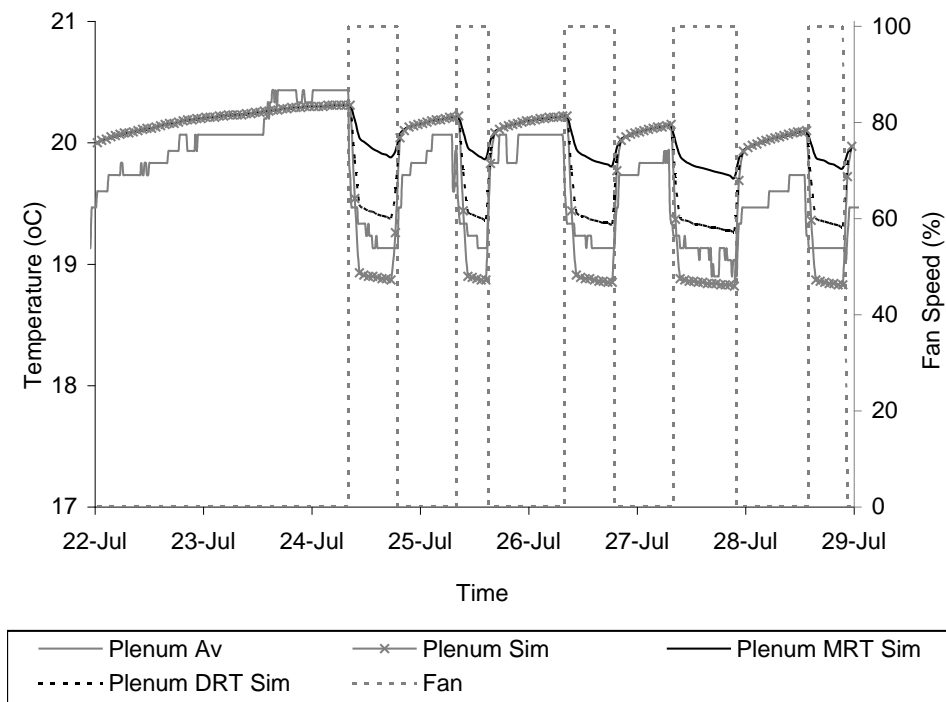


Figure 4—24 Comparison of monitored and simulated results for the labyrinth in Lowry in summer 2006

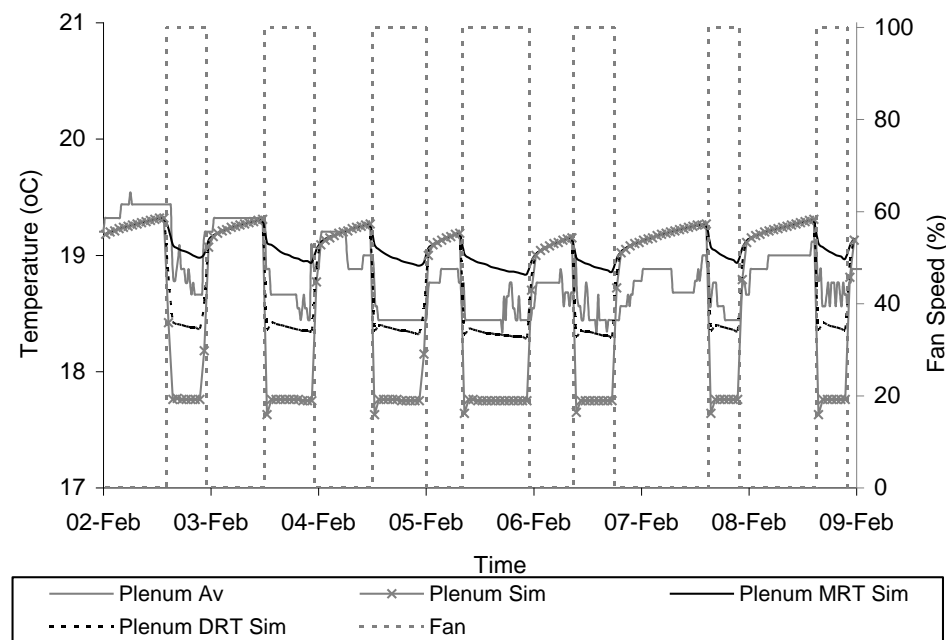


Figure 4—25 Comparison of monitored and simulated results for the labyrinth in Lowry in winter 2007

The simulated temperatures in the void in the summer (Figure 4—24) and in the winter (Figure 4—25) show a good comparison with the monitored temperatures, but the simulated temperatures are lower than those monitored, with the difference being greater in the summer. Again the simulated mean radiant temperature (MRT) in the plenum has been considered together with the dry resultant temperature (DRT). The mean radiant temperatures are higher than the measured air temperatures, but the temperature sensors were not positioned as close to the concrete of the plenum as they were when monitoring the hollow core slabs. It is therefore felt that the monitored temperatures would lie in between the mean radiant temperature and the air temperature as the simulated data shows, ie dry resultant temperature as indicated in Figure 4—24 and Figure 4—25.

4.5 Summary

This chapter 4 described the development of models for four activated thermal mass strategies within a commercially available dynamic thermal simulation program (IES, 2008). The strategies studied are (a) earth-to-air heat exchanger, (b) hollow core concrete floor slabs, (c) floor void with thermal mass and (d) thermal labyrinth. The method of modelling these strategies has been described and all simplifications for easiness of modelling are stated; this includes changes in physical representation. The input parameters for the simulations have been determined from monitoring three buildings integrating active thermal mass strategies for typical periods in the year. It was possible to isolate the performance of the thermal mass by using measurements of the adjacent space temperatures, supply air temperatures into the thermal mass, ambient air temperatures and fan running times as input data into the simulation models. Simulation results of the air temperatures within the active thermal mass strategies have shown good comparison with the monitored data.

The next chapter 5 will now use the calibrated modelling methods to outline the development of a simplified design tool, TMAir (Thermal Mass Activation – Air Medium),

5.0 DEVELOPMENT OF A CONCEPT DESIGN TOOL

5.1 Introduction

The previous chapter 4 demonstrated that a commercially available dynamic thermal modelling software program (IES, 2008) can be used to model the performance of active thermal mass strategies with results that show a good comparison with monitored data.

This chapter 5 outlines the development of a simplified design tool, TMAir (Thermal Mass Activation – Air Medium), that can be used by designers at the concept stages of a project to quickly analyse the effects, in terms of energy and comfort, of integrating active thermal mass strategies into UK office buildings based in South East England for a range of design parameters. This was developed by carrying out simulations using the calibrated modelling methods developed in chapter 4. Four active thermal mass strategies are considered (a) hollow core slabs (b) earth-to-air heat exchanger (c) floor void with mass and (d) thermal labyrinth in addition to a standard office with no active thermal mass. Key design parameters were identified for each system and parametric analysis carried out to determine the resulting environmental conditions and energy consumption in the office.

All of the possible combinations of the user selected parameters have been simulated and the results have been fed into the excel based tool TMAir.

The tool has an easy-to-use interface which allows direct comparison of the different active thermal mass strategies together with the effects of changing key design parameters. Results are presented in terms of thermal comfort and energy consumption. Figure 5—1 shows a process diagram for the TMAir design tool.

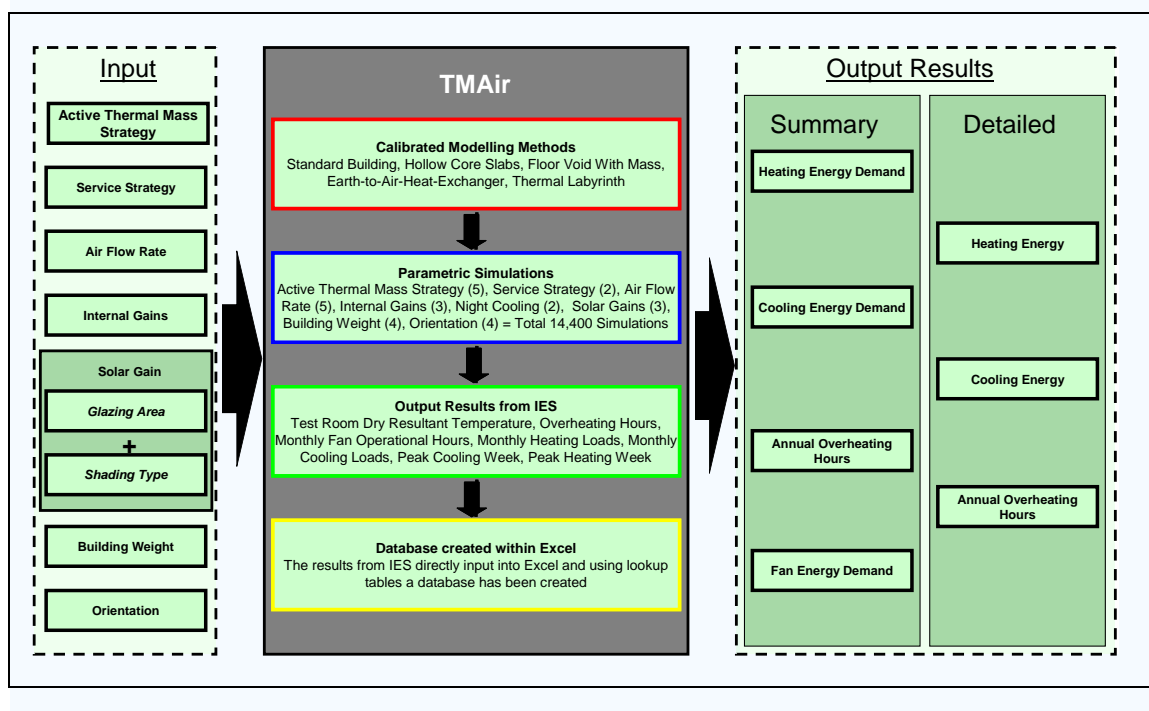


Figure 5—1 Process diagram for TMAir

5.2 Selection of Parameters

To allow the effects of integrating an active thermal mass strategy into an office building to be determined, a number of parameters have been explored.

These parameters can be split into two categories:

- The fixed parameters - pre-selected for the design tool and have to be a fair representation of the projects that the tool will be used for.
- The user selected parameters - chosen by the user to represent the way the building will be used, and to look at the effect of key design decisions on the performance of the building.

5.2.1 Fixed Parameters

The office type, weather data, site terrain and the site terrain have been fixed to be a fair representation of the projects that the tool will be used for.

5.2.1.1 Office Type

The simulation results are based on a single office cell 10m wide, 6m deep and 3m high (Tindale et al, 1995; Kolokotroni et al, 1997; CIBSE, 2002a; Kolokotroni et al, 2004). The cell has one external wall and is located on a middle floor with the rooms above and below conditioned similarly to the test room (Figure 5—2).

To allow a North, East, South and West facing test cell to be simulated within the same model, two separate office blocks have been created – one with North and South facing facades and one with East and West facing facades. A 3m wide corridor separates the two sides of the office block, representing a typical corridor space and also creating a thermal separation between the test rooms within the model.

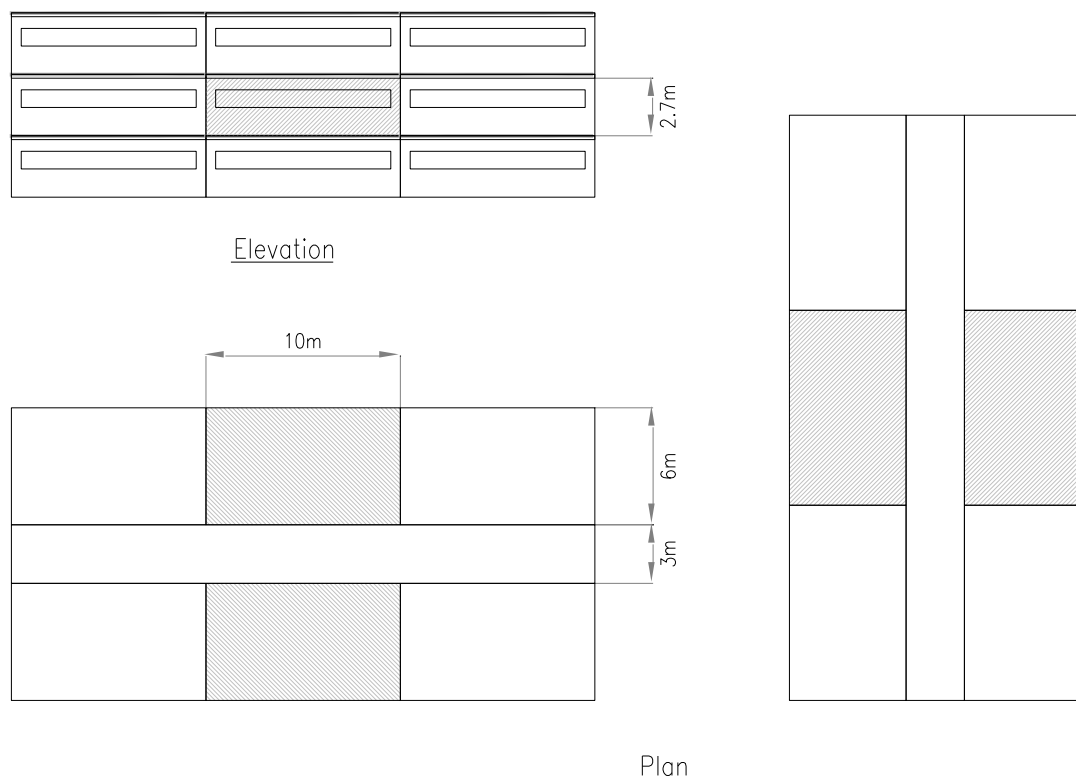


Figure 5—2 Plan and elevation of office blocks with test rooms highlighted

Originally the internal walls and floors were going to be set to isothermal so the adjacent spaces would have had no effect on the test spaces. This cannot be done within IES and to

stop heat transfer between the internal spaces insulation would have to be placed on the outside of the surfaces. This would then effect the thermal capacity of the surfaces. Also the floor and ceiling cannot be set to isothermal for the floor void with mass and hollow core slabs strategies because this would set the adjacent room temperatures to the same temperature as the air in the void or slab.

The rooms adjacent to the test rooms will have the same service strategy, air flow rate, internal heat gains, night cooling control strategy, solar gain, building weight and orientations as the test room. However, due to the increase in simulation time as a result of adding the active thermal mass strategies to all rooms, the active thermal mass strategies are only applied to the test rooms. The adjacent spaces will therefore have a temperature that is close to the test room temperatures.

5.2.1.2 Weather Data

CIBSE Design Summer Year (DSY) 2005 weather file for London has been selected because the data is at the centre of the upper quartile of rankings obtained from the previous 20 years and is intended to be used in the assessment of overheating risk (CIBSE, 2002b). To calculate the energy required for heating ideally the CIBSE Kew Example Weather Year (EWY) would have been used as this is the weather file usually used for heating load calculations. However, this would have resulted in double the number of simulations required. Also the tool is to be used as a comparison tool and when comparing the winter months of the CIBSE DSY and the CIBSE EWY, although the overall average is lower for the EWY, the data show periods with similar patterns.

5.2.2 User Selected Parameters

The user selected parameters can be selected by the user to represent the way the building will be used, and to look at the effect of key design decisions on the performance of the building.

TMAir tool allows the user to select five options for comparison (Figure 5—3). For each of the five options the user selected parameters can be changed. Option 1 is classed as the

‘BASE Case’ because the results of all of the other options are compared against this option (section 5.4).

	B	C	D	E	F	G
1		Option 1- BASE Case	Option 2	Option 3	Option 4	Option 5
2						
3						
4	Active Thermal Mass Strategy	Standard Building	Active Hollow Core Slabs	Floor Void with Mass	ETAHE	Thermal Labyrinth
5	Service Strategy	Standard Building	Mechanical Ventilation	Mechanical Ventilation	Mechanical Ventilation	Mechanical Ventilation
6	Air Flow Rate (ach ⁻¹)		6	6	6	6
7	Internal Heat Gains (W/m ²)	Medium	Medium	Medium	Medium	Medium
8	Night cooling	No	No	No	No	No
9	Glazing Area	40	40	40	40	40
10	Shading Type	Internal venetian blinds, closed, light	Internal venetian blinds, closed, light	Internal venetian blinds, closed, light	Internal venetian blinds, closed, light	Internal venetian blinds, closed, light
11	Building Weight	Lightweight	Lightweight	Lightweight	Lightweight	Lightweight
12	Orientation	East	East	East	East	East
13						

Figure 5—3 Opening tab of TMAir – input parameter selection

As a default the BASE Case Option 1 input parameters were selected to represent typical values (Table 5—1) and comply with typical benchmark values and energy consumption in the UK (ECON 19, 2000). It should be noted that the user can change them from a pull down menu.

Table 5—1 TMAir BASE Case Default Values

User Selected Parameter	DEFAULT Value
Active Thermal Mass Strategy	Standard Building
Service Strategy	Mechanical Ventilation
Air Flow Rate	6 ach-1
Internal Heat Gains	Medium
Night Cooling	No
Glazing Area	40%
Shading Type	Internal Venetian Blinds, Closed, Light
Building Weight	Lightweight
Orientation	East

5.2.2.1 Active Thermal Mass Strategy

Four Active Thermal Mass Strategies can be selected:

Hollow Core Slabs (HCS)

The standard hollow core slab available is 1200mm in width and can be extruded to be the desired width for the room. Each test room will therefore have 8 active hollow core slabs 6m in length, each with 5 x 185mm diameter hollow cores (Figure 5—4). The centre 3 cores of each slab will be actively used to supply air to the test room at high level.

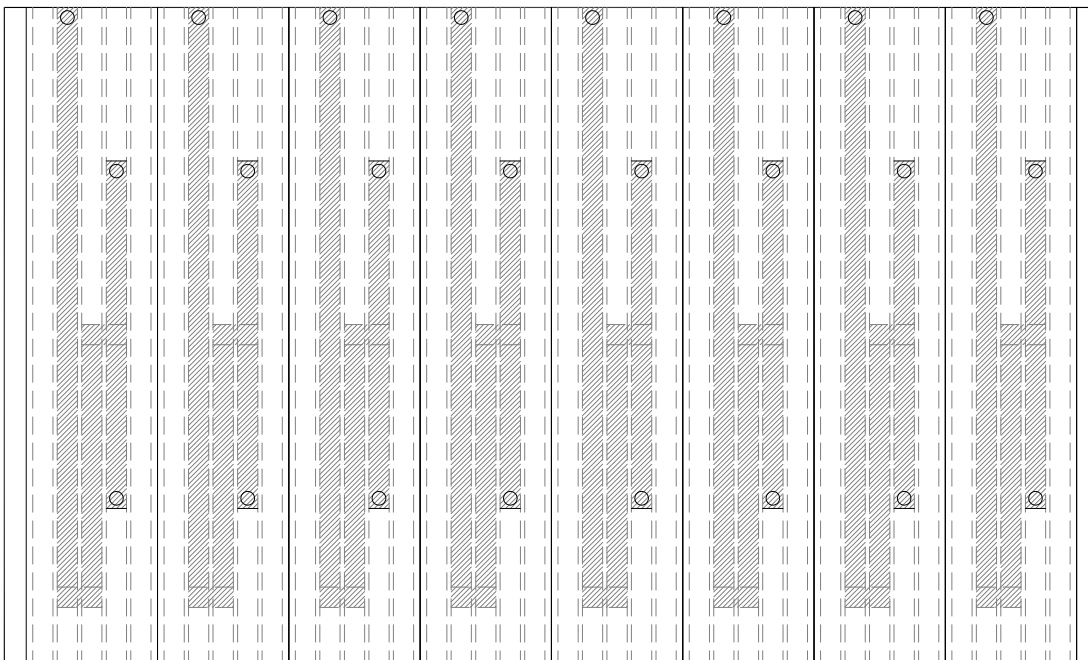


Figure 5—4 Layout of hollow core slabs in test room.

Within the IES model the hollow core has been simplified, as described in section 4.3.4 and validated in section 4.4.2, as two parallel plates with air passing between them, one in contact with the room above and one in contact with the room below.

Table 5—2 shows the materials and their properties used for the hollow core modelling (CIBSE 2006a).

Table 5—2 Materials and properties of Hollow Core Slab for TMAir

	Thickness (m)	Conductivity ($\text{W}\cdot\text{m}^{-1}\cdot\text{K}^{-1}$)	Density ($\text{kg}\cdot\text{m}^{-3}$)	Specific Heat Capacity ($\text{J}\cdot\text{kg}^{-1}\cdot\text{K}^{-1}$)
Top of Hollow Core Slab				
- Carpet	0.005	0.600	200.0	1300.0
- Screed	0.075	0.410	1200.0	840.0
- Pre-cast Concrete	0.0565	1.900	2300.0	840.0
Bottom of Hollow Core Slab				
- Pre-cast Concrete	0.0565	1.900	2300.0	840.0

The selected air flow rate for the test room (section 5.2.2.3) will determine the velocity of air through the hollow core slabs and using Equation 3-6 the heat transfer coefficient is calculated (Table 5—3).

Table 5—3 Hollow Core Slab air flow rate, air velocity and heat transfer coefficient

	Air Flow Rate ($\text{AC}\cdot\text{h}^{-1}$)				
	1	2	6	8	10
Volume Flow Rate ($\text{m}^3\cdot\text{s}^{-1}$)	0.045	0.090	0.270	0.360	0.450
Velocity ($\text{m}\cdot\text{s}^{-1}$)	0.21	0.42	1.26	1.67	2.09
Heat Transfer Coefficient ($\text{W}\cdot\text{m}^{-2}\cdot\text{K}^{-1}$)	CIBSE Variable h_c	CIBSE Variable h_c	6.08	7.65	9.15

Floor Void With Mass (FVWM)

To represent a typical raised floor void, a 150mm floor void air supply plenum will be created between the exposed concrete slab base and a suspended floor with carpet finish. The test room supply air is supplied into the floor void and then transferred to the test room by diffusers in the suspended floor, which is then extracted at high level via extract fan.

The model is created in IES using the same method described in section 4.3.3 and validated in section 4.4.1.

Table 5—4 shows the materials and their properties used for the floor void with mass modelling (CIBSE 2006a).

Table 5—4 Materials and properties of Floor Void with Mass for TMAir

	Thickness (m)	Conductivity (W.m ⁻¹ .K ⁻¹)	Density (kg.m ⁻³)	Specific Heat Capacity (J.kg ⁻¹ .K ⁻¹)
Suspended Floor				
- Carpet	0.005	0.600	200.0	1300.0
- Chipboard	0.028	0.120	630.0	2260.0
Bottom of Floor void				
- Pre-cast Concrete	0.200	1.900	2300.0	840.0

Earth-to-Air-Heat-Exchanger (ETAHE)

Comprehensive early design guidance on earth to air heat exchangers has been produced as one of the outputs of IEA-BCS Annex 28 (Zimmermann & Remund, 2001). This has been used to optimise the design of the earth-to-air heat exchanger for this concept design tool.

- Length of heat exchanger: 45 m
- Diameter of heat exchanger: 0.25 m
- Air velocity: 2 m.s⁻¹
- Span between ducts: 1.0 m
- Duct depth: 3.0 m

The air velocity through the earth-to-air heat exchanger will remain set at 2 m.s⁻¹. To achieve this for the different air flow rates different numbers of earth tubes will used (Table 5—5).

Table 5—5 Air flow rate and the number of earth tubes required for each test room

	Air Flow Rate (AC.h ⁻¹)				
	1	2	6	8	10
Volume Flow Rate (m ³ .s ⁻¹)	0.045	0.090	0.270	0.360	0.450
N ^o Earth Tubes required per room	0.5	0.9	2.8	3.7	4.6

Using the method described in section 4.3.5 and validated in section 4.4.3 the earth tube has been simplified as two parallel plates with air passing between them, one in contact with the ambient air temperature / room above and one in contact with the undisturbed ground temperature.

Table 5—6 shows the materials and their properties used for the earth to air heat exchanger modelling (CIBSE 2006a).

Table 5—6 Materials and properties of Earth to Air Heat Exchanger for TMAir

	Thickness (m)	Conductivity (W.m ⁻¹ .K ⁻¹)	Density (kg.m ⁻³)	Specific Heat Capacity (J.kg ⁻¹ .K ⁻¹)
Above Earth Duct				
- Soil	2.50	1.210	1960.0	840.0
- PVC	0.10	0.160	1380.0	1000.0
Below Earth Duct				
- Soil	0.50	1.210	1960.0	840.0
- PVC	0.10	0.160	1380.0	1000.0

Due to the reduced diameter of earth duct the depth of soil beneath the earth duct has been reduced to 0.5m as recommended by Jacovides and Mihalakakou (1995).

The ground temperature at a depth of 2.75m has been calculated for each month using Equation 3-11 and used as the boundary condition within the model.

When the ambient temperature is sufficient to provide space conditioning the ETAHE will be bypassed. This will prevent the heat sink being drained unnecessarily.

Thermal Labyrinth

A thermal labyrinth will be created beneath each of the office blocks, having a floor plate of 30 m wide x 15 m deep. The height and depth of the voids in the thermal labyrinth are determined by health and safety regulations to allow access for cleaning so a height and depth of 2.0 m has been chosen (Figure 5—5).

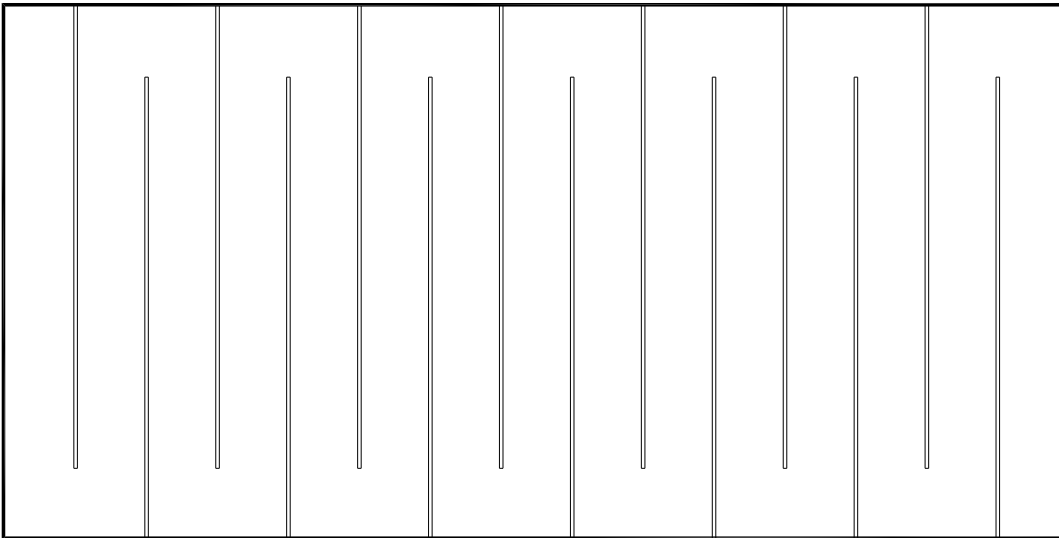


Figure 5—5 Layout of thermal labyrinth beneath each office block

The method described in section 4.3.5 and validated in section 4.4.3 has been used for the thermal labyrinth.

Table 5—7 shows the materials and their properties used for the earth to air heat exchanger modelling (CIBSE 2006a).

Table 5—7 Materials and properties of Thermal Labyrinth for TMAir

	Thickness (m)	Conductivity ($\text{W}\cdot\text{m}^{-1}\cdot\text{K}^{-1}$)	Density ($\text{kg}\cdot\text{m}^{-3}$)	Specific Heat Capacity ($\text{J}\cdot\text{kg}^{-1}\cdot\text{K}^{-1}$)
Labyrinth roof				
- Pre-cast concrete	0.20	1.900	2300.0	840.0
-Polyurethane Insulation	0.10	0.028	30.0	1470.0
Labyrinth floor				
- Soil	4.60	1.210	1960.0	840.0
- Cast concrete	0.40	1.330	2000.0	1000.0
Labyrinth External Walls				
- Dense concrete block	0.20	1.330	2000.0	1000.0
- Soil	0.50	1.210	1960.0	840.0
Labyrinth Internal Walls				
- Concrete Block	0.20	1.310	2240.0	840.0

The ground temperature at a depth of 1.0m (labyrinth external walls) and 7.0m (labyrinth floor) have been calculated for each month using Equation 3-11 and used as the boundary condition within the model.

When the ambient temperature is sufficient to provide space conditioning the thermal labyrinth will be bypassed. This will prevent the heat sink being drained unnecessarily.

5.2.2.2 Service Strategy

When a space has high internal heat gains an active thermal mass strategy may not have enough storage capacity to overcome these loads and provide a comfortable environment. In these cases cooling may be required. To analyse the effect an active thermal mass strategy has when coupled with a cooling system two different service strategies can be selected.

- Mechanical Ventilation – the supply air is heated to maintain the test room at an air temperature of 21°C; in the summer period ambient air is supplied directly to the test room.
- Comfort Cooling - the supply air is heated as above; additionally the supply air is cooled to maintain the test room at an air temperature of 24°C.

The selected air flow rate (section 5.2.2.3) is supplied to the room between the hours of 0800 and 1800hrs, and night cooling is applied if selected (section 5.2.2.5).

5.2.2.3 Air Flow Rate

The internal heat gains (section 5.2.2.4), together with the solar gains (section 5.2.2.6) to the test room are changeable within the tool. The amount of air required to achieve the minimum fresh air rate or the amount of air required to meet the cooling demand of the space therefore varies. Air change rates of 1, 2, 6, 8 and 10 achr^{-1} have been included to allow the user to select an air flow rate suitable for the internal and solar gains that have been selected.

The air supplied to the test room is supplied by a mechanical system. An allowance for the heat gain added to the supply air from the supply fan has therefore been added.

To meet the requirements of Building Regulations Approved Document L2A (ODPM, 2006) a centralised air distribution system must achieve a specific fan power (SFP) of $1.8 \text{ W.l}^{-1}.\text{s}^{-1}$ is used. This is for system with heating, heating and cooling or heating cooling and ventilation. This was chosen to simplify the difference between the simulations and because it is felt that if an active thermal mass strategy is being considered the air distribution system will be designed at a level deemed to be industry best practice.

Since:

Equation 5-1

$$Q_s = m c_p \Delta t_f$$

Where:

Q_s sensible heat gain/loss (kW)

m mass flow rate of supply air ($\text{kg}\cdot\text{s}^{-1}$)

c_p specific heat capacity ($\text{kJ}\cdot\text{kg}^{-1}\cdot\text{K}^{-1}$)

Δt_f fan heat gain ($^{\circ}\text{C}$)

The heat gain added by the fan to each $1.\text{s}^{-1}$ will therefore be 0.00216kW (2.16W). This translates to a heat gain of 2.12°C . This is for air distribution system and includes the supply and extract fan. The heat gain for the supply fan and the extract fan has been assumed to be split equally at 1.059°C .

5.2.2.4 Internal Heat Gains

The internal heat gains were defined using data from CIBSE Guide A (CIBSE, 2006a).

Three levels of internal heat gain can be selected (Table 5—8).

Table 5—8 TMAir internal heat gains

	Density of occupation / person m ⁻²	Sensible heat gain / W.m ⁻²				Latent heat gain / W.m ⁻²		
		People	Lighting	Equip't	Total	People	Other	Total
High	4	20	12	25	57	15	-	15
Medium	8	10	12	20	42	7.5	-	7.5
Low	20	4	12	10	26	3	-	3

The sensible heat gains from the lighting and equipment is made up of radiant and conducted/convective heat gains.

The internal lighting is assumed to be fluorescent and a 30% radiant and 70% conducted/convective split has been used (CIBSE 2006a).

The equipment sensible heat gains will be made up of mainly desktop computers and monitors. The radiant component for a desktop computer is 14% and for a monitor is 35% (CIBSE 2006a). The exact make up of the equipment heat gains in the office space is not known exactly and will be assumed to be 50% monitors and 50% desktop computers. For equipment the heat gain will be 24.5% radiant and 75.5% conducted/convective.

The internal heat gains are controlled by time profiles.

Occupancy

The test room is assumed to be a typical office and will be occupied between 0800 and 1800 hours. It is assumed the first occupants will arrive at 0800 hours and by 0900 hours the office will be fully occupied (Figure 5—6). Lunch hour is assumed to be between 1300 and 1400 hours and it is assumed half the occupants will leave the room. At 1700 hours it is assumed the first occupants will leave the room and by 1800 hours the room will be empty.

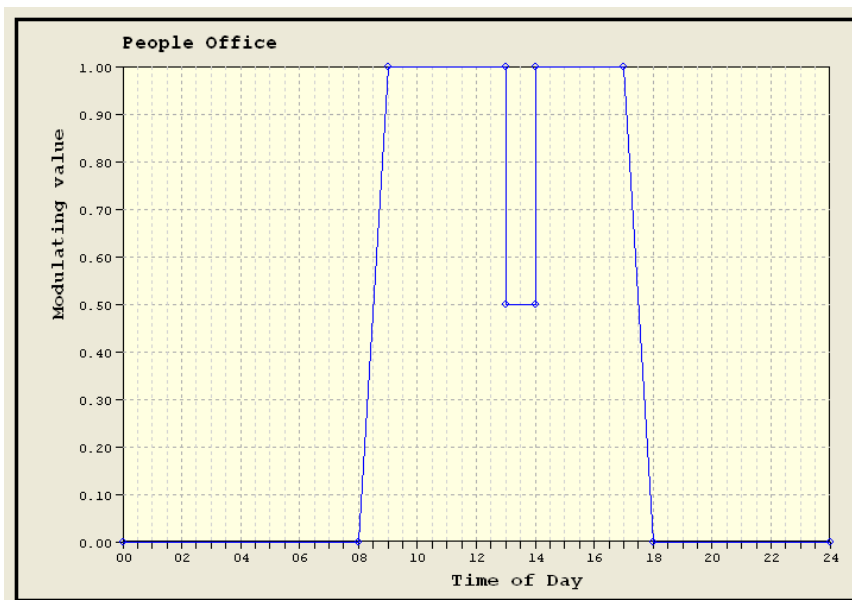


Figure 5—6 Office occupancy profile

Lighting

It is assumed the internal lighting will be on for the full occupancy period 0800 to 1800 hours (Figure 5—7).

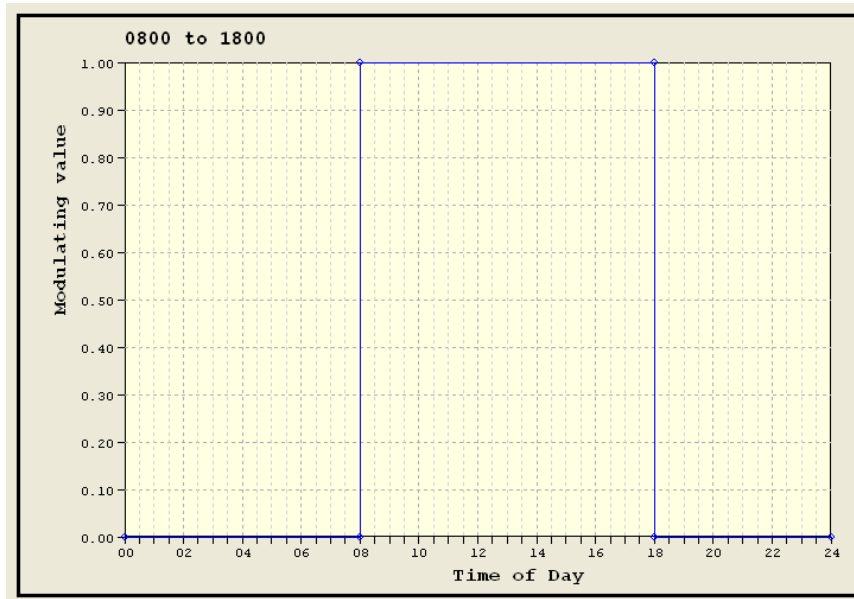


Figure 5—7 Office lighting profile

Equipment

It is assumed the office equipment profile will follow the same profile as the occupancy profile (Figure 5—8).

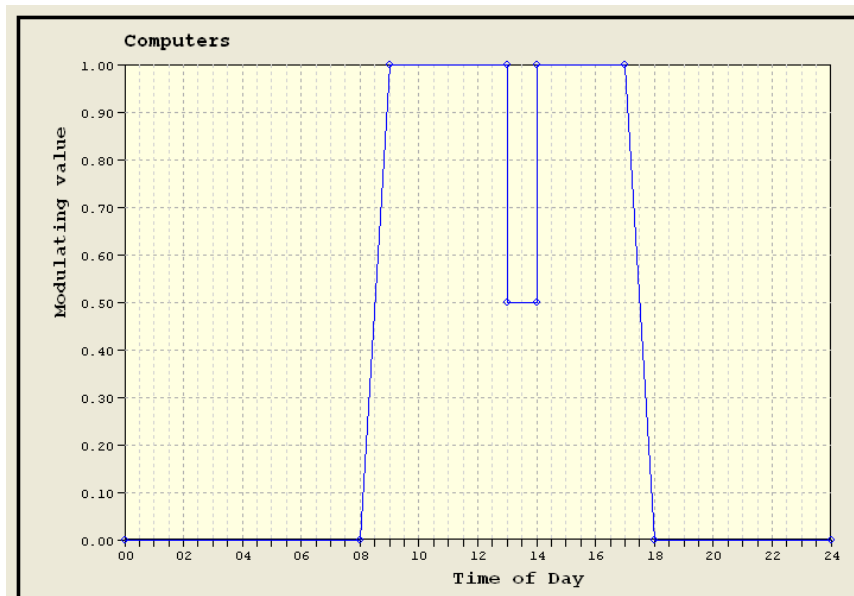


Figure 5—8 Office equipment profile

5.2.2.5 Night Cooling

Night cooling can be selected and is controlled based on the strategy developed within BSRIA Technical Appraisal 14/96 (Fletcher & Martin, 1996).

- Time is between 00:00 and 07:00
- Room air temperature > 18°C
- Outside air temperature > 12°C
- Outside air temperature < inside air temperature

For the Thermal Labyrinth Strategy, to allow the thermal mass to be cooled further, when the test room reaches 18°C the thermal labyrinth will not supply air to the occupied space, but will bypass to outside. This will allow the labyrinth to be cooled further to 16°C.

5.2.2.6 Solar Gains

The method outlined in CIBSE TM37 (CIBSE, 2006b) has been used to classify the solar gains to the test room in terms of solar gain per unit floor area (m²) over the period 0630 to 1630 Solar Time (GMT).

The solar gain per unit floor area averaged over the period 0630 to 1630 Solar Time (GMT) is given by:

$$\phi_{sl} = \left(\frac{1}{A_p} \right) \sum (A_g \phi_s g_{eff}) \quad \text{Equation 5-2}$$

Where:

ϕ_{sl} solar load per unit floor area (W·m⁻²)

A_p perimeter zone floor area (m²)

A_g	net area of glazing (m^2)
ϕ_s	external solar radiation on outside of window ($\text{W}\cdot\text{m}^{-2}$)
g_{eff}	effective g-value of the window and solar shading device

The perimeter zone of floor area is defined as the area that is within 6m on plan from a window. The test room is only 6m in depth so the whole floor plate is considered to be the perimeter zone floor area.

The external solar radiation for London for the different orientations are (CIBSE 2006b):

North	124 $\text{W}\cdot\text{m}^{-2}$
East/West	319 $\text{W}\cdot\text{m}^{-2}$
South	355 $\text{W}\cdot\text{m}^{-2}$

BRE has defined an ‘effective g-value’ for the shading performance of a window with shading device as follows (Littlefair, 2005):

$$g_{eff} = \frac{\text{Solar gain in period of potential overheating through window with shading device}}{\text{Solar gain through unshaded, unglazed aperture for the same period}}$$

The solar load per unit floor area for different combinations of effective g-value and window area have been calculated (Table 5—9, Table 5—10 and

Table 5—11).

Only effective g-values of up to 0.6 have been calculated for the North and South and up to 0.7 for the East/West. This is because of the following g_{eff} values for a low emissivity double glazed window (Littlefair, 2005):

- North 0.57
- East/West 0.66
- South 0.59

Table 5—9 Solar load per unit floor area for different combinations of g_{eff} and window area – North Facing Facade

g_{eff}	Window Area (%)									
	10	20	30	40	50	60	70	80	90	100
0.1	0.56	1.12	1.67	2.23	2.79	3.35	3.91	4.46	5.02	5.58
0.2	1.12	2.23	3.35	4.46	5.58	6.70	7.81	8.93	10.04	11.16
0.3	1.67	3.35	5.02	6.70	8.37	10.04	11.72	13.39	15.07	16.74
0.4	2.23	4.46	6.70	8.93	11.16	13.39	15.62	17.86	20.09	22.32
0.5	2.79	5.58	8.37	11.16	13.95	16.74	19.53	22.32	25.11	27.90
0.6	3.35	6.70	10.04	13.39	16.74	20.09	23.44	26.78	30.13	33.48

Table 5—10 Solar load per unit floor area for different combinations of g_{eff} and window area – East/West Facing Facade

g_{eff}	Window Area (%)									
	10	20	30	40	50	60	70	80	90	100
0.1	1.44	2.87	4.31	5.74	7.18	8.61	10.05	11.48	12.92	14.36
0.2	2.87	5.74	8.61	11.48	14.36	17.23	20.10	22.97	25.84	28.71
0.3	4.31	8.61	12.92	17.23	21.53	25.84	30.15	34.45	38.76	43.07
0.4	5.74	11.48	17.23	22.97	28.71	34.45	40.19	45.94	51.68	57.42
0.5	7.18	14.36	21.53	28.71	35.89	43.07	50.24	57.42	64.60	71.78
0.6	8.61	17.23	25.84	34.45	43.07	51.68	60.29	68.90	77.52	86.13
0.7	10.05	20.10	30.15	40.19	50.24	60.29	70.34	80.39	90.44	100.5

Table 5—11 Solar load per unit floor area for different combinations of g_{eff} and window area – South Facing Facade

g_{eff}	Window Area (%)									
	10	20	30	40	50	60	70	80	90	100
0.1	1.60	3.20	4.79	6.39	7.99	9.59	11.18	12.78	14.38	15.98
0.2	3.20	6.39	9.59	12.78	15.98	19.17	22.37	25.56	28.76	31.95
0.3	4.79	9.59	14.38	19.17	23.96	28.76	33.55	38.34	43.13	47.93
0.4	6.39	12.78	19.17	25.56	31.95	38.34	44.73	51.12	57.51	63.90
0.5	7.99	15.98	23.96	31.95	39.94	47.93	55.91	63.90	71.89	79.88
0.6	9.59	19.17	28.76	38.34	47.93	57.51	67.10	76.68	86.27	95.85

To categorise the solar gains into levels; low, medium and high, the solar load factors have been analysed. To achieve a low solar gain on the south façade it is assumed that either a small window area or a low g_{eff} will need to be achieved (10% window area and g_{eff} 0.6, $9.59 \text{ W}\cdot\text{m}^{-2}$, 60% window area and g_{eff} 0.1, $9.59 \text{ W}\cdot\text{m}^{-2}$). It is also assumed that when a 30% window area and a low emissivity double glazed window (g_{eff} 0.59) is selected that the solar gains ($28.76 \text{ W}\cdot\text{m}^{-2}$) should be classified as high. The levels for solar gains have therefore been set as:

$$\text{Low} \leq 10 < \text{Medium} \leq 20 < \text{High} \leq 30$$

Within the calculations for the design tool a window area and g_{eff} combination for each orientation has been selected to achieve $10 \text{ W}\cdot\text{m}^{-2}$ (low), $20 \text{ W}\cdot\text{m}^{-2}$ (medium) and $30 \text{ W}\cdot\text{m}^{-2}$ (high).

To reduce the differences in heat gains or losses through the glazing it has been chosen to try and fix the window area at an area that can be coupled with an effective g-value to achieve 10 , 20 and $30 \text{ W}\cdot\text{m}^{-2}$. A glazing area of 40% can achieve except for 20 and $30 \text{ W}\cdot\text{m}^{-2}$ on the North façade. It is only possible to achieve $20 \text{ W}\cdot\text{m}^{-2}$ with a window area of 60% and $30 \text{ W}\cdot\text{m}^{-2}$ with a window area of 90% . Therefore, to achieve these solar gains the window areas would have to be these sizes and the associated heat gains or losses associated with the larger window areas would be unavoidable.

The effective g-values have been interpolated for a glazing area of 40% for the East/West and South to achieve a solar load factor of 10, 20 and 30 $\text{W}\cdot\text{m}^{-2}$, and for a glazing area of 40%, 60% and 90% for the North to achieve 10, 20 and 30 $\text{W}\cdot\text{m}^{-2}$ respectively (see Table 5—12).

Table 5—12 Glazing areas and g_{eff} to achieve solar categories for each orientation

	Glazing Area (%)	g_{eff}
North		
- Low	40	0.45
- Medium	60	0.60
- High	90	0.60
East/West		
- Low	40	0.17
- Medium	40	0.35
- High	40	0.52
South		
- Low	40	0.16
- Medium	40	0.31
- High	40	0.47

To calculate the g value, based on the required g_{eff} values above, the inverse of factors to convert normal incidence g value to effective g value for double glazing have been used (see Table 5—13) (Littlefair, 2005).

Table 5—13 g-values for different solar gains and orientations

	Factor	g-value
North		
- Low	0.810	0.556
- Medium	0.810	0.733
- High	0.810	0.733
East/West		
- Low	0.918	0.185
- Medium	0.918	0.381
- High	0.918	0.566
South		
- Low	0.817	0.196
- Medium	0.817	0.379
- High	0.817	0.575

Therefore 4 different glazing combinations will be used to give g values of; 0.19, 0.38, 0.56 and 0.73 (

Table 5—14).

Table 5—14 Glazing configurations used within calculations for TMAir

	Window Area (%)	g-value
North		
- Low	40	0.56
- Medium	60	0.73
- High	90	0.73
East/West		
- Low	40	0.19
- Medium	40	0.38
- High	40	0.56
South		
- Low	40	0.19
- Medium	40	0.38
- High	40	0.56

The glazing configurations have been created by using the Building Regulations Approved Document Part L2A National Calculation Method (NCM) window construction within IES Virtual Environment as a template (Table 5—15). The values of transmittance and outside and inside reflectance have then been adjusted to achieve the required g-value.

Table 5—15 Glazing constructions used within IES for TMAir

Description	Thickness (m)	Conductivity ($\text{W}\cdot\text{m}^{-1}\cdot\text{K}^{-1}$)	Gas	Convection coefficient ($\text{W}\cdot\text{m}^{-2}\cdot\text{K}^{-1}$)	Resistance ($\text{m}^2\cdot\text{K}\cdot\text{W}^{-1}$)	Transmittance	Outside Reflectance	Inside Reflectance	Refractive Index	Outside emissivity	Inside emissivity
g-value 0.19											
NCM low-e 4mm	0.004	1.06				0.14	0.04	0.04	1.526	0.837	0.170
Cavity			Air	1.614	0.407						
NCM clear 4mm	0.004	1.06				0.82	0.07	0.07	1.526	0.837	0.837
g-value 0.38											
NCM low-e 4mm	0.004	1.06				0.37	0.05	0.05	1.526	0.837	0.170
Cavity			Air	1.614	0.407						
NCM clear 4mm	0.004	1.06				0.82	0.07	0.07	1.526	0.837	0.837
g-value 0.56											
NCM low-e 4mm	0.004	1.06				0.58	0.06	0.06	1.526	0.837	0.170
Cavity			Air	1.614	0.407						
NCM clear 4mm	0.004	1.06				0.82	0.07	0.07	1.526	0.837	0.837
g-value 0.73											
NCM low-e 4mm	0.004	1.06				0.79	0.08	0.08	1.526	0.837	0.170
Cavity			Air	1.614	0.407						

NCM clear 4mm	0.004	1.06				0.82	0.07	0.07	1.526	0.837	0.837
---------------	-------	------	--	--	--	------	------	------	-------	-------	-------

The window frame is assumed to be wood with an average thickness of 50mm with a U-value is $2.02 \text{ W}\cdot\text{m}^{-2}\cdot\text{K}^{-1}$ (CIBSE 2006a), the corresponding resistance is $0.3250 \text{ m}^2\cdot\text{K}\cdot\text{W}^{-1}$. The window frame is assumed to be 10% of the window area. The outside and inside surface resistances are set as default.

The CIBSE U-value for the glass only is $1.6719 \text{ W}\cdot\text{m}^{-2}\cdot\text{K}^{-1}$ and including the frame is $1.8019 \text{ W}\cdot\text{m}^{-2}\cdot\text{K}^{-1}$.

5.2.2.7 Building Thermal Weight

Rennie and Parand (1998) defined the thermal mass by the room admittance per m^2 floor area and categorised the different levels as: Very Light 6 to $8 \text{ W}\cdot\text{m}^{-2}\cdot\text{K}^{-1}$, Light 8 to $10 \text{ W}\cdot\text{m}^{-2}\cdot\text{K}^{-1}$, Heavy 14 to $18 \text{ W}\cdot\text{m}^{-2}\cdot\text{K}^{-1}$ and Very Heavy 18 to $24 \text{ W}\cdot\text{m}^{-2}\cdot\text{K}^{-1}$.

To give a fair representation of this spectrum four typical groups of construction have been created allowing the user to select the level of thermal mass (Table 5—16 and Figure 5—9).

Table 5—16 Admittance values to be used in the development of TMAir

Element	Very Lightweight (VLW)	Lightweight (LW)	Heavyweight (HW)	Very Heavyweight (VHW)
External Wall	0.85	2.73	5.53	5.53
Internal Wall	0.75	2.65	4.13	4.13
Floor	2.57	2.57	2.72	6.26
Ceiling	2.86	2.86	6.09	6.13
Admittance per m^2 floor area	6.39	8.78	14.39	17.96

The amount of insulation in the external walls has been set to achieve a CIBSE U-value of $0.35 \text{ W.m}^{-2}.\text{K}^{-1}$, which is the limiting area weighted average U-value required to meet the requirements of Building Regulations Approved Documents Part L2A for England and Wales (OPDM, 2006).

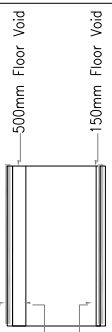
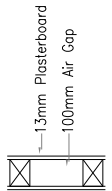
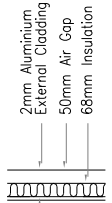
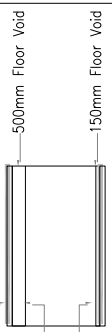
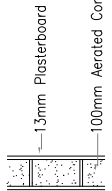
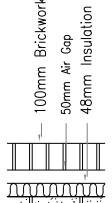
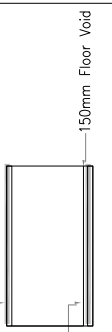
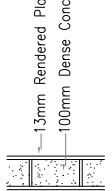
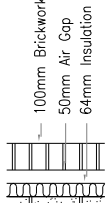
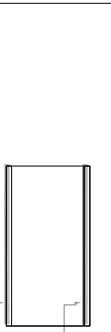
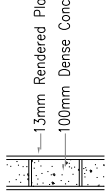

Element Weight	Floor & Ceiling	Internal Partitions	External Walls
Very Light	 <p>200mm Concrete Floor 15mm Suspended Ceiling 30mm Suspended Floor with Carpet Finish 500mm Floor Void 150mm Floor Void</p>	 <p>13mm Plasterboard 100mm Air Gap</p>	 <p>13mm Plasterboard 2mm Aluminium External Cladding 50mm Air Gap 68mm Insulation</p>
Light	 <p>200mm Concrete Floor 15mm Suspended Ceiling 30mm Suspended Floor with Carpet Finish 500mm Floor Void 150mm Floor Void</p>	 <p>13mm Plasterboard 100mm Aerated Concrete Block</p>	 <p>13mm Plasterboard 100mm Aerated Concrete Block 50mm Air Gap 48mm Insulation</p>
Heavy	 <p>200mm Concrete Floor 30mm Suspended Floor with Carpet Finish 150mm Floor Void</p>	 <p>13mm Rendered Plaster 100mm Dense Concrete Block</p>	 <p>13mm Rendered Plaster 100mm Brickwork 50mm Air Gap 64mm Insulation</p>
Very Heavy	 <p>200mm Concrete Floor 15mm Marble Tiles 20mm Tile Bedding 65mm Screed 150mm Floor Void</p>	 <p>13mm Rendered Plaster 100mm Dense Concrete Block</p>	 <p>13mm Rendered Plaster 2mm Aluminium External Cladding 50mm Air Gap 67mm Insulation</p>

Figure 5—9 Constructions to be used in the development of TMAir

Table 5—17 shows the materials and their properties (CIBSE 2006a) and Table 5—18 shows the construction properties (CIBSE 2006a).

Table 5—17 Material properties to be used in the development of the TMAir

Material	Density (kg.m ⁻³)	Thermal Conductivity (W.m ⁻¹ .K ⁻¹)	Specific Heat Capacity (J.kg ⁻¹ .K ⁻¹)
Aerated Concrete Block	750	0.24	1000
Aluminium Cladding	7680	45	420
Cast Concrete	2000	1.33	1000
Dense Concrete Block	2240	1.31	840
External Brickwork	1700	0.84	800
Limestone	2180	1.5	720
Marble	2750	2.9	840
Perforated Ceiling	2700	230	880
Plaster Ceiling Tiles	1120	0.38	840
Plasterboard	950	0.16	840
Polyurethane Insulation	30	0.028	1470
Pre-cast concrete	2300	1.9	840
PVC	1380	0.16	1000
Rendered Plaster, Sand Aggregate	1680	0.82	840
Screed	1200	0.41	840
Suspended Floor - particle board (28mm)	630	0.12	2260
- stainless steel (1mm top & bottom)	7850	29	480
Synthetic Carpet	200	0.6	1300
Tile bedding	2100	1.4	840

Table 5—18 Construction properties to be used in the development of the TMAir

	CIBSE U-Value (W.m ⁻² .K ⁻¹)	Emissivity		Solar Absorptance	
		Inside	Outside	Inside	Outside
External Walls					
VLW	0.35	0.91	0.72	0.5	0.65
LW	0.35	0.91	0.85	0.5	0.63
HW	0.35	0.91	0.85	0.5	0.63
VHW	0.35	0.91	0.72	0.5	0.65
Internal Partitions					
VLW	1.70	0.91	0.91	0.50	0.50
LW	1.21	0.91	0.91	0.50	0.50
HW	2.83	0.91	0.91	0.50	0.50
VHW	2.83	0.91	0.91	0.50	0.50
Internal Ceilings/Floors					
VLW	1.00	0.91	0.89	0.50	0.55
LW	1.00	0.91	0.89	0.50	0.55
HW	1.28	0.94	0.89	0.56	0.55
VHW	2.81	0.94	0.93	0.56	0.59

5.2.2.8 Orientation

Although the selected solar gains controls the amount of solar heat gain to the space, the orientation still effects the time of day that the gains are experienced by the room.

Orientations of North, East, South or West can be compared.

5.2.3 Additional Options

Additional to the main user selected parameters described above, the user can also select options that will affect the amount of energy consumed by the fan and the amount of energy consumed for heating and cooling.

	A	B	C	D	E	F	G	H
13								
14		Supply System Pressure (Pa)	1000	1000	1000	1000	1000	
15		Return System Pressure (Pa)	700		700	700	700	
16		Fan Total Efficiency (%)	80		80	80	80	
17		Fan Motor Efficiency (%)	80		80	80	80	
18		Boiler Efficiency (%)	85	85	85	85	85	
19		CSOP	2.8	2.8	2.8	2.8	2.8	
20								
21								
22								
23								

Figure 5—10 Additional options within TMAir

The system pressure and the fan efficiency alter the energy consumption of the fan. If it is known at the early stages of design that long lengths of ductwork will be needed or energy efficient fans are to be used this will greatly effect the energy consumption. The system pressure and the fan efficiency can therefore be selected by the user.

The boiler efficiency and chiller coefficient of seasonal performance together with the distribution losses directly effect the energy consumption and can also be selected by the user.

5.3 Simulation Settings

Within APACHE Simulation there are a number of simulation choices that determine the way that the simulations are carried out. The selected choices are summarised in Table 5—19.

Table 5—19 Simulation settings

Simulation Parameter	Simulation Option Selected
External Convection Model	McAdams empirical equations model the external convective heat transfer coefficient dependent on wind speed
Internal Convection Model	CIBSE variable values have been used because convection coefficients are calculated as a function of surface orientation, air-surface temperature difference and mean room air velocity as part of an iterative procedure (CIBSE 2007).
Sky and Ground Long Wave Radiation Model	On - The most significant effect of air emissivity is its influence on radiant temperature and the absorption of long-wave radiation (IES, 2008)
Internal Air Emissivity Model	On
Solar Radiation Model	Anisotropic - Anisotropic diffuse radiation model applies a model where the intensity of the radiation is greater in the region near the sun, whereas an isotropic model only treats the diffuse component of solar radiation as radiating with equal intensity from all parts of the sky vault (IES, 2008).
Simulation Time Step	10 minute time step.
Reporting Interval	The results of interest will not be rapidly changing and hourly values will give accurate results whilst reducing the amount of data to be handled within the design tool
Preconditioned Period	30 days.

5.4 Description Of Output Results

The output results from TMAir are presented on two levels; summary results and detailed results.

5.4.1 Summary Results

The summary results are a single page printout intended to give a quick snapshot of the performance of the different options. The results are presented in a graphical format of the actual values and in a tabular format that express the results as a percentage of the BASE Case Option 1 allowing quick comparison between the different options.

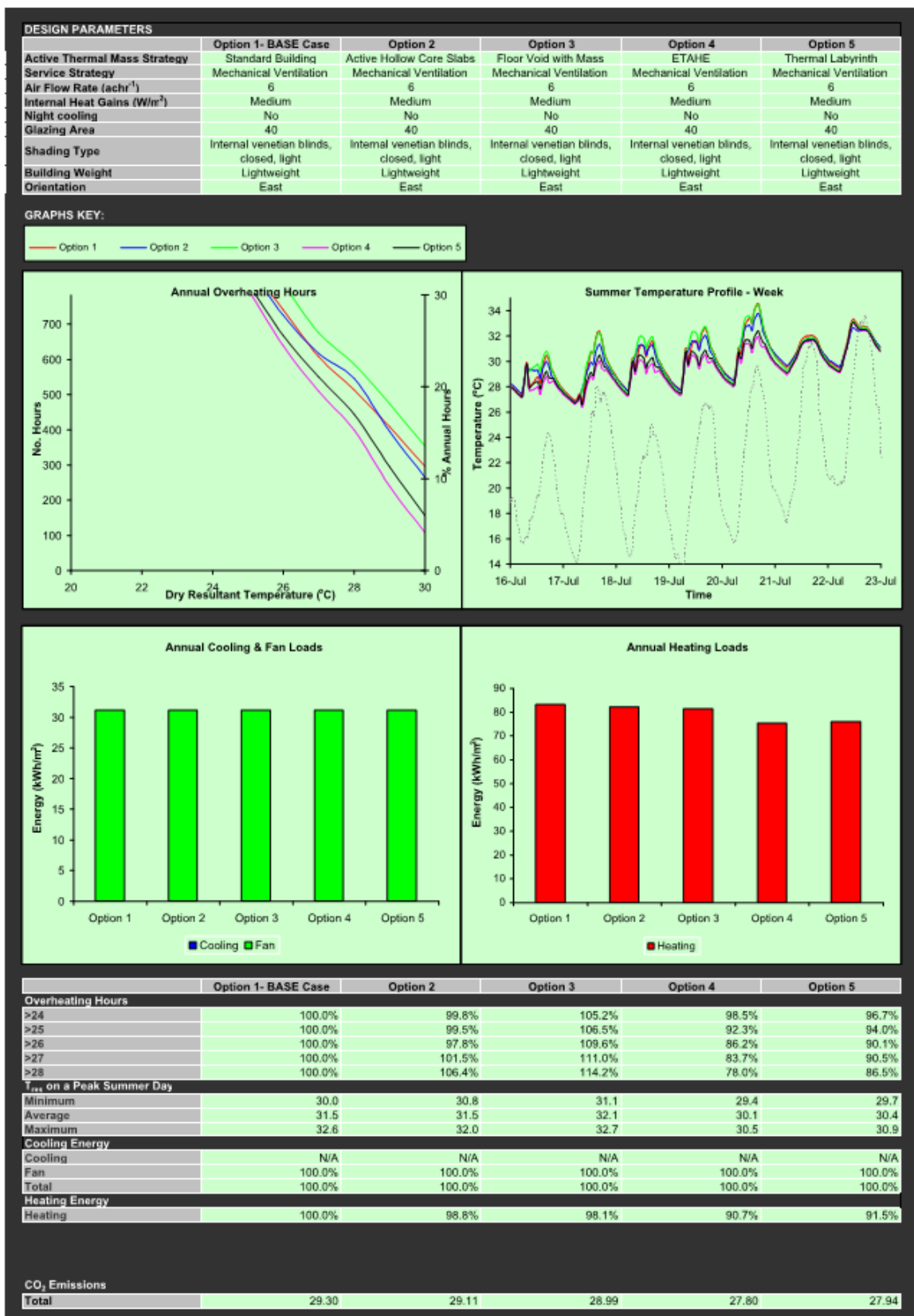


Figure 5—11 TMAir Summary Results single page printout

5.4.1.1 Heating Energy Demand

The heating energy demand presented is the energy (normalised per m² floor area) required to maintain the test room air temperature above the heating setpoint (21°C) during the occupied hours for a full year.

5.4.1.2 Cooling Energy Demand

The cooling energy demand presented is the energy (normalised per m² floor area) required to maintain the test room air temperature below the cooling set point (24°C) during the occupied hours for a full year.

Only applies if comfort cooling is selected.

5.4.1.3 Overheating Hours

The overheating hours presented are the number of hours the dry resultant temperature in the test room exceeds 24, 25, 26, 27 and 28°C.

5.4.1.4 Fan Energy Demand

The fan energy demand presented is the energy required to run the fan to supply the air to the test room. This allows the benefits of adding night cooling to be compared against the additional energy required by the fan.

The fan power is calculated from (CIBSE, 2005a):

$$w_f = \frac{p_{tF} Q}{\eta_t} \quad \text{Equation 5-3}$$

Where:

p_{tF} fan total pressure (N.m⁻²)

Q volumetric airflow rate (m³.s⁻¹)

η_t total fan efficiency

5.4.2 Detailed Results

To allow the user to look at the results in more detail there is a separate page for heating energy, cooling energy and overheating hours that break the results down into monthly energy consumption and looks at the energy and room temperatures during a peak week and a peak day. The results are again presented in a graphical format for the actual results and in a tabular format that express the results as a percentage of the BASE Case Option 1.

5.5 Summary

This chapter 5 described the methodology used for the development of a concept design tool to help designers analyse the effects, in terms of energy and comfort, of integrating active thermal mass strategies into office buildings for a range of design parameters. The tool was developed using South East England (Heathrow) weather data and typical construction details for office buildings in the UK

The results from simulations using a calibrated dynamic thermal model have been used to create a database within Microsoft Excel. The user can select one BASE Case Option and four other options for comparison.

The results are then presented in two levels; summary results and detailed results:

- (i) Summary results - present the heat energy demand, cooling energy demand, fan energy demand normalised per m² floor area together with overheating hours in a graphical format of the actual values and in a tabular format that express the results as a percentage of the base option allowing quick comparison between the different options.
- (ii) Detailed results - to allow the user to look at the results in more detail there is a separate page for heating energy, cooling energy and overheating hours that break the results down into monthly energy consumption and looks at the energy and room temperatures during a peak week and a peak day. The results

are again presented in a graphical format for the actual results and in a tabular format that express the results as a percentage of the base option.

This chapter 6 and the following three chapters present the analysis of the results to identify the benefit that adding the active thermal mass strategies have compared to the standard strategy. Each strategy will be looked at in turn for the five parameters mentioned in the previous paragraph; the actual results for each strategy are presented in Appendix A. These are presented in terms of annual overheating hours, annual cooling load and annual heating load.

TMAir will now be used to carry out a parametric analysis to look at the impact of changing the user selected parameters. The actual results for each strategy are presented in Appendix A.

The next chapter 6, will present the results of the hollow core slab strategy in comparison to the standard strategy

6.0 HOLLOW CORE SLAB MODEL: RESULTS AND ANALYSIS

6.1 Introduction

The previous chapter 5 presented the development of the concept design tool, TMAir, and its parameters. Using TMAir a parametric analysis can be performed for the standard model and each of the four active thermal mass strategies to investigate the effect of (a) thermal mass (b) night cooling, (c) solar gain (d) internal gain and (e) air change rate on the performance of the strategy. The performance is analysed in terms of (a) number of overheating hours (b) annual cooling load and (c) annual heating load. The results of this parametric analysis are presented in Appendix A, starting with the standard model and continuing with the hollow core slab (HCS), floor void with mass (FVWM), air-to-earth heat exchanger (ETAHE) and finally thermal labyrinth (TL).

This chapter 6 and the following three chapters present the analysis of the results to identify the benefit that adding the active thermal mass strategies have compared to the standard strategy. Each strategy will be looked at in turn for the five parameters mentioned in the previous paragraph; the actual results for each strategy are presented in Appendix A. These are presented in terms of annual overheating hours, annual cooling load and annual heating load.

In this chapter the results of the hollow core slab model are presented as a percentage of the standard strategy. The T_{res} maximum is presented as a difference from the standard strategy. Chapters 7, 8 and 9 present the results of the other three investigated active thermal mass strategies in a similar way, while chapter 10 discusses all results together.

6.2 Overheating Hours

6.2.1 Thermal Mass

Comparing the results of the different levels of thermal mass for the Standard and HCS strategies show that for all levels of thermal mass the HCS strategy increases the annual overheating hours (Figure 6—1). The T_{res} maximum is reduced for the VLW and LW test rooms, but remains the same for the HW and VHW rooms.

The number of overheating hours are increased by 4.3% and 6.4% for the VLW and LW test rooms and by 12.8% and 16.9% for the HW and VHW test rooms.

The T_{res} maximum is reduced by 0.4°C and 0.3°C for the VLW and LW rooms. The T_{res} maximum remains the same for the HW and VHW rooms.

On a peak summer day, passing the supply air through the hollow core slab results in the air being heated for the full day (appendix A). The HCS strategy exposes the underside of the hollow core slab to the room below. Looking at the surface temperature of the ceiling for the standard and HCS strategies on a peak summer day show the dampening effect the exposed slab has on the surface temperature (Figure 6—3). The reduction in T_{res} maximum is therefore as a result of adding the exposed concrete soffit to the room.

The T_{res} maximum for the HW and VHW remain the same due to the supply air temperature leaving the core being only slightly higher than that entering the slab (the same temperature as the supply air for the standard strategy) at the time of T_{res} maximum.

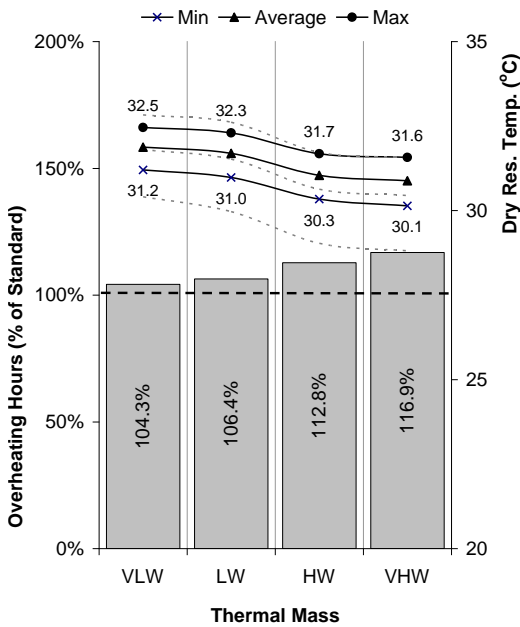


Figure 6—1 HCS vs Standard Strategy Annual Overheating Hours – Thermal Mass

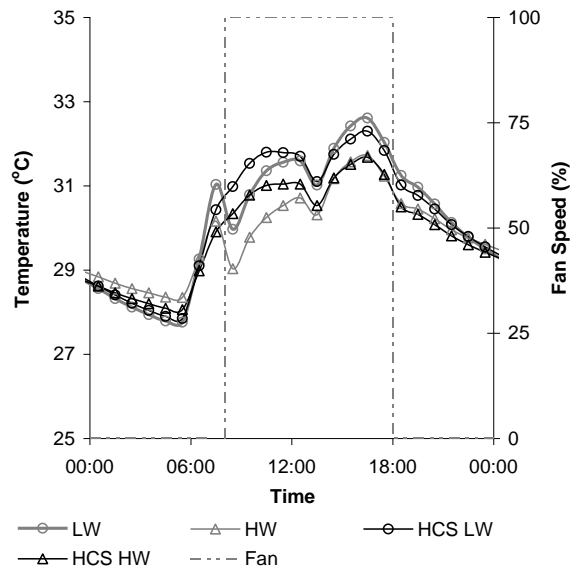


Figure 6—2 HCS vs Standard Strategy T_{res} on a peak summer day – Thermal Mass

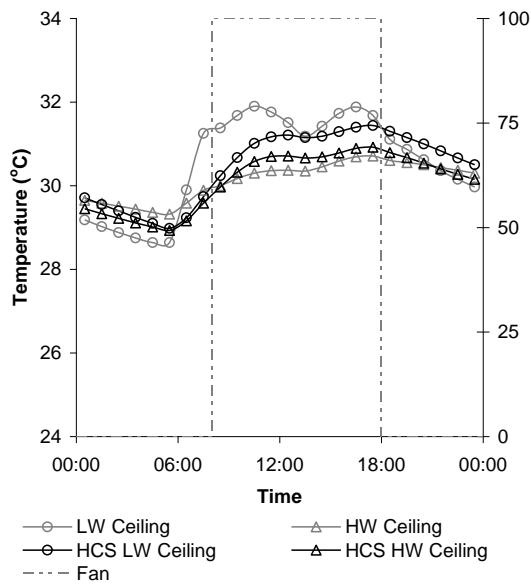


Figure 6—3 HCS vs Standard Strategy Ceiling Surface Temperature – Thermal Mass

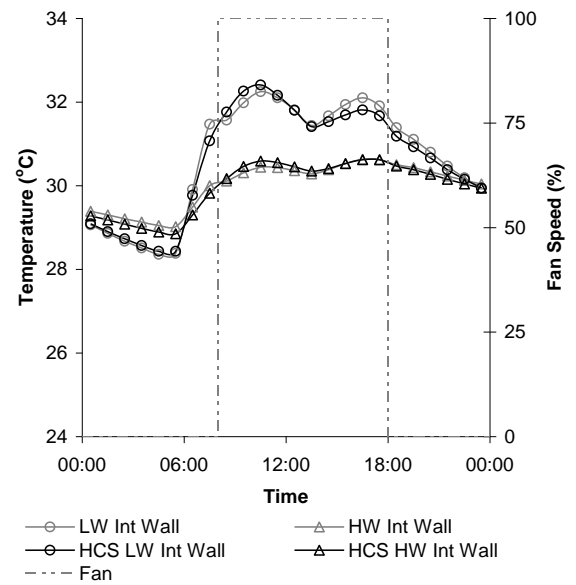


Figure 6—4 HCS vs Standard Strategy Internal Wall Surface Temperature – Thermal Mass

6.2.2 Thermal Mass with Night Cooling

Comparing the results with night cooling of the different levels of thermal mass for the Standard and HCS strategies show that for all, but the VHW levels of thermal mass the annual overheating hours are reduced (Figure 6—5). The T_{res} maximum on a peak summer day is also reduced for all but the VHW room (Figure 6—6).

The number of overheating hours are reduced by 13.7% and 16.5% for the VLW and LW test rooms. The number of overheating hours are reduced by 3.0% for the HW test room and increased by 5.0% for the VHW test room.

The T_{res} maximum is reduced by 0.9°C for the VLW and LW rooms and by 0.3°C and 0.2°C for the HW and VHW rooms.

The T_{res} maximum on a peak summer day is reduced for the HW and VHW test rooms as a result of the supply air being cooled in the late afternoon by the hollow core slab. The additional reduction for the VLW and LW rooms is again as a result of the exposed concrete soffit of the HCS strategy.

The HCS strategy doesn't allow the test room to be cooled as much as the standard strategy due to the core being cooled by the air, resulting in the air entering the room during the night being hotter.

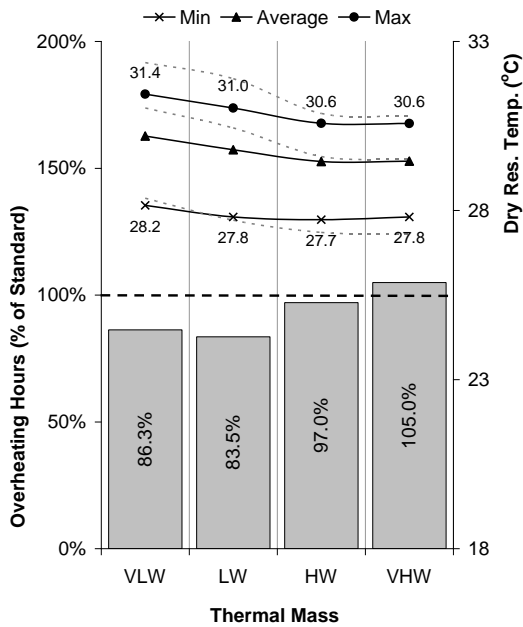


Figure 6—5 HCS vs Standard Strategy Annual Overheating Hours – Thermal Mass with Night Cooling

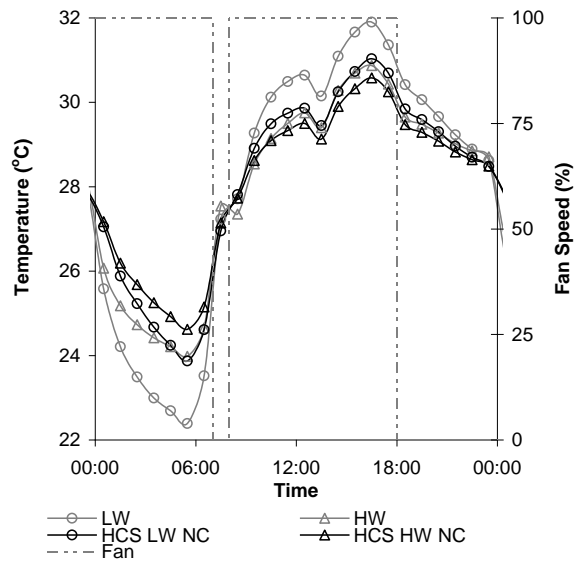
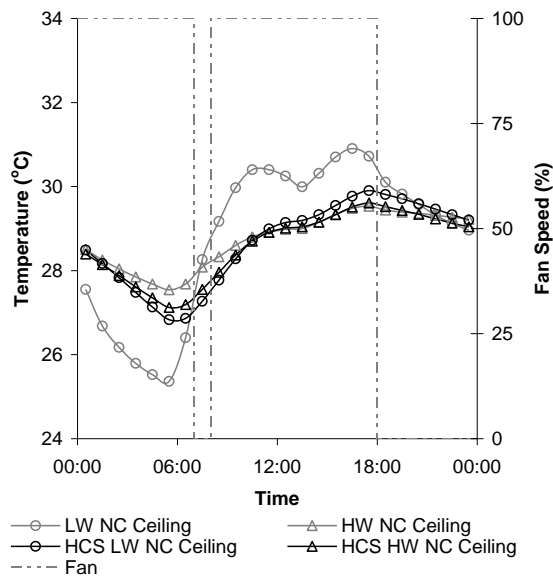


Figure 6—6 HCS vs Standard Strategy T_{res} on a peak summer day – Thermal Mass with Night Cooling



**Figure 6—7 HCS vs Standard Strategy
Ceiling Surface Temperature – Thermal
Mass with Night Cooling**

6.2.3 Solar Gains

Comparing the results of the different levels of solar gain for the Standard and HCS strategies show that for all levels of solar gain the annual overheating hours are increased (Figure 6—8). However, for all levels of solar gain the T_{res} maximum on a peak summer day is reduced (Figure 6—9).

The number of overheating hours are increased by 2.7% for the low solar gain test room, 7.6% for the medium solar gain test room and 6.4% for the high solar gain test room.

The T_{res} maximum is reduced by 0.5°C for the low solar gain test room, by 0.4°C for the medium solar gain test room and by 0.3°C for the high solar gain test rooms.

A greater reduction in the T_{res} maximum is found as the solar gains are reduced because reducing the solar gains reduces the surface temperature of the ceiling, which in turn

reduces the supply air temperature leaving the hollow core slabs. This lower supply air temperature

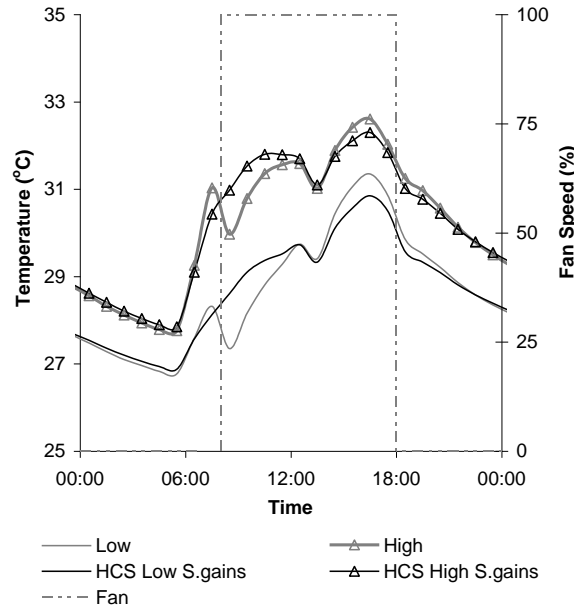
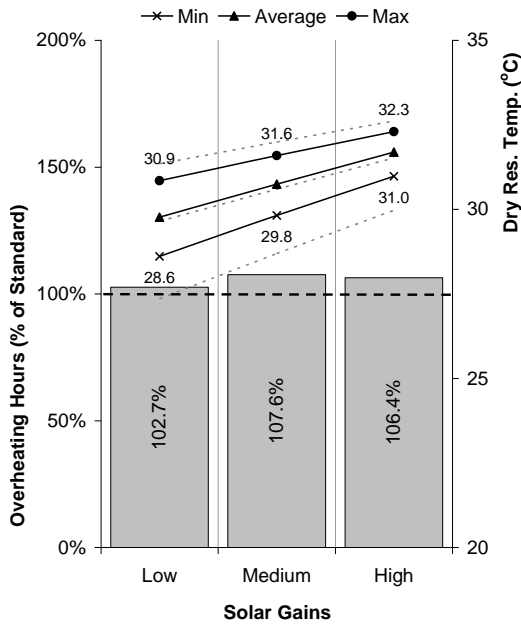


Figure 6—8 HCS vs Standard Strategy Annual Overheating Hours – Solar Gain

Figure 6—9 HCS vs Standard Strategy T_{res} on a peak summer day – Solar Gain

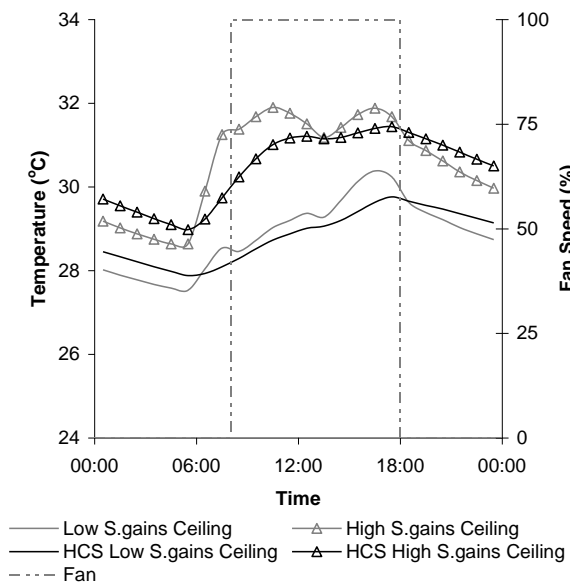


Figure 6—10 HCS vs Standard Strategy Ceiling Surface Temperature – Solar Gain

6.2.4 Internal Gains

Comparing the results of the different levels of internal gain for the Standard and HCS strategies show that the annual overheating hours for all levels of internal gain are increased (Figure 6—11). However, for all levels of internal gain the T_{res} maximum on a peak summer day is reduced (Figure 6—12).

The number of overheating hours are increased by 6.8% for the low internal gain test room, 6.4% for the medium internal gain test room and 2.4% for the high internal gain test room.

The T_{res} maximum is reduced by 0.3°C for the low and medium internal gain test rooms and by 0.4°C high internal gain test rooms.

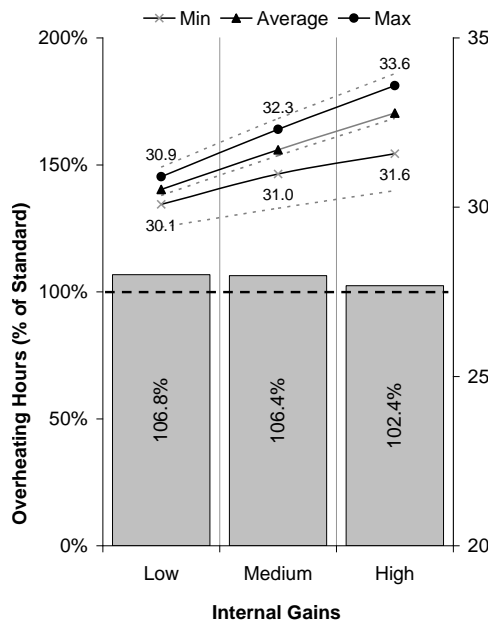


Figure 6—11 HCS vs Standard Strategy Annual Overheating Hours – Internal Gain

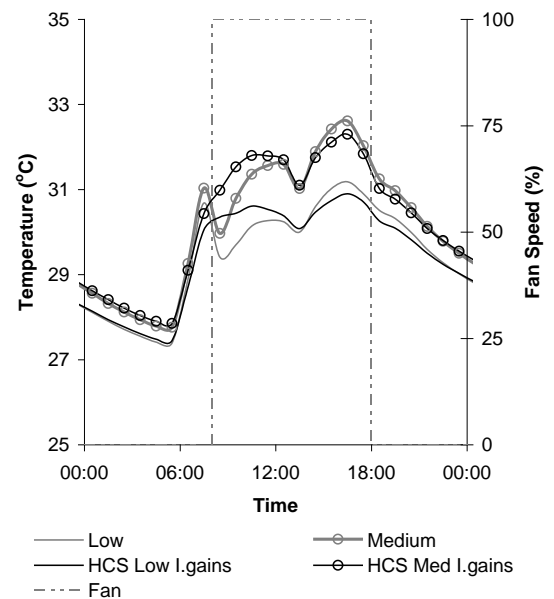
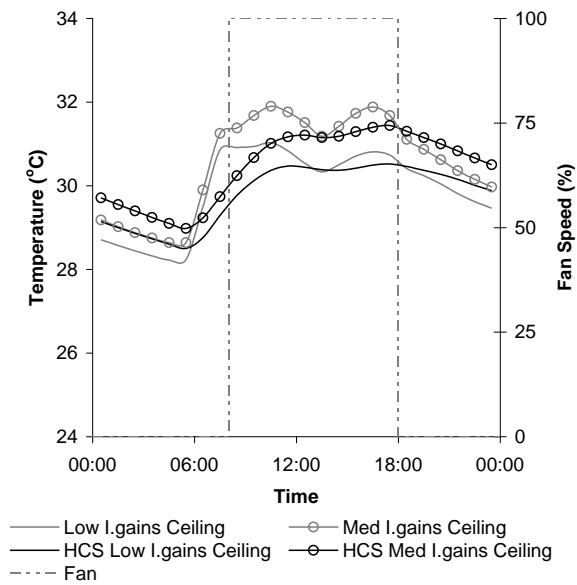


Figure 6—12 HCS vs Standard Strategy T_{res} on a peak summer day – Internal Gain



**Figure 6—13 HCS vs Standard Strategy
Ceiling Surface Temperature – Internal Gain**

6.2.5 Air Change Rate

Comparing the results of the different levels of air change rate for the Standard and HCS strategies show that the annual overheating hours for all levels of air change rate are increased (Figure 6—14). However, for all levels of air change rate the T_{res} maximum on a peak summer day is reduced (Figure 6—15).

The number of overheating hours are increased by 6.4% for the test room with 6ach^{-1} , 4.2% for the test room with 8ach^{-1} and 2.2% for the test room with 10ach^{-1} .

For 6ach^{-1} T_{res} maximum is reduced by 0.3°C . For medium 8ach^{-1} T_{res} maximum is reduced by 0.4°C . For medium 10ach^{-1} T_{res} maximum is reduced by 0.5°C .

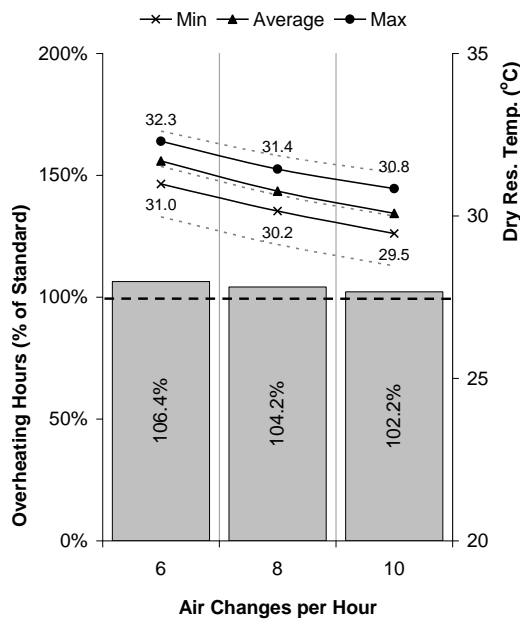


Figure 6—14 HCS vs Standard Strategy Annual Overheating Hours – Air Change Rate

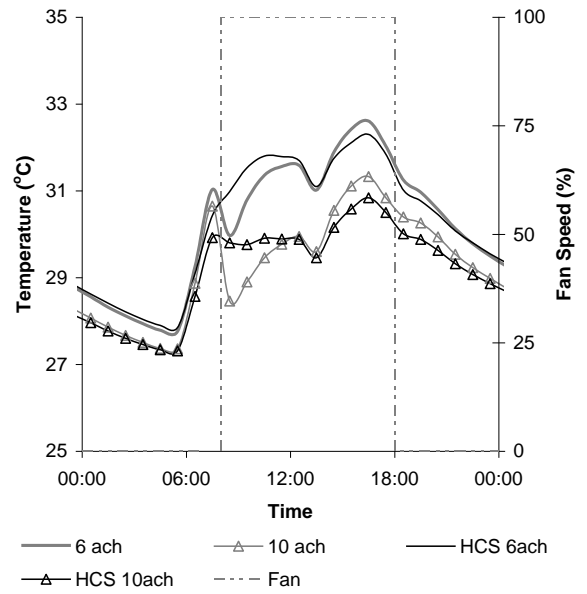


Figure 6—15 HCS vs Standard Strategy T_{res} on a peak summer day – Air Change Rate

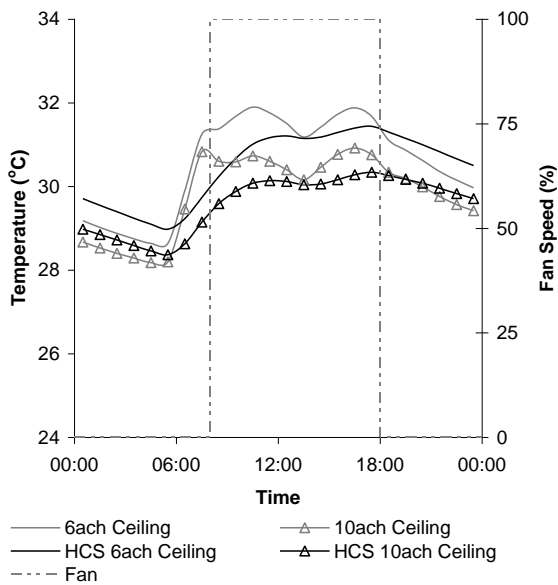


Figure 6—16 HCS vs Standard Strategy Ceiling Surface Temperature – Air Change Rate

6.3 Annual Cooling Load

6.3.1 Thermal Mass

Comparing the results of the different levels of thermal mass for the Standard and HCS strategies show that for all levels of thermal mass the annual cooling load is increased (Figure 6—17). The T_{res} maximum on a peak summer day is also increased for all levels of thermal mass (Figure 6—18).

The annual cooling load is increased by 14.8% and 14.9% for the VLW and LW test rooms and by 21.0% and 25.2% for the HW and VHW test rooms.

The T_{res} maximum is increased by 0.3°C and 0.4°C for the VLW and LW rooms and by 0.8°C and 1.0°C for the HW and VHW rooms.

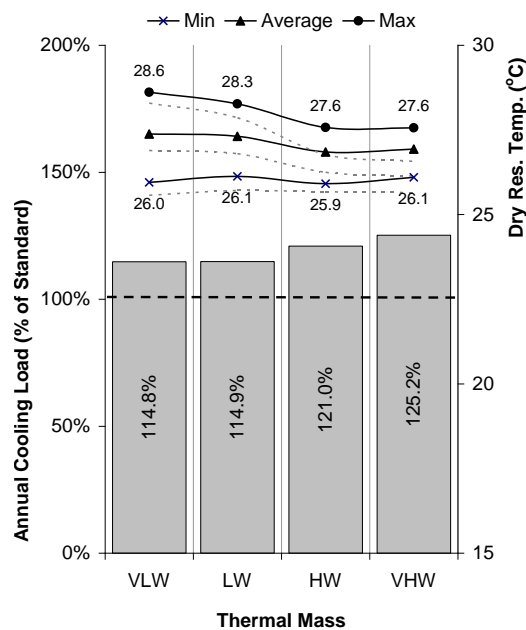


Figure 6—17 HCS vs Standard Strategy Annual Cooling Load– Thermal Mass

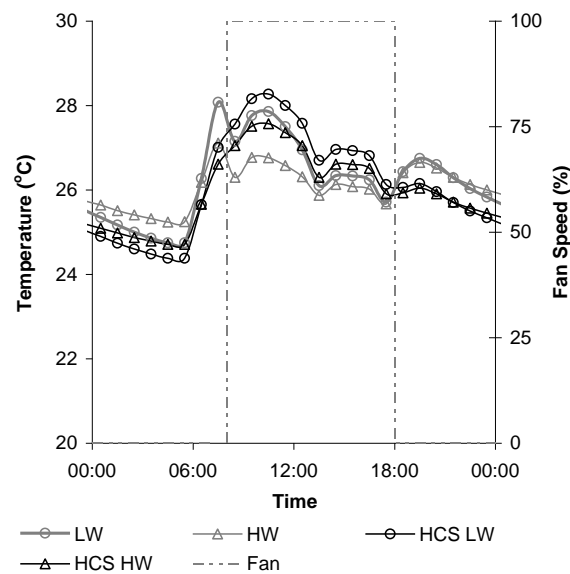


Figure 6—18 HCS vs Standard Strategy with cooling T_{res} on a peak summer day – Thermal Mass

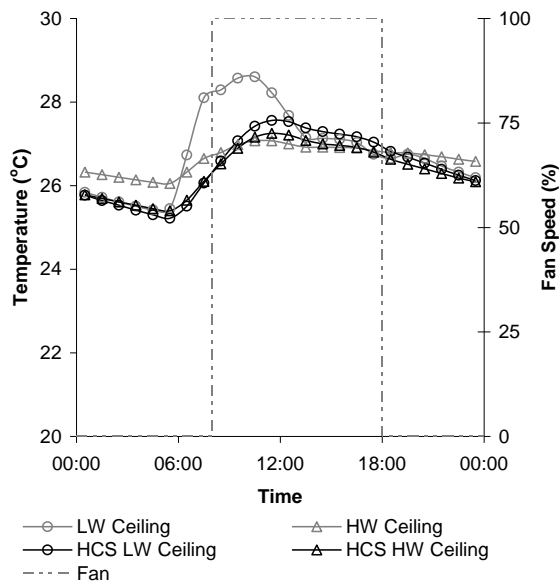


Figure 6—19 HCS vs Standard Strategy with Cooling Ceiling Surface Temperature – Thermal Mass

6.3.2 Thermal Mass with Night Cooling

Comparing the results of the different levels of thermal mass with night cooling for the Standard and HCS strategies show that for all levels thermal mass the annual cooling load is increased (Figure 6—20). The T_{res} maximum on a peak summer day is reduced for the VLW and LW test rooms (Figure 6—21).

The annual cooling load is increased by 6.7% and 7.5% for the VLW and LW test rooms and by 14.4% and 21.7% for the HW and VHW test rooms..

The T_{res} maximum is reduced by 0.5°C and 0.3°C for the VLW and LW rooms. The T_{res} maximum is increased by 0.2°C and 0.4°C for the HW and VHW rooms.

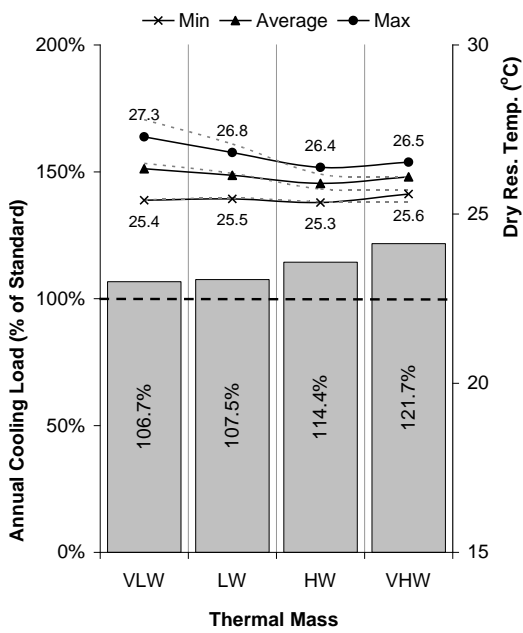


Figure 6—20 HCS vs Standard Strategy Annual Cooling Load– Thermal Mass with Night Cooling

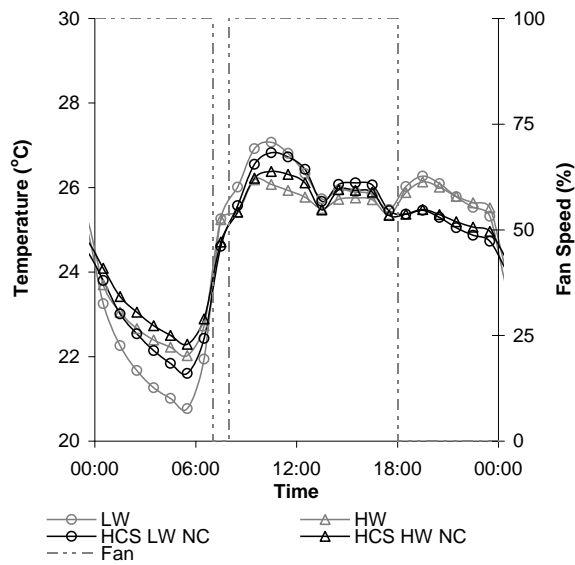


Figure 6—21 HCS vs Standard Strategy with cooling T_{res} on a peak summer day – Thermal Mass with Night Cooling

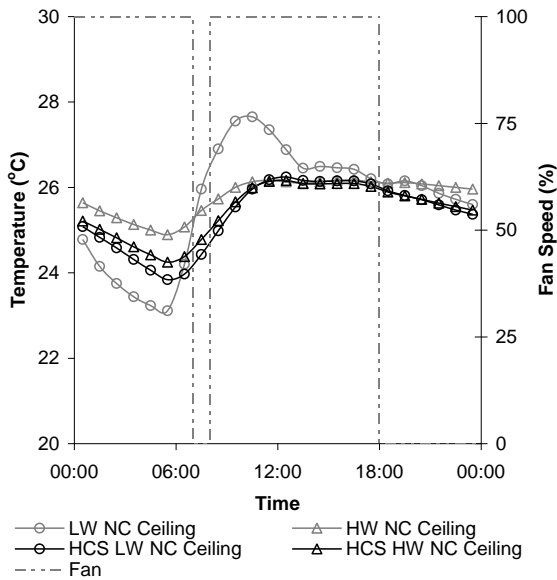


Figure 6—22 HCS vs Standard Strategy with Cooling Ceiling Surface Temperature – Thermal Mass with Night Cooling

6.3.3 Solar Gains

Comparing the results of the different levels of solar gain for the Standard and HCS strategies show that for all levels of solar gain the annual cooling load is increased (Figure 6—23). The T_{res} maximum on a peak summer day for all levels of solar gain is also increased (Figure 6—24).

The annual cooling load is increased by 24.4% for the low internal gain test room, 19.4% for the medium internal gain test room and 14.9% for the high internal gain test room.

The T_{res} maximum is increased by 0.1°C for the low solar gain test room and by 0.4°C for the medium and high solar gain test rooms.

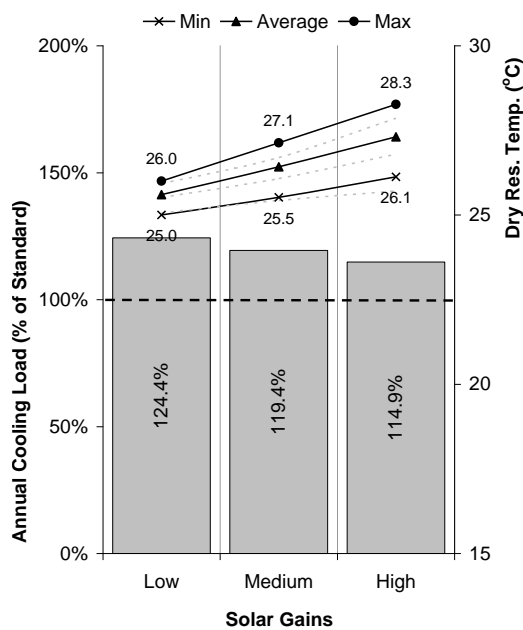


Figure 6—23 HCS vs Standard Strategy Annual Cooling Load– Solar Gain

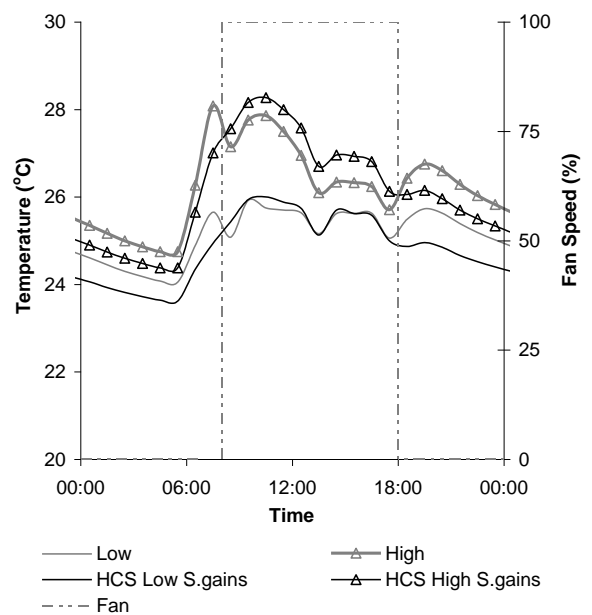


Figure 6—24 HCS vs Standard Strategy with cooling T_{res} on a peak summer day – Solar Gain

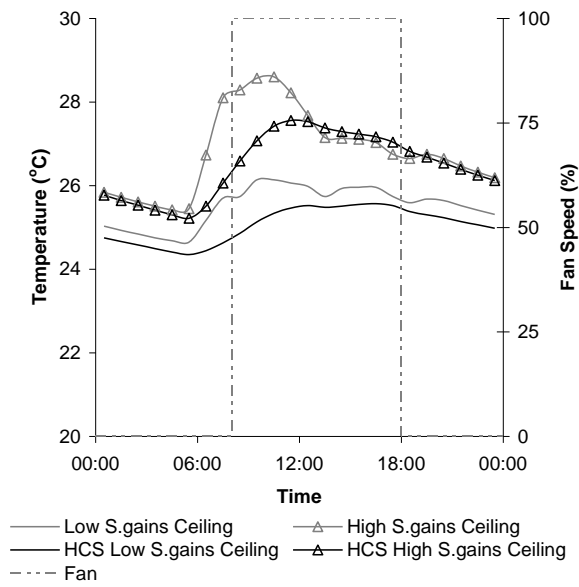


Figure 6—25 HCS vs Standard Strategy with Cooling Ceiling Surface Temperature – Solar Gain

6.3.4 Internal Gains

Comparing the results of the different levels of internal gain for the Standard and HCS strategies show that for all levels of internal gain the annual cooling load is increased (Figure 6—26). The T_{res} maximum on a peak summer day for all levels of internal gain is also increased (Figure 6—27).

The annual cooling load is increased by 24.5% for the low internal gain test room, 14.9% for the medium internal gain test room and 8.6% for the high internal gain test room.

The T_{res} maximum is increased by 0.4°C for all levels of internal gain.

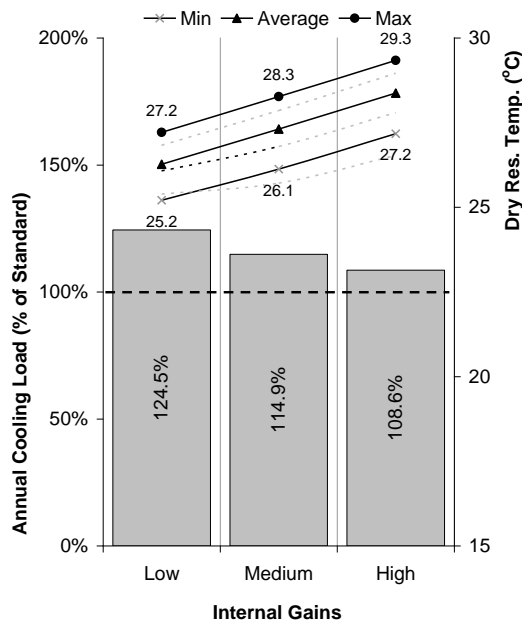


Figure 6—26 HCS vs Standard Strategy Annual Cooling Load– Internal Gain

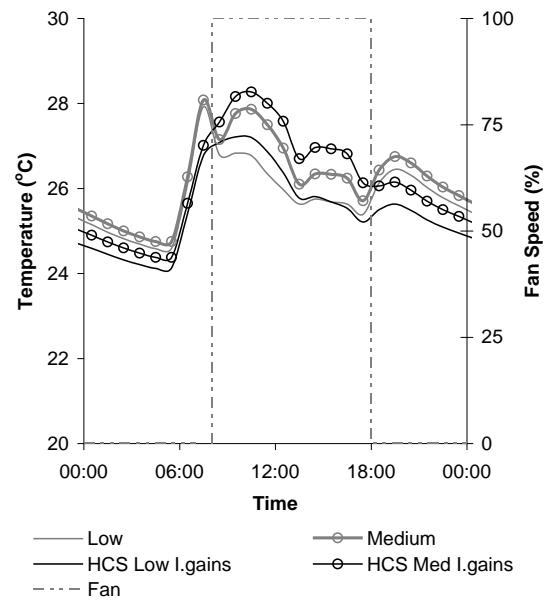


Figure 6—27 HCS vs Standard Strategy with cooling T_{res} on a peak summer day – Internal Gain

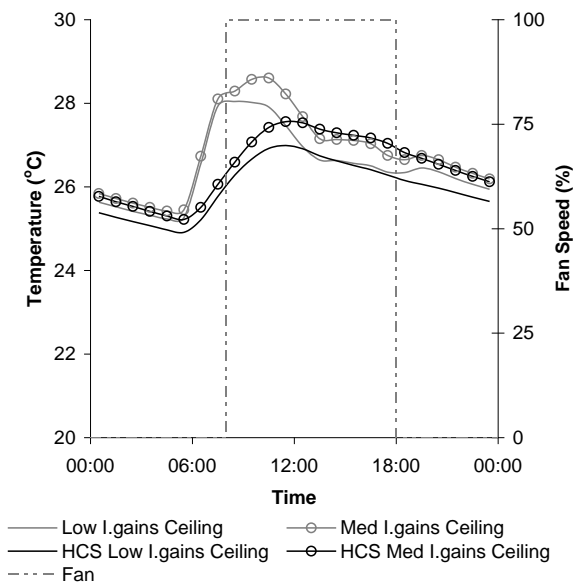


Figure 6—28 HCS vs Standard Strategy with Cooling Ceiling Surface Temperature – Internal Gain

6.3.5 Air Change Rate

Comparing the results of the different levels of air change rate for the Standard and HCS strategies show that for all levels of air change rate the annual cooling load is increased (Figure 6—29). The T_{res} maximum on a peak summer day for all levels of air change rate is also increased (Figure 6—30).

The annual cooling load is increased by 14.9% for the test room with 6ach^{-1} , 22.1% for the test room with 8ach^{-1} and 24.2% for the test room with 10ach^{-1} .

For 6ach^{-1} T_{res} maximum is increased by 0.4°C . For medium 8ach^{-1} T_{res} maximum is increased by 0.3°C . For medium 10ach^{-1} T_{res} maximum remains the same.

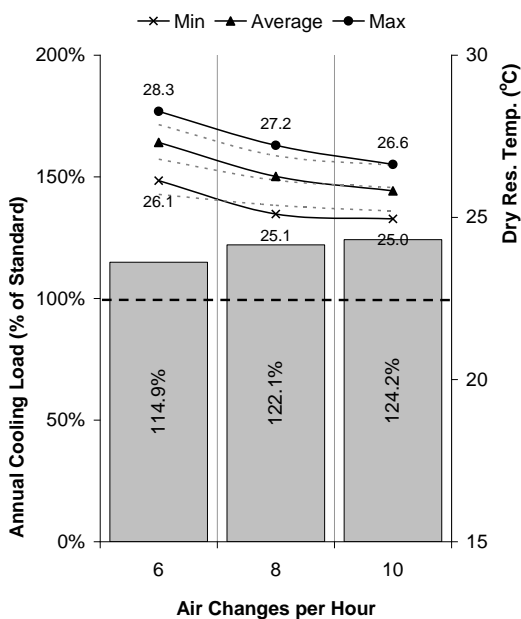


Figure 6—29 HCS vs Standard Strategy Annual Cooling Load– Air Change Rate

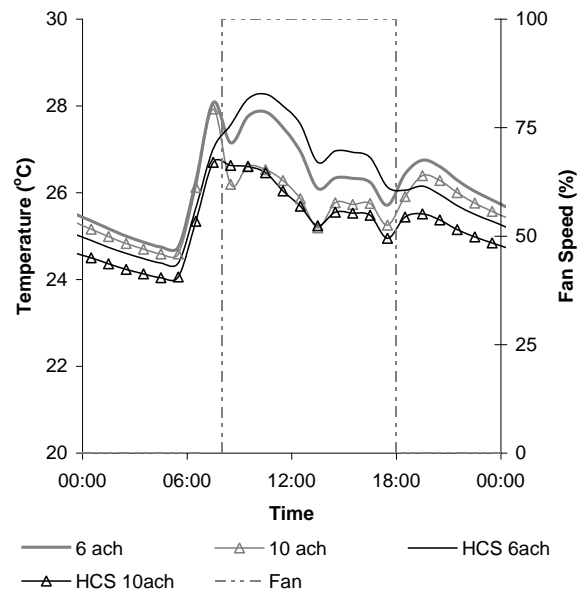


Figure 6—30 HCS vs Standard Strategy with cooling T_{res} on a peak summer day – Air Change Rate

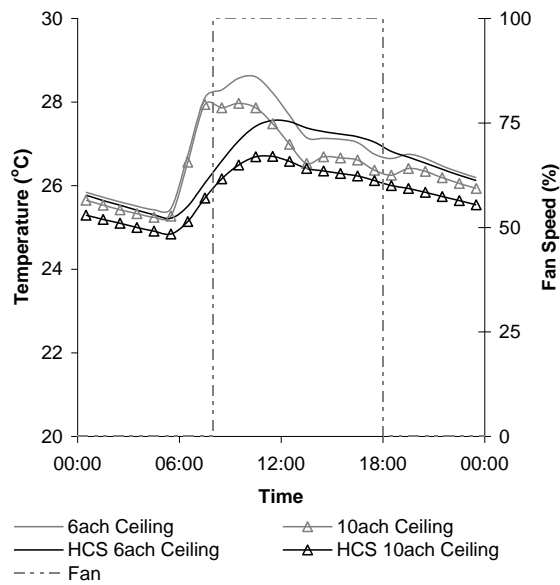


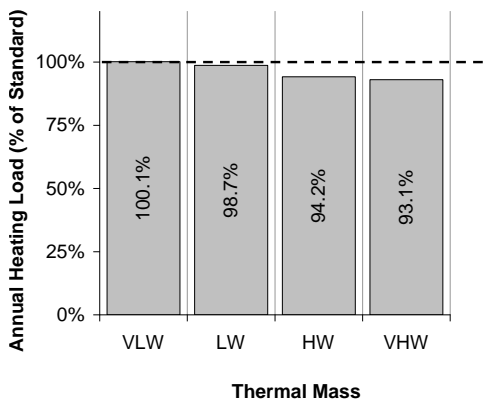
Figure 6—31 HCS vs Standard Strategy with Cooling Ceiling Surface Temperature – Air Change Rate

6.4 Annual Heating Load

6.4.1 Thermal Mass

Comparing the results of the different levels of thermal mass for the Standard and HCS strategies show that for the VLW and LW test rooms the annual heating load remains very similar, however for the HW and VHW test rooms the annual heating load is slightly reduced (Figure 6—32).

The annual heating load is increased by 0.1% for the VLW test room, reduced by 1.3% for the LW test room, reduced by 5.8% for the HW room and reduced by 6.9% for the VHW test room.

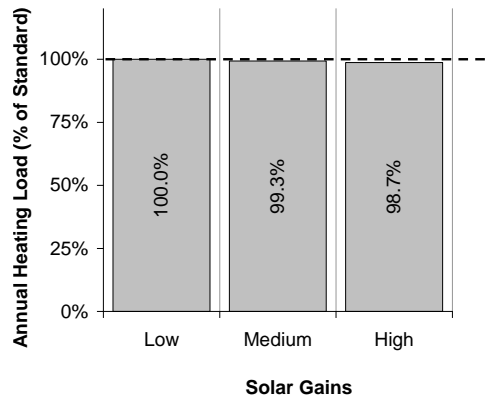


**Figure 6—32 HCS vs Standard Strategy
Annual Heating Load – Thermal Mass**

6.4.2 Solar Gain

Comparing the results of the different levels of solar gain for the Standard and HCS strategies show that the annual heating load for the test room with low solar gain remains the same and is slightly reduced for the test rooms with medium and high solar gains (Figure 6—33).

The annual heating load remains the same for test room with low solar gains, is reduced by 0.7% for the test room with medium solar gains and is reduced by 1.3% for the test room with high solar gain.



**Figure 6—33 HCS vs Standard Strategy
Annual Heating Load – Solar Gain**

6.4.3 Internal Gain

Comparing the results of the different levels of internal gain for the Standard and HCS strategies show that the annual heating load for the test room with low internal gain is slightly increased, whereas it is slightly reduced for the test rooms with medium and high internal gains (Figure 6—34).

The annual heating load is increased by 1.8% for the test room with low internal gain, reduced by 1.3% for the test room with medium internal gain and reduced by 3.7% for the test room with high internal gain.

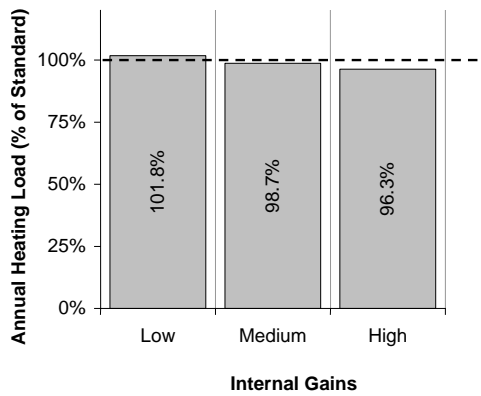


Figure 6—34 HCS vs Standard Strategy

Annual Heating Load – Internal Gain

6.4.4 Air Change Rate

Comparing the results of the different air change rates for the Standard and HCS strategies show that the annual heating load for the test room with low internal gain is slightly reduced for all air change rates (Figure 6—35).

The annual heating load is reduced by 1.3% for the test room with 6ach^{-1} , by 1.0% for the test room with 8ach^{-1} and by 1.4% for the test room with 10ach^{-1} .

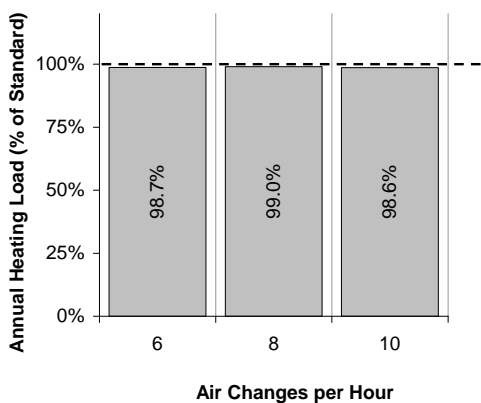


Figure 6—35 HCS vs Standard Strategy

Annual Heating Load – Air Change Rate

6.5 Chapter Summary

This chapter presented the results of the hollow core slab strategy in comparison to the standard strategy. It has argued that the hollow core slab strategy has the following characteristics in comparison to the standard strategy:

- Hollow core slab without night cooling results in an increase of annual overheating hours and only a slight reduction of T_{res} maximum for the lightweight building types..
- Adding night cooling results to a reduction of annual overheating hours for all but the VHW level of thermal mass and a reduction in T_{res} maximum for all levels of thermal mass.
- There is an increase of annual overheating hours for all levels of solar gain and internal gain. However, T_{res} maximum is reduced on a peak summer day for all levels of solar gain and internal gain..
- Similarly, there is an increase of annual overheating hours and reduction of T_{res} maximum for all levels of air change rate.
- The annual cooling load is increased for all investigated cases.
- The annual heating load remains similar and in some cases slightly reduced for all cases investigated.

The next chapter 7, presents the results and analysis for the floor void with mass strategy in a similar method.

7.0 FLOOR VOID WITH MASS: RESULTS AND ANALYSIS

7.1 Introduction

This chapter presents the results and analysis for the floor void with mass model in a similar method as for the hollow core model in chapter 6. As before the performance is analysed in terms of (a) number of overheating hours (b) annual cooling load and (c) annual heating load and the results are presented as a percentage of the standard strategy. The T_{res} maximum is presented as a difference from the standard strategy.

7.2 Overheating Hours

7.2.1 Thermal Mass

Comparing the results of the different levels of thermal mass for the Standard and FVWM strategies show that for all levels of thermal mass the FVWM strategy increases the annual overheating hours (Figure 7—1). The T_{res} maximum is also increased for all levels of thermal mass (Figure 7—2).

The number of overheating hours are increased by 14.0% and 14.2% for the VLW and LW test rooms. The number of overheating hours are increased by 16.4% and 21.7% for the HW and VHW test rooms.

The T_{res} maximum is increased by 0.1°C for the VLW, LW and HW test rooms and is increased by 0.3 °C for the VHW test room.

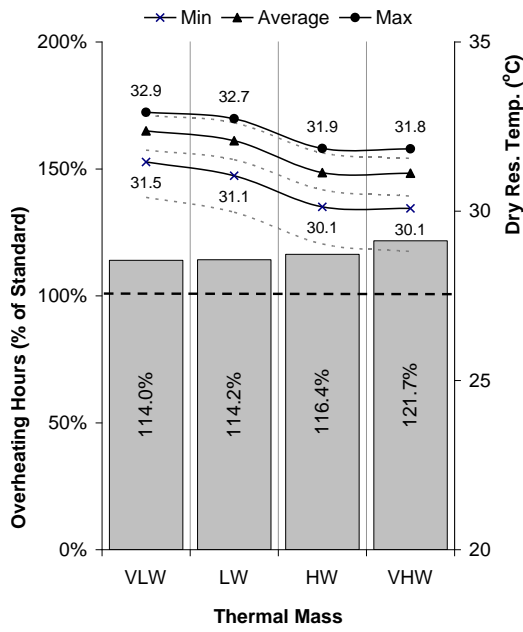


Figure 7—1 FVWM vs Standard Strategy Annual Overheating Hours – Thermal Mass

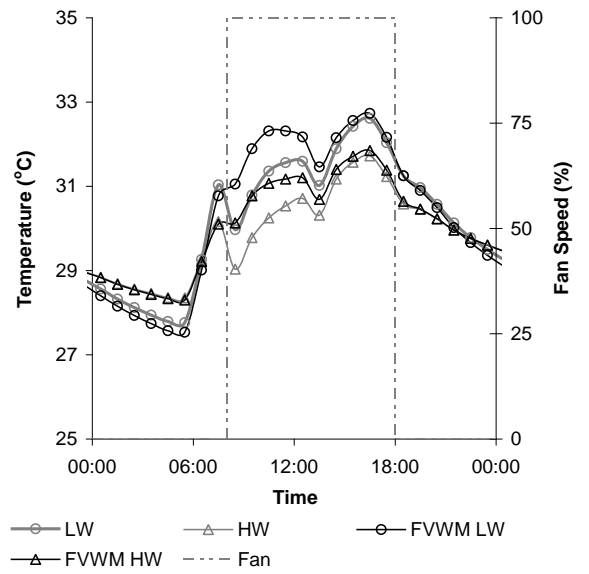


Figure 7—2 FVWM vs Standard Strategy T_{res} on a peak summer day – Thermal Mass

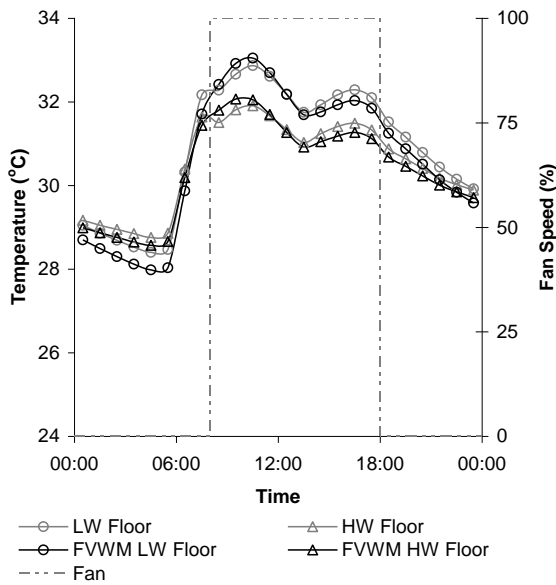


Figure 7—3 FVWM vs Standard Strategy Floor Surface Temperature – Thermal Mass

7.2.2 Thermal Mass with Night Cooling

Comparing the results with night cooling of the different levels of thermal mass for the Standard and FVWM strategies show that for all levels of thermal mass the annual overheating hours are increased (Figure 7—4). The T_{res} maximum on a peak summer day is also reduced for the VLW and LW test rooms, but increased for the HW and VHW test rooms (Figure 7—5).

The number of overheating hours are increased by 7.1% and 9.9% for the VLW and LW and by 15.8% and 21.7% for the HW and VHW test rooms.

The T_{res} maximum is reduced by 0.2°C for the VLW and LW rooms. The T_{res} maximum remains the same for the HW test room and is increased by 0.2°C for the VHW test room.

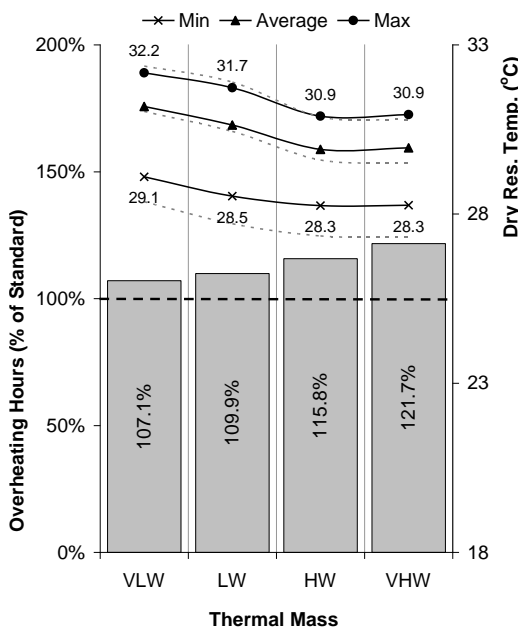


Figure 7—4 FVWM vs Standard Strategy Annual Overheating Hours – Thermal Mass with Night Cooling

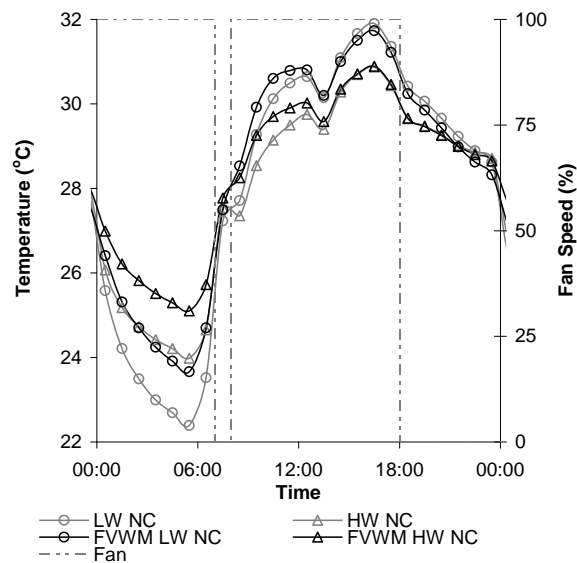
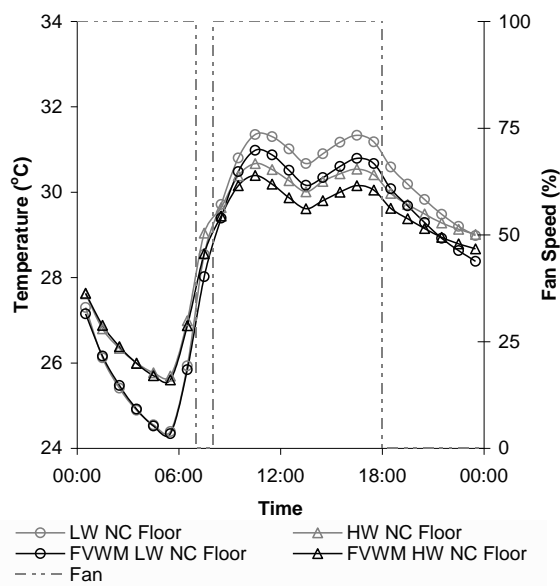


Figure 7—5 FVWM vs Standard Strategy T_{res} on a peak summer day – Thermal Mass with Night Cooling



**Figure 7—6 FVWM vs Standard Strategy
Floor Surface Temperature – Thermal Mass
with Night Cooling**

7.2.3 Solar Gains

Comparing the results of the different levels of solar gain for the Standard and FVWM strategies show that for all levels of solar gain the annual overheating hours are increased (Figure 7—7). the T_{res} maximum on a peak summer day is remains the same for the test rooms with low and medium solar gains and is increased for the test room with high solar gains (Figure 7—8).

The number of overheating hours are increased by 15.9% for the low internal gain test room, 16.4% for the medium internal gain test room and 14.2% for the high internal gain test room.

The T_{res} maximum remains the same for the low and medium solar gain test rooms, and is increased by 0.1°C for the high solar gain test room.

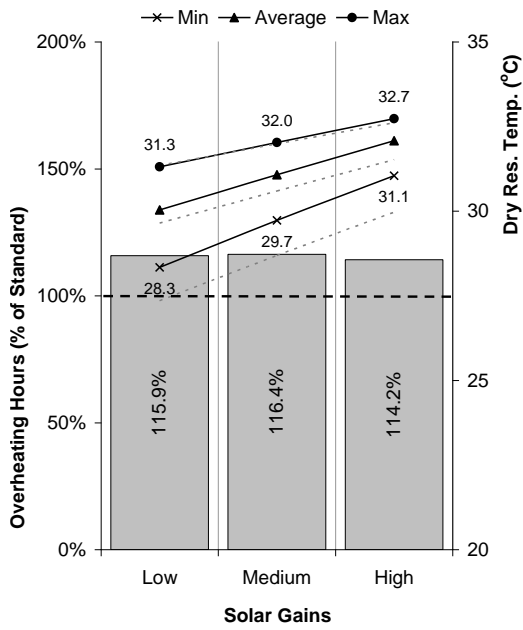


Figure 7—7 FVWM vs Standard Strategy Annual Overheating Hours – Solar Gain

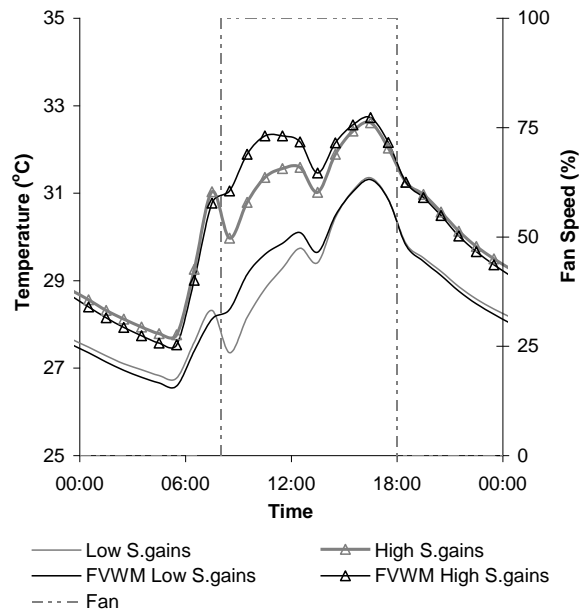


Figure 7—8 FVWM vs Standard Strategy T_{res} on a peak summer day – Solar Gains

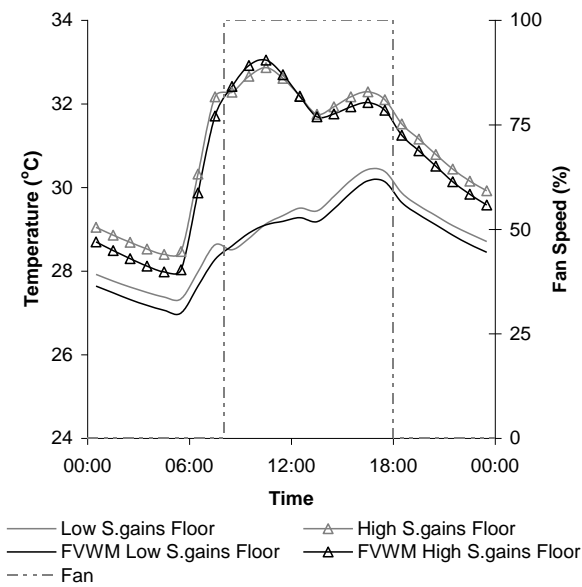


Figure 7—9 FVWM vs Standard Strategy Floor Surface Temperature – Solar Gain

7.2.4 Internal Gains

Comparing the results of the different levels of internal gain for the Standard and FVWM strategies show that the annual overheating hours for all levels of internal gain are increased (Figure 7—10). The T_{res} maximum on a peak summer day is also increased for all levels of internal gain (Figure 7—11).

The number of overheating hours are increased by 17.4% for the low internal gain test room, by 14.2% for the medium internal gain test room and by 11.5% for the high internal gain test room.

The T_{res} maximum is increased by 0.1°C for the low and medium internal gain test rooms and by 0.2°C high internal gain test rooms.

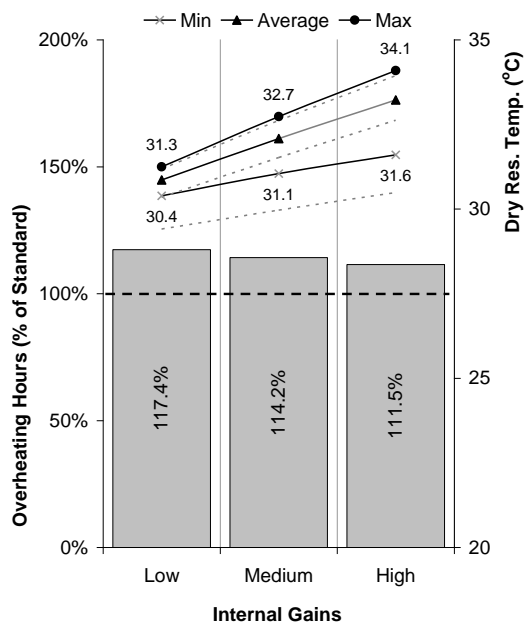


Figure 7—10 FVWM vs Standard Strategy Annual Overheating Hours – Internal Gain

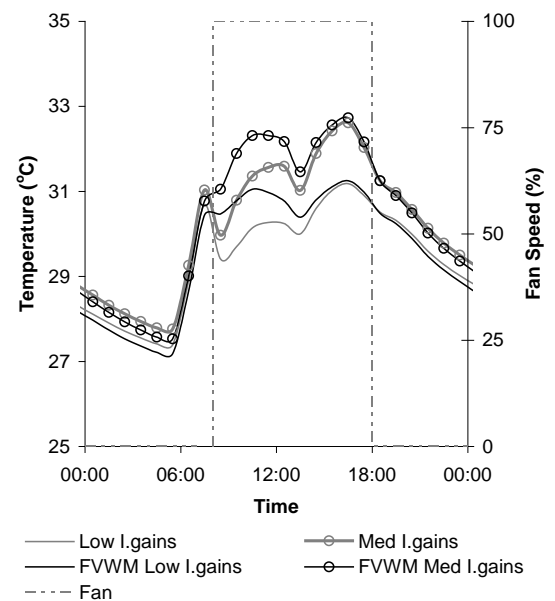
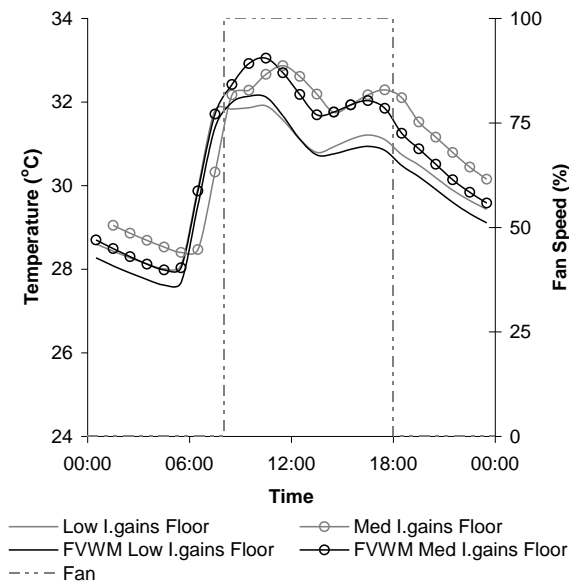


Figure 7—11 FVWM vs Standard Strategy T_{res} on a peak summer day – Internal Gains



**Figure 7—12 FVWM vs Standard Strategy
Floor Surface Temperature – Internal Gain**

7.2.5 Air Change Rate

Comparing the results of the different levels of air change rate for the Standard and FVWM strategies show that the annual overheating hours for all levels of air change rate are increased (Figure 7—13). The T_{res} maximum on a peak summer day is increased for the 6ach^{-1} test room and remains the same for the 8ach^{-1} and 10ach^{-1} test rooms (Figure 7—14).

The number of overheating hours are increased by 14.2% for the test room with 6ach^{-1} , 12.6% for the test room with 8ach^{-1} and 11.7% for the test room with 10ach^{-1} .

For the 6ach^{-1} test room the T_{res} maximum is increased by 0.1°C . For the 8ach^{-1} and 10ach^{-1} test rooms the T_{res} maximum remains the same.

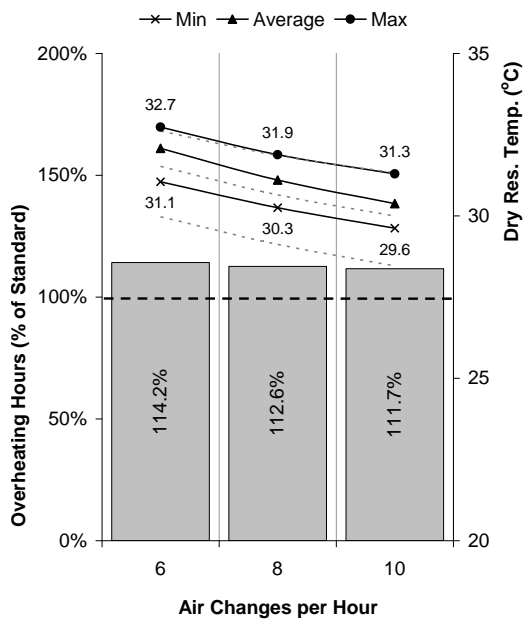


Figure 7—13 FVWM vs Standard Strategy Annual Overheating Hours – Air Change Rate

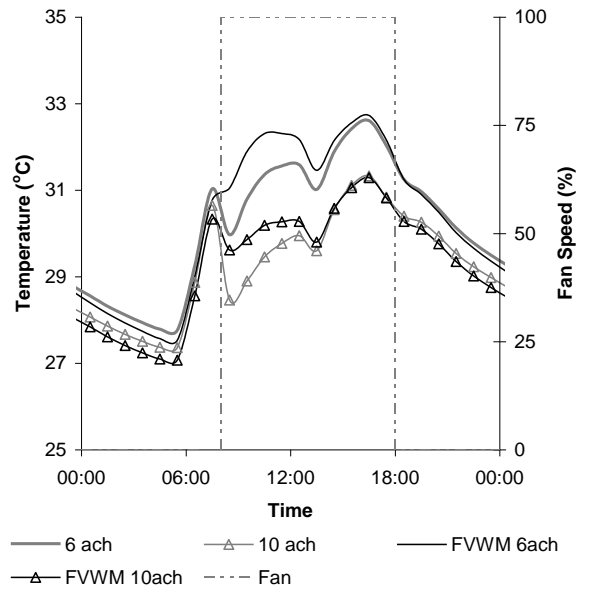


Figure 7—14 FVWM vs Standard Strategy T_{res} on a peak summer day – Air Change Rate

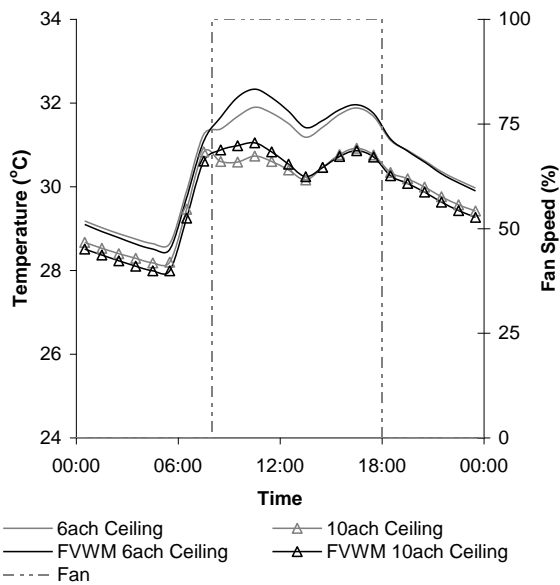


Figure 7—15 FVWM vs Standard Strategy Floor Surface Temperature – Air Change Rate

7.3 Annual Cooling Load

7.3.1 Thermal Mass

Comparing the results of the different levels of thermal mass for the Standard and FVWM strategies show that for all levels thermal mass the annual cooling load is increased (Figure 7—16). The T_{res} maximum on a peak summer day is also increased for all levels of thermal mass (Figure 7—17).

The annual cooling load is increased by 13.8% and 13.6% for the VLW and LW test rooms and by 18.6% and 20.9% for the HW and VHW test rooms.

The T_{res} maximum is increased by 1.1°C and 1.0°C for the VLW and LW rooms and by 0.9°C and 1.1°C for the HW and VHW rooms.

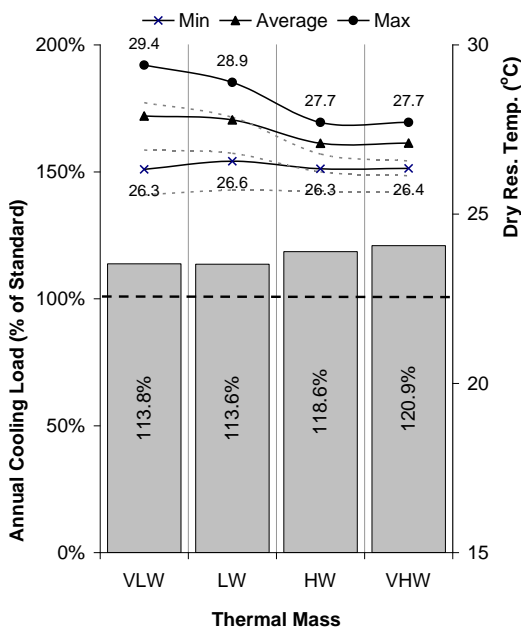


Figure 7—16 FVWM vs Standard Strategy Annual Cooling Load— Thermal Mass

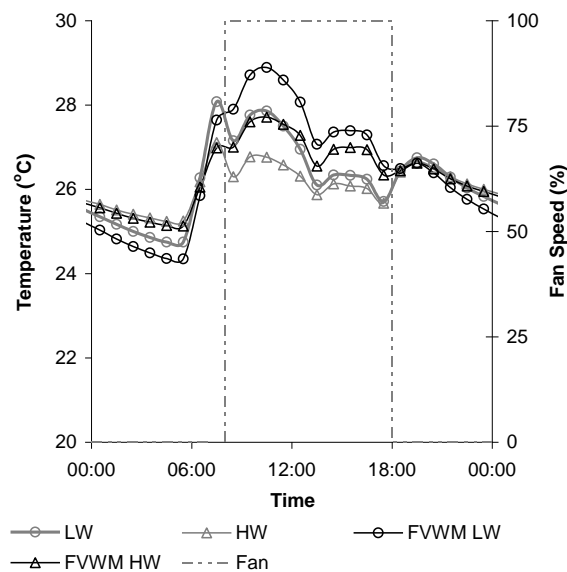


Figure 7—17 FVWM vs Standard Strategy with cooling T_{res} on a peak summer day – Thermal Mass

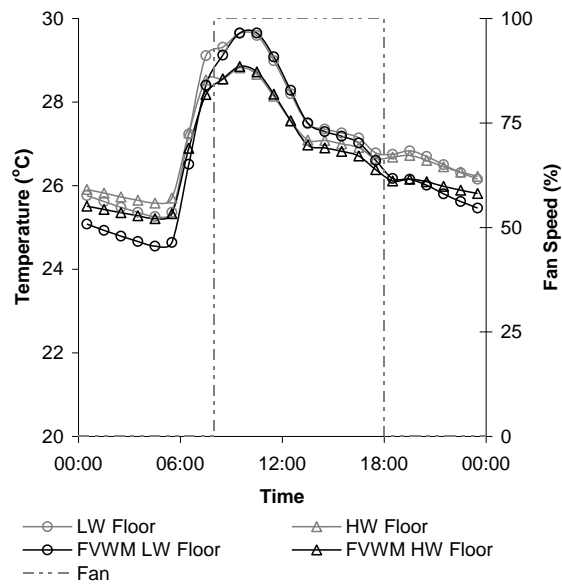


Figure 7—18 FVWM with Standard Strategy with Cooling Floor Surface Temperature – Thermal Mass

7.3.2 Thermal Mass with Night Cooling

Comparing the results of the different levels of thermal mass with night cooling for the Standard and FVWM strategies show that for all levels thermal mass the annual cooling load is increased (Figure 7—19). The T_{res} maximum on a peak summer day is also increased for all levels of thermal mass (Figure 7—20).

The annual cooling load is increased by 13.3% and 14.5% for the VLW and LW test rooms and by 21.1% and 23.6% for the HW and VHW test rooms..

The T_{res} maximum is increased by 0.8°C and 0.7°C for the VLW and LW rooms. The T_{res} maximum is increased by 0.7°C and 0.8°C for the HW and VHW rooms.

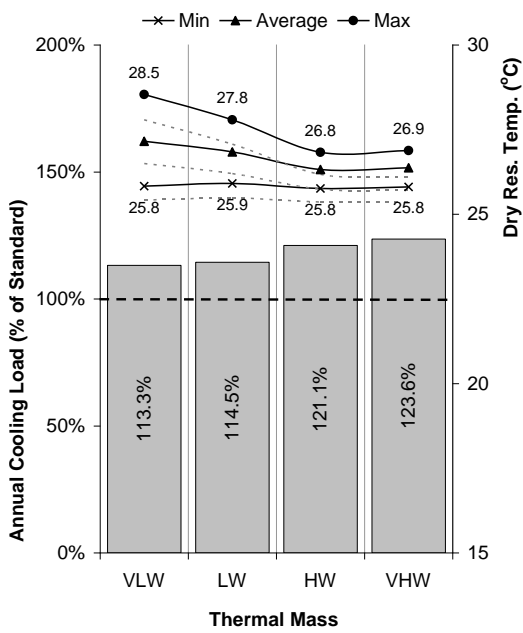


Figure 7—19 FVWM vs Standard Strategy Annual Cooling Load– Thermal Mass with Night Cooling

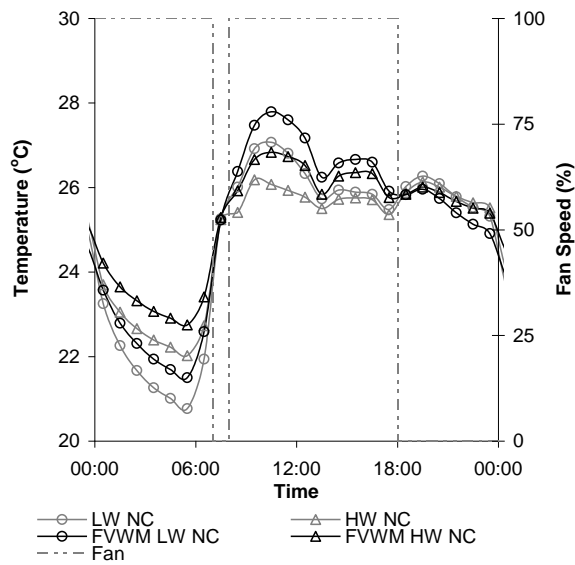


Figure 7—20 FVWM vs Standard Strategy with cooling T_{res} on a peak summer day – Thermal Mass with Night Cooling

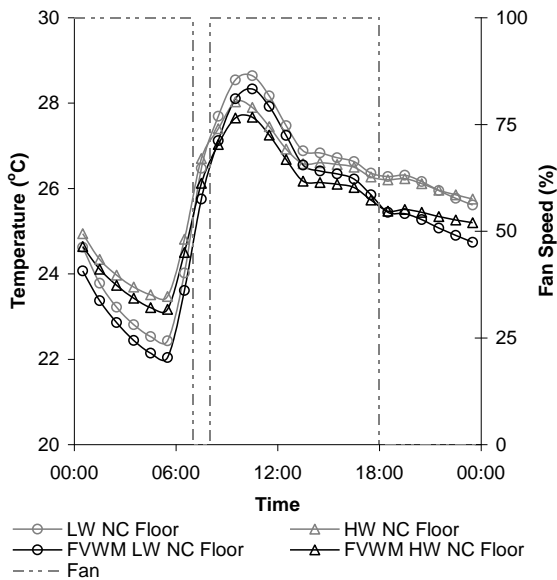


Figure 7—21 FVWM vs Standard Strategy with Cooling Floor Surface Temperature – Thermal Mass with Night Cooling

7.3.3 Solar Gains

Comparing the results of the different levels of solar gain for the Standard and FVWM strategies show that for all levels of solar gain the annual cooling load is increased (Figure 7—22). The T_{res} maximum on a peak summer day for all levels of solar gain is also increased (Figure 7—23).

The annual cooling load is increased by 23.5% for the low solar gain test room, 18.6% for the medium solar gain test room and 13.6% for the high solar gain test room.

The T_{res} maximum is increased by 0.4°C for the low solar gain test room, by 0.9°C for the medium internal gain test room and by 1.0°C for the high solar gain test rooms.

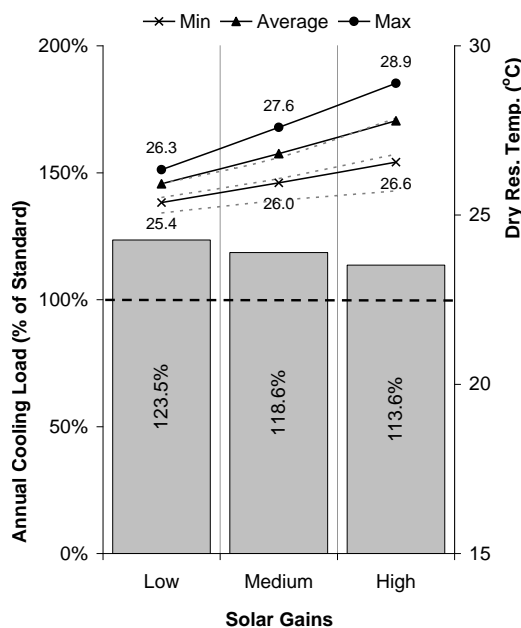


Figure 7—22 FVWM vs Standard Strategy Annual Cooling Load– Solar Gain

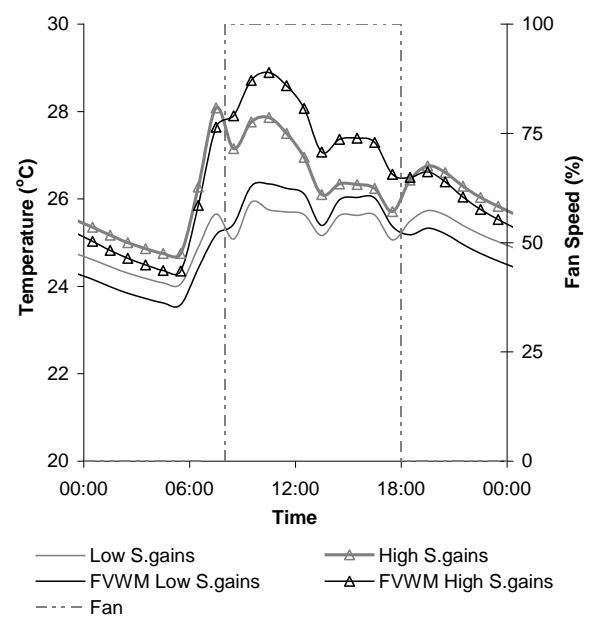


Figure 7—23 FVWM vs Standard Strategy with cooling T_{res} on a peak summer day – Solar Gain

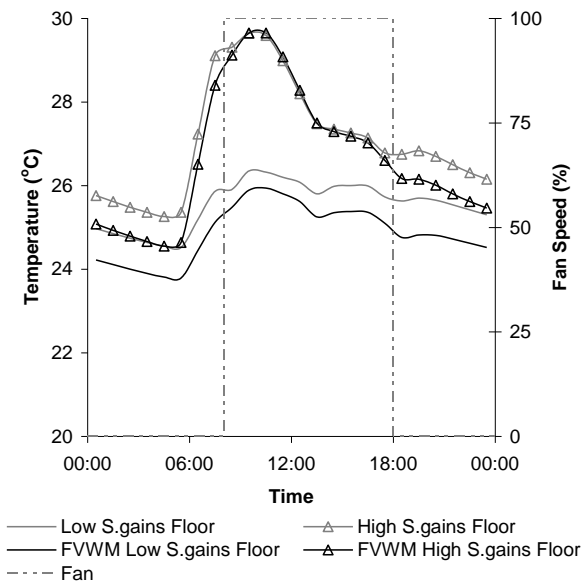


Figure 7—24 FVWM vs Standard Strategy with Cooling Floor Surface Temperature – Solar Gain

7.3.4 Internal Gains

Comparing the results of the different levels of internal gain for the Standard and FVWM strategies show that for all levels of internal gain the annual cooling load is increased (Figure 7—25). The T_{res} maximum on a peak summer day for all levels of internal gain is also increased (Figure 7—26).

The annual cooling load is increased by 23.7% for the low internal gain test room, 13.6% for the medium internal gain test room and 6.2% for the high internal gain test room.

The T_{res} maximum is increased by 0.9°C for the low internal gain test room, by 1.0°C for the medium internal gain test room and 1.1°C for the high internal gain test room.

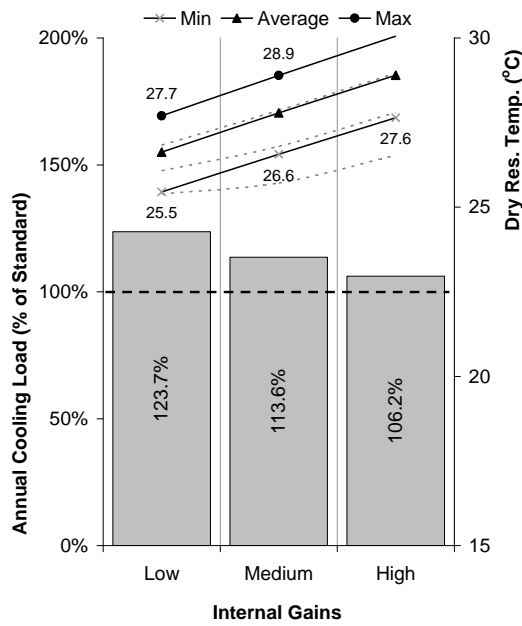


Figure 7—25 FVWM vs Standard Strategy Annual Cooling Load— Internal Gain

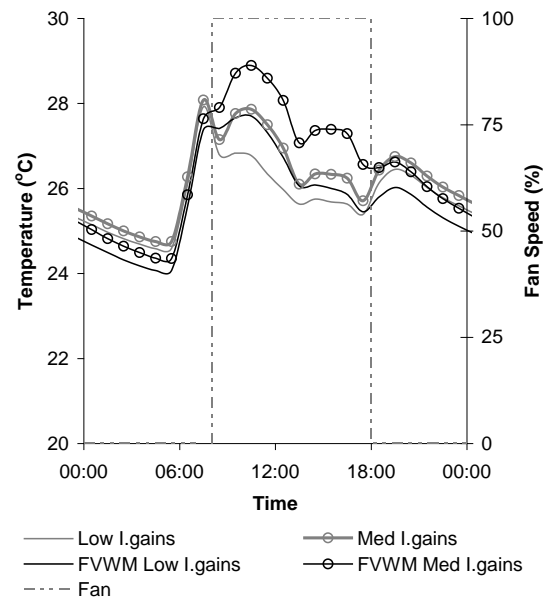


Figure 7—26 FVWM vs Standard Strategy with cooling T_{res} on a peak summer day – Internal Gain

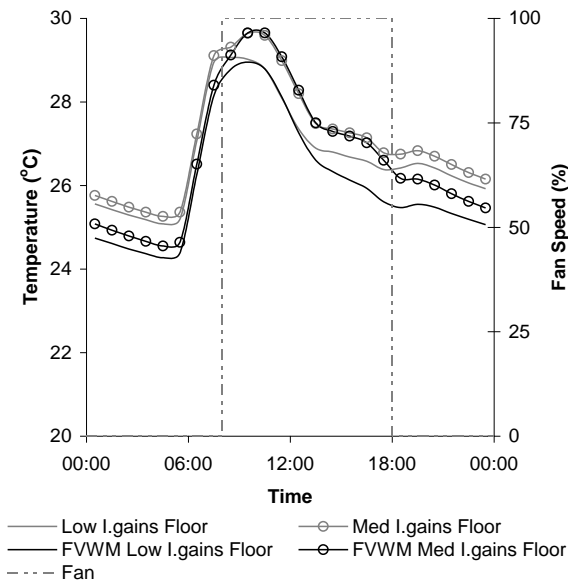


Figure 7—27 FVWM vs Standard Strategy with Cooling Floor Surface Temperature – Internal Gain

7.3.5 Air Change Rate

Comparing the results of the different levels of air change rate for the Standard and FVWM strategies show that for all levels of air change rate the annual cooling load is increased (Figure 7—28). The T_{res} maximum on a peak summer day for all levels of air change rate is also increased (Figure 7—29).

The annual cooling load is increased by 14.2% for the test room with 6ach^{-1} , 12.6% for the test room with 8ach^{-1} and 11.7% for the test room with 10ach^{-1} .

For 6ach^{-1} T_{res} maximum is increased by 1.0°C . For 8ach^{-1} the T_{res} maximum is increased by 0.7°C . For medium 10ach^{-1} the T_{res} maximum is increased by 0.4°C .

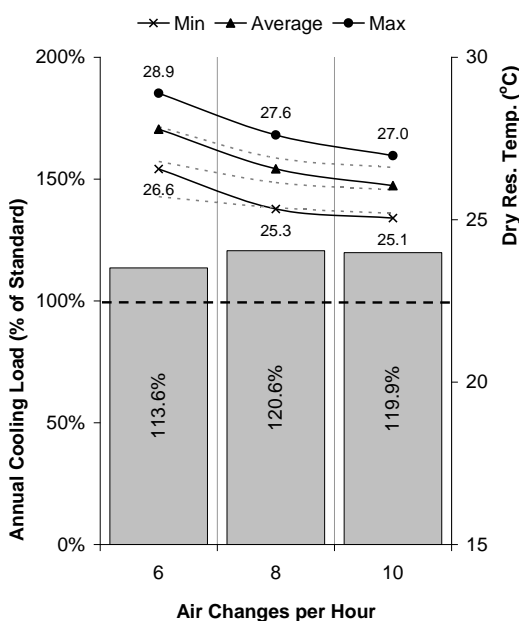


Figure 7—28 FVWM vs Standard Strategy Annual Cooling Load– Air Change Rate

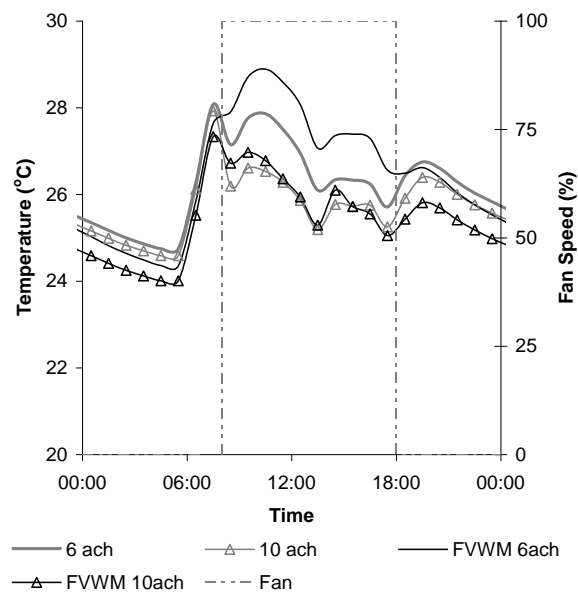


Figure 7—29 FVWM vs Standard Strategy with cooling T_{res} on a peak summer day – Air Change Rate

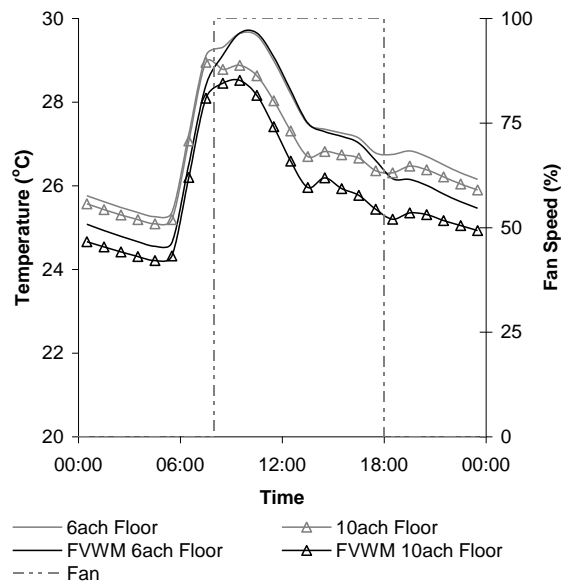


Figure 7—30 FVWM vs Standard Strategy with Cooling Floor Surface Temperature – Air Change Rate

7.4 Annual Heating Load

7.4.1 Thermal Mass

Comparing the results of the different levels of thermal mass for the Standard and FVWM strategies show that for all levels of thermal mass the annual heating load is slightly reduced (Figure 7—31).

The annual heating load is reduced by 0.8% for the VLW test room, by 1.9% for the LW test room, by 2.7% for the HW room and by 3.5% for the VHW test room.

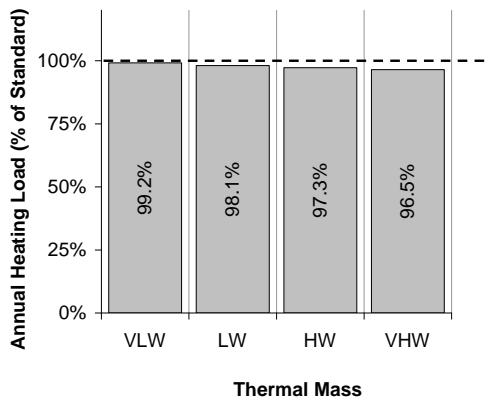


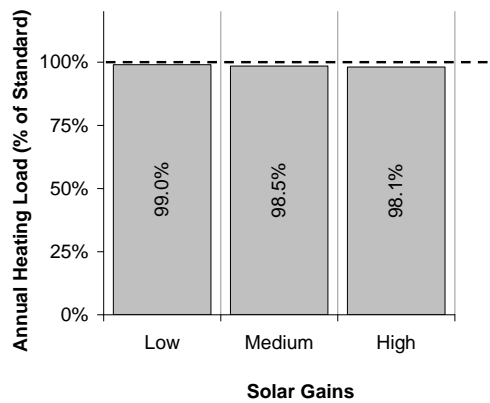
Figure 7—31 FVWM vs Standard Strategy

Annual Heating Load – Thermal Mass

7.4.2 Solar Gain

Comparing the results of the different levels of solar gain for the Standard and FVWM strategies show that the annual heating load is slightly reduced for all levels of solar gain (Figure 7—32).

The annual heating load is reduced by 1.0% for the test room with low solar gain, by 1.5% for the test room with medium solar gains and by 1.9% for the test room with high solar gain.



**Figure 7—32 FVWM vs Standard Strategy
Annual Heating Load – Solar Gain**

7.4.3 Internal Gain

Comparing the results of the different levels of internal gain for the Standard and FVWM strategies show that the annual heating load for the test room with low internal gain is slightly increased, whereas it is slightly reduced for the test rooms with medium and high internal gains (Figure 7—33).

The annual heating load is increased by 1.0% for the test room with low internal gain, reduced by 1.9% for the test room with medium internal gain and reduced by 1.7% for the test room with high internal gain.

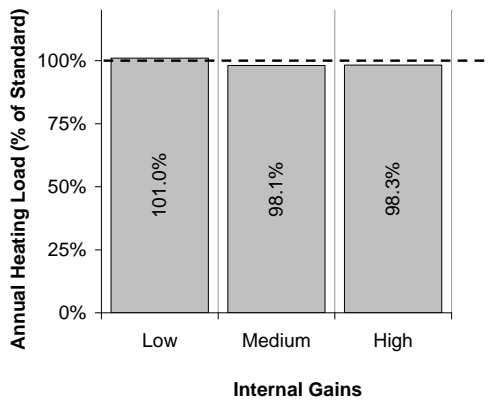


Figure 7—33 FVWM vs Standard Strategy

Annual Heating Load – Internal Gain

7.4.4 Air Change Rate

Comparing the results of the different air change rates for the Standard and FVWM strategies show that the annual heating load is slightly reduced for the 6 ach⁻¹ and 8ach⁻¹ air change rates and remains the same for the 10ach⁻¹ air change rate (Figure 7—34).

The annual heating load is reduced by 1.9% for the test room with 6ach⁻¹, by 0.5% for the test room with 8ach⁻¹ and remains the same for the test room with 10ach⁻¹.

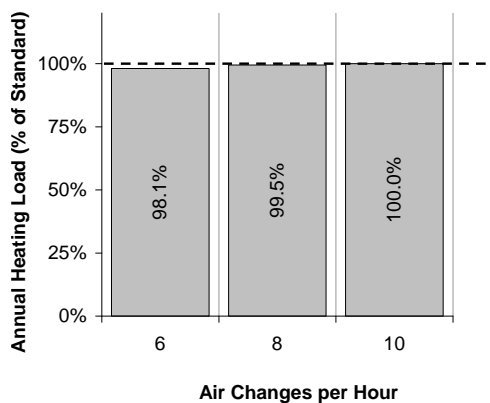


Figure 7—34 FVWM vs Standard Strategy

Annual Heating Load – Air Change Rate

7.5 Chapter Summary

This chapter presented the results of the Floor Void with Mass (FVWM) strategy in comparison to the standard strategy. It has argued that the Floor Void with Mass strategy has the following characteristics in comparison to the standard strategy:

- All levels of thermal mass without night cooling result in an increase of annual overheating hours and a slight increase of T_{res} maximum.
- Adding night cooling still results in an increase of annual overheating hours. The T_{res} maximum for the lightweight building types is slightly reduced.
- There is an increase of annual overheating hours for all levels of solar gain and internal gain. There is little if any change in T_{res} maximum on a peak summer day for all levels of solar gain and internal gain.
- Similarly, there is an increase of annual overheating hours and minimal change in T_{res} maximum for all levels of air change rate.
- The annual cooling load is increased for all investigated cases.
- The annual heating load remains similar and in some cases slightly reduced for all cases investigated.

The next chapter 8, presents the results and analysis for the Earth to Air Heat Exchanger (ETAHE) strategy in a similar method.

8.0 EARTH TO AIR HEAT EXCHANGER MODEL: RESULTS AND ANALYSIS

8.1 Introduction

This chapter presents the results and analysis for the earth to air heat exchanger model in a similar method as for the hollow core model in chapter 6. As before the performance is analysed in terms of (a) number of overheating hours (b) annual cooling load and (c) annual heating load and the results are presented as a percentage of the standard strategy. The T_{res} maximum is presented as a difference from the standard strategy.

8.2 Overheating Hours

8.2.1 Thermal Mass

Comparing the results of the different levels of thermal mass for the Standard and ETAHE strategies show that for all levels of thermal mass the ETAHE strategy reduces the annual overheating hours (Figure 8—1) and the T_{res} maximum on a peak summer day (Figure 8—2).

The number of overheating hours are reduced by 20.2% and 22.0% for the VLW and LW test rooms. The number of overheating hours are reduced by 27.4% and 28.2% for the HW and VHW test rooms.

The T_{res} maximum is reduced by 1.9°C and 2.1°C for the VLW and LW rooms. The T_{res} maximum is reduced by 1.7°C and 1.6°C for the HW and VHW rooms.

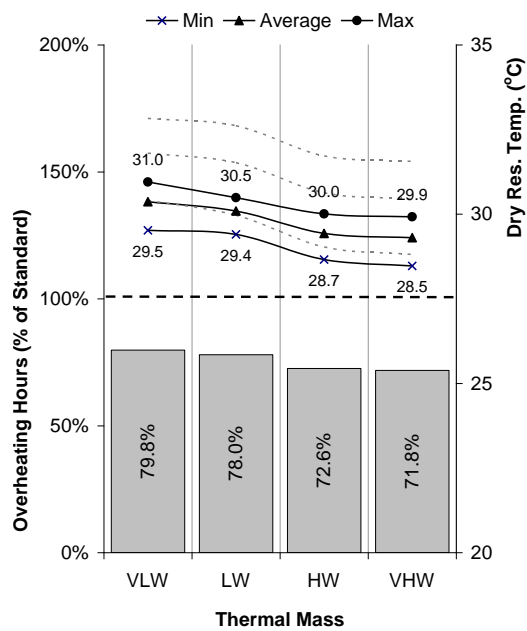


Figure 8—1 ETAHE vs Standard Strategy
Annual Overheating Hours – Thermal Mass

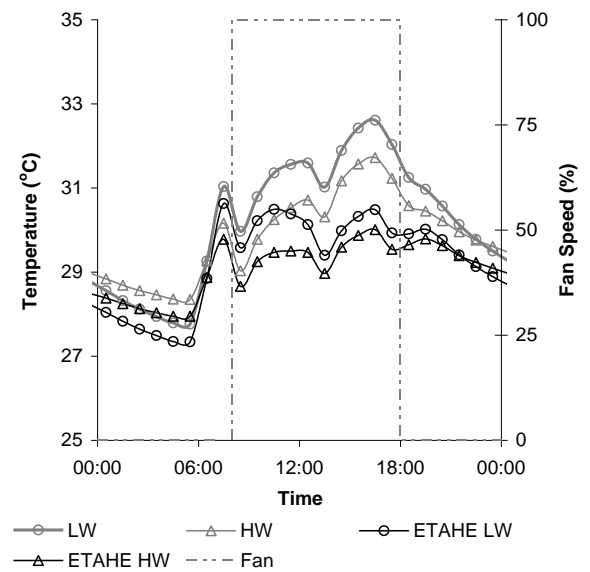


Figure 8—2 ETAHE vs Standard Strategy
 T_{res} on a peak summer day – Thermal Mass

8.2.2 Thermal Mass with Night Cooling

Comparing the results of the different levels of thermal mass with night cooling for the Standard and ETAHE strategies show that for all levels of thermal mass the ETAHE strategy reduces the annual overheating hours (Figure 8—3) and the T_{res} maximum on a peak summer day (Figure 8—4).

The number of overheating hours are reduced by 27.4% and 36.9% for the VLW and LW test rooms. The number of overheating hours are reduced by 49.7% and 49.2% for the HW and VHW test rooms.

The T_{res} maximum is reduced by 2.2°C and 2.1°C for the VLW and LW rooms. The T_{res} maximum is reduced by 1.6°C for the HW and VHW rooms.

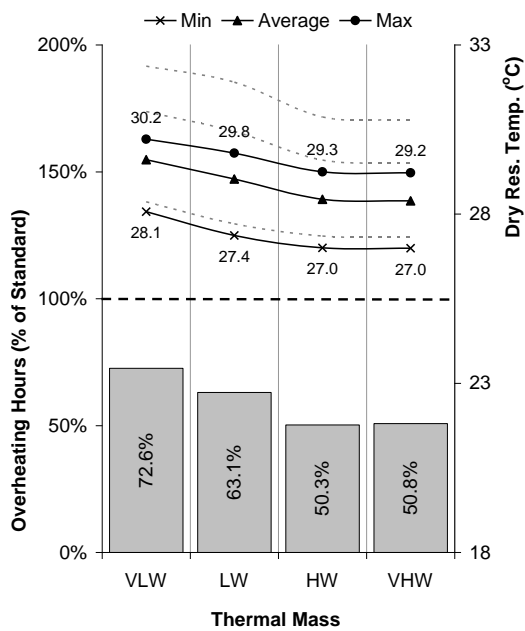


Figure 8—3 ETAHE vs Standard Strategy Annual Overheating Hours – Thermal Mass with Night Cooling

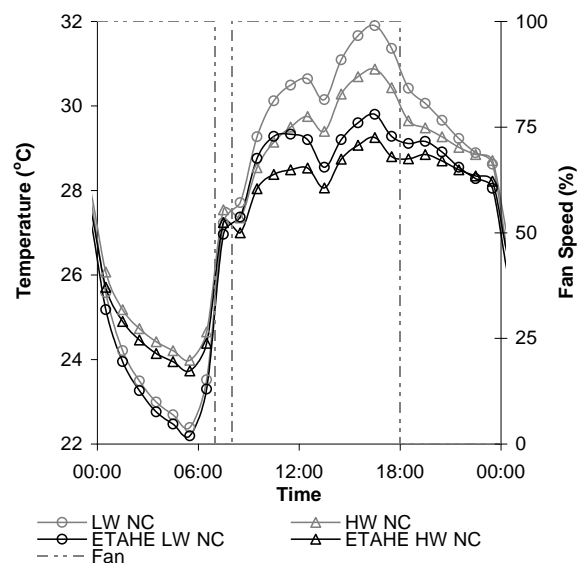


Figure 8—4 ETAHE vs Standard Strategy T_{res} on a peak summer day – Thermal Mass with Night Cooling

8.2.3 Solar Gain

Comparing the results of the different levels of solar gain for the Standard and ETAHE strategies show that for all levels of thermal mass the ETAHE strategy reduces the annual overheating hours (Figure 8—5) and the T_{res} maximum on a peak summer day (Figure 8—6).

Reducing the solar gain in the test room reduces the heat gain that needs to be overcome by the supply air. This then gives the supply air greater opportunity to control the T_{res} below 28°C.

The number of overheating hours are reduced by 57.8% for the low solar gain test room, 41.0% for the medium solar gain test room and 22.0% for the high solar gains test room.

The T_{res} maximum is reduced by 2.1°C for all levels of solar gain.

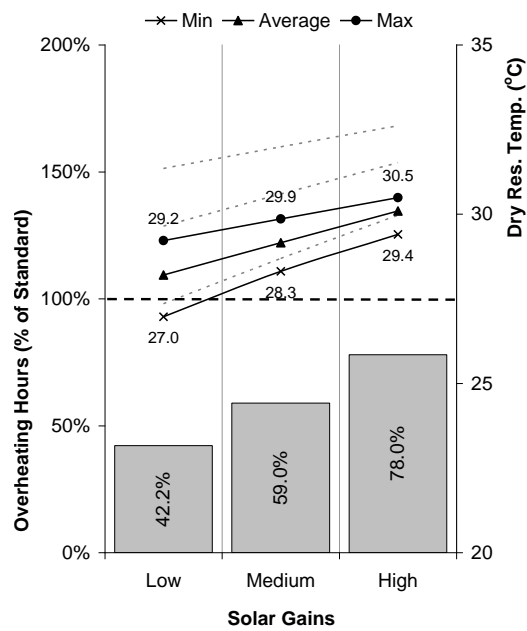


Figure 8—5 ETAHE vs Standard Strategy
Annual Overheating Hours – Solar Gain

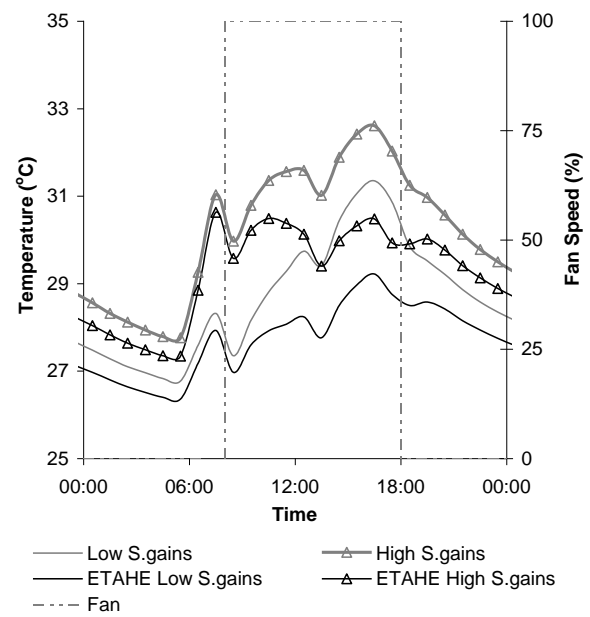


Figure 8—6 ETAHE vs Standard Strategy
T_{res} on a peak summer day – Solar Gain

8.2.4 Internal Gains

Comparing the results of the different levels of internal gain for the Standard and ETAHE strategies show that for all levels of thermal mass the ETAHE strategy reduces the annual overheating hours (Figure 8—7) and the T_{res} maximum on a peak summer day (Figure 8—8).

The number of overheating hours are reduced by 43.6% for the low internal gain test room, 22.0% for the medium internal gain test room and 16.0% for the high internal gain test room.

The T_{res} maximum is reduced by 1.9°C for the low internal gain test room and 2.1°C for the medium and high internal gain test rooms.

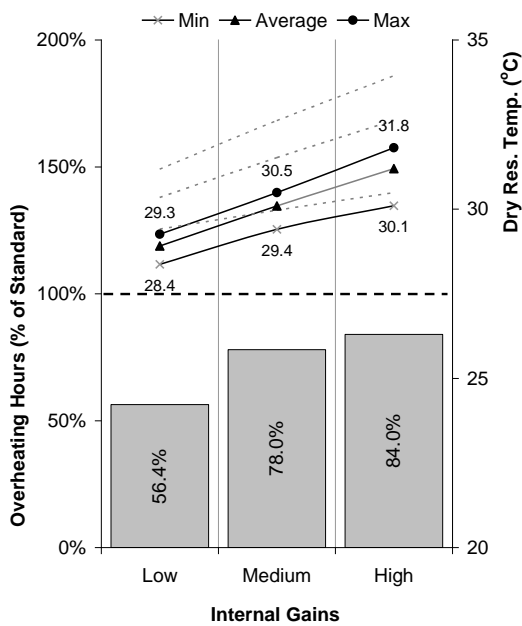


Figure 8—7 ETAHE vs Standard Strategy
Annual Overheating Hours – Internal Gain

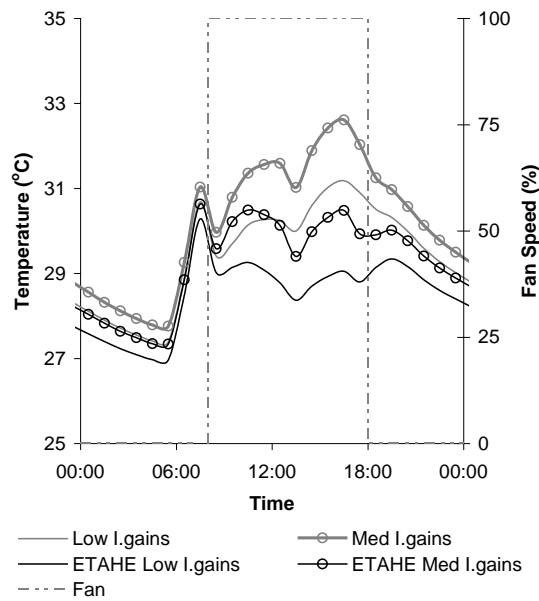


Figure 8—8 ETAHE vs Standard Strategy
 T_{res} on a peak summer day – Internal Gain

8.2.5 Air Change Rate

Comparing the results of the different levels of air change rate for the Standard and ETAHE strategies show that for all levels of thermal mass the ETAHE strategy reduces the annual overheating hours (Figure 8—9) and the T_{res} maximum on a peak summer day (Figure 8—10).

The number of overheating hours are reduced by 22.0% for the test room with 6ach^{-1} , 44.8% for the test room with 8ach^{-1} and 61.7% for the test room with 10ach^{-1} .

For 6ach^{-1} T_{res} maximum is reduced by 2.1°C . For medium 8ach^{-1} T_{res} maximum is reduced by 2.4°C . For medium 10ach^{-1} T_{res} maximum is reduced by 2.6°C .

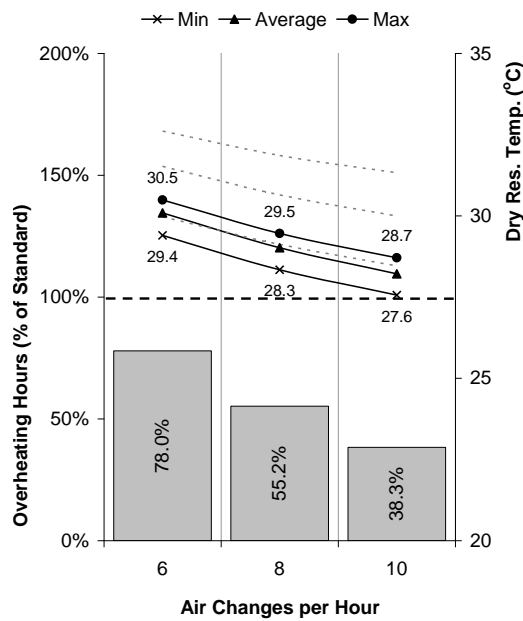


Figure 8—9 ETAHE vs Standard Strategy Annual Overheating Hours – Air Change Rate

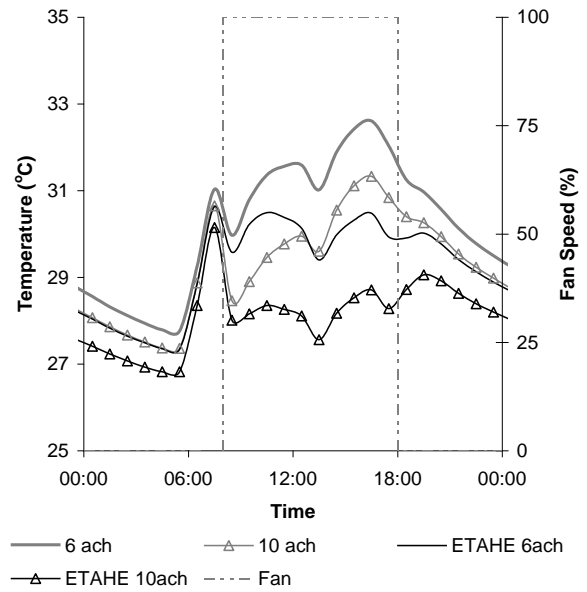


Figure 8—10 ETAHE vs Standard Strategy T_{res} on a peak summer day – Air Change Rate

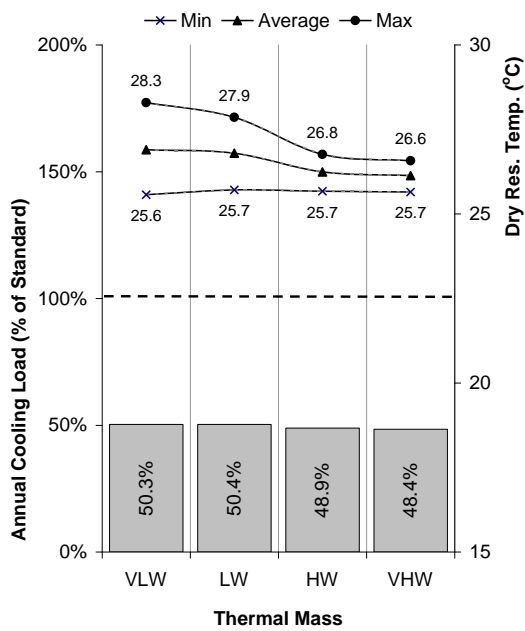
8.3 Annual Cooling Load

The ETAHE provides a source of cooling before the supply air is passed into the air handling unit. The air temperature leaving the air handling unit (after being cooled) is therefore the same for the Standard and ETAHE strategies. The T_{res} in the test room is therefore the same for both the Standard and ETAHE strategies (Figure 8—11 to Figure 8—15).

8.3.1 Thermal Mass

Comparing the results of the different levels of thermal mass for the Standard and ETAHE strategies show that for all levels of thermal mass the ETAHE strategy reduces the annual cooling load (Figure 8—11).

The annual cooling load is reduced by 49.7% and 49.6% for the VLW and LW test rooms. The annual cooling load is reduced by 51.1% and 51.6% for the HW and VHW test rooms.

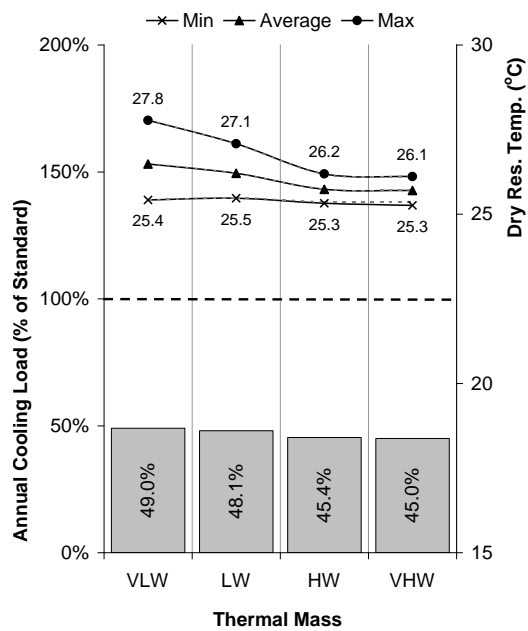


**Figure 8—11 ETAHE vs Standard Strategy
Annual Cooling Load– Thermal Mass**

8.3.2 Thermal Mass with Night Cooling

Comparing the results of the different levels of thermal mass with night cooling for the Standard and ETAHE strategies show that for all levels of thermal mass the ETAHE strategy reduces the annual cooling load (Figure 8—12).

The annual cooling load is reduced by 51.0% and 51.9% for the VLW and LW test rooms. The annual cooling load is reduced by 54.6% and 55.0% for the HW and VHW test rooms.

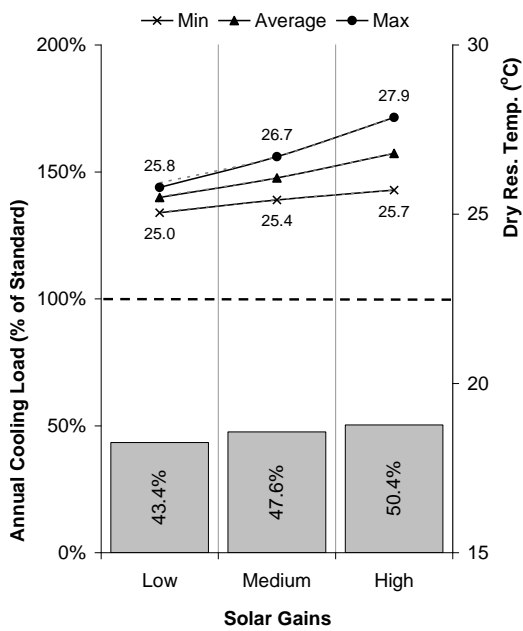


**Figure 8—12 ETAHE vs Standard Strategy
Annual Cooling Load– Thermal Mass with
Night Cooling**

8.3.3 Solar Gain

Comparing the results of the different levels of solar gain for the Standard and ETAHE strategies show that for all levels of solar gain the ETAHE strategy reduces the annual cooling load (Figure 8—13).

The annual cooling load is reduced by 56.6% for the low solar gain test room, 52.4% for the medium solar gain test room and 49.6% for the high solar gains test room.

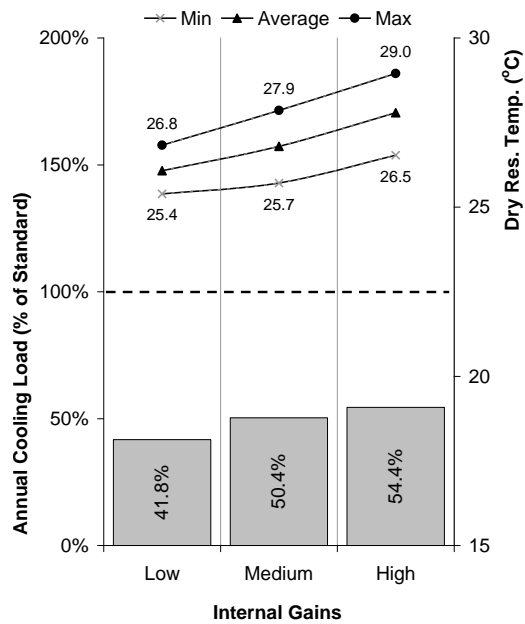


**Figure 8—13 ETAHE vs Standard Strategy
Annual Cooling Load– Solar Gain**

8.3.4 Internal Gain

Comparing the results of the different levels of internal gain for the Standard and ETAHE strategies show that for all levels of internal gain the ETAHE strategy reduces the annual cooling load (Figure 8—14).

The annual cooling load is reduced by 58.2% for the low internal gain test room, 49.6% for the medium internal gain test room and 45.6% for the high internal gains test room.



**Figure 8—14 ETAHE vs Standard Strategy
Annual Cooling Load– Internal Gain**

8.3.5 Air Change Rate

Comparing the results of the different levels of air change rate for the Standard and ETAHE strategies show that for all levels of air change rate the ETAHE strategy reduces the annual cooling load (Figure 8—15).

The annual cooling load is reduced by 49.6% for the test room with 6ach^{-1} , 57.7% for the test room with 8ach^{-1} and 64.1% for the test room with 10ach^{-1} .

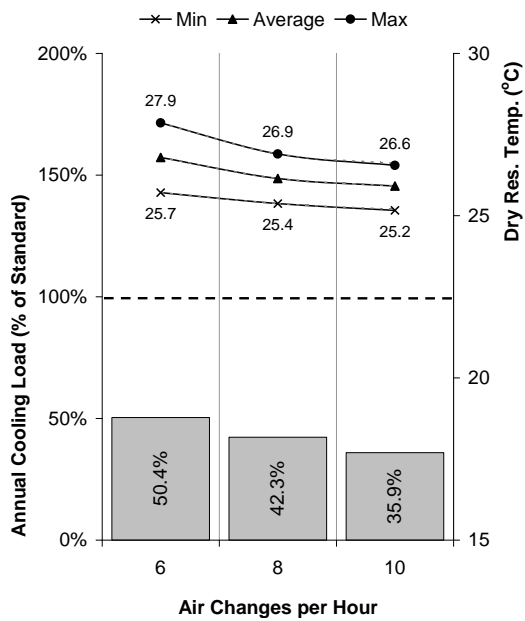


Figure 8—15 ETAHE vs Standard Strategy
Annual Cooling Load– Air Change Rate

8.4 Annual Heating Load

8.4.1 Thermal Mass

Comparing the results of the different levels of thermal mass for the Standard and ETAHE strategies show that for all levels of thermal mass the annual heating load is reduced (Figure 8—16).

The annual heating load is reduced by 9.2% for all levels of thermal mass.

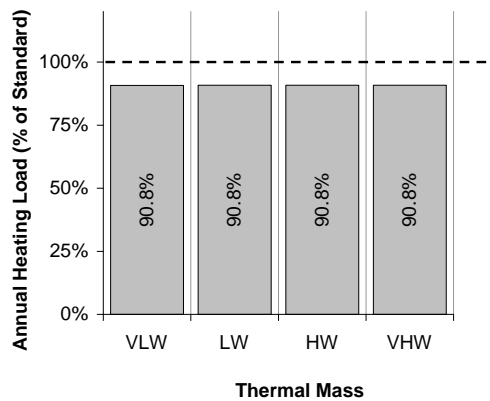


Figure 8—16 ETAHE vs Standard Strategy

Annual Heating Load – Thermal Mass

8.4.2 Solar Gain

Comparing the results of the different levels of solar gain for the Standard and ETAHE strategies show that for all levels of solar gain the annual heating load is reduced (Figure 8—17).

The annual heating load is reduced by 9.2% for test rooms with low and high solar gains and by 9.3% for the test room with medium solar gain.

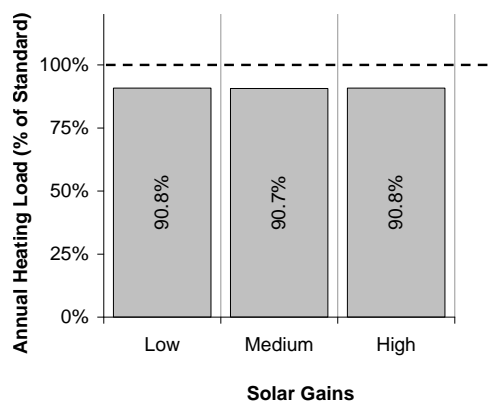


Figure 8—17 ETAHE vs Standard Strategy

Annual Heating Load – Solar Gain

8.4.3 Internal Gain

Comparing the results of the different levels of internal gain for the Standard and ETAHE strategies show that for all levels of internal gain the annual heating load is reduced (Figure 8—18).

The annual heating load is reduced by 8.7% for the test room with low internal gain, by 9.2% for the test room with medium internal gain and by 7.3% for the test room with high internal gain.

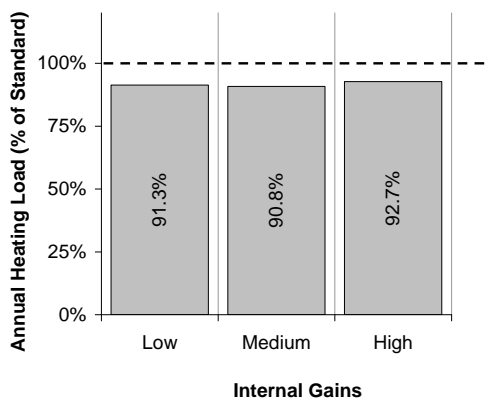


Figure 8—18 ETAHE vs Standard Strategy

Annual Heating Load – Internal Gain

8.4.4 Air Change Rate

Comparing the results of the different levels of air change rate for the Standard and ETAHE strategies show that for all levels of air change rate the annual heating load is reduced (Figure 8—19).

The annual heating load is reduced by 9.2% for the test room with 6ach^{-1} , by 9.1% for the test room with 8ach^{-1} and by 8.8% for the test room with 10ach^{-1} .

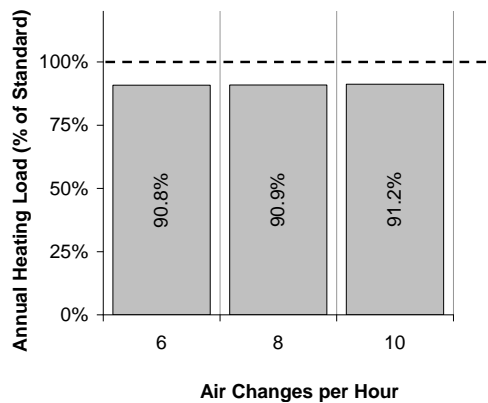


Figure 8—19 ETAHE vs Standard Strategy
Annual Heating Load – Air Change Rate

8.5 Chapter Summary

This chapter presented the results of the Earth to Air Heat Exchanger (ETAHE) strategy in comparison to the standard strategy. It has argued that the Earth to Air Heat Exchanger has the following characteristics in comparison to the standard strategy:

- All levels of thermal mass without night cooling result in an reduction of annual overheating hours and a reduction of T_{res} maximum.
- Adding night cooling results in a greater reduction of annual overheating hours and a greater reduction of T_{res} maximum.
- There is a reduction of annual overheating hours and a reduction of T_{res} maximum for all levels of solar gain and internal gain.
- Similarly, there is a reduction of annual overheating hours and a reduction of T_{res} maximum for all levels of air change rate.
- The annual cooling load is reduced by around 50% for all investigated cases.
- The annual heating load is reduced by around 10% for all cases investigated.

The next chapter 9, presents the results and analysis for the Thermal Labyrinth (TL) strategy in a similar method.

9.0 THERMAL LABYRINTH MODEL: RESULTS AND ANALYSIS

9.1 Introduction

This chapter presents the results and analysis for the thermal labyrinth model in a similar method as for the hollow core model in chapter 6. As before the performance is analysed in terms of (a) number of overheating hours (b) annual cooling load and (c) annual heating load and the results are presented as a percentage of the standard strategy. The T_{res} maximum is presented as a difference from the standard strategy.

9.2 Overheating Hours

9.2.1 Thermal Mass

Comparing the results of the different levels of thermal mass for the Standard and TL strategies show that for all levels of thermal mass the TL strategy reduces the annual overheating hours and the T_{res} maximum on a peak summer day (Figure 9—1 and Figure 9—2).

The number of overheating hours are reduced by 12.0% and 13.5% for the VLW and LW test rooms. The number of overheating hours are reduced by 19.0% and 18.0% for the HW and VHW test rooms.

The T_{res} maximum is reduced by 1.6°C and 1.7°C for the VLW and LW rooms. The T_{res} maximum is reduced by 1.4°C and 1.3°C for the HW and VHW rooms.

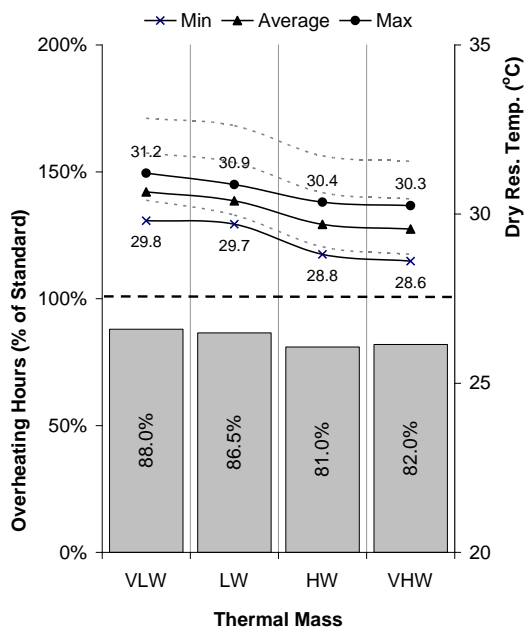


Figure 9—1 TL vs Standard Strategy Annual Overheating Hours – Thermal Mass

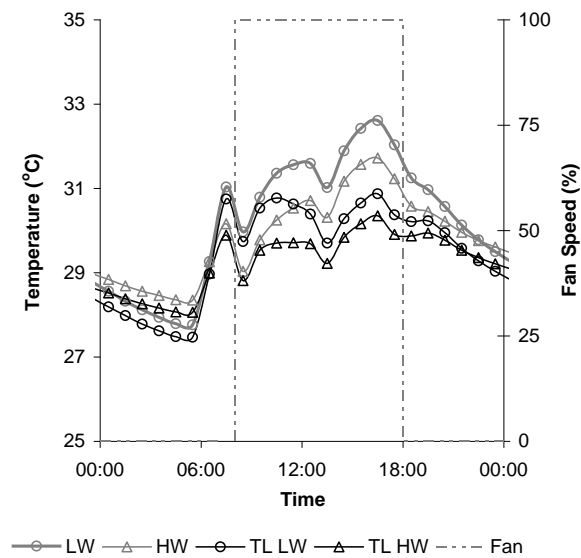


Figure 9—2 TL vs Standard Strategy T_{res} on a peak summer day – Thermal Mass

9.2.2 Thermal Mass with Night Cooling

Comparing the results of the different levels of thermal mass with night cooling for the Standard and TL strategies show that for all levels of thermal mass the TL strategy reduces the annual overheating hours and the T_{res} maximum on a peak summer day (Figure 9—3 and Figure 9—4).

The number of overheating hours are reduced by 14.3% and 17.6% for the VLW and LW test rooms. The number of overheating hours are reduced by 26.5% and 26.0% for the HW and VHW test rooms.

The T_{res} maximum is reduced by 1.7°C and 1.6°C for the VLW and LW rooms. The T_{res} maximum is reduced by 1.1°C for the HW and VHW rooms.

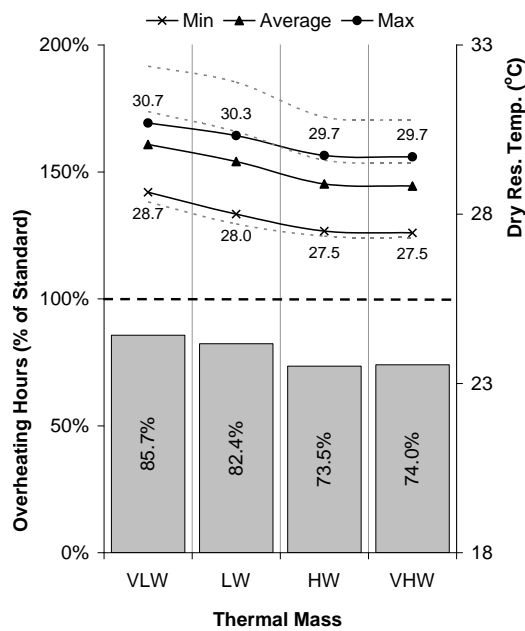


Figure 9—3 TL vs Standard Strategy Annual Overheating Hours – Thermal Mass with Night Cooling

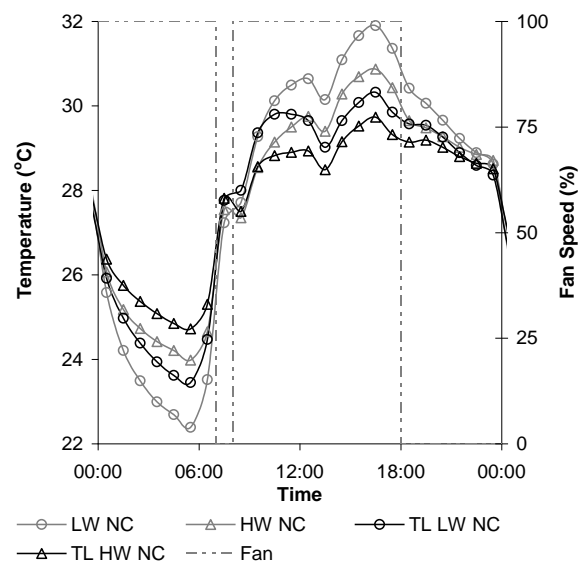


Figure 9—4 TL vs Standard Strategy T_{res} on a peak summer day – Thermal Mass with Night Cooling

9.2.3 Solar Gains

Comparing the results of the different levels of solar gain for the Standard and TL strategies show that for all levels of thermal mass the TL strategy reduces the annual overheating hours and the T_{res} maximum on a peak summer day (Figure 9—5 and Figure 9—6).

The number of overheating hours are reduced by 42.5% for the low solar gain test room, 24.9% for the medium solar gain test room and 13.5% for the high solar gains test room.

The tT_{res} maximum is reduced by 1.7°C for all levels of solar gain.

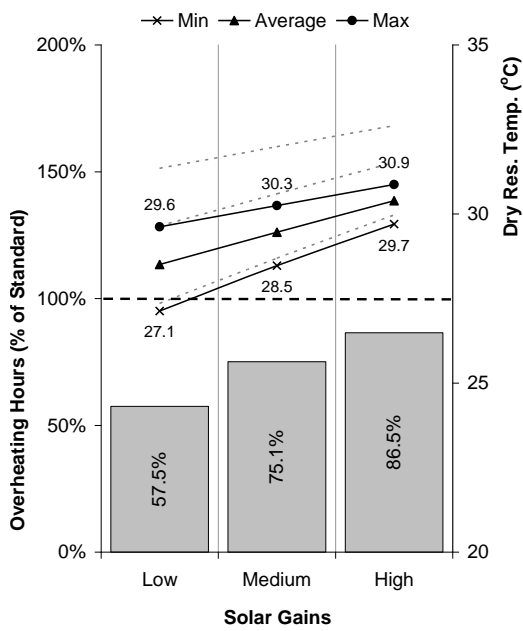


Figure 9—5 TL vs Standard Strategy Annual Overheating Hours – Solar Gain

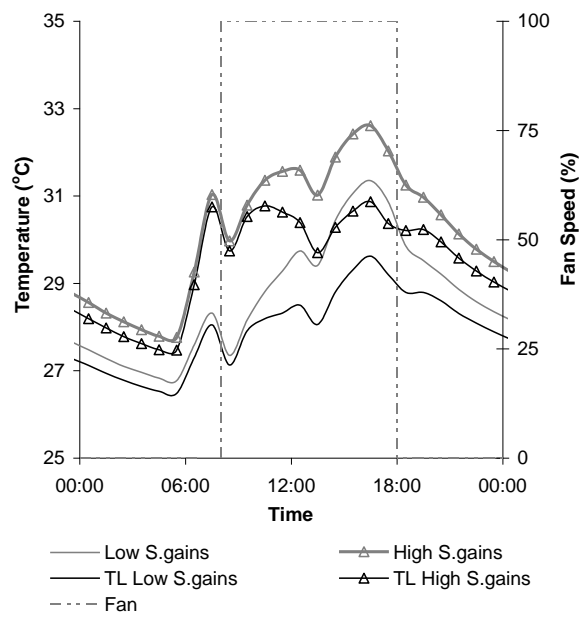


Figure 9—6 TL vs Standard Strategy T_{res} on a peak summer day – Solar Gain

9.2.4 Internal Gains

Comparing the results of the different levels of internal gain for the Standard and TL strategies show that for all levels of thermal mass the TL strategy reduces the annual overheating hours and the T_{res} maximum on a peak summer day (Figure 9—7 and Figure 9—8).

The number of overheating hours are reduced by 32.5% for the low internal gain test room, 13.5% for the medium internal gain test room and 10.0% for the high internal gain test room.

The T_{res} maximum is reduced by 1.6°C for the low internal gain test room and 1.7°C for the medium and high internal gain test rooms.

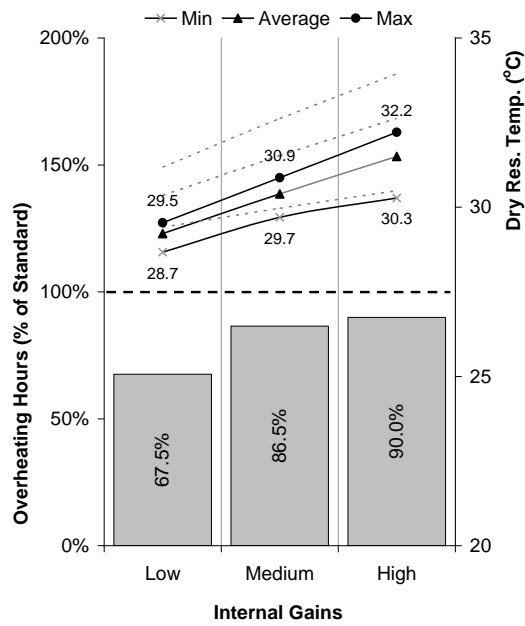


Figure 9—7 TL vs Standard Strategy Annual Overheating Hours – Internal Gain

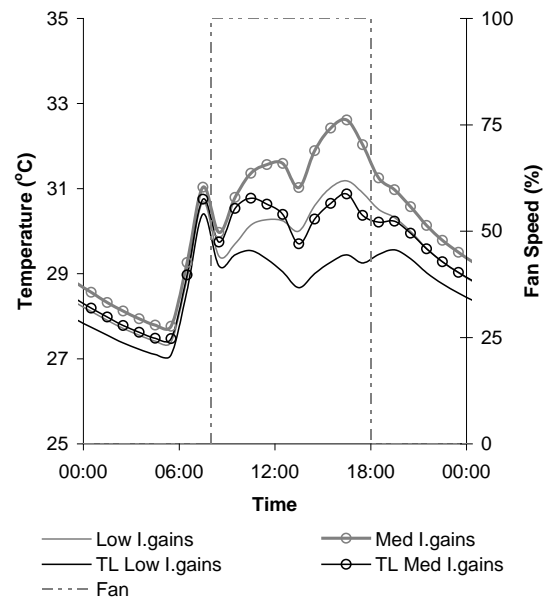


Figure 9—8 TL vs Standard Strategy T_{res} on a peak summer day – Internal Gain

9.2.5 Air Change Rate

Comparing the results of the different levels of air change rate for the Standard and TL strategies show that for all levels of thermal mass the TL strategy reduces the annual overheating hours and the T_{res} maximum on a peak summer day (Figure 9—9 and Figure 9—10).

The number of overheating hours are reduced by 13.5% for the test room with 6ach^{-1} , 29.1% for the test room with 8ach^{-1} and 45.3% for the test room with 10ach^{-1} .

For 6ach^{-1} T_{res} maximum is reduced by 1.7°C . For medium 8ach^{-1} T_{res} maximum is reduced by 2.0°C . For medium 10ach^{-1} T_{res} maximum is reduced by 2.1°C .

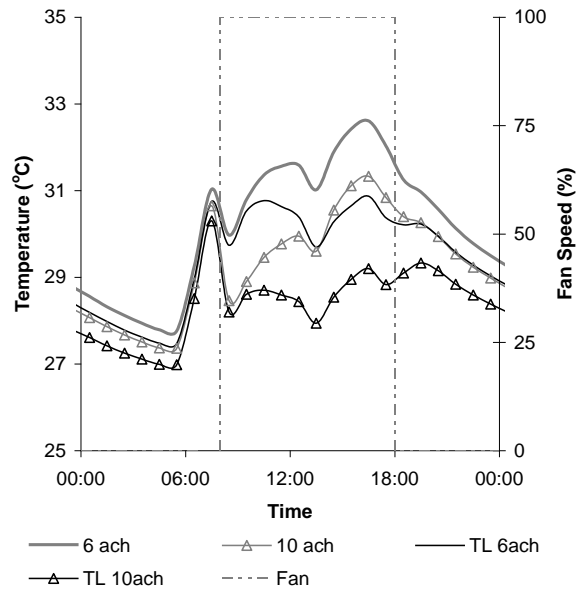
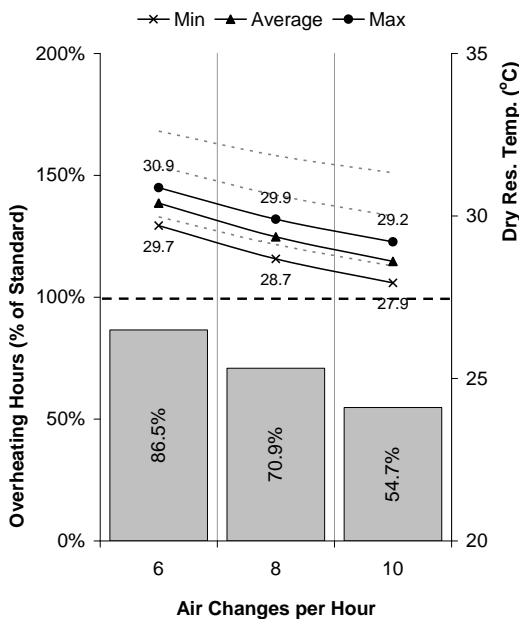


Figure 9—9 TL vs Standard Strategy Annual Overheating Hours – Air Change Rate

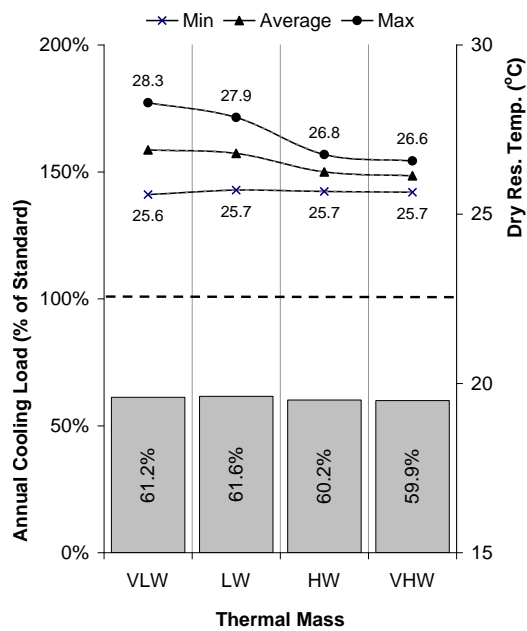
Figure 9—10 TL vs Standard Strategy T_{res} on a peak summer day – Air Change Rate

9.3 Annual Cooling Load

9.3.1 Thermal Mass

Comparing the results of the different levels of thermal mass for the Standard and TL strategies show that for all levels of thermal mass the TL strategy reduces the annual cooling load (Figure 9—11).

The annual cooling load is reduced by 38.8% and 38.4% for the VLW and LW test rooms. The annual cooling load is reduced by 39.8% and 40.1% for the HW and VHW test rooms.



**Figure 9—11 TL vs Standard Strategy
Annual Cooling Load– Thermal Mass**

9.3.2 Thermal Mass with Night Cooling

Comparing the results of the different levels of thermal mass with night cooling for the Standard and TL strategies show that for all levels of thermal mass the TL strategy reduces the annual cooling load (Figure 9—12).

The annual cooling load is reduced by 39.0% and 38.9% for the VLW and LW test rooms. The annual cooling load is reduced by 40.8% and 40.9% for the HW and VHW test rooms.

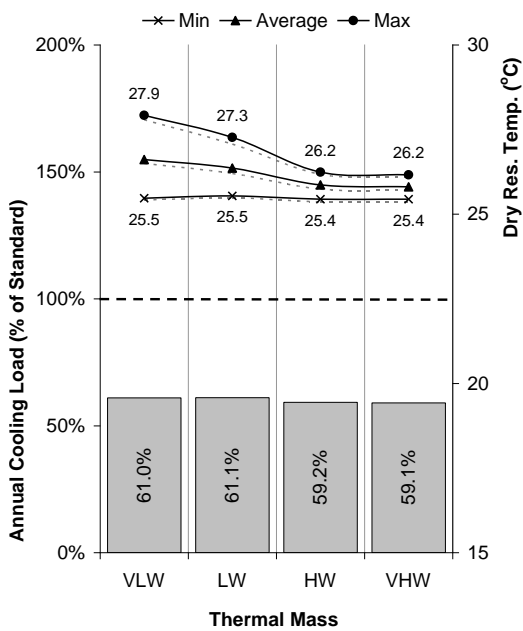
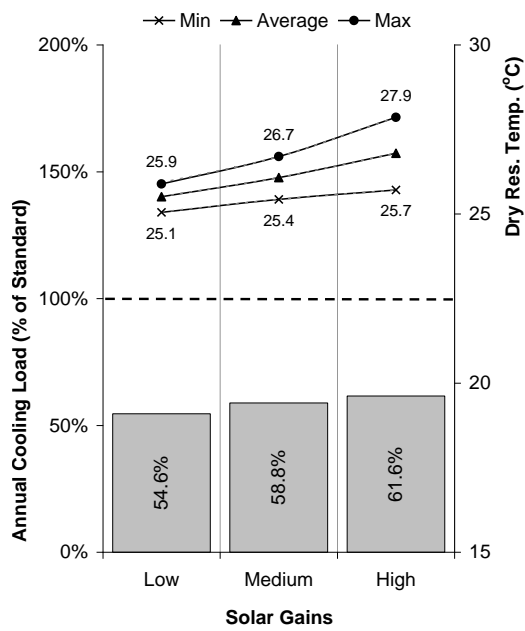


Figure 9—12 TL vs Standard Strategy
Annual Cooling Load— Thermal Mass with
Night Cooling

9.3.3 Solar Gain

Comparing the results of the different levels of solar gain for the Standard and TL strategies show that for all levels of solar gain the TL strategy reduces the annual cooling load (Figure 9—13).

The annual cooling load is reduced by 45.4% for the low solar gain test room, 41.2% for the medium solar gain test room and 38.4% for the high solar gains test room.

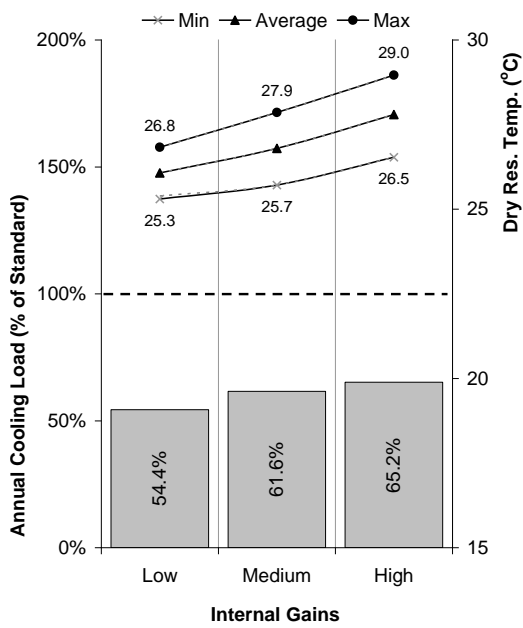


**Figure 9—13 TL vs Standard Strategy
Annual Cooling Load– Solar Gain**

9.3.4 Internal Gains

Comparing the results of the different levels of internal gain for the Standard and TL strategies show that for all levels of internal gain the TL strategy reduces the annual cooling load (Figure 9—14).

The annual cooling load is reduced by 45.6% for the low internal gain test room, 38.4% for the medium internal gain test room and 34.8% for the high internal gains test room.

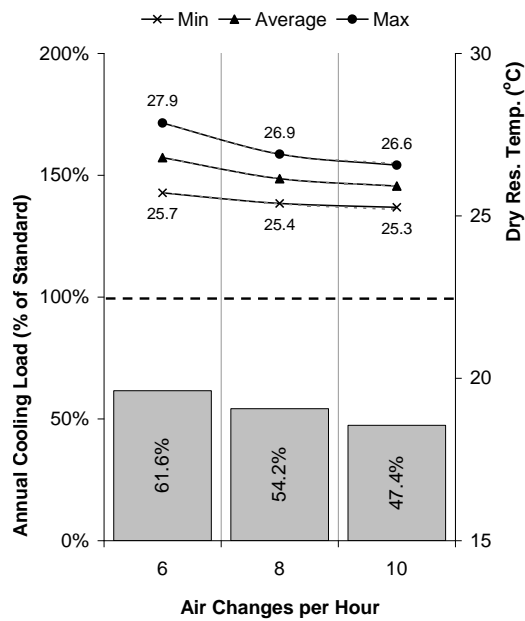


**Figure 9—14 TL vs Standard Strategy
Annual Cooling Load– Internal Gain**

9.3.5 Air Change Rate

Comparing the results of the different levels of air change rate for the Standard and TL strategies show that for all levels of air change rate the TL strategy reduces the annual cooling load (Figure 9—15).

The annual cooling load is reduced by 38.4% for the test room with 6ach^{-1} , 45.8% for the test room with 8ach^{-1} and 52.6% for the test room with 10ach^{-1} .



**Figure 9—15 TL vs Standard Strategy
Annual Cooling Load– Air Change Rate**

9.4 Annual Heating Load

9.4.1 Thermal Mass

Comparing the results of the different levels of thermal mass for the Standard and TL strategies show that for all levels of thermal mass the annual heating load is reduced (Figure 9—16).

The annual heating load is reduced by 8.7% for all the VLW and LW test rooms, by 8.8% for the HW test rooms and by 8.9% for the VHW test room.

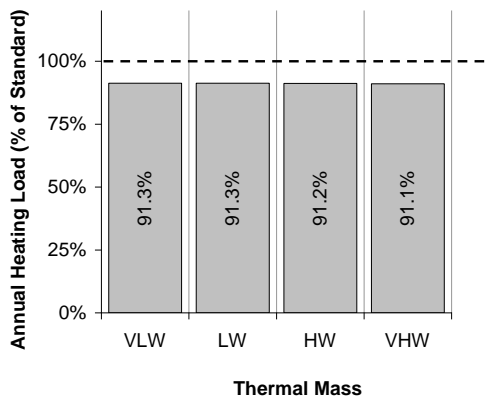
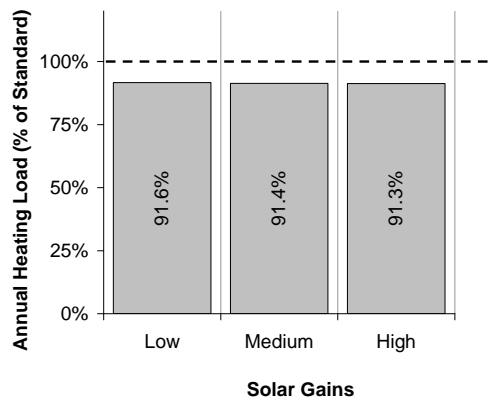


Figure 9—16 TL vs Standard Strategy
Annual Heating Load – Thermal Mass

9.4.2 Solar Gain

Comparing the results of the different levels of solar gain for the Standard and TL strategies show that for all levels of solar gain the annual heating load is reduced (Figure 9—17).

The annual heating load is reduced by 8.4% for the test room with low high solar gain, by 8.6% for the test room with medium solar gain and by 8.7% for the test room with high solar gain.

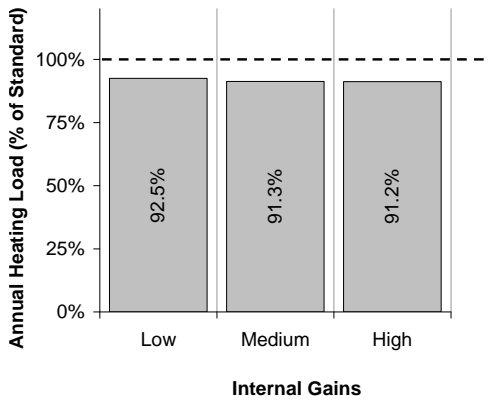


**Figure 9—17 TL vs Standard Strategy
Annual Heating Load – Solar Gain**

9.4.3 Internal Gain

Comparing the results of the different levels of internal gain for the Standard and TL strategies show that for all levels of internal gain the annual heating load is reduced (Figure 9—18).

The annual heating load is reduced by 7.5% for the test room with low internal gain, by 8.7% for the test room with medium internal gain and by 8.8% for the test room with high internal gain.



**Figure 9—18 TL vs Standard Strategy
Annual Heating Load – Internal Gain**

9.4.4 Air Change Rate

Comparing the results of the different levels of air change rate for the Standard and TL strategies show that for all levels of air change rate the annual heating load is reduced (Figure 9—19).

The annual heating load is reduced by 8.7% for the test room with 6ach^{-1} , by 8.6% for the test room with 8ach^{-1} and by 8.3% for the test room with 10ach^{-1} .

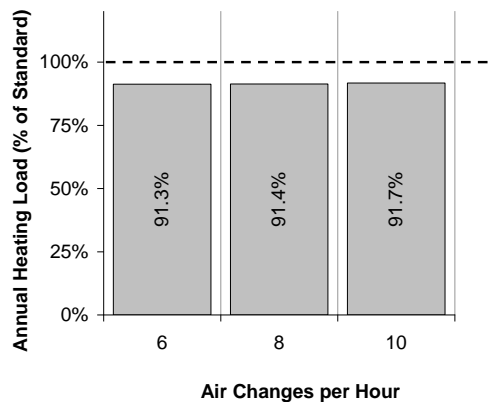


Figure 9—19 TL vs Standard Strategy
Annual Heating Load – Air Change Rate

9.5 Chapter Summary

This chapter presented the results of the Thermal Labyrinth (TL) strategy in comparison to the standard strategy. It has argued that the Thermal Labyrinth has the following characteristics in comparison to the standard strategy:

- All levels of thermal mass without night cooling result in a reduction of annual overheating hours and a reduction of T_{res} maximum.
- Adding night cooling results in a greater reduction of annual overheating hours and a greater reduction of T_{res} maximum.
- There is a reduction of annual overheating hours and a reduction of T_{res} maximum for all levels of solar gain and internal gain.
- Similarly, there is a reduction of annual overheating hours and a reduction of T_{res} maximum for all levels of air change rate.
- The annual cooling load is reduced by around 40% for all investigated cases.
- The annual heating load is reduced by around 10% for all cases investigated.

The next chapter 10, presents the discussion of results of the four active thermal mass strategies.

10.0 DISCUSSION

10.1 Introduction

The previous Chapters 6 to 9 analysed the results comparing the performance of each Active Thermal Mass Strategy against the Standard Strategy.

This chapter 10 will now use the concept design tool, TMAir (Thermal Mass Activation – Air Medium), to compare the performance of the different active thermal mass strategies against one another in terms of (a) number of overheating hours (b) annual cooling load and (c) annual heating load and the results are presented as a percentage of the standard strategy.

10.2 Base Case

Comparing the annual overheating hours (% of Standard strategy) for each of the strategies (Figure 10—1) shows that both the HCS and FVWM strategies result in an increase in annual overheating hours, whereas both the ETAHE and TL strategies result in a reduction in annual overheating hours.

The dampening effect of the additional thermal mass of the HCS and FVWM strategies can be seen in T_{res} on a peak summer day (Figure 10—2).

For the HCS Strategy this results in the peak temperature in the afternoon being lower than that for the Standard Strategy. However, the dampening effect results in the temperature in the morning being higher than that of the Standard Strategy.

The free cooling benefit of both the ETAHE and TL strategies can also be seen in the T_{res} on a peak summer day (Figure 10—2).

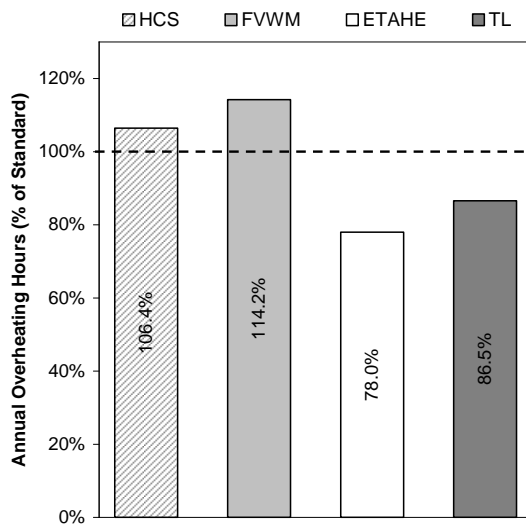


Figure 10—1 Comparison of Strategies Annual Overheating Hours – Base Case

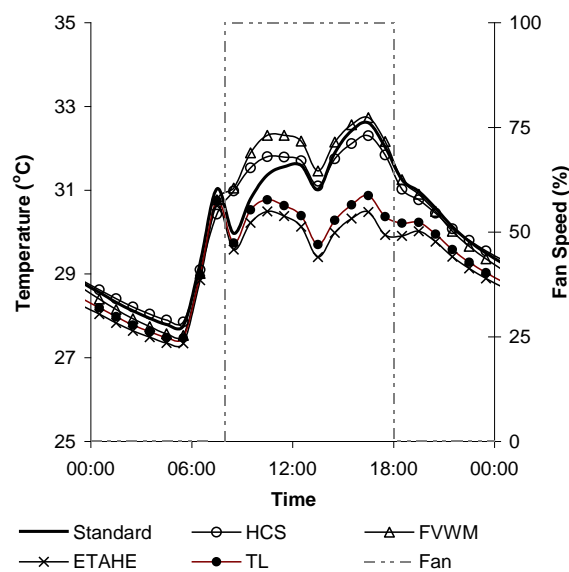


Figure 10—2 Comparison of Strategies T_{res} on a peak summer day – Base Case

When comfort cooling is introduced, both the HCS and FVWM strategies result in around a 15% increase in annual cooling load (% of Standard Strategy), whereas both the ETAHE and TL result in substantial reductions (Figure 10—3).

The HCS and FVWM strategies result in an increase in cooling load due to the temperature of the air being supplied into the floor void being lower than that of the internal surface temperature of the cores or floor void (see sections A.2.2 and A.3.2.). This results in the supply air being heated, and less cooling provided to the test room per cooling energy delivered. The materials within the cores and void are cooled, but never to a temperature less the supply air being passed into the cores or floor void. The materials will also provide a cooling benefit to the rooms above and below the hollow core slabs or floor void. However, since the material does not act as a perfect heat exchanger the annual cooling load is increased.

Comparing the T_{res} on a peak summer day shows that the temperature for the ETAHE and TL strategies is the same as the Standard strategy as a result of these strategies only providing pre-cooling to the supply air. The T_{res} on a peak summer day for the HCS and FVWM strategies is higher as a result of these strategies heating the supply air as it is passed through the cores or floor void.

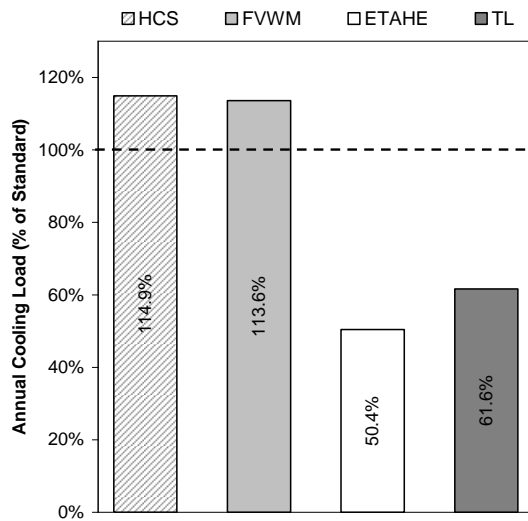


Figure 10—3 Comparison of Strategies Annual Cooling Load – Base Case

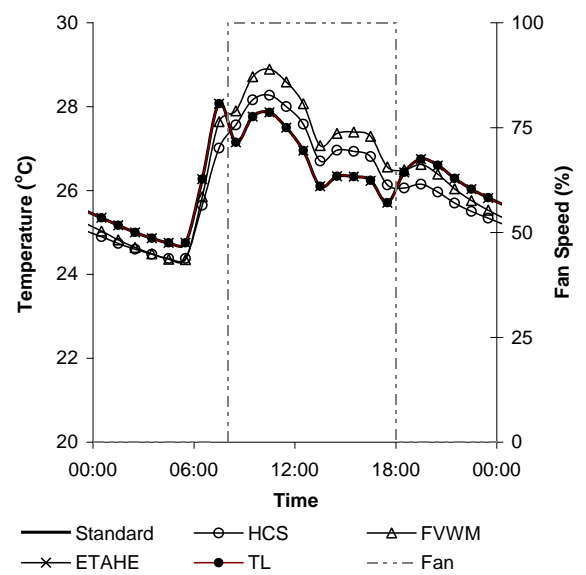
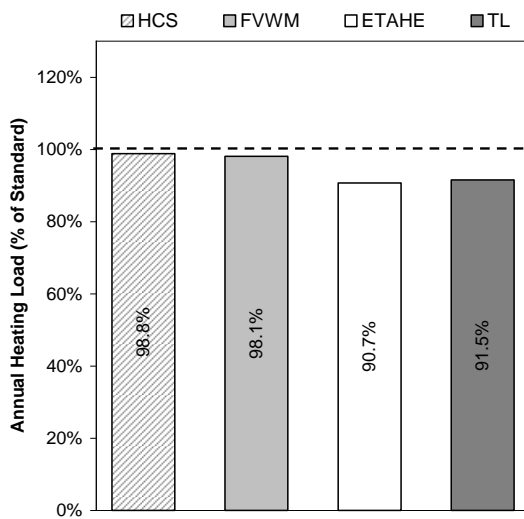


Figure 10—4 Comparison of Strategies T_{res} on a peak summer day with Cooling – Base Case

When the HCS and FVWM strategies are added to the Base Case test room the annual heating load (% of Standard strategy) is reduced by a small amount (Figure 10—5). When the ETAHE and TL Strategies are added to the Base Case test room the annual heating load is reduced by around 10% due to the preheating effect of these strategies.



**Figure 10—5 Comparison of Strategies
Annual Heating Load – Base Case**

10.3 Thermal Mass

Increasing the level of thermal mass from LW to HW results in the annual overheating hours (% of Standard strategy) increasing for the HCS (+6.4%) and FVWM (+2.2%) strategies and reduced slightly for the ETAHE (-5.4%) and TL (-5.5%) strategies (Figure 10—6). This results in the annual overheating hours for both the HCS and FVWM strategies being even higher than that of the Standard strategy and the annual overheating hours for both the ETAHE and TL strategies being slightly lower.

This demonstrates that there is even less benefit in integrating a HCS or FVWM strategy and a slightly greater benefit in integrating an ETAHE or TL strategy when there is a HW level of thermal mass.

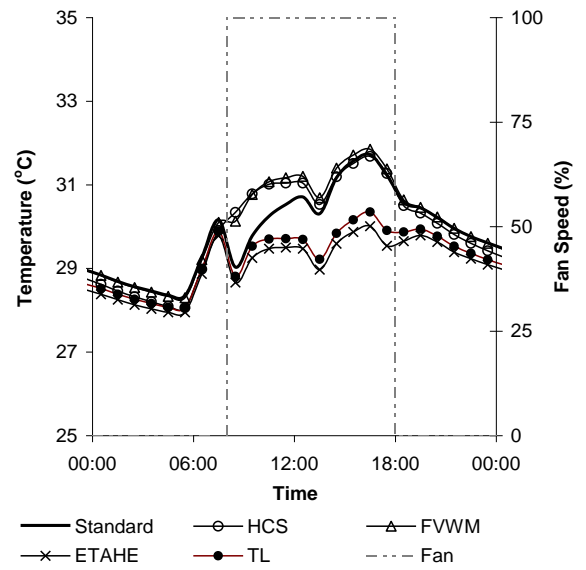
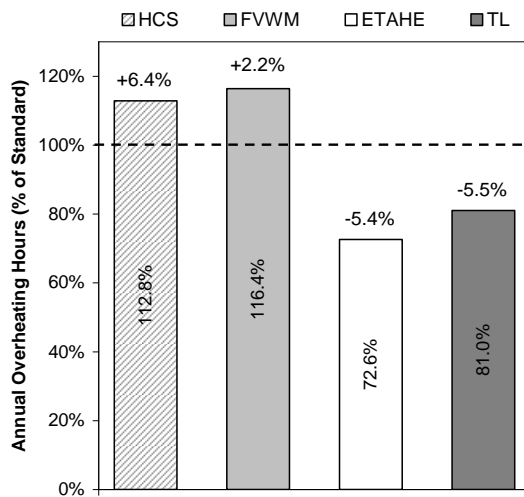


Figure 10—6 Comparison of Strategies Annual Overheating Hours – Thermal Mass

Figure 10—7 Comparison of Strategies Temperature on a peak summer day – Thermal Mass

The annual cooling load (% of Standard) is increased for both the HCS (+6.1%) and FVWM (+5.0%) strategies and reduced moderately for the ETAHE (-1.5%) and TL (-1.4%) strategies (Figure 10—8).

This demonstrates that there is slightly less benefit in integrating a HCS or FVWM strategy and a slightly greater benefit in integrating an ETAHE or TL strategy when there is a HW level of thermal mass.

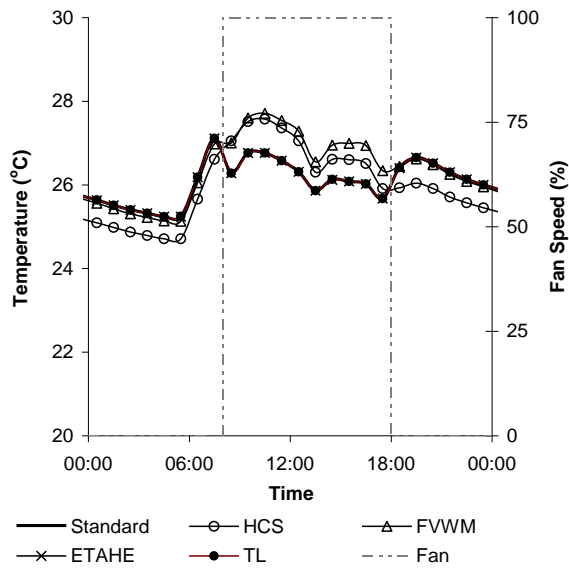
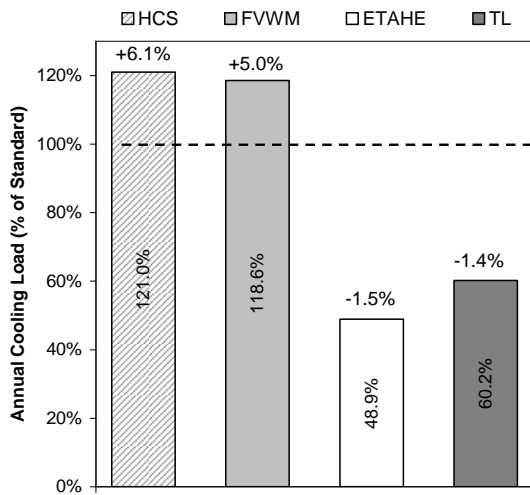
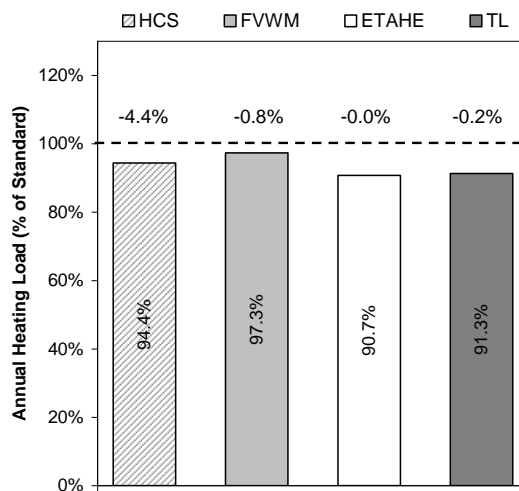


Figure 10—8 Comparison of Strategies Annual Cooling Load – Thermal Mass

Figure 10—9 Comparison of Strategies Temperature on a peak summer day with Cooling – Thermal Mass

The annual heating load (% of Standard) is reduced for all of the active thermal mass strategies (Figure 10—15). The reduction for the FVWM (-0.8%), ETAHE (-0.0%) and TL (-0.2%) is only very small. The reduction for the HCS (-4.4%) strategy is higher.

There is therefore still a small benefit in integrating a HCS and FVWM strategy and a still around a 10% reduction in annual heating load when a ETAHE or TL strategy are integrated when there is a HW level of thermal mass.



**Figure 10—10 Comparison of Strategies
Annual Heating Load – Thermal Mass**

10.4 Thermal Mass with Night Cooling

Introducing night cooling together with increasing the level of thermal mass from LW to HW results in the annual overheating hours (% of Standard strategy) being reduced for the HCS strategy (-9.4%) (Figure 10—11). It is however still increased for the FVWM strategy (+1.6%). There is a substantial reduction for the ETAHE strategy (-27.7%) and a moderate reduction for the TL strategy (-13.0%). This results in the annual overheating hours for the FVWM strategy being even higher than that of the Standard strategy. The annual overheating hours for the HCS strategy are now slightly below that of the Standard strategy and the annual overheating hours for both the ETAHE and TL strategies being substantially lower.

This demonstrates that there is now a benefit in integrating a HCS strategy when the level of thermal mass is HW and there is night cooling. There is again even less benefit in integrating FVWM strategy and a there is a greater benefit in integrating an ETAHE or TL strategy.

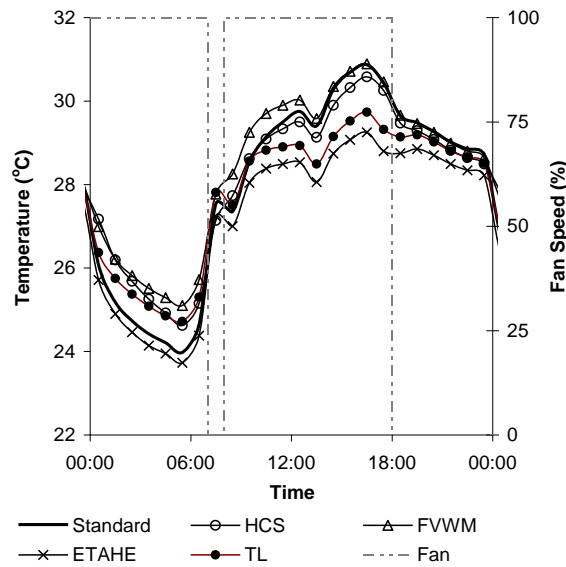
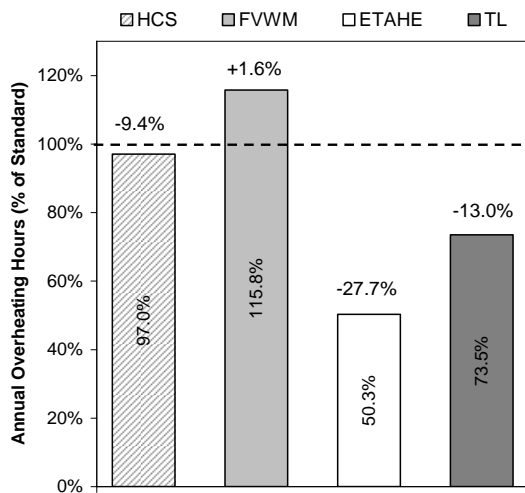


Figure 10—11 Comparison of Strategies Annual Overheating Hours – Thermal Mass with Night Cooling

Figure 10—12 Comparison of Strategies Temperature on a peak summer day – Thermal Mass with Night Cooling

The annual cooling load (% of Standard) is increased for the FVWM strategy (+7.5%), reduced slightly for the HCS strategy (-0.5%) strategy and reduced moderately for the ETAHE (-5.0%) and TL (-2.4%) strategies (Figure 10—13).

This demonstrates that there is still no benefit in integrating a HCS strategy, less benefit in integrating a FVWM strategy and a slightly greater benefit in integrating an ETAHE or TL strategy when there is a HW level of thermal mass with night cooling.

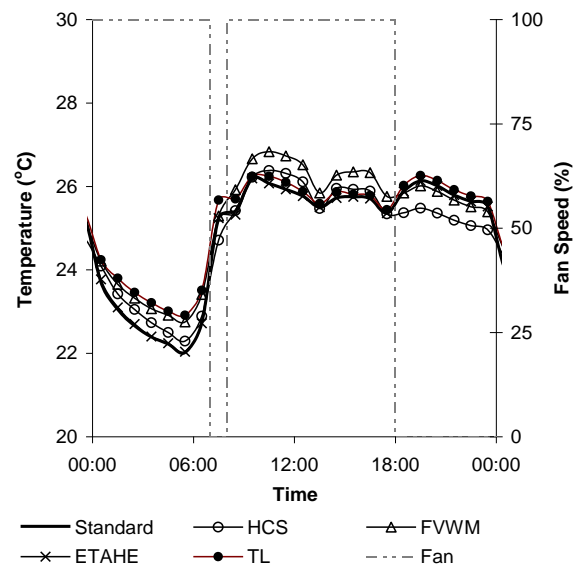
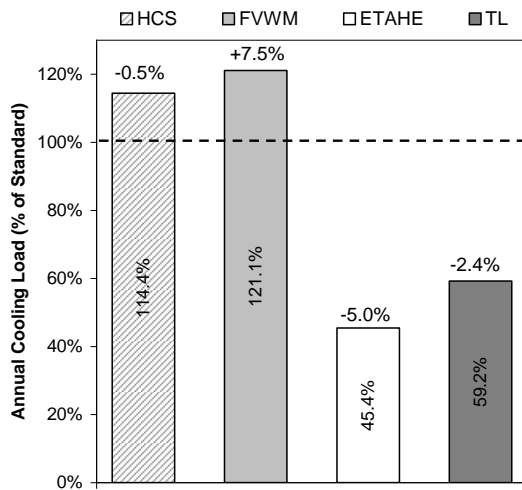
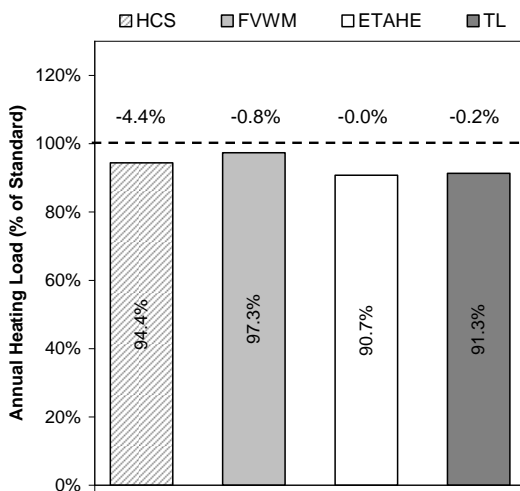


Figure 10—13 Comparison of Strategies Annual Cooling Load – Thermal Mass with Night Cooling

Figure 10—14 Comparison of Strategies Temperature on a peak summer day with Cooling – Thermal Mass with Night Cooling

The annual heating load (% of Standard) is reduced for all of the active thermal mass strategies (Figure 10—15). The reduction for the FVWM (-0.8%), ETAHE (-0.0%) and TL (-0.2%) is only very small. The reduction for the HCS (-4.4%) strategy is higher.

There is therefore still a small benefit in integrating a HCS and FVWM strategy and a still around a 10% reduction in annual heating load when a ETAHE or TL strategy are integrated when there is a HW level of thermal mass.



**Figure 10—15 Comparison of Strategies
Annual Heating Load – Thermal Mass with
Night Cooling**

10.5 Solar Gains

Reducing the level of solar gain to low results in the HCS strategy performing slightly better in terms of annual overheating hours, however it is still higher than that for the Standard strategy (). The FVWM strategy performs slightly worse. There is a substantial improvement in the performance, in terms of annual overheating hours, for both the ETAHE and TL strategies.

Reducing the level of solar gain from high to low results in the annual overheating hours (% of Standard strategy) increasing for the FVWM strategy (+1.7%), slightly reducing for the HCS strategy (-3.7%) and reducing substantially for the ETAHE (-35.8%) and TL (-29.0%) strategies (Figure 10—15). This results in the annual overheating hours for the HCS strategy still being higher and the FVWM strategy being even higher than that of the Standard strategy and the annual overheating hours for both the ETAHE and TL strategies being much lower.

This demonstrates that there is still isn't a benefit in integrating a HCS strategy, there is even less benefit in integrating a FVWM strategy and there is a greater benefit in integrating an ETAHE or TL strategy when there is a low level of solar gain.

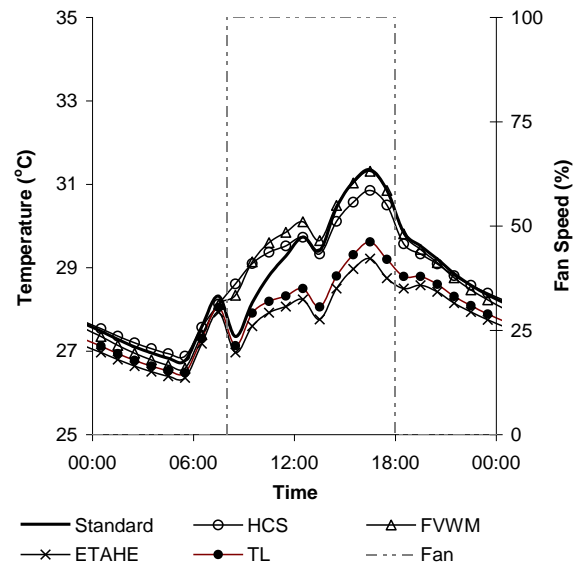
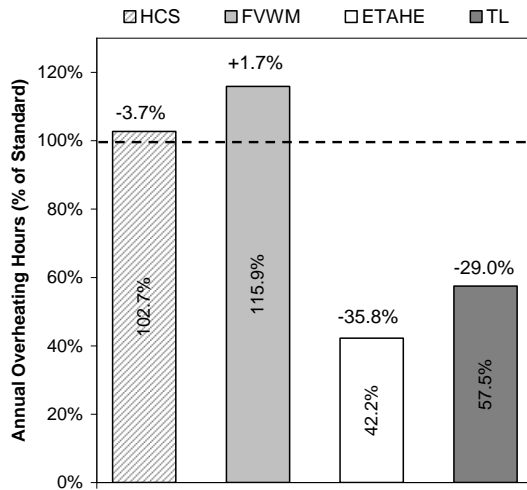


Figure 10—16 Comparison of Strategies Annual Overheating Hours – Solar Gains

Figure 10—17 Comparison of Strategies Temperature on a peak summer day – Solar Gains

The annual cooling load (% of Standard) is increased for both the HCS (+9.5%) and FVWM (+9.9%) strategies and reduced moderately for the ETAHE (-7.0%) and TL (-7.0%) strategies (Figure 10—18).

This demonstrates that there is slightly less benefit in integrating a HCS or FVWM strategy and a moderately greater benefit in integrating an ETAHE or TL strategy when there is a low level of solar gain.

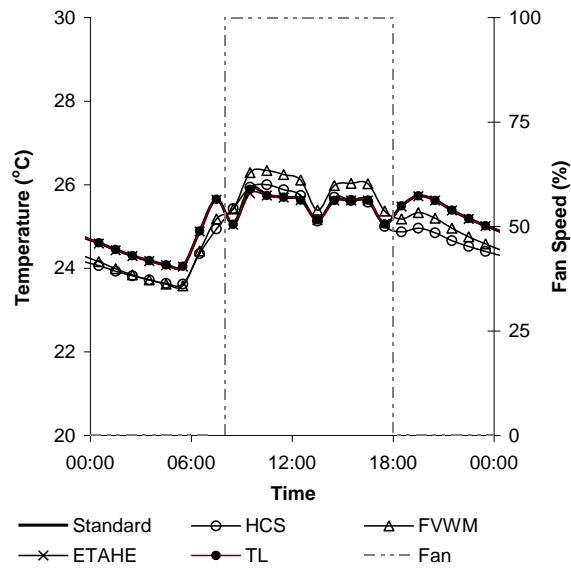
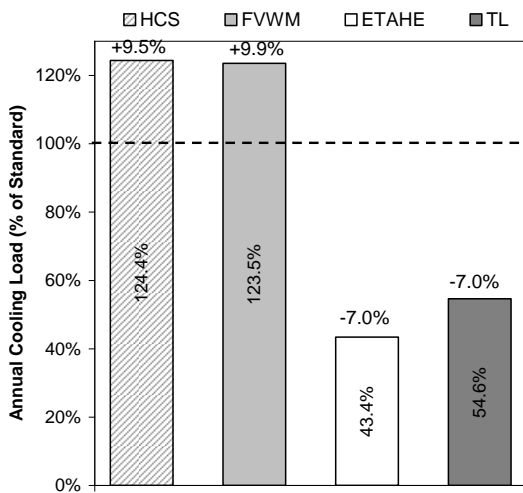
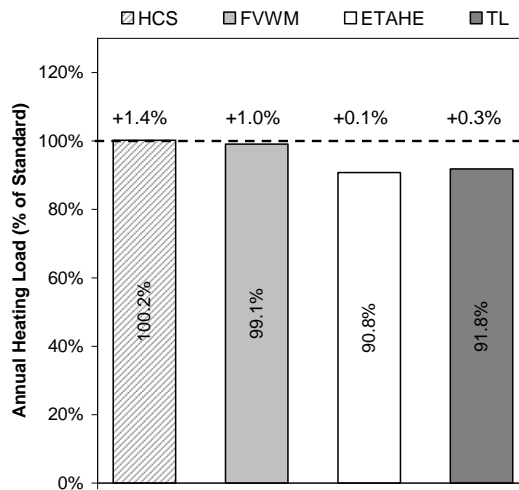


Figure 10—18 Comparison of Strategies Annual Cooling Load – Solar Gain

Figure 10—19 Comparison of Strategies Temperature on a peak summer day with Cooling – Solar Gain

The annual heating load (% of Standard) is increased for all of the active thermal mass strategies (Figure 10—20). The reductions for the ETAHE (+0.1%) and TL (+0.3%) strategies are only very small. The reduction for the HCS (+1.4%) and FVWM (+1.0%) strategies are slightly more.

This now results in the HCS strategy resulting in a higher annual heating load than the Standard strategy, the FVWM strategy only providing a very small benefit. There is still around a 10% reduction in annual heating load when a ETAHE or TL strategy are integrated when there is a low level of solar gain.



**Figure 10—20 Comparison of Strategies
Annual Heating Load – Solar Gain**

10.6 Internal Gains

Reducing the level of internal gain from medium to low results in the annual overheating hours (% of Standard strategy) increasing for the HCS (+0.4%) and FVWM (+3.2%) strategies and reduced substantially for the ETAHE (-21.6%) and TL (-19.0%) strategies (Figure 10—21). This results in the annual overheating hours for both the HCS and FVWM strategies being even higher than that of the Standard strategy and the annual overheating hours for both the ETAHE and TL strategies being much lower.

This demonstrates that there is even less benefit in integrating a HCS or FVWM strategy and a greater benefit in integrating an ETAHE or TL strategy when there is a low level of internal gain.

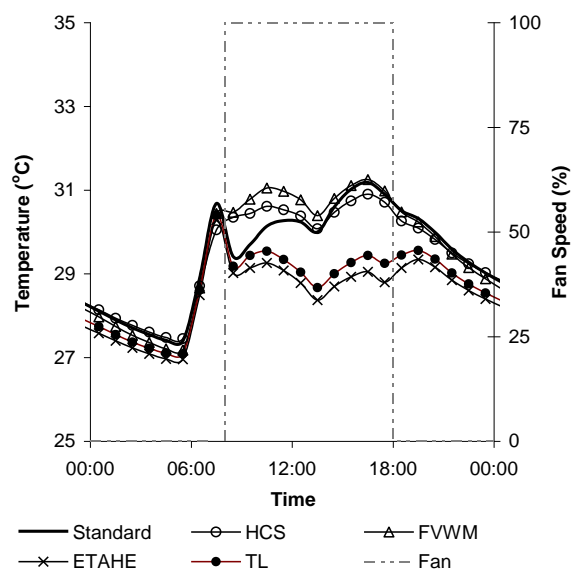
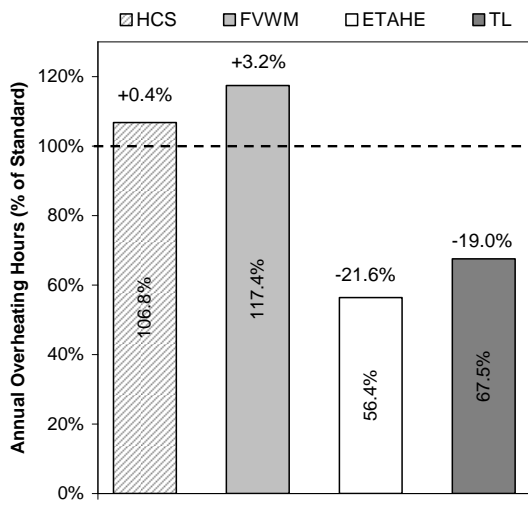


Figure 10—21 Comparison of Strategies Annual Overheating Hours – Internal Gains

Figure 10—22 Comparison of Strategies Temperature on a peak summer day – Internal Gains

The annual cooling load (% of Standard) is increased by around 10% for both the HCS and FVWM strategies and reduced moderately for the ETAHE (-8.6%) and TL (-7.2%) strategies.

This demonstrates that there is even less benefit in integrating a HCS or FVWM strategy and a greater benefit in integrating an ETAHE or TL strategy when there is a low level of internal gain.

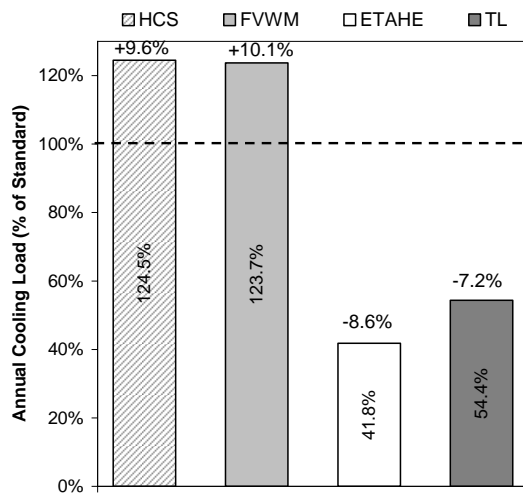


Figure 10—23 Comparison of Strategies Annual Cooling Load – Internal Gain

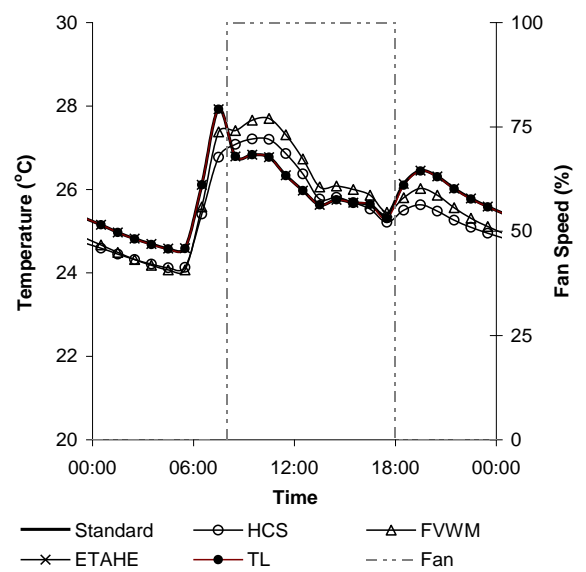
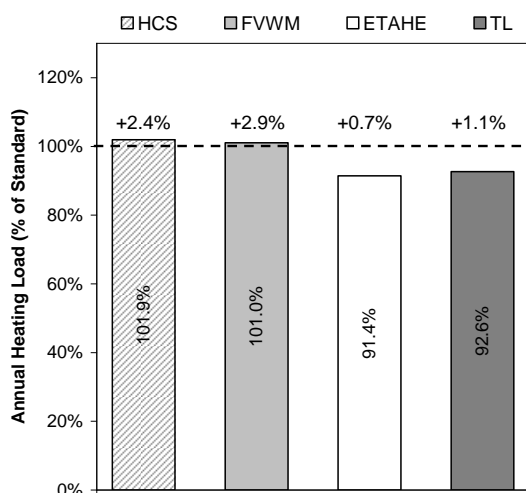


Figure 10—24 Comparison of Strategies Temperature and Fan Speed on a Peak Summer Day with Cooling – Internal Gain

The annual heating load (% of Standard) is increased for all of the active thermal mass strategies (Figure 10—25). The reductions for the ETAHE (+0.7%) and TL (+1.1%) strategies are only small. The reduction for the HCS (+2.4%) and FVWM (+2.9%) strategies are slightly more.

This now results in the HCS strategy resulting in a higher annual heating load than the Standard strategy, the FVWM strategy only providing a very small benefit. There is still around a 10% reduction in annual heating load when a ETAHE or TL strategy are integrated when there is a low level of internal gain.



**Figure 10—25 Comparison of Strategies
Annual Heating Load – Internal Gain**

10.7 Air Change Rate

Increasing the air change rate from 6 to 8 air changes per hour results in the annual overheating hours (% of Standard strategy) slightly reducing for the HCS (-2.2%) and FVM (-1.6%) strategies and reduced substantially for the ETAHE strategy (-22.8%) and moderately for the TL strategy (-15.6%) (Figure 10—26). This results in the annual overheating hours for both the HCS and FVM strategies still being higher than that of the Standard strategy and the annual overheating hours for both the ETAHE and TL strategies being much lower.

This demonstrates that there still isn't a benefit in integrating a HCS or FVM strategy and that there is a greater benefit in integrating an ETAHE or TL strategy when the air change rate is 8 air changes per hour.

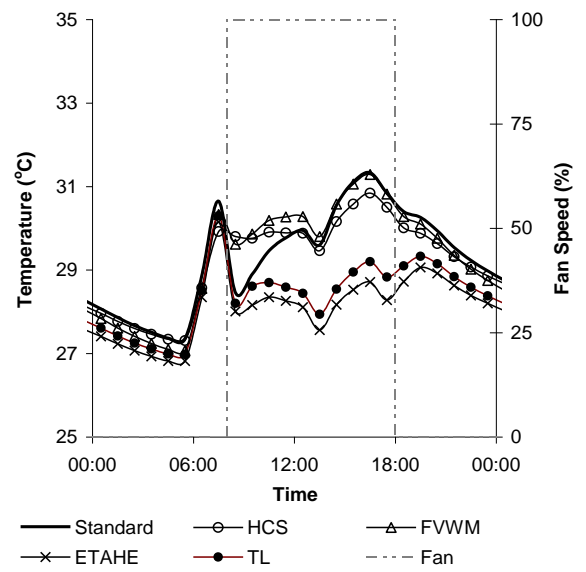
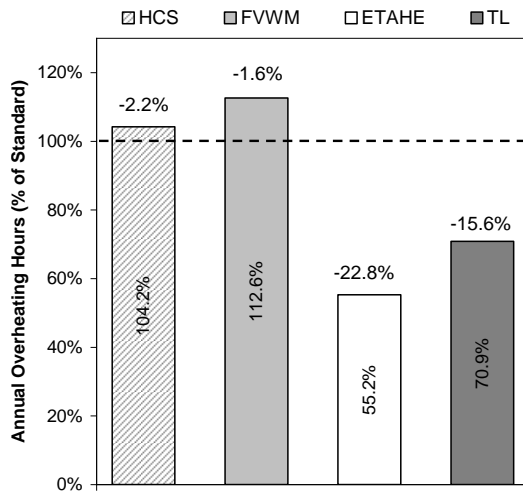


Figure 10—26 Comparison of Strategies Annual Overheating Hours – Air Change rate **Figure 10—27 Comparison of Strategies Temperature on a peak summer day – Air Change rate**

The annual cooling load (% of Standard) is increased for both the HCS (+7.2%) and FVWM (+7.0%) strategies and reduced moderately for the ETAHE (-8.1%) and TL (-7.4%) strategies (Figure 10—28).

This demonstrates that there is less benefit in integrating a HCS or FVWM strategy and a moderately greater benefit in integrating an ETAHE or TL strategy when there is an air change rate of 8 air changes per hour.

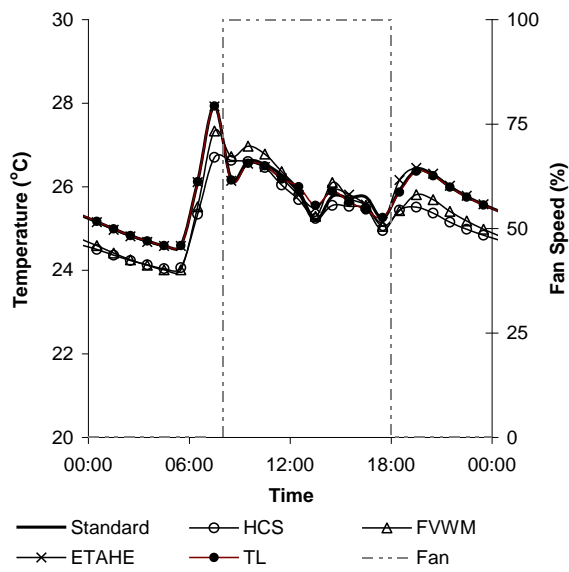
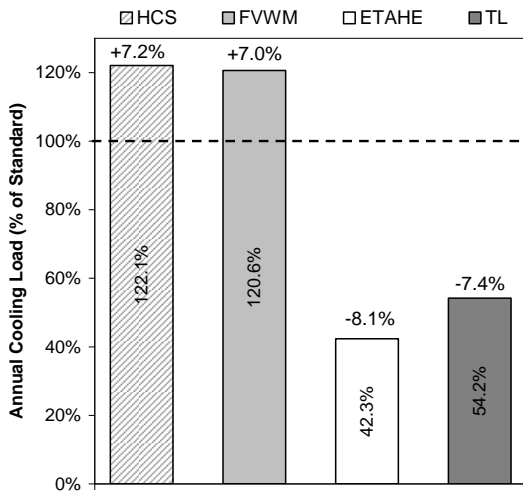
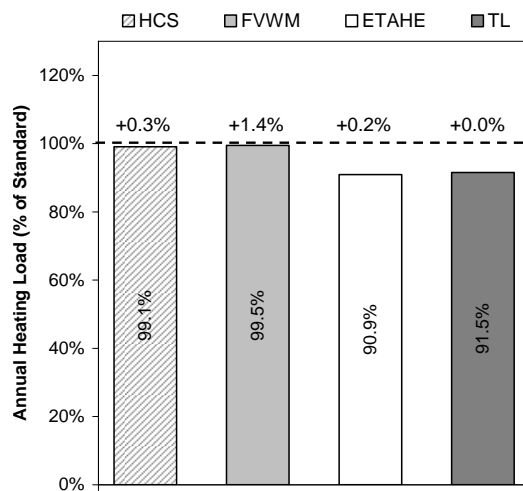


Figure 10—28 Comparison of Strategies Annual Cooling Load – Air Change rate

Figure 10—29 Comparison of Strategies T_{res} on a peak summer day with Cooling – Air Change rate

The annual heating load (% of Standard) is increased for all of the active thermal mass strategies (Figure 10—20). The reductions for the HCS (+0.3%), ETAHE (+0.2%) and TL (+0.0%) strategies are only very small. The reduction for the FVWM strategy (+1.4%) is slightly more.

This now results in the HCS and the FVWM strategy only providing a very small benefit. There is still around a 10% reduction in annual heating load when a ETAHE or TL strategy are integrated when there is an air change rate of 8 air changes per hour.



**Figure 10—30 Comparison of Strategies
Annual Heating Load – Air Change rate**

10.8 Combinations of Parameters

When the improvements are applied to the test room in sequence the results show that all of the active thermal mass strategies can provide a reduction in annual overheating hours when compared to the Standard Strategy (Figure 10—31).

Only a small benefit is found for the FVWM Strategy, however around a 25% reduction is found for the HCS Strategy, over a 50% reduction for the TL Strategy and nearly a 75% reduction for the ETAHE Strategy.

This demonstrates the importance of applying a low energy, passive approach when considering the application of active thermal mass strategies.

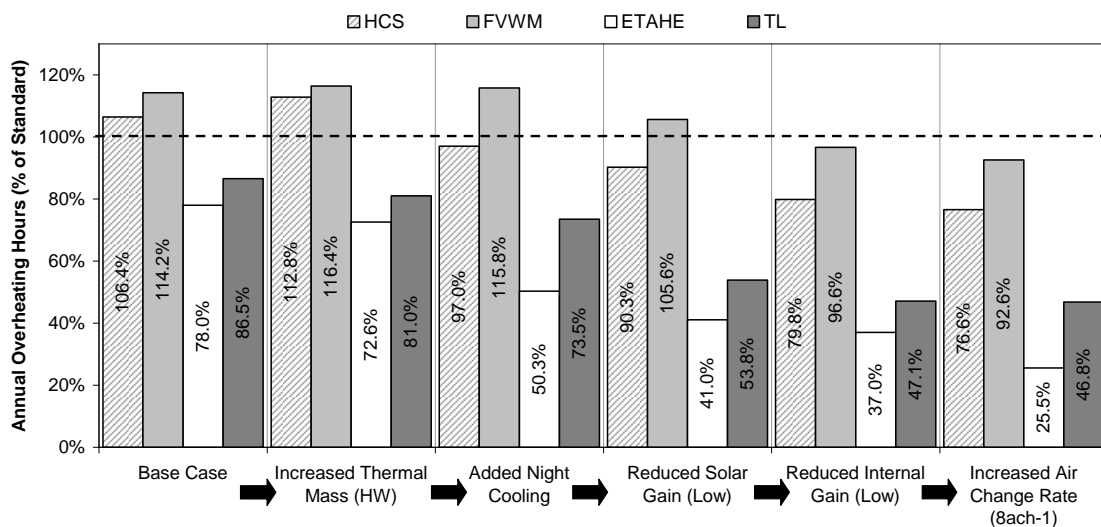


Figure 10—31 Comparison of Strategies Annual Overheating Hours – Combinations of Parameters

However, even when all of the when all of the improvements are applied to the test room both the HCS and FVWM strategies still result in an increase in annual cooling load when compared to the Standard strategy, although the benefit of the ETAHE and TL strategies can be improved further (Figure 10—32).

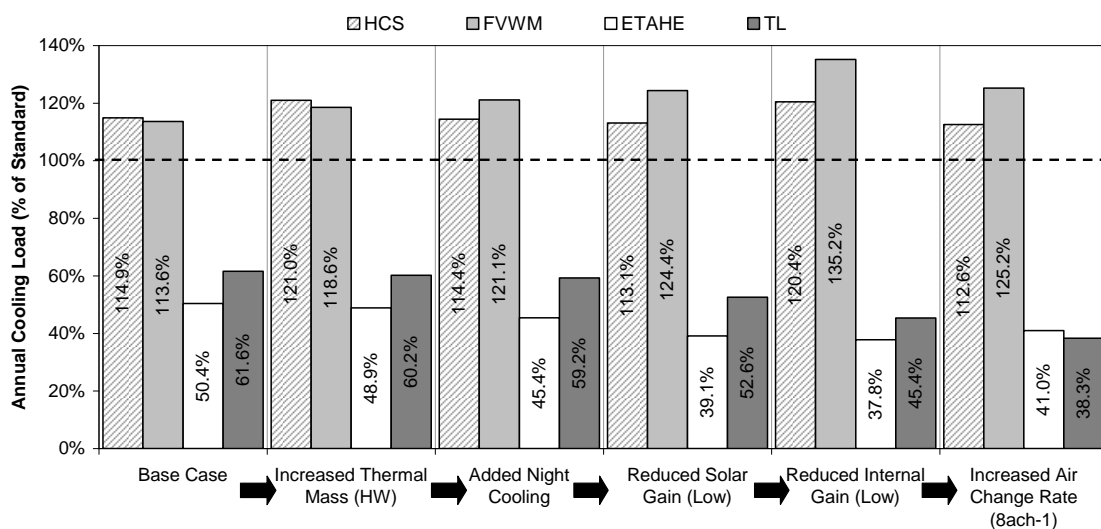


Figure 10—32 Comparison of Strategies Annual Cooling Load – Combinations of Parameters

Applying all of the improvements only has a small impact on the Annual Heating Load (% of Standard) with the HCS and FVWM strategies providing a small benefit, unless the internal gains are reduced to low, and the ETAHE and TL strategies resulting in around a 10% reduction in annual heating load when compared to the Standard strategy (Figure 10—33).

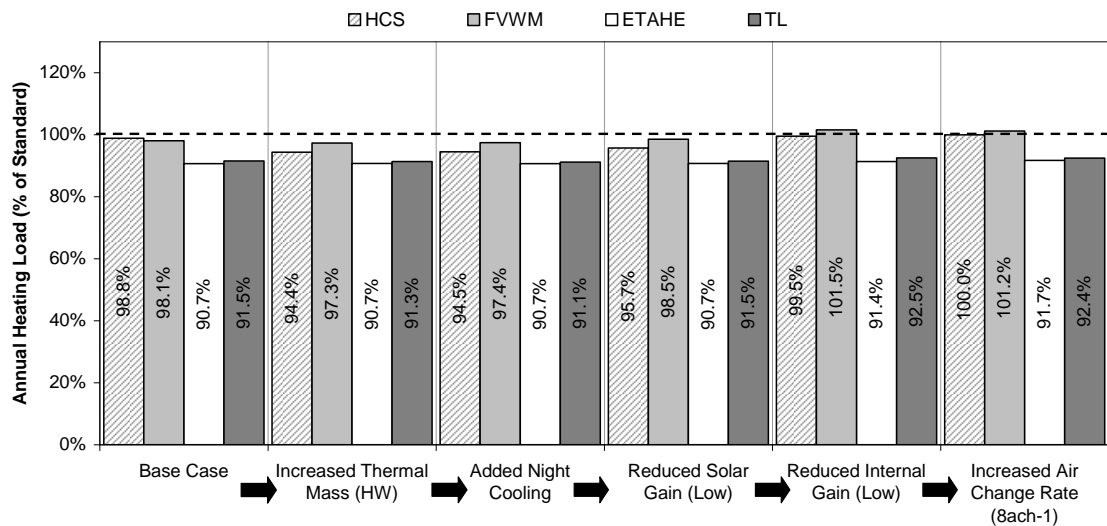


Figure 10—33 Comparison of Strategies Annual Heating Load – Combinations of Parameters

The concept design tool developed TMAir (Thermal Mass Activation – Air Medium) also allows different combinations of parameter improvements to be compared.

10.9 Summary

The Annual Overheating Hours, Annual Cooling Load and Annual Heating Load, expressed as a percentage of the Standard strategy have been investigated for the improvement of five parameters in turn, for the four active thermal mass strategies: Hollow Core Slabs (HCS), Floor Void with Mass (FVWM), Earth to Air Heat Exchanger (ETAHE) and Thermal Labyrinth (TL).

A summary of the annual overheating hours (% of Standard Strategy) results are given in Table 10—1. The results show that for the Base Case test room studied :

- There is only a benefit in integrating a HCS strategy when night cooling is introduced.
- There is no benefit in integrating a FVWM strategy when only one parameter is improved.
- An ETAHE and TL strategy will always provide a benefit, although the benefits are greater when night cooling is introduced, solar and internal gains are reduced and when the air change rate is increased

Table 10—1 Annual Overheating Hours

	HCS	FVWM	ETAHE	TL
Base Case	106.4%	114.2%	78.0%	86.5%
HW	112.8%	116.4%	72.6%	81.0%
HW+NC	97.0%	115.8%	50.3%	73.5%
Low S Gains	102.7%	115.9%	42.2%	57.5%
Low I Gains	106.8%	117.4%	56.4%	67.5%
8 ach ⁻¹	104.2%	112.6%	55.2%	70.9%

A summary of the annual cooling load (% of Standard Strategy) results are given in Table 10—2. The results show that for the Base Case test room studied:

- Adding a HCS or FVWM strategy always results in an increase in the annual cooling load.
- Due to the pre cooling effect of the ETAHE and TL strategies, these strategies always result in a reduction in the annual cooling load.

Table 10—2 Annual Cooling

	HCS	FVWM	ETAHE	TL
Base Case	114.9%	113.6%	50.4%	61.6%
HW	121.0%	118.6%	48.9%	60.2%
HW+NC	114.4%	121.1%	45.4%	59.2%
Low S Gains	124.4%	123.5%	43.4%	54.6%
Low I Gains	124.5%	123.7%	41.8%	54.4%
8 ach ⁻¹	122.1%	120.6%	42.3%	54.2%

A summary of the annual heating load (% of Standard Strategy) results are given in Table 10—3. The results show that for the Base Case test room studied:

- The HCS strategy reduces the annual heating load by a small amount, unless the solar gains or internal gains are reduced.
- The FVWM strategy reduces the annual heating load by a small amount, unless the internal gains are reduced.
- The ETAHE and TL strategies always result in a around a 10% reduction in annual heating load as a result of the preheating effect these strategies have on the supply air.

Table 10—3 Annual Heating

	HCS	FVWM	ETAHE	TL
Base Case	98.8%	98.1%	90.7%	91.5%
HW	94.4%	97.3%	90.7%	91.3%
HW+NC	94.5%	97.4%	90.7%	91.1%
Low S Gains	100.2%	99.1%	90.8%	91.8%
Low I Gains	101.9%	101.0%	91.4%	92.6%
8 ach ⁻¹	99.1%	99.5%	90.9%	91.5%

11.0 CONCLUSION

11.1 Introduction

The thesis has investigated the integration of active thermal mass strategies in responsive buildings focussing on improving the understanding of architects, building services engineers and building physicists of the performance of active thermal mass strategies in operational buildings, and also to provide guidance for their use in suitable future buildings.

The literature review highlighted that active methods enhance the performance of thermal mass by passing air or fluid across or through the materials with high thermal mass. Such systems have been applied to buildings but there is still uncertainty on how to incorporate them in new designs and how to carry out accurate (but as simple as possible) modelling during the detailed design of a building. Therefore the solution must be provided in two parts. The first must deal with simplified guidelines on how activated thermal mass could reduce energy consumption (and by how much) and possibly improve environmental conditions. The second must deal with building up confidence in dynamic thermal models used by building services engineers to accurately predict environmental conditions in a building incorporating active thermal mass strategies.

This thesis addresses this in three ways:

- (i) by developing a profile of the performance of active thermal mass strategies in operational buildings
- (ii) by determining the accuracy of commercially available dynamic thermal models and
- (iii) by creating simple design guidance for the use at the concept design stages of a project.

11.2 Building Monitoring & Simulation

The monitoring of three operational buildings incorporating four different active thermal mass strategies allowed a profile of the performance of active thermal mass strategies in operational buildings to be developed.

Using construction record drawings and on-site measures a model of each building, focusing on the active thermal mass strategies, was constructed within the commercially available dynamic building thermal program IES Virtual Environment. Each building was monitored for a minimum of two periods in different climatic weather periods (winter, mid season or summer) to create two sets of data to calibrate the dynamic thermal models against.

IES Virtual Environment has been extensively validated in the simulation of standard building types previously. The interest of the validation was therefore only concerned with the accuracy of simulating the active thermal mass strategy.

All of the buildings monitored had varying levels of internal and solar gains that would have been difficult to monitor accurately without severely disrupting the running of the buildings and at a cost that could not be justified. To isolate the performance of the active thermal mass strategy in each model it was therefore chosen to monitor the temperatures adjacent to the thermal mass, which varies with the internal and solar gains, and set these as boundary conditions within the simulation models.

For Booth's HQ and Longley Park case studies these were the air temperatures in the rooms above and below the floor void or hollow core slab. For the Lowry ETAHE, this was the surrounding ground temperature and the ambient air temperature and for the Lowry Plenum, this is the theatre above and the ground below.

For the ground temperature the temperature of the ground at 10m below the surface would ideally have been used, this is because at this depth the undisturbed ground temperature is almost equal to the average annual temperature (Carslaw and Jaeger 1959). However, the amount of soil that could be added to the model was limited to 4.5m. This reached almost 8m below ground and was considered a good approximation to the undisturbed ground

temperature. A depth of soil has also been included within the ETAHE and Plenum models to allow the dynamic effect of the ground temperature on the ETAHE/Plenum to be simulated and also the effect of the ETAHE/Plenum on the ground.

The air temperature entering the active thermal mass was then used as an input into the model and the air temperature leaving the active thermal mass strategy as the output of the model. The flow rates from the monitored data have also been used as input into the model.

The geometry for the Floor Void with Mass (FVWM) Strategy at Booths HQ was added to the model as the actual building due to the simple geometry, however simplifications for easiness of modelling were made in the geometry of the other active thermal mass strategies within the models.

The Hollow Core Slab (HCS) Strategy at Longley Park and the Earth to Air Heat Exchanger (ETAHE) Strategy at The Lowry were simplified as two parallel plates with air passing between them, one in contact with the room/ground above and one in contact with the room/ground below. The models were constructed to create air paths with the same cross sectional area and internal surface area. The depth of concrete added to the Hollow Core Slab model created the same volume of thermal mass of the actual slab.

The geometry of the plenum beneath the theatre at The Lowry is complex as it is formed beneath the raked theatre stalls seating. To represent the amount of mass that the plenum has, in the model a rectangular room with the same surface area and air volume was constructed. The same exposed area of internal sleeper wall was also included within the model.

The CIBSE variable heat transfer coefficients were used for the FVWM at Booths and the Plenum at The Lowry as a result of the low air turbulence created. The increased turbulence created within the HCS at Longley Park and the ETAHE at The Lowry required the heat transfer coefficients to be calculated using a correlation for turbulent flow in circular and non-circular ducts. The effect that the surface roughness and bends have on the heat transfer have also been explored. The effect on the temperature of the air leaving the slab (air temperature and mean radiant temperature) was found to be minimal for both the surface roughness and the bends.

Simulation results of the air temperatures within all of the active thermal mass strategies have shown good comparison with the monitored data.

11.3 Development of a Concept Design Tool

Using the calibrated modelling methods a concept design tool, TMAir (Thermal Mass Activation – Air Medium), was developed to help designers analyse the effects, in terms of energy and comfort, of integrating active thermal mass strategies into office buildings for a range of design parameters.

To allow the effects of integrating an active thermal mass strategy into an office building to be determined, a number of parameters have been explored.

These parameters were split into two categories:

- (i) The fixed parameters - pre-selected for the design tool and were chosen to be a fair representation of the projects that the tool will be used for.
- (ii) The user selected parameters - chosen by the user to represent the way the building will be used, and to look at the effect of key design decisions on the performance of the building.

The simulation results are based on a single office cell 10m wide, 6m deep and 3m high and use CIBSE Design Summer Year (DSY) 2005 weather data for London. These were determined to give a fair representation of the majority of the projects that the sponsoring design organisation will use the tool for.

The user selected parameters can be selected by the user to represent the way the building will be used, and to look at the effect of key design decisions on the performance of the building.

The user can select the following parameters:

- Active Thermal Mass Strategy

- Service Strategy
- Air Flow Rate
- Internal Heat Gain
- Night Cooling
- Glazing Area
- Shading Type
- Building Weight
- Orientation

All of the possible combinations of the user selected parameters have been simulated and the results have been fed into the excel based concept design tool TMAir.

The tool has been developed with an easy-to-use interface which allows direct comparison of the different active thermal mass strategies together with the effects of changing key design parameters. Results are presented in terms of thermal comfort and energy consumption

TMAir tool allows the user to select five options for comparison. For each of the five options the user selected parameters can be changed. Option 1 is classed as the 'BASE Case' because the results of all of the other options are compared against this option. As a default the BASE Case Option 1 input parameters were selected to represent typical values and comply with typical benchmark values and energy consumption in the UK.

The output results from TMAir are presented on two levels; summary results and detailed results:

- Summary Results - a single page printout intended to give a quick snapshot of the performance of the different options. The results are presented in a graphical format of the actual values and in a tabular format that express the results as a percentage

of the BASE Case Option 1 allowing quick comparison between the different options.

- Detailed Results - to allow the user to look at the results in more detail there is a separate page for heating energy, cooling energy and overheating hours. The results are broken down into monthly energy consumption and look at the energy and room temperatures during a peak week and a peak day. The results are again presented in a graphical format for the actual results and in a tabular format that express the results as a percentage of the BASE Case Option 1.

11.4 Main Findings

Using TMAir a parametric analysis was then performed for the Standard Strategy model and each of the active thermal mass strategies to investigate the effects of changing the user selected parameters.

The thesis has argued that the hollow core slab strategy has the following characteristics in comparison to the standard strategy:

- (i) Hollow core slab without night cooling results in an increase of annual overheating hours and only a slight reduction of T_{res} maximum for the lightweight building types..
- (ii) Adding night cooling results to a reduction of annual overheating hours for all but the VHW level of thermal mass and a reduction in T_{res} maximum for all levels of thermal mass.
- (iii) There is an increase of annual overheating hours for all levels of solar gain and internal gain. However, T_{res} maximum is reduced on a peak summer day for all levels of solar gain and internal gain..
- (iv) Similarly, there is an increase of annual overheating hours and reduction of T_{res} maximum for all levels of air change rate.
- (v) The annual cooling load is increased for all investigated cases.

- (vi) The annual heating load remains similar and in some cases slightly reduced for all cases investigated.

The thesis has argued that the Floor Void with Mass strategy has the following characteristics in comparison to the standard strategy:

- (i) All levels of thermal mass without night cooling result in an increase of annual overheating hours and a slight increase of T_{res} maximum.
- (ii) Adding night cooling still results in an increase of annual overheating hours. The T_{res} maximum for the lightweight building types is slightly reduced.
- (iii) There is an increase of annual overheating hours for all levels of solar gain and internal gain. There is little if any change in T_{res} maximum on a peak summer day for all levels of solar gain and internal gain.
- (iv) Similarly, there is an increase of annual overheating hours and minimal change in T_{res} maximum for all levels of air change rate.
- (v) The annual cooling load is increased for all investigated cases.
- (vi) The annual heating load remains similar and in some cases slightly reduced for all cases investigated.

The thesis has argued that the Earth to Air Heat Exchanger has the following characteristics in comparison to the standard strategy:

- (i) All levels of thermal mass without night cooling result in a reduction of annual overheating hours and a reduction of T_{res} maximum.
- (ii) Adding night cooling results in a greater reduction of annual overheating hours and a greater reduction of T_{res} maximum.
- (iii) There is a reduction of annual overheating hours and a reduction of T_{res} maximum for all levels of solar gain and internal gain.

- (iv) Similarly, there is a reduction of annual overheating hours and a reduction of T_{res} maximum for all levels of air change rate.
- (v) The annual cooling load is reduced by around 50% for all investigated cases.
- (vi) The annual heating load is reduced by around 10% for all cases investigated.

The thesis has argued that the Thermal Labyrinth has the following characteristics in comparison to the standard strategy:

- (i) All levels of thermal mass without night cooling result in an reduction of annual overheating hours and a reduction of T_{res} maximum.
- (ii) Adding night cooling results in a greater reduction of annual overheating hours and a greater reduction of T_{res} maximum.
- (iii) There is a reduction of annual overheating hours and a reduction of T_{res} maximum for all levels of solar gain and internal gain.
- (iv) Similarly, there is a reduction of annual overheating hours and a reduction of T_{res} maximum for all levels of air change rate.
- (v) The annual cooling load is reduced by around 40% for all investigated cases.
- (vi) The annual heating load is reduced by around 10% for all cases investigated.

The results from the parametric analysis were then further analysed to identify the benefit that adding the active thermal mass strategy have compared to one another for the improvement of the five parameters in turn.

The key results have shown that when only mechanical ventilation is provided (i.e. no cooling) the performance of the Hollow Core Slab (HCS) and Floor Void with Mass (FVWM) strategies are dependent on the performance of the test room and will only result in a reduction in annual overheating hours when the performance of the test room is optimised (i.e. solar gains reduced, night cooling introduced, etc), whereas the Earth to Air Heat Exchanger (ETAHE) and Thermal Labyrinth (TL) strategies will always provide a reduction in annual overheating hours. When only one parameter is improved from the BASE Case Option:

- There is only a benefit in integrating a HCS strategy when night cooling is introduced
- There is no benefit in integrating a FVWM strategy when only one parameter is improved
- An ETAHE and TL strategy will always provide a benefit, although the benefits are greater when night cooling is introduced, solar and internal gains are reduced and when the air change rate is increased

When all of the parametric improvements are applied to the test room the results show that all of the active thermal mass strategies can provide a reduction in annual overheating hours when compared to the Standard Strategy.

Only a small benefit is found for the FVWM Strategy, however around a 25% reduction in annual overheating hours is found for the HCS Strategy, over a 50% reduction for the TL Strategy and nearly a 75% reduction for the ETAHE Strategy. This demonstrates the importance of applying a low energy, passive approach when considering the application of active thermal mass strategies.

The key results have shown that when comfort cooling is provided, adding a HCS or FVWM strategy always results in an increase in the annual cooling load. This is as a result of the temperature of the air being supplied into the cores or floor void being higher than that of the internal surface temperatures of the cores or void. This results in the supply air being heated, and less cooling provided to the test room per cooling energy delivered. Due to the pre cooling effect of the ETAHE and TL strategies, these strategies always result in a reduction in the annual cooling load.

The key results have shown that the annual heating load is reduced by a small amount for the HCS and FVWM strategies unless the solar gains or internal gains are reduced, whereas the ETAHE and TL strategies always result in a around a 10% reduction in annual heating load as a result of the preheating effect these strategies have on the supply air.

Originality and Contribution to Knowledge

The project makes contributions to the field of building engineering in three distinct ways:

- i) Developed a profile of four active thermal mass strategies in three operational buildings

The monitored data provides real data on the actual performance of operational buildings in the UK integrating active thermal mass strategies.

- ii) This research has shown that commercial models with these capabilities can be used successfully to predict the performance of active thermal mass strategies.

Previous research has shown the validation of simulation methods when applied to active thermal mass strategies, however this has not previously been done using commercially available software commonly used with building services design consultancies.

- iii) The creation of a simplified design tool that can be used by designers at the concept stages of a project to quickly analyse the effects of integrating active thermal mass strategies into UK office buildings

There is currently limited design guidance on the performance of active thermal mass strategies, other than for Night Cooling or Earth-to-Air Heat Exchangers (ETAHE). The concept design tool TMAir presents results in terms of thermal comfort and energy consumption and allows the direct comparison of the four active thermal mass strategies; Hollow Core Slabs (HCS), Floor Void with Mass (FVWM), Earth to Air Heat Exchangers (ETAHE) and Thermal Labyrinth (TL), and a Standard Strategy, together with the effects of changing key design parameters.

Contribution to IEA-ECBCS Annex 44

This research project was part of the UK contribution to the IEA-ECBCS Annex 44

“Integrating Environmentally Responsive Elements in Buildings”. A description of Annex 44 is included in Appendix B and more details can be found in its website.

It was beneficial to participate in the project and the 6-monthly meeting where progress by all participating countries was presented. The interaction with international researchers working on similar technologies was invaluable.

Further Research

The tool was developed using South East England (Heathrow) weather data and typical construction details for office buildings in the UK. For this reason it's applicability is restricted. It is hoped that this thesis can be used as a basis for further development for other weather conditions, construction methods and building types

12.0 REFERENCES

Action Energy, 2003. Energy consumption guide 19: Energy use in offices. London: Action Energy.

Al-Homoud, M.S., 2001. Computer-aided building energy analysis techniques. *Building and Environment*, 36, pp. 421-433.

Artmann, N., Manz, H., Heiselberg, P., 2007. Climatic potential for passive cooling of buildings by night-time ventilation in Europe. *Applied Energy*, 84, pp. 187-201.

Babiak J, Olesen B W, Petráš D. 2007 REHVA Guidebook no. 7, Low temperature heating and high temperature cooling – Embedded water based surface systems, Forssan Kirjapaino Oy- Forssan, Finland.

Balaras, C.A., 1996. The role of thermal mass on the cooling load of buildings. An overview of computational methods. *Energy and Buildings*, 24, pp. 1-10.

Barnard, N 1994. Technical Report 9/94 Dynamic Energy Storage in the Building Fabric. Bracknell: Building Services Research and Information Association.

Barnard, N., Jaunzens, D., 2001. IEA Annex 28 Low Energy Cooling: Technology selection and early design guidance.. International Energy Agency.

Barton, P., Beggs, C.B., Sleigh, P.A., 2002. A theoretical study of the thermal performance of the termodeck hollow core slab system. *Applied thermal engineering*, 22, pp. 1485-1499.

Batty, W.J., Swann, B., 1997. Integration of computer based modelling and interdisciplinary based approach to building design in post-graduate education. Proceedings of the Fifth International IBPSA Conference. Prague, Czech Republic.

Becker, R., Paciuk, M., 2002. Inter-related effects of cooling strategies and building features on energy performance of office buildings. *Energy and Buildings*, 34, pp. 25-31.

Birtles, A.B., Kolokotroni, Perera, M.D.A.E.S., 1996. Night cooling and ventilation design for office-type buildings. *Proceedings of World Renewable Energy Conference (WREC)*.

Blondeau, P., Sperandio, M. and Allard, F., 1997. Night ventilation for building cooling in summer. *Solar Energy*, 61(5), pp. 327-335.

Bordass, B., Leaman, A., Ruyssevelt, P., 1999. PROBE strategic review: Report 4 Strategic Conclusions, Department of the Environment, Transport and the Regions.

Braham, D., Barnard, N., Jaunzens, D. 2001a. Digest 454 Part 1: Thermal mass in office buildings: an introduction. Garston: Building Research Establishment (BRE).

Braham, D., Barnard, N., Jaunzens, D. 2001b. Digest 454 Part 2: Thermal mass in office buildings: Design Criteria. Garston: Building Research Establishment (BRE).

BRE., 2001. Information Paper 6/01 Modelling the performance of thermal mass.. Garston: Building Research Establishment (BRE).

BRE., 2006. BR 489 Part L Explained – The BRE Guide. Garston: Building Research Establishment (BRE).

Breesch, H., Bossaer, A., Janssens, A., (2005). Passive cooling in a low-energy office building. *Solar Energy*, 79, 682-696

BRESCU., 2002. General information report 085: New ways of cooling – information for building designers. Garston: Building Research Establishment (BRE).

Butler, D., Swainson, M., Perry, A., 2002. Information Paper 6/02 Free cooling with displacement ventilation. Garston: Building Research Establishment (BRE).

Carslaw, H.S., Jaeger, J.C., 1959. Conduction of heat in solids, 2nd edition. Oxford University Press, New York.

Cheng, V., NG, E., Givoni., 2005. Effect of envelope colour and thermal mass on indoor temperatures in hot and humid climates. *Solar Energy*, 78, pp. 528-534.

CIBSE, 1986. CIBSE Guide Volume C – Reference Data. London: Chartered Institute of Building Services Engineers.

CIBSE, 1986. Guide A: Environmental Design. Chartered Institute of Building Services Engineers.

Cibse, 1998. Cibse AM11 – Building energy and environmental modelling. London: Chartered Institute of Building Services Engineers.

CIBSE, 2002. TM29 HVAC strategies for well insulated airtight buildings. London: Chartered Institute of Building Services Engineers.

CIBSE, 2002b. Guide J Weather, solar and illuminance data. London: Chartered Institute of Building Services Engineers.

CIBSE, 2004a. Guide F Energy efficiency in buildings. 2nd Edition. London: Chartered Institute of Building Services Engineers.

CIBSE, 2004b. TM34 Climatic change with weather change scenario. London: Chartered Institute of Building Services Engineers.

CIBSE, 2005a. Guide B Heating, ventilation, air conditioning and refrigeration. London: Chartered Institute of Building Services Engineers.

CIBSE, 2005b. CIBSE knowledge series: KS3 – Sustainable low energy cooling: an overview. London: Chartered Institute of Building Services Engineers.

CIBSE, 2006a. Guide A: Environmental Design. Chartered Institute of Building Services Engineers.

CIBSE, 2006b. TM37 Design for improved solar shading control. London: Chartered Institute of Building Services Engineers.

CIBSE, 2007. Guide C Reference Data. London: Chartered Institute of Building Services Engineers.

Clarke, J.A., Johnstone, C.M., Kondratenko, I., Lever, M., McElroy, L.B., Prazeres, L., Strachan, P.A., McKenzie, F., Peart, G., 2004. Using simulation to formulate domestic sector upgrading strategies for Scotland. *Energy and Buildings*, 36, pp. 759-770.

Cook, M.J., and Rees, S.J., 2006. Low energy design of community healthcare buildings : a case study. *Proceedings of World Renewable Energy Congress IX, Florence, Italy*

Corgnati SP, and Kindinis A, (2007). Thermal mass activation by hollow core slab coupled with night ventilation to reduce summer cooling loads, *Building and Environment* 42 (2007) 3285–3297.

Crawley D.B.,_Hand J.W., Kummert M. and Griffith B.T. (2008). Contrasting the capabilities of building energy performance simulation programs, *Building and Environment* 43 (2008) 661–673

De Paepe, M. and JANSSENS, A., 2003. Thermo-hydraulic design of earth-air heat exchangers. *Energy and Buildings*, 35(4), pp. 389-397.

De Wit, S., Augenbroe, G., 2002. Analysis of uncertainty in building design evaluations and its implications. *Energy and Buildings*, 34, pp. 951-958.

ECON 19, (2000). Energy Use in Offices, Best Practice Programme (can be downloaded from www.cibse.org/pdfs/ECG019.pdf)

Eicker, U., Huber, M, Seeberger, P., Vorshulze, C., 2006. Limits and potentials of office building climatisation with ambient air. *Energy and Buildings*, 38, pp. 574-581.

Ellis, M.W., Mathews, E.H., 2001. A new simplified thermal design tool for architects. *Building and Environment*, 36, pp. 1009-1021.

Ellis, M.W., Mathews, E.H., 2002. Needs and trends in building and HVAC system design tools. *Building and Environment*, 37, pp. 461-470.

EN 15377. 2008. Design of embedded water based surface heating and cooling systems, Part1: Determination of the design heating and cooling capacity, Part2: Design, dimensioning and installation, Part 3: Optimizing for use of renewable energy sources; CEN Brussels, Belgium, 2007

Evans, B., 1998. Through the labyrinth. *The Architect's Journal*, 44, pp. 44-46.

Fernandez, J.L., Porta-Gandara, M.A., Chargoy, N., 2005. Rapid on-site evaluation of thermal comfort through heat capacity in buildings. *Energy and Buildings*, 37, pp. 1205-1211.

Fletcher, J., Martin, A, J., 1996. Technical Appraisal 14/96 Night cooling control strategies. Bracknell: Building Services Research and Information Association (BSRIA).

Gan, G., 2001. Analysis of mean radiant temperature and thermal comfort, *Building Services Engineering Research and Technology*, 22(2), 95-101.

Garde-Bentaleb, F., Miranville, F., Boyer, H., Depecker, P., 2002. Bringing scientific knowledge from research to the professional fields: the case of the thermal and airflow design of buildings in tropical climates. *Energy and Buildings*, 34, pp. 511-521.

Geros, V., Santamouris, M., Tsangrasoulis, A., Guarracino, G., 1999. Experimental evaluation of night ventilation phenomena. *Energy and Buildings*, 29, pp. 141-154.

Ghiaus, C., Allard, F., 2006. Potential for free cooling by ventilation. *Solar Energy*, 80, pp. 402-413.

Ghiaus, C., Allard, F., 2006. Potential for free cooling by ventilation. *Solar Energy*, 80, pp. 402-413.

Ghosal, M.K., Tiwari, G.N., Das, D.K. And Pandey, K.P., 2005. Modelling and comparative thermal performance of ground air collector and earth air heat exchanger for heating of greenhouse. *Energy and Buildings*, 37(6), 613-621

Givoni, B., 1992. Comfort, climate analysis and building design guidelines. *Energy and Buildings*, 18(1), pp. 11-23.

Golove, W.H., Eto, J.H., 1996. Market barriers to energy efficiency: a critical reappraisal of the rationale for public policies to promote energy efficiency. LBL-38059, Lawrence Berkeley Laboratory, University of California, Berkeley.

Gratia, E., De Herde, A., 2002. A simple design tool for the thermal study of an office building. *Energy and Buildings*, 34, pp. 279-289.

Grosso M and Raimondo L, (2008). Horizontal Air-to-Earth heat exchangers in northern Italy – Testing, Designing and Monitoring, *International Journal of Ventilation*, Vol 7, No1, pp1-10

Gwerder M, Lehmann B, Todtli J, Dorer V, and Renggli F, (2008). Control of thermally-activated building systems (TABS), *Applied Energy* 85 (2008) 565–581

Holm. D., 1993. Building thermal analyses: what the industry needs: the architect's perspective. *Building and Environment*, 28(4), 405-407.

Holman, J. P. (1990). *Heat Transfer – 6th Edition*. McGraw-Hill. (Out of print). [7th edition 1990 ISBN 0-412-34280-4].

Hong, T, Zhang, J., Jiang, Y., 1997. IISABRE: an integrated building simulation environment. *Building and Environment*, 32 (3), pp. 219-224.

Høseggen, R., Mathisen, H.M., Hanssen, S.O., 2009. The effect of suspended ceilings on energy performance and thermal comfort. *Energy and Buildings*, 41(2), pp234-245.

IES (2008). *Virtual Environment – Building Performance Modelling*, www.iesve.com

Jacovides, C.P. And Mihalakakou, G., 1995. An underground pipe system as an energy source for cooling/heating purposes. *Renewable Energy*, 6(8), pp. 893-900.

JRAIA, 2002. *Air Conditioning Market*. Tokyo, Japan.

Kalay, Y.E., Khemlani, L., Choi, Jinwon., 1998. An integrated model to support distributed collaborative design of buildings. *Automation in Construction*, 7, pp. 177-188.

Kolarik J and Yang L (2009). Thermal Mass Activation, Chapter 5 in *Expert Guide Part 2: RBE*, Aschehoug O and Perino M (Eds), IEA ECBSC Annex 44, *Integrating Environmentally Responsive Elements in Buildings*.

Kolokotroni, M (1998). *Information Paper 4/98 Night ventilation for cooling office buildings*. Garston: Building Research Establishment (BRE).

Kolokotroni, M. and Aronis, A., 1999. Cooling-energy reduction in air-conditioned offices by using night ventilation. *Applied Energy*, 63(4), pp. 241-253.

Kolokotroni, M. Robinson-Gayle, S., Tanno, S., Cripps, A., 2004. Environmental impact analysis for typical office facades. *Building Research and Information*, 32(1), pp. 2-16.

Kolokotroni, M., Tindale, A., Irving, S.J., 1997. Nitecool: office ventilation pre-design tool. Proceedings of 18th annual AIVC conference. Athens, Greece.

Kolokotroni, M., Webb, B.C., Hayes, S.D., 1998. Summer cooling with night ventilation for office buildings in moderate climates. *Energy and Buildings*, 27, pp. 231-237.

Kurpaska, S., Slipek, Z., 2000. Optimization of Greenhouse Substrate Heating. *Journal of Agricultural Engineering Research*, 76(2), pp. 129-139.

La Roche, P., Milne, M., 2004. Effects of window size and thermal mass on building comfort using an intelligent ventilation controller. *Solar Energy*, 77(4), pp. 421-434.

Lehmann B, Dorer V and Koschenz M (2007). Application range of thermally activated building systems tabs, *Energy and Buildings* 39 (2007) 593–598.

Li, Y., P. Xu. (2006). Thermal mass design in buildings – heavy or light? *International Journal of Ventilation*, Special Edition 5(1): 143 - 150

Lin, Y.J.P., Linden, P.F., 2005. A model for an under floor air distribution system. *Energy and Buildings*, 37, pp. 299-409.

Littlefair, P.J., 2005. Summertime solar performance of windows with shading devices. Watford: Building Research Establishment (BRE).

Lovins, A., 1992. *Energy Efficient Buildings: Institutional Barriers and Opportunities*. Strategic Issues Paper No. 1. E Source Inc., Boulder, CO.

Mahdavi, A., El-Bellahy, S., 2005. Effort and effectiveness considerations in computational design evaluation: a case study. *Building and Environment*, 40, pp. 1651-1664

Mihalakakou, G., Lewis, J.O., Santamouris, M., 1996b. The influence of different ground covers on the heating potential of earth-to-air heat exchangers. *Renewable Energy*, 7(1), pp. 33-46.

Mihalakakou, G., Lewis, J.O., Santamouris, M., 1996a. On the heating potential of buried pipes techniques -- application in Ireland. *Energy and Buildings*, 24(1), pp. 19-25.

Mihalakakou, G., Santamouris, M., Asimakopoulos, D., Tselepidaki, I., 1995. Parametric prediction of the buried pipes cooling potential for passive cooling applications. *Solar Energy*, 55(3), pp. 163-173.

Mohammad., Al-Homoud, S., 2005. Performance characteristics and practical applications of common building thermal insulation materials. *Building and Environment*, 40(3), pp. 353-366.

MYERS, G.E., 1971. *Analytical Methods in Conduction Heat Transfer*. McGraw-Hill.

Nagano, K., Takeda, S., Mochida, T., Shimakura, K., Nakamura, T., 2006. Study of a floor supply air conditioning system using granular phase change material to augment building mass thermal storage – Heat response in small scale experiments. *Energy and Buildings*, 38, pp. 436-446

ODPM., 2005. *Low or zero carbon energy sources – strategic guide (interim publication)*. Office of the Deputy Prime Minister: London.

ODPM., 2006. *The building regulations 2000 approved document L2A Conservation of fuel and power in buildings other than dwellings*. London: NBS.

Olsen, E.L., Chen, Q.Y., 2003. Energy consumption and comfort analysis for different low-energy cooling systems in a mild climate. *Energy and Buildings*, 35, pp. 561-571.

Pfafferott, J., Herkel, S., Wambsganb, M., 2004. Design, monitoring and evaluation of a low energy office building with passive cooling by night ventilation. *Energy and Buildings*, 36(5), pp. 455-465.

Pout, C., Mackenzie, F., Bettle, R., 2002. Carbon dioxide emissions from non-domestic buildings: 2000 and beyond. Garston: Building Research Establishment (BRE).

RCEP, 2000. Energy – Changing the climate: 22nd report. The Royal Commission for Environmental Pollution – presented to parliament June 2000

Ren, M.J., Wright, J.A., 1997. A ventilated slab thermal storage system. *Building and Environment*, 33(1), pp. 43-52.

Rennie, D., Parand, F., 1998. BR 345: Environmental design guide for naturally ventilated and daylit offices. Garston: Building Research Establishment (BRE).

Richards, P.G., 1992. A design tool for thermal performance of buildings. PhD Thesis, Mechanical Engineering, University of Pretoria.

RUSSELL, M.B., SURENDRAN, P.N., 2001. Influence of active heat sinks on fabric thermal storage in building mass. *Applied Energy*, 70(1), pp. 17-33.

Santamouris, M., 2006. Ventilation Information Paper No 11 - Use of earth to air heat exchangers for cooling. Air Infiltration and Ventilation Centre (AIVC)

Santamouris, M., Asimakopoulos, D., 1997. *Passive Cooling of Buildings*. James & James, London, 2nd reprint

Santamouris, M., Mihalakakou, G., Balaras, C.A., Lewis, J.O., Vallindras, M. and Argiriou, A., (1996). Energy conservation in greenhouses with buried pipes. *Energy*, 21(5), 353-360.

Seaman, A., Martin, A., Sands, J. 2000. Application Guide 11/2000 HVAC Thermal Storage: Practical application and performance issues. Bracknell: Building Services Research and Information Association.

Shaviv, E., 1998. Computer aided energy conscious building design. *Renewable Energy*, 15, pp.343-348.

Shaviv, E., 1999. Design Tools for bio-climatic and passive solar buildings. *Solar Energy*, 67, pp. 189-204.

Shaviv, E., Yezioro, A., Capeluto, I.G., 2001. Thermal mass and night ventilation as passive cooling design strategy. *Renewable Energy*, 24, pp. 445-452.

Sorrell, S., 2003. Making the link: climate policy and the reform of the UK construction industry. *Energy Policy*, 31, pp. 865-878.

Standeven, M., Cohen, R., Bordass, B., Leaman, A., 1998. PROBE 14: Elizabeth fry building, *Building Services Journal*, 20, pp. 37-42.

Stevens, G., 1991. The impact of computing on architecture. *Building and Environment*, 26(1), pp. 3-11.

Stevens, J.W., 2004. Optimal placement depth for air-ground heat transfer systems. *Applied Thermal Engineering*, 24(2-3), pp. 149-157.

The Concrete Centre, 2009. Thermal Mass Explained. Camberly: The Concrete Centre.

The Concrete Centre., 2005. Thermal mass: a concrete solution for the changing future. The Concrete Centre. Camberly, Surrey.

Tindale, A.W., Irving, S.J., Concannon, P.J., Kolokotroni, M., 1995. Simplified method for night cooling. Proceedings of CIBSE National Conference Vol I, p8-13. Eastbourne, England.

UNDERWOOD, C.P., YIK, W.H., 2004. Modelling Methods for Energy in Buildings. Blackwell Publishing, Oxford, UK.

Voss, K., Herkel, S., Pfafferott, J., Lohnert, G., Wagner., 2006. Energy efficient office buildings with passive cooling – results and experiences from a research and demonstration programme. Solar Energy, xx, pp. xxx-xxx.

Vossa, K., Herkelb, S., Pfafferottb, J., Löhnertc, G., Wagner, A., 2007. Energy efficient office buildings with passive cooling – Results and experiences from a research and demonstration programme. Solar Energy, 81(3), pp 424-434.

Wagner, R., Beisel, S., Spieler, A., Vajen, K., 2000. Measurement, modelling and simulation of an earth-to-air heat exchanger in Marburg (Germany). Proceedings of ISES Europe Solar Congress. Kopenhagen, Denmark.

Weber T and Jo´ hannesson G (2005). An optimized RC-network for thermally activated building Components, Building and Environment 40 (2005) 1–14.

Yohanis, Y.G., Norton, B., 2002. Useful solar heat gains in multi-zone non-domestic buildings as a function of orientation and thermal time constant. Renewable Energy, 27(1), pp. 87-95.

Zhou, J., Zhang, G., Lin, Y., Yuguo, L., 2008. Coupling of thermal mass and natural ventilation in buildings. Energy and Buildings, 40, pp. 979-986.

Zimmerman M and Remund S, (2001). Ground coupled air systems, Chapter F in Early design Guidance for low energy cooling, IEA-BCS Annex 28.

APPENDIX A: Parametric Analysis Results

A

A.1 Standard

A.1.1 Overheating Hours

A.1.1.1 Thermal Mass

Increasing the thermal mass from LW (base case) to HW reduces the overheating hours by 11.9% and decreases T_{res} maximum by 0.9°C (Figure A—1). Increasing the thermal mass further to VHW only results in a further 3.7% reduction in annual overheating hours with and a further reduction T_{res} maximum of 0.1°C . Alternatively, decreasing the thermal mass from LW to VLW only increases the annual overheating hours by 0.4% and an increase in T_{res} maximum of 0.2°C .

The dampening effect of the thermal mass on the fluctuation of T_{res} can be seen in Figure A—2.

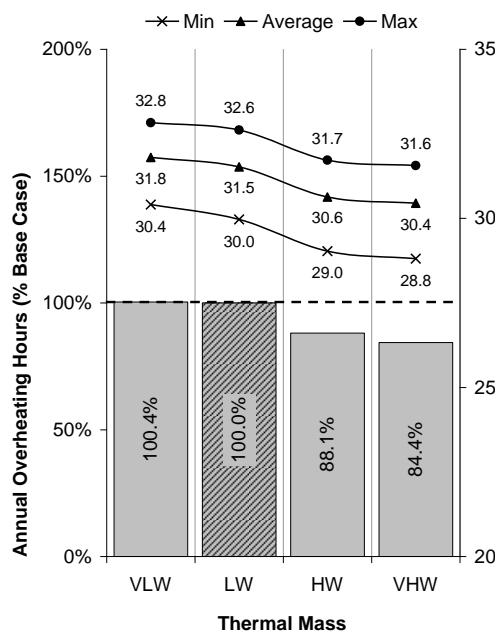


Figure A—1 Standard Strategy Annual Overheating Hours – Thermal Mass

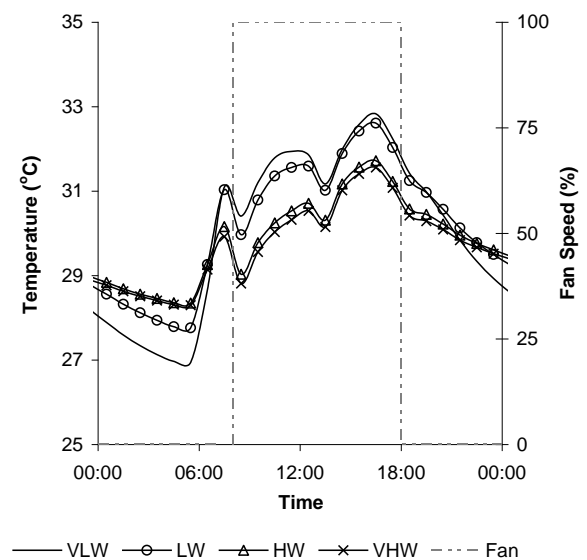
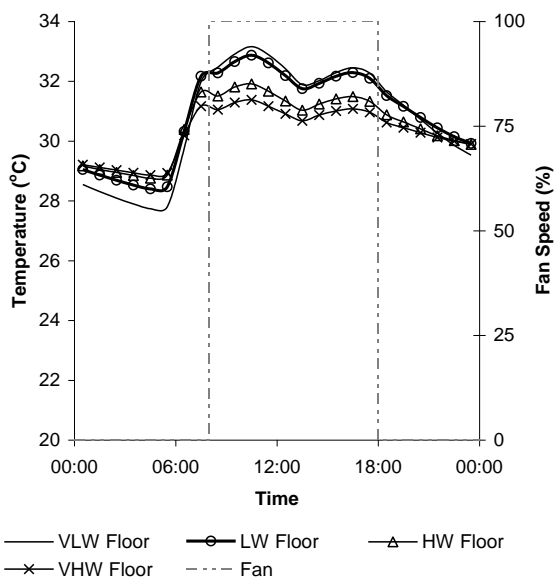


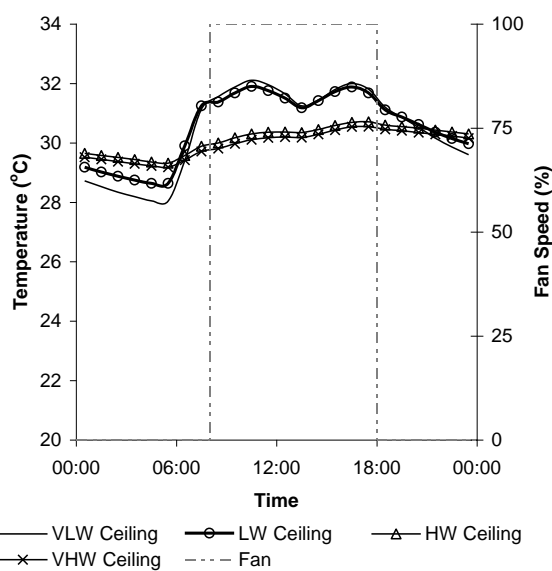
Figure A—2 Standard Strategy T_{res} on a peak summer day – Thermal Mass

The internal surface temperatures of the floor (Figure A—3), the ceiling (Figure A—4) and the internal walls (Figure A—5) on a peak summer day demonstrate the effect of the different levels of thermal mass.

The surface temperatures of the floor closely follows the temperatures of the room, however the surface temperatures of the HW and VHW ceilings and internal walls show a dampening effect, demonstrating the thermal mass of these surfaces. The HW and VHW rooms both have the same exposed concrete ceiling, however the VHW ceiling is slightly lower than the HW ceiling due to the average temperature in the VHW room being lower than the HW room.



**Figure A—3 Standard Strategy Floor
Surface Temperature – Thermal Mass**



**Figure A—4 Standard Strategy Ceiling
Surface Temperature – Thermal Mass**

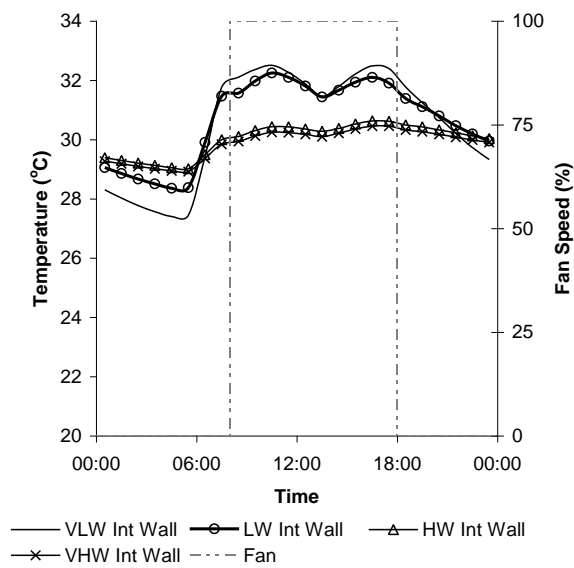


Figure A—5 Standard Strategy Internal Wall Surface Temperature – Thermal Mass

A.1.1.2 Thermal Mass with Night Cooling

Night cooling reduces the temperature of the test room during the unoccupied period for all levels of thermal mass (Figure A—7). The T_{res} in the VLW and LW rooms reach a low of around 22°C and the HW and VHW reach a low of around 24°C . This then results in T_{res} at the start of the occupied period being 2.0°C lower in the VLW room, 2.3°C lower in the LW room, 1.6°C lower in the HW room and 1.5°C lower in the VHW room.

Night cooling reduces the annual overheating hours by 17.2% for the LW (base case) reducing the maximum T_{res} on a peak summer day by 0.7°C (Figure A—6).

Introducing night cooling to the HW room reduces the annual overheating hours by 22.6%, and the maximum T_{res} by 0.8°C . For the VHW room the annual overheating hours are reduced by 21.4%, reducing the maximum T_{res} by 0.8°C . There is still little difference between the HW and VHW rooms in terms of both annual overheating hours or T_{res} .

A greater difference is now found between the VLW and LW rooms. Adding night cooling to the VLW room reduces the annual overheating hours by 9.4% and the T_{res} maximum by 0.4°C.

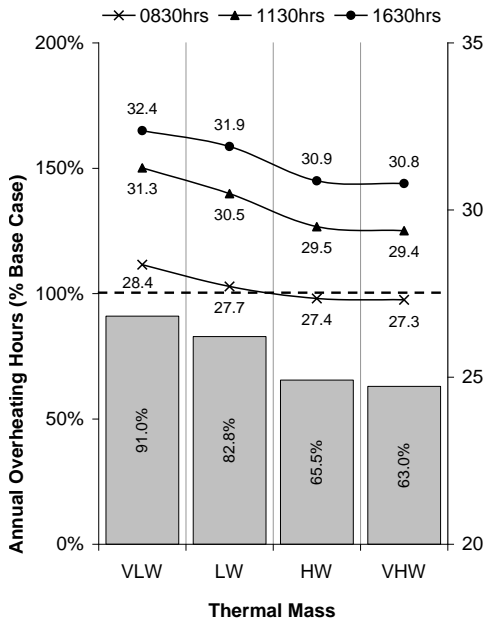


Figure A—6 Standard Strategy Annual Overheating Hours – Thermal Mass with Night Cooling

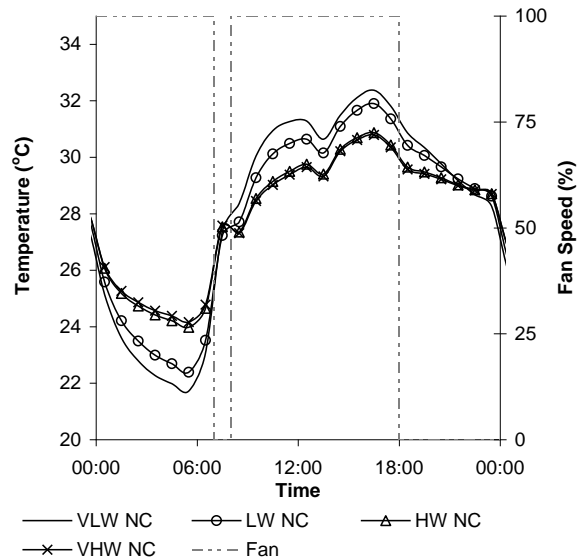


Figure A—7 Standard Strategy T_{res} on a peak summer day – Thermal Mass with Night Cooling

The surface temperatures of the ceiling (Figure A—9) and internal wall (Figure A—10) for the HW and VHW rooms again demonstrate the additional thermal mass. However, there is now only a small difference between the ceiling and internal wall surface temperatures for the HW and VHW rooms.

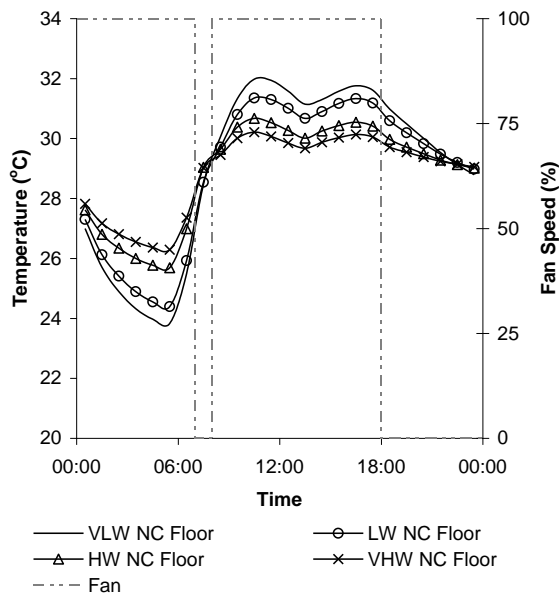


Figure A—8 Standard Strategy Floor Surface Temperature – Thermal Mass with Night Cooling

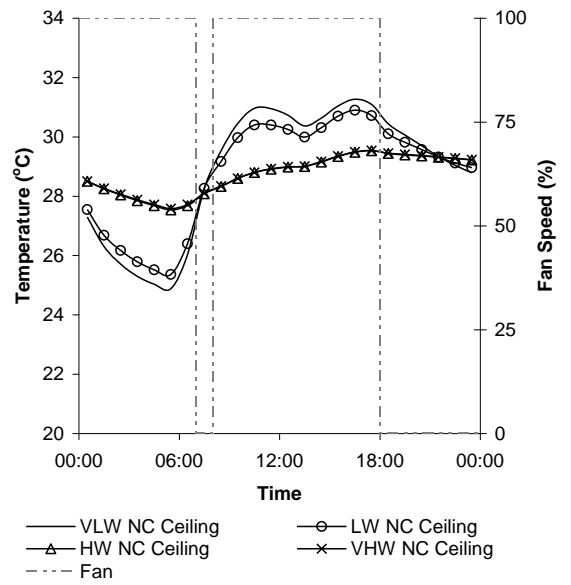


Figure A—9 Standard Strategy Ceiling Surface Temperature – Thermal Mass with Night Cooling

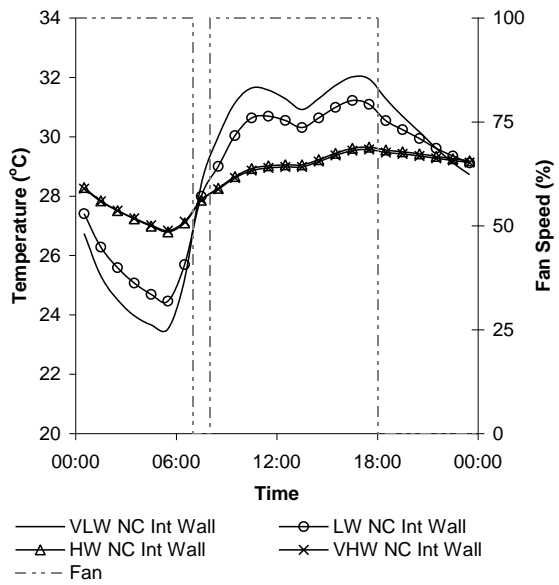


Figure A—10 Standard Strategy Internal Wall Surface Temperature – Thermal Mass with Night Cooling

A.1.1.3 Solar Gains

Reducing the solar gain reduces the heat gain experienced by the room and therefore reduces the temperature in the room (Figure A—11). Reducing the solar gains to medium reduces the annual overheating hours by 15.4% and the T_{res} maximum by 0.6°C. Reducing the solar gains to low reduces the annual overheating hours by 34.9% and the T_{res} maximum by 1.2°C.

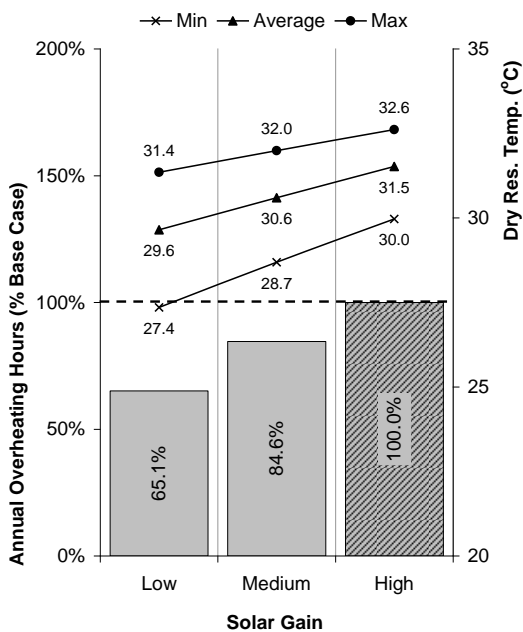


Figure A—11 Standard Strategy Annual Overheating Hours – Solar Gain

A.1.1.4 Internal Gains

Reducing the internal gain again reduces the heat gain experienced by the room and again reduces the temperature (Figure A—12). Reducing the internal gains to low reduces the annual overheating hours by 25% and the T_{res} maximum by 1.4°C. Increasing the internal gains to high increases the annual overheating hours by 10.7% and the T_{res} maximum by 1.3°C.

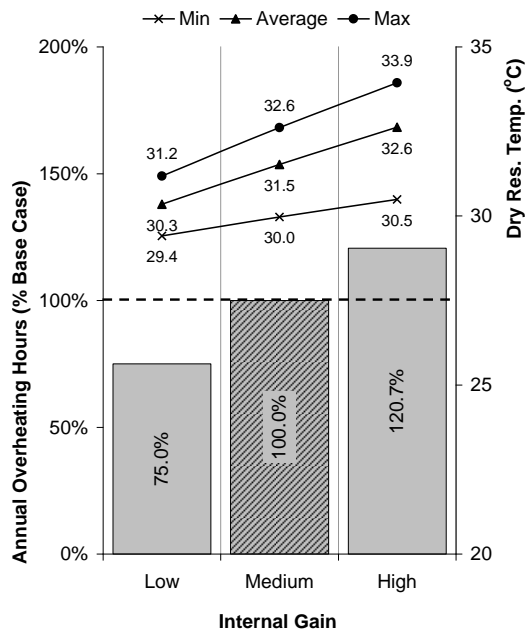


Figure A—12 Standard Strategy Annual Overheating Hours – Internal Gain

A.1.1.5 Air Change Rate

Increasing the air change rate increases the amount of free cooling that can be provided to the room (Figure A—13). Increasing the air change rate from 6 ach^{-1} (base case) to 8 ach^{-1} reduces the annual overheating hours by 16.4% and reduces T_{res} maximum by 0.7°C . Increasing the air change rate to 10 ach^{-1} reduces the annual overheating hours by 29.8% and the T_{res} maximum by 1.3°C .

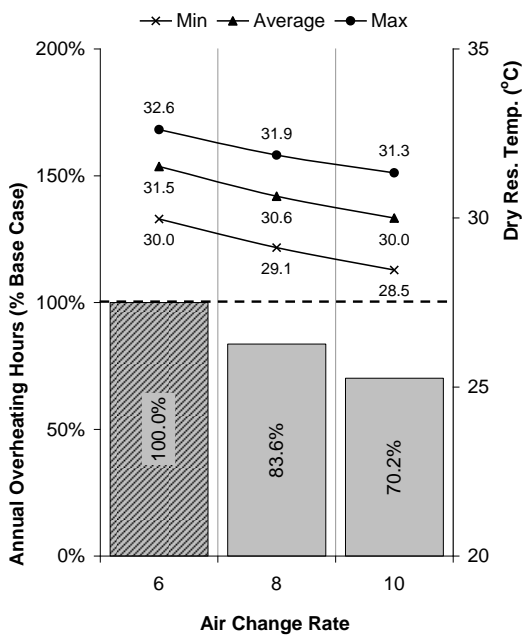


Figure A—13 Standard Strategy Annual Overheating Hours – Air Change Rate

A.1.2 Annual Cooling Load

A.1.2.1 Thermal Mass

The set point control temperature for the cooling is $t_{\text{air}} 24^{\circ}\text{C} \pm 2^{\circ}\text{C}$. To maintain comfort and to avoid discomfort, as a result of cold drafts, the supply air temperature to the room is limited to a minimum of 16°C .

During the peak summer day the VLW and LW levels of thermal mass cannot meet the comfort criteria of $T_{\text{res}} 24^{\circ}\text{C} \pm 2^{\circ}\text{C}$.

Figure A—14 and Figure A—15 show that the VLW and LW rooms cannot achieve the setpoint temperature in the morning period (morning period due to test room being east facing and receiving direct solar gain in the morning period). Due to the dampening effect of the HW and VHW levels of thermal mass these rooms come much closer to achieving the setpoint temperature, and only exceed them for a very short period.

Increasing the amount of thermal mass in the test room from LW (base case) to HW reduces the annual cooling load by 7.6% (see Figure A—14). Increasing the thermal mass further to VHW only reduces this by a further 1.7%. Reducing the thermal mass from LW to VLW only results in an increase in annual cooling load of 0.4%.

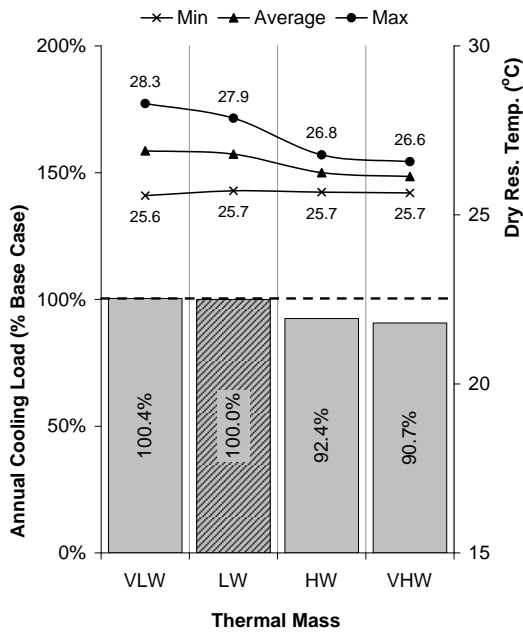


Figure A—14 Standard Strategy Annual Cooling Load– Thermal Mass

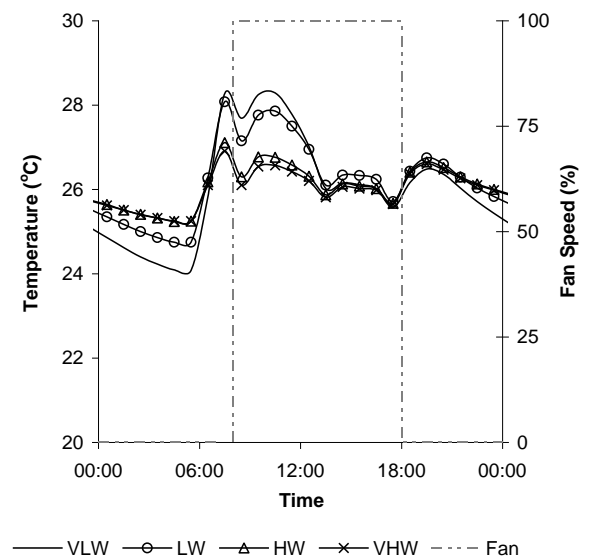


Figure A—15 Standard Strategy with cooling T_{res} on a peak summer day – Thermal Mass

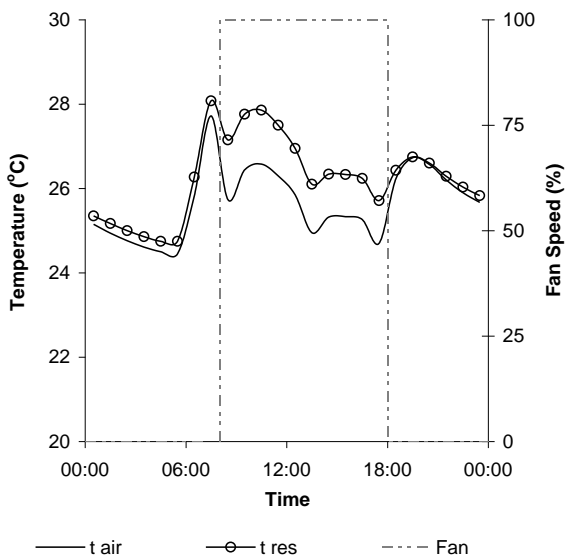


Figure A—16 Comparison of T_{air} and T_{res} for Standard Strategy Base Case test room

The internal surface temperatures of the floor (Figure A—17), the ceiling (Figure A—18) and the internal walls (Figure A—19) on a peak summer day demonstrate the effect of the different levels of thermal mass.

The surface temperatures of the floor closely follows the temperatures of the room, however the surface temperatures of the HW and VHW ceilings and internal walls show a dampening effect, demonstrating the thermal mass of these surfaces. The HW and VHW rooms both have the same exposed concrete ceiling, however the VHW ceiling is slightly lower than the HW ceiling due to the average temperature in the VHW room being lower than the HW room.

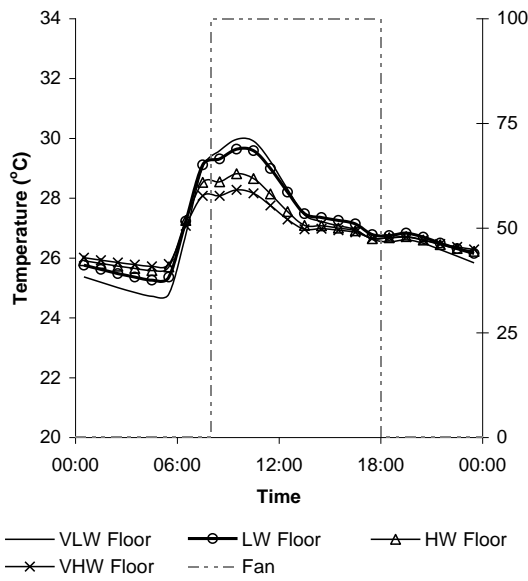


Figure A—17 Standard Strategy with Cooling Floor Surface Temperature – Thermal Mass

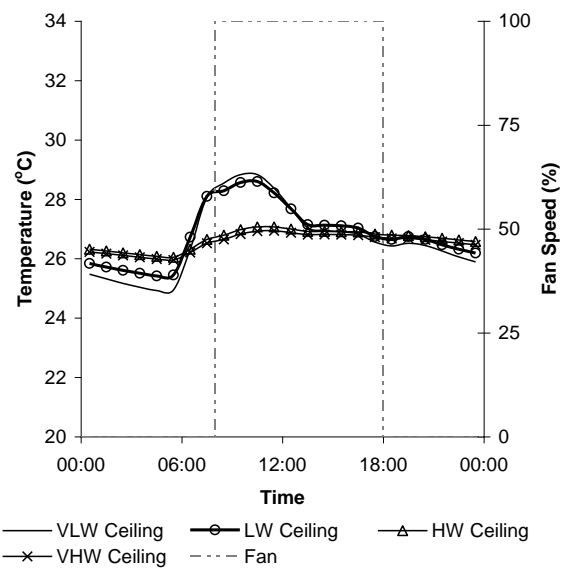


Figure A—18 Standard Strategy with Cooling Ceiling Surface Temperature – Thermal Mass

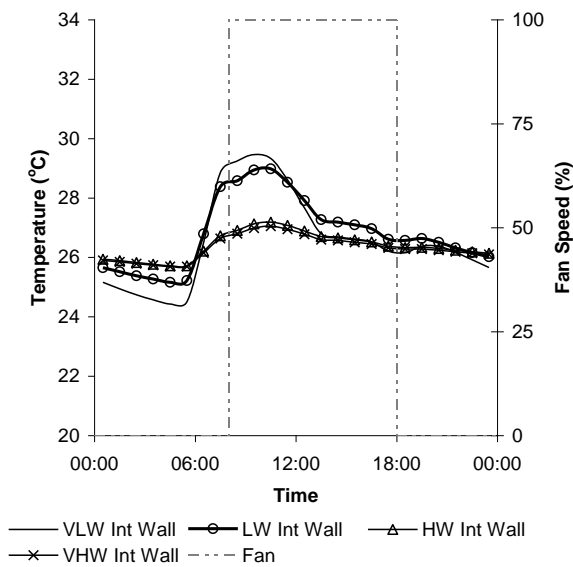


Figure A—19 Standard Strategy with Cooling Internal Wall Surface Temperature – Thermal Mass

A.1.2.2 Thermal Mass with Night Cooling

Night cooling reduces the temperature of the test room during the unoccupied period for all levels of thermal mass (Figure A—21). The T_{res} in the VLW and LW rooms reach a low of around 20°C and 21°C and the HW and VHW reach a low of around 22°C.

Again the VLW and LW rooms do not achieve the comfort criteria of $T_{res} 24^{\circ}\text{C} \pm 2^{\circ}\text{C}$ in the morning period on the peak summer day (Figure A—20 and Figure A—21) and increasing the thermal mass to HW or VHW almost allows this criteria to be met.

Introducing night cooling reduces the annual cooling load for the VLW room by 4.8%, the LW room by 7.5%, the HW room by 8.7% and the VHW room by 8.2%.

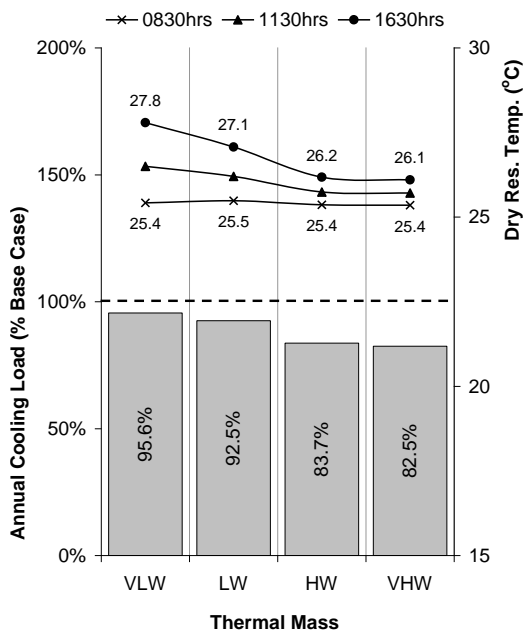


Figure A—20 Standard Strategy Annual Cooling Load– Thermal Mass with Night Cooling

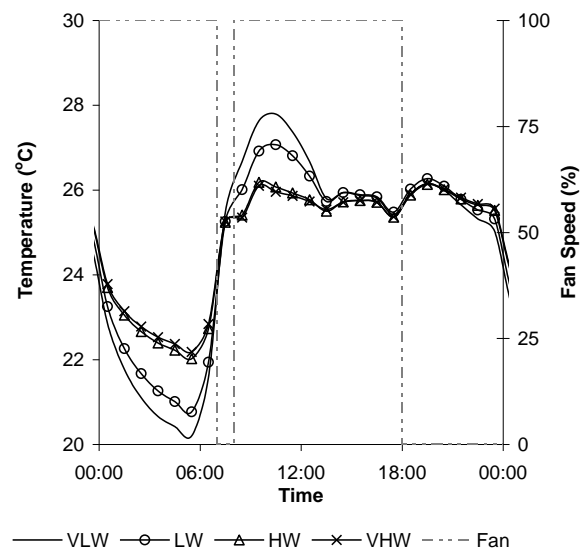


Figure A—21 Standard Strategy with cooling T_{res} on a peak summer day – Thermal Mass with Night Cooling

The surface temperatures of the ceiling (Figure A—22) and internal wall (Figure A—23) for the HW and VHW rooms again demonstrate the additional thermal mass. However, there is now only a small difference between the ceiling and internal wall surface temperatures for the HW and VHW rooms.

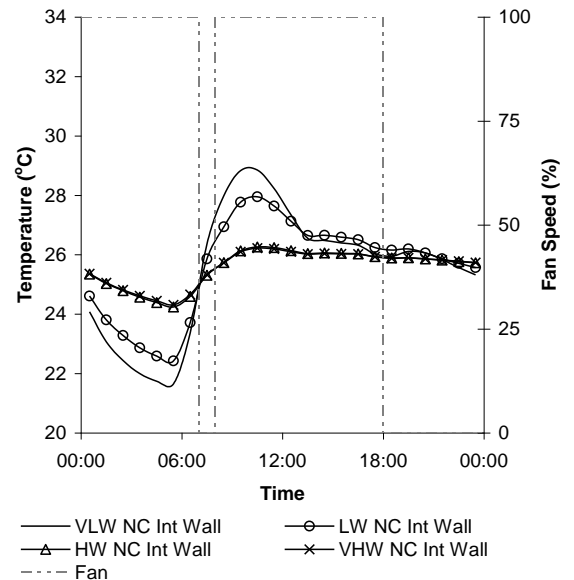
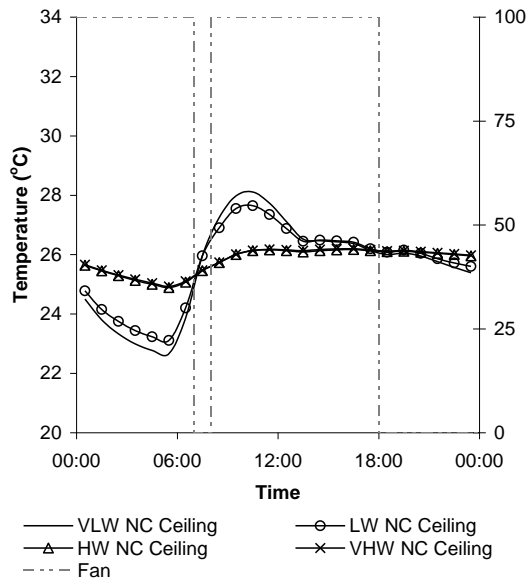


Figure A—22 Standard Strategy with Cooling Ceiling Surface Temperature – Thermal Mass with Night Cooling

Figure A—23 Standard Strategy with Cooling Internal Wall Surface Temperature – Thermal Mass with Night Cooling

A.1.2.3 Solar Gains

Reducing the amount of solar gain reduces the amount of heat gain the cooling needs to overcome. Figure A—24 shows that by reducing the solar gain the maximum T_{res} on a peak summer day becomes closer to the comfort criteria of $T_{res} 24^{\circ}\text{C} \pm 2^{\circ}\text{C}$.

Reducing the solar gains from high (base case) to medium reduces the annual cooling load by 9.5%. Reducing the solar gains to low reduces the annual cooling load by 21.0%.

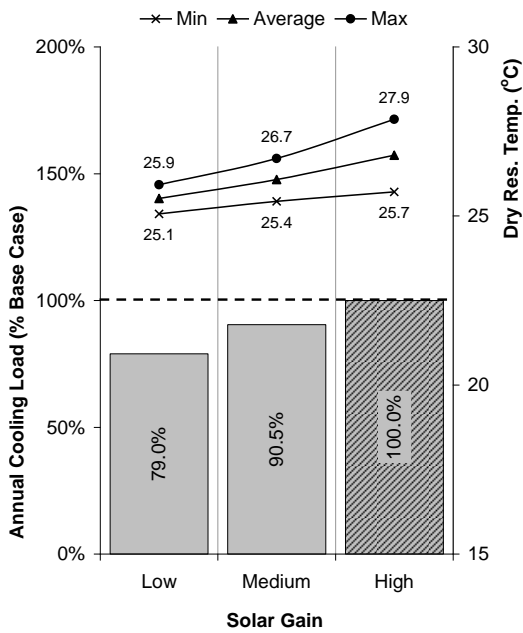


Figure A—24 Standard Strategy Annual Cooling Load – Solar Gain

A.1.2.4 Internal Gains

Reducing the internal gain also reduces the amount of heat gain that needs to be overcome by the cooling system. Figure A—25 shows that by reducing the internal gain the maximum T_{res} becomes closer to achieving the comfort criteria of $T_{res} 24^{\circ}\text{C}\pm 2^{\circ}\text{C}$

Reducing the internal gains from medium (base case) to low reduces the annual cooling load by 24.5%. Increasing the solar gains to high increase the annual cooling load by 16.0%.

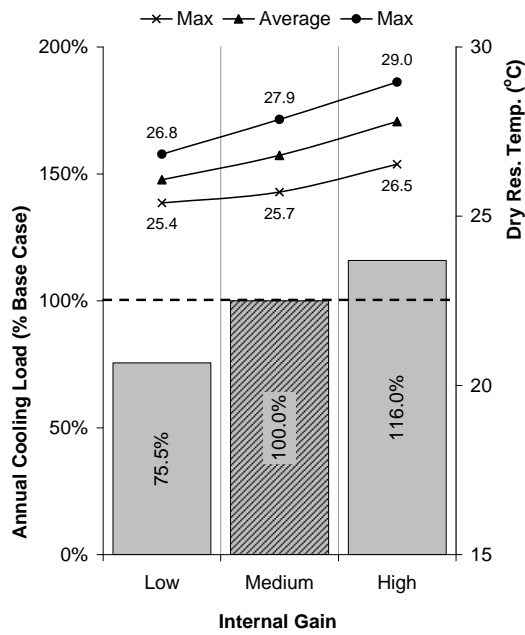


Figure A—25 Standard Strategy Annual Cooling Load – Internal Gain

A.1.2.5 Air Change Rate

Increasing the air change rate increases the amount of free cooling that can be provided when the ambient air temperature is below that of the required supply air temperature, but also increases the amount of air that needs to be cooled when the ambient air is above that of the required supply air temperature.

Increasing the air change rate from 6ach^{-1} (base case) to 8ach^{-1} increases the annual cooling load by 5.0% (Figure A—26). Increasing the air change rate to 10ach^{-1} increases the annual cooling load by 7.5%.

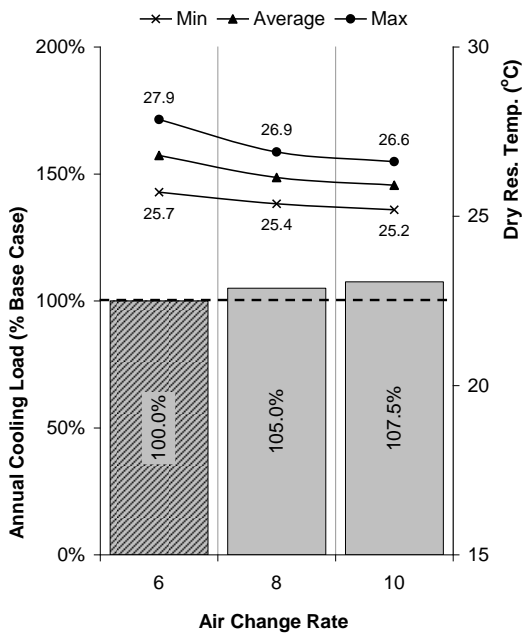


Figure A—26 Standard Strategy Annual Cooling Load – Air Change Rate

A.1.3 Annual Heating Load

A.1.3.1 Thermal Mass

Increasing the thermal mass from LW (base case) to HW increases the annual heating load by 2.8% (Figure A—27), increasing the thermal mass to VHW increases the annual heating load by 3.3%. Reducing the thermal mass reduces the annual heating load by 1.7%.

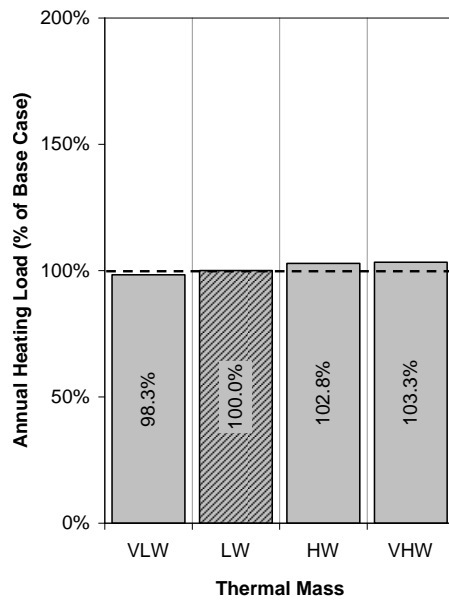


Figure A—27 Standard Strategy Annual Heating Load – Thermal Mass

A.1.3.2 Solar Gain

Reducing the solar gains from high (base case) to medium increases the annual heating load by 2.3% (Figure A—28). Reducing the solar gains to low increases the annual heating load by 4.8%.

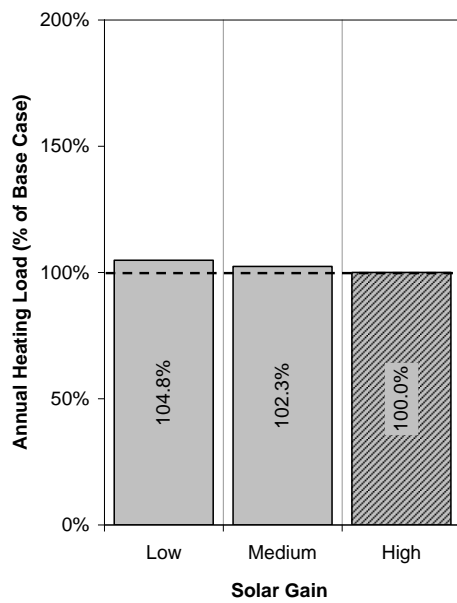


Figure A—28 Standard Strategy Annual Heating Load – Solar Gain

A.1.3.3 Internal Gain

Reducing the internal gains from medium (base case) to low increases the annual heating load by 18.6% (Figure A—29). Increasing the internal gains to high reduces the annual heating load by 14.4%.

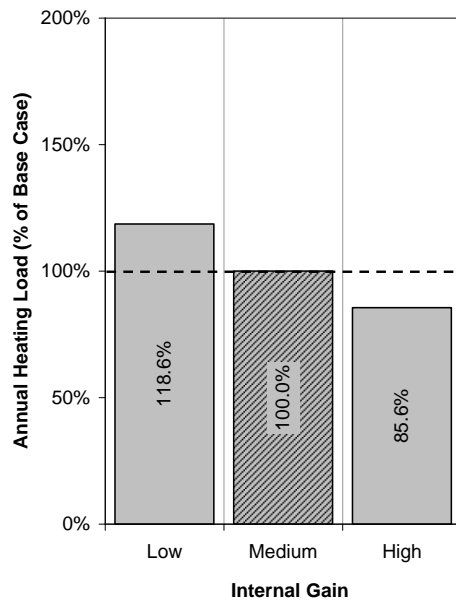


Figure A—29 Standard Strategy Annual Heating Load – Internal Gain

A.1.3.4 Air Change Rate

Increasing the air change rate from 6ach^{-1} (base case) to 8ach^{-1} increases the annual heating load by 41.7% (Figure A—30). Increasing the air change rate to 10ach^{-1} increases the annual heating load by 84.8%.

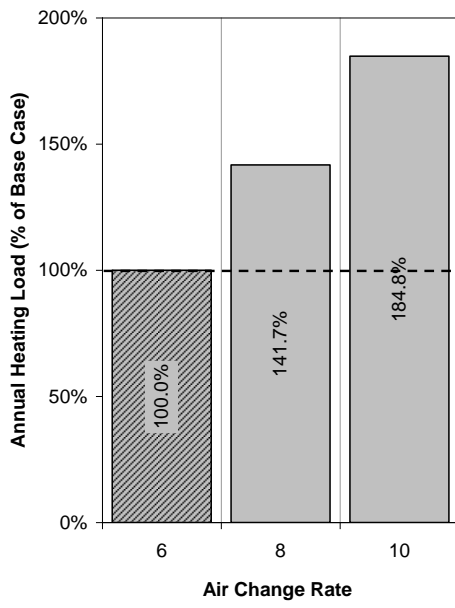


Figure A—30 Standard Strategy Annual Heating Load – Air Change Rate

A.2 Hollow Core Slabs

A.2.1 Overheating Hours

Passing the supply air through the Hollow Core Slab dampens the fluctuations in the air entering into the core. Figure A—31 shows the effect that passing the air through the core has on a peak summer day.

For the base case model the surface temperatures of the core base and the core top are relatively constant. Due to this temperature being higher than that of the air entering into the core the strategy has the unwanted effect of heating the air.

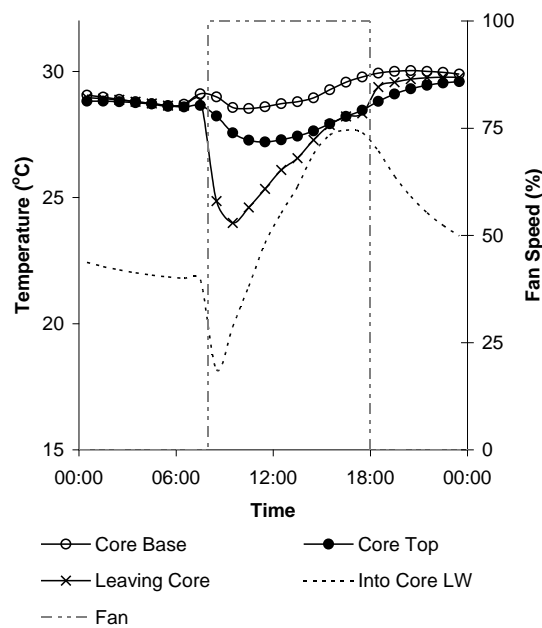


Figure A—31 HCS Strategy core and supply air temperatures

Table A—1 shows the temperatures of the core surfaces together with the air temperature into the core and leaving the core. The heat exchange efficiency of the core has also been calculated. The efficiency ranges between 35.9% at the start of the day to 64.4% in the

early afternoon, however a 50% efficiency provides a good agreement with all but the beginning of the day with an accuracy of between 99.9% and 100.8%.

Table A—1 HCS Efficiency

Time	Surface Temperatures (°C)			Air Temperatures (°C)		Heat Exchange Efficiency	50% Efficiency	
	Core Base	Core Top	Average Core	Into Core	Leaving Core		Leaving Core	Accuracy
08:30	28.99	28.23	28.61	18.17	24.86	35.9%	23.39	94.1%
09:30	28.57	27.56	28.06	19.87	23.99	49.7%	23.97	99.9%
10:30	28.53	27.27	27.90	21.47	24.60	51.3%	24.69	100.3%
11:30	28.60	27.20	27.90	23.17	25.34	54.1%	25.54	100.8%
12:30	28.72	27.29	28.00	24.37	26.09	52.7%	26.19	100.4%
13:30	28.80	27.43	28.11	25.42	26.56	57.7%	26.77	100.8%
14:30	28.95	27.64	28.29	26.72	27.28	64.4%	27.51	100.8%
15:30	29.27	27.92	28.59	27.47	27.88	63.6%	28.03	100.5%
16:30	29.57	28.21	28.89	27.67	28.21	55.7%	28.28	100.2%
17:30	29.78	28.46	29.12	27.57	28.34	50.3%	28.35	100.0%

A.2.1.1 Thermal Mass

Increasing the thermal mass from LW (base case) to HW reduces the overheating hours by 6.6% and decreases T_{res} maximum by 0.60°C (Figure A—32). Increasing the thermal mass further to VHW only results in a further 0.7% reduction in annual overheating hours with and a further reduction T_{res} maximum of 0.1°C. Alternatively, decreasing the thermal mass from LW to VLW also reduces the annual overheating hours by 1.6%, but increases the T_{res} maximum by 0.2°C.

The dampening effect of the thermal mass on the fluctuation in the temperature can be seen in Figure A—33.

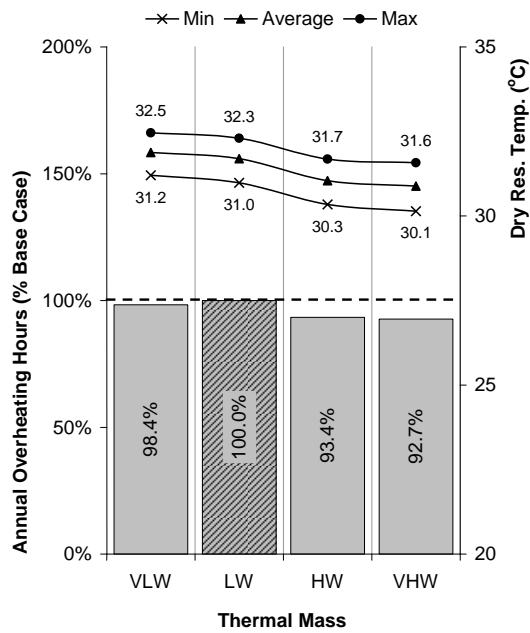


Figure A—32 HCS Strategy Annual Overheating Hours – Thermal Mass

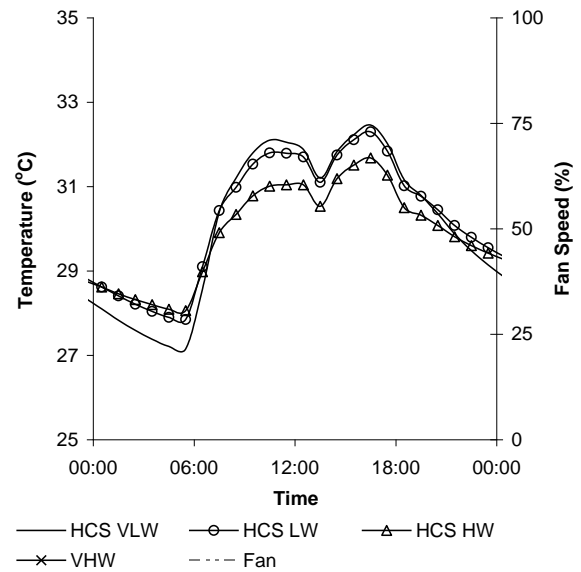


Figure A—33 HCS Strategy T_{res} on a peak summer day – Thermal Mass

The internal surface temperatures of the floor (Figure A—34), the ceiling (Figure A—35) and the internal walls (Figure A—36) on a peak summer day demonstrate the effect of the different levels of thermal mass.

The surface temperatures of the floor closely follows the temperatures of the room, however the surface temperatures of the HW and VHW internal walls and all of the ceiling surface temperatures show a dampening effect, demonstrating the thermal mass of these surfaces. All of the levels of thermal mass have an exposed concrete soffit as part of the hollow core slab strategy. The surface temperatures of the ceiling for all levels of thermal mass follow the same profile, however the VLW and LW remain higher than the HW and VHW due to the higher temperatures in the room below.

To look at the effect of increasing the level of thermal mass in the room on the core surface temperatures and the air temperature leaving the core the results for the LW and HW levels of thermal mass are presented in Figure A—37. As a result of the ceiling surface temperature in the room being lower in the HW room, the core base surface temperature is lower. However there is minimal effect on the core top surface temperature. The heat exchanger efficiency of the hollow core slab still remains close to 50% (Table A—2). The

heat transfer of the top and bottom of the core are the same due to the air being turbulent within the core. The difference between the air temperature leaving the core for the LW and HW levels of thermal mass is therefore minimal.

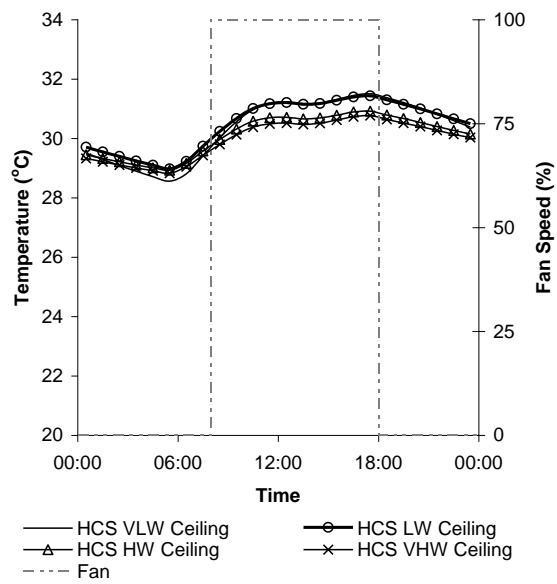
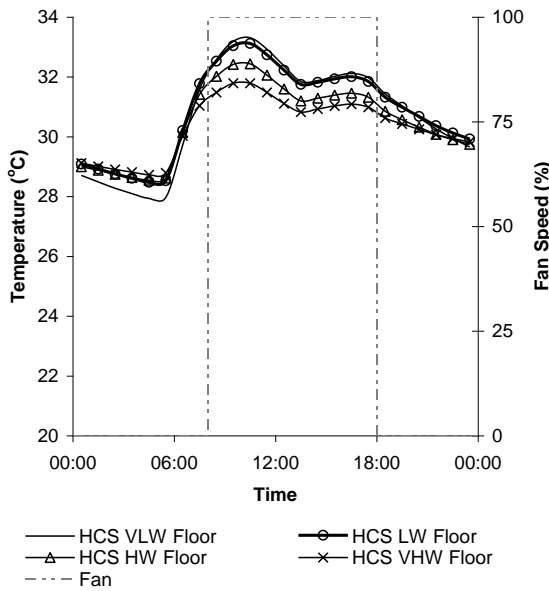


Figure A—34 HCS Strategy Floor Surface Temperature – Thermal Mass

Figure A—35 HCS Strategy Ceiling Surface Temperature – Thermal Mass

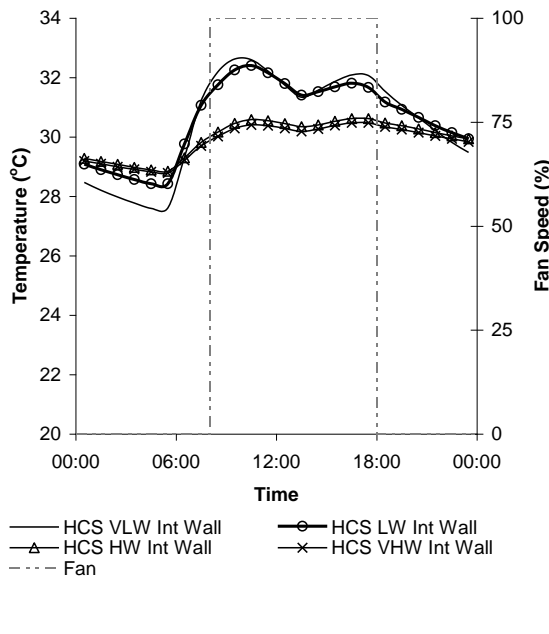


Figure A—36 HCS Strategy Internal Wall Surface Temperature – Thermal Mass

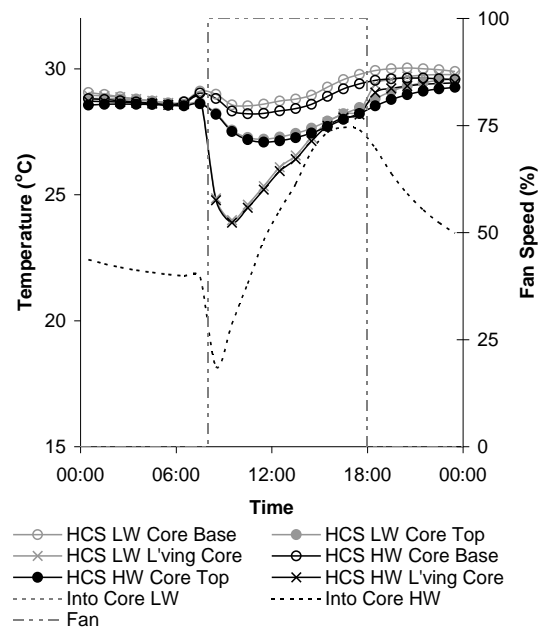


Figure A—37 HCS Strategy core and supply air temperatures – Thermal Mass

Table A—2 HCS Heat Exchange Efficiency – HW Thermal Mass

Time	Surface Temperatures (°C)			Air Temperatures (°C)		Heat Exchange Efficiency	50% Efficiency	
	Core Base	Core Top	Average Core	Into Core	Leaving Core		Leaving Core	Accuracy
08:30	28.82	28.19	28.51	18.17	24.78	36.0%	23.34	94.2%
09:30	28.32	27.51	27.92	19.87	23.89	50.0%	23.89	100.0%
10:30	28.21	27.19	27.70	21.47	24.48	51.7%	24.59	100.4%
11:30	28.23	27.09	27.66	23.17	25.20	54.8%	25.42	100.9%
12:30	28.33	27.14	27.74	24.37	25.94	53.3%	26.05	100.4%
13:30	28.42	27.26	27.84	25.42	26.41	59.1%	26.63	100.8%
14:30	28.59	27.45	28.02	26.72	27.13	68.5%	27.37	100.9%
15:30	28.90	27.71	28.31	27.47	27.73	68.9%	27.89	100.6%
16:30	29.20	27.99	28.60	27.67	28.06	57.8%	28.13	100.3%
17:30	29.40	28.22	28.81	27.57	28.18	50.8%	28.19	100.0%

A.2.1.2 Thermal Mass with Night Cooling

Night cooling reduces the temperature of the test room during the unoccupied period for all of the levels of thermal mass (Figure A—39). The T_{res} in the VLW and LW rooms reach a low of around 24°C and the HW and VHW reach a low of around 25°C.

Night cooling reduces the annual overheating hours by 35.0% for the LW (base case) reducing the maximum T_{res} on a peak summer day by 1.3°C (Figure A—38).

Introducing night cooling to the HW room reduces the annual overheating hours by 33.7%, and the maximum T_{res} by 1.1°C. For the VHW room the annual overheating hours are reduced by 30.6%, reducing the maximum T_{res} by 1.0°C. There is still little difference between the HW and VHW rooms in terms of both annual overheating hours or T_{res} .

A greater difference is now found between the VLW and LW rooms. Adding night cooling to the VLW room reduces the annual overheating hours by 24.6% and the T_{res} maximum by 1.1°C.

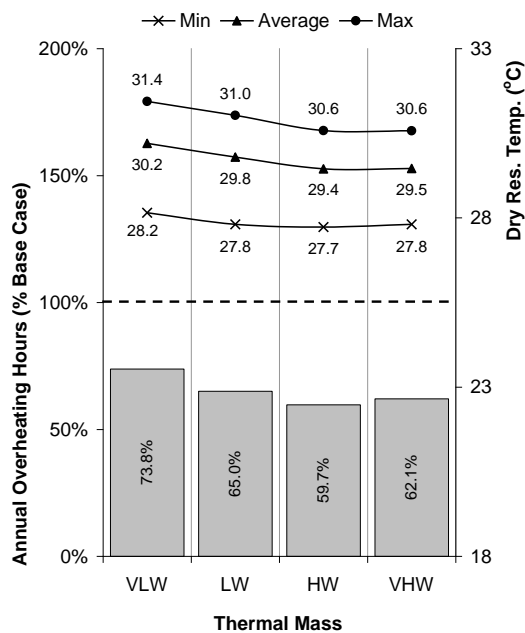


Figure A—38 HCS Strategy Annual Overheating Hours – Thermal Mass with Night Cooling

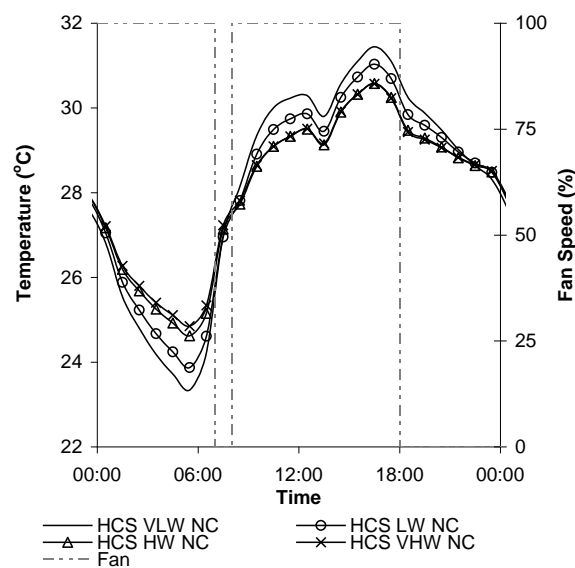


Figure A—39 HCS Strategy T_{res} on a peak summer day – Thermal Mass with Night Cooling

The surface temperatures of the ceiling (Figure A—40) is around 1°C lower for all levels of thermal mass. The difference between the various levels of thermal mass is now reduced.

To look at the effect of adding night cooling on the core surface temperatures and the air temperature leaving the core the results for the LW and HW levels of thermal mass with night cooling are presented in Figure A—41. As a result of the ceiling surface temperatures in the room being similar, the core base surface temperature are also similar. Again the core top surface temperature is also similar. The difference between the air temperature leaving the core for the LW and HW levels of thermal mass with night cooling is therefore minimal. The heat exchanger efficiency of the hollow core slab still remains close to 50% (Table A—3).

As a result of adding night cooling to both the LW and HW levels of thermal mass the surface temperature of the core top is reduced below that of the supply air going into the core in the afternoon. The core base surface temperature still remains higher resulting in the average core surface temperature being slightly below that of the supply air going into the core in the afternoon, resulting in the supply air being cooled by up to 0.6°C.

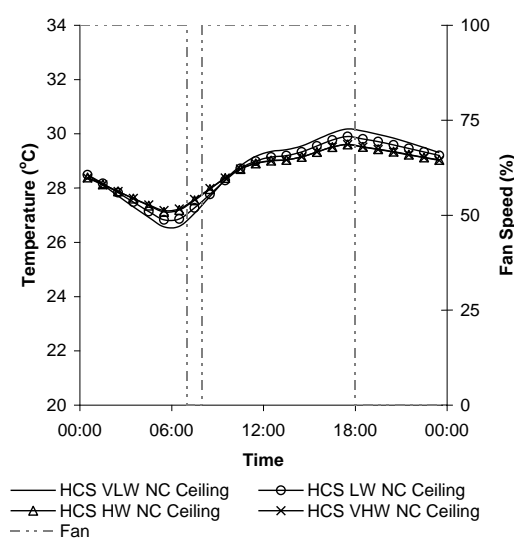


Figure A—40 HCS Strategy Ceiling Surface Temperature – Thermal Mass with Night Cooling

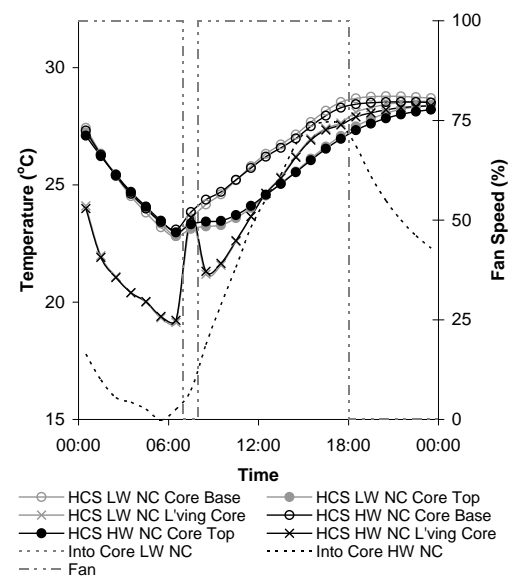


Figure A—41 HCS Strategy core and supply air temperatures – Thermal Mass with Night Cooling

Table A—3 HCS Heat Exchange Efficiency – HW Thermal Mass with Night Cooling

Time	Surface Temperatures (°C)			Air Temperatures (°C)		Heat Exchange Efficiency	50% Efficiency	
	Core Base	Core Top	Average Core	Into Core	Leaving Core		Leaving Core	Accuracy
00:30	27.32	27.10	27.21	17.78	23.99	34.1%	22.50	93.8%
01:30	26.28	26.22	26.25	16.68	21.91	45.4%	21.47	98.0%
02:30	25.39	25.43	25.41	15.93	21.05	46.0%	20.67	98.2%
03:30	24.62	24.70	24.66	15.73	20.40	47.7%	20.20	99.0%
04:30	23.99	24.07	24.03	15.43	20.02	46.6%	19.73	98.6%
05:30	23.42	23.47	23.45	14.98	19.39	47.9%	19.21	99.1%
06:30	23.09	22.97	23.03	15.43	19.22	50.1%	19.23	100.1%
08:30	24.37	23.43	23.90	18.18	21.31	45.3%	21.04	98.7%
09:30	24.70	23.46	24.08	19.88	21.65	57.9%	21.98	101.5%
10:30	25.21	23.71	24.46	21.48	22.62	61.7%	22.97	101.5%
11:30	25.72	24.10	24.91	23.18	23.65	72.8%	24.05	101.7%
12:30	26.20	24.58	25.39	24.38	24.63	75.2%	24.89	101.0%
13:30	26.58	25.04	25.81	25.43	25.29	136.8%	25.62	101.3%
14:30	26.98	25.54	26.26	26.73	26.18	-17.0%	26.50	101.2%
15:30	27.50	26.05	26.78	27.48	26.91	19.1%	27.13	100.8%
16:30	27.95	26.54	27.25	27.68	27.34	21.8%	27.46	100.4%
17:30	28.29	26.96	27.63	27.58	27.56	144.4%	27.60	100.2%

A.2.1.3 Solar Gains

Reducing the solar gain reduces the heat gain experienced by the room and therefore reduces the temperature (Figure A—42). Reducing the solar gains to medium reduces the annual overheating hours by 14.5% and the T_{res} maximum by 0.7°C. Reducing the solar gains to low reduces the annual overheating hours by 37.2% and the T_{res} maximum by 1.4°C.

To look at the effect of reducing the level on solar gain on the core surface temperatures and the air temperature leaving the core the results for the High and Low levels of solar gain are presented in Figure A—44. As a result of the ceiling surface temperatures in the room being much lower for the Low level of solar gain (Figure A—43), the core base surface temperature and core top surface temperature are much lower.

As a result of reducing the solar gain to Low the surface temperature of the core top is reduced below that of the supply air going into the core in the late afternoon (15:30hrs and 16:30hrs). However, the core base surface temperature still remains higher. The average core surface temperature remains above the air temperature supplied into the slab, however the air temperature leaving the core is slightly lower than that going into the core at 14:30hrs and 15:30hrs.

The heat exchanger efficiency of the hollow core slab still remains close to 50% (Table A—4).

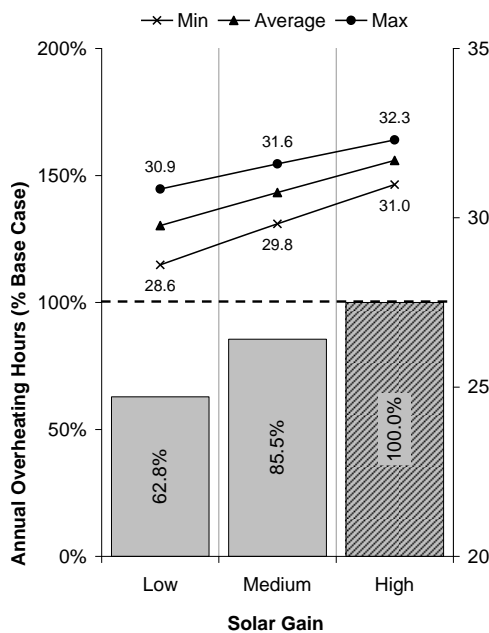


Figure A—42 HCS Strategy Annual Overheating Hours – Solar Gain

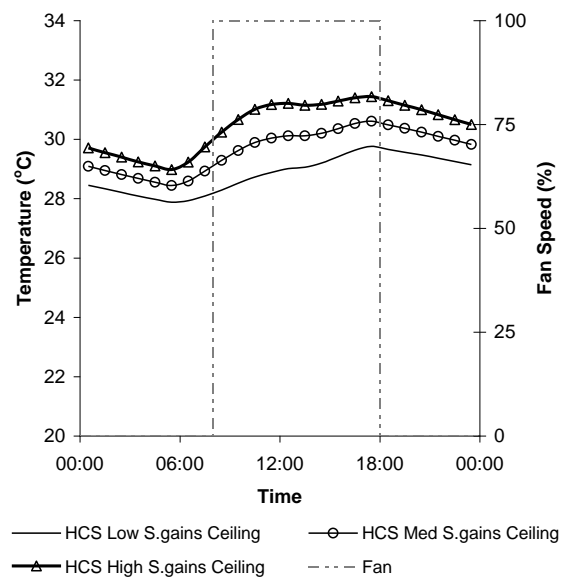


Figure A—43 HCS Strategy Ceiling Surface Temperature – Solar Gain

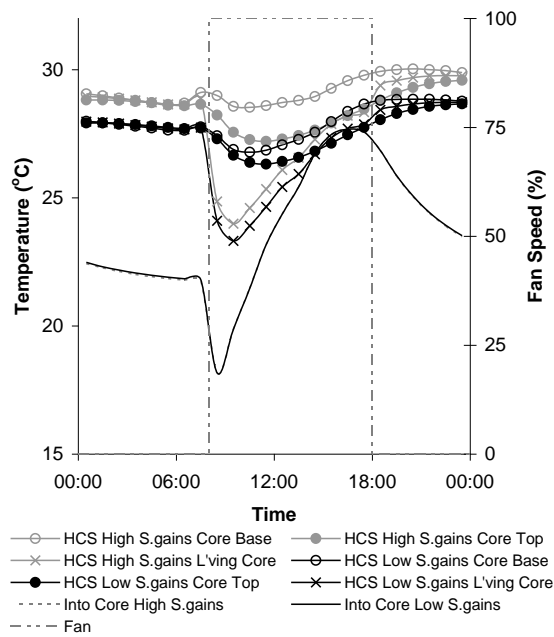


Figure A—44 HCS Strategy core and supply air temperatures – Solar Gain

Table A—4 HCS Heat Exchange Efficiency - Low Solar Gain

Time	Surface Temperatures (°C)			Air Temperatures (°C)		Heat Exchange Efficiency	50% Efficiency	
	Core Base	Core Top	Average Core	Into Core	Leaving Core		Leaving Core	Accuracy
08:30	27.42	27.30	27.36	18.17	24.10	35.5%	22.77	94.5%
09:30	26.89	26.66	26.78	19.87	23.32	50.0%	23.32	100.0%
10:30	26.78	26.38	26.58	21.47	23.91	52.3%	24.03	100.5%
11:30	26.86	26.31	26.59	23.17	24.65	56.7%	24.88	100.9%
12:30	27.07	26.42	26.75	24.37	25.42	55.8%	25.56	100.5%
13:30	27.28	26.58	26.93	25.42	25.93	66.2%	26.18	100.9%
14:30	27.56	26.82	27.19	26.72	26.70	104.3%	26.96	101.0%
15:30	27.97	27.13	27.55	27.47	27.34	262.5%	27.51	100.6%
16:30	28.37	27.46	27.92	27.67	27.70	87.8%	27.79	100.3%
17:30	28.66	27.75	28.21	27.57	27.87	52.8%	27.89	100.1%

A.2.1.4 Internal Gains

Reducing the internal gain again reduces the heat gain experienced by the room and again reduces the temperature (Figure A—45). Reducing the internal gains to low reduces the

annual overheating hours by 24.7% and the T_{res} maximum by 1.4°C. Increasing the internal gains to high increases the annual overheating hours by 16.1% and the T_{res} maximum by 1.3°C.

To look at the effect of reducing the level on internal gain on the core surface temperatures and the air temperature leaving the core the results for the Medium and Low levels of internal gain are presented in Figure A—47. Again as a result of the ceiling surface temperatures in the room being much lower for the Low level of internal gain, the core base surface temperature and core top surface temperature are much lower.

As a result of reducing the internal gain to Low the surface temperature of the core top is reduced below that of the supply air going into the core in the late afternoon (14:30hrs). However, the core base surface temperature still remains higher. The average core surface temperature remains above the air temperature supplied into the slab, with the supply being heated during the full occupied period.

The heat exchanger efficiency of the hollow core slab still remains close to 50% (Table A—5).

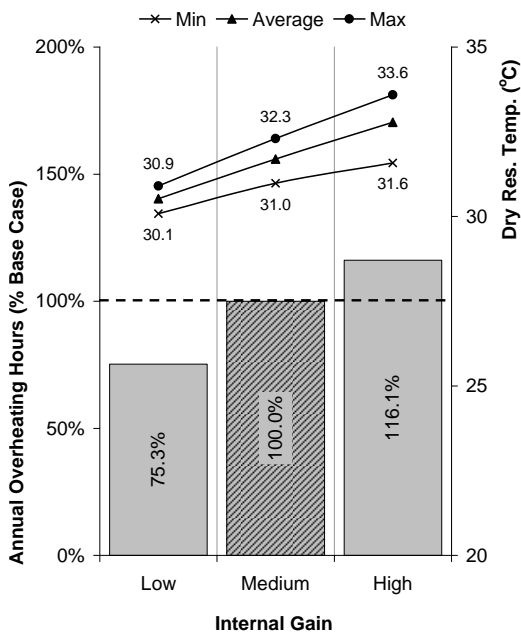


Figure A—45 HCS Strategy Annual Overheating Hours – Internal Gain

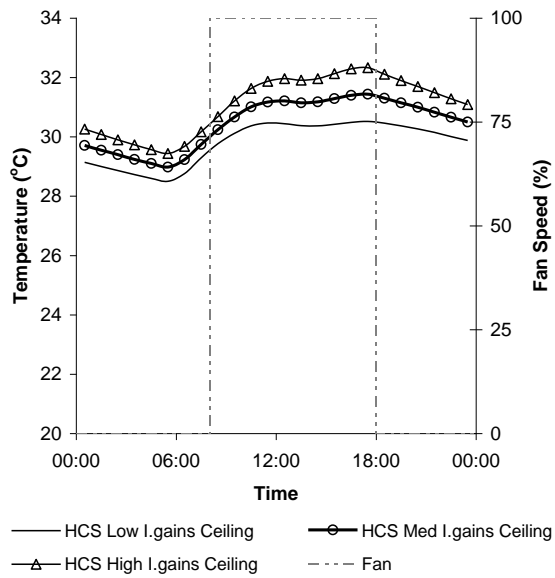


Figure A—46 HCS Strategy Ceiling Surface Temperature – Internal Gain

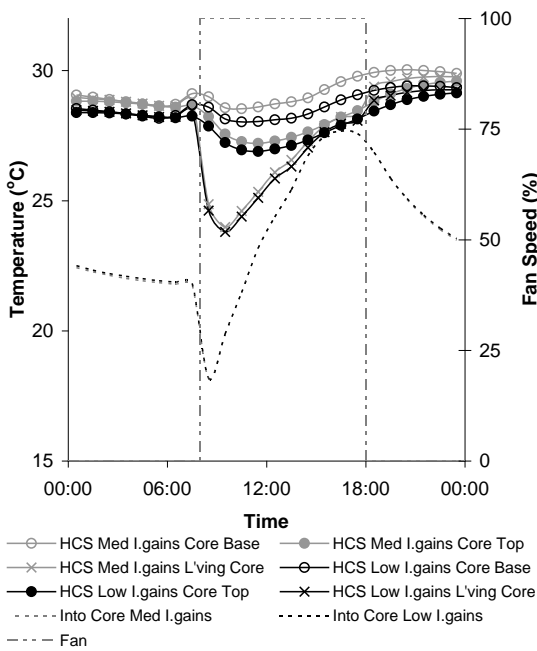


Figure A—47 HCS Strategy core and supply air temperatures – Internal Gain

Table A—5 HCS Heat Exchange Efficiency - Low Internal Gain

Time	Surface Temperatures (°C)			Air Temperatures (°C)		Heat Exchange Efficiency	50% Efficiency	
	Core Base	Core Top	Average Core	Into Core	Leaving Core		Leaving Core	Accuracy
08:30	28.59	27.86	28.23	18.17	24.62	35.9%	23.20	94.2%
09:30	28.14	27.23	27.69	19.87	23.80	49.7%	23.78	99.9%
10:30	28.03	26.95	27.49	21.47	24.39	51.5%	24.48	100.4%
11:30	28.04	26.89	27.47	23.17	25.11	54.8%	25.32	100.8%
12:30	28.11	26.99	27.55	24.37	25.85	53.5%	25.96	100.4%
13:30	28.17	27.12	27.65	25.42	26.31	60.0%	26.53	100.8%
14:30	28.33	27.33	27.83	26.72	27.04	71.2%	27.28	100.9%
15:30	28.60	27.61	28.11	27.47	27.63	74.8%	27.79	100.6%
16:30	28.87	27.89	28.38	27.67	27.95	60.6%	28.03	100.3%
17:30	29.07	28.14	28.61	27.57	28.07	51.7%	28.09	100.1%

A.2.1.5 Air Change Rate

Increasing the air change rate increases the amount of free cooling that can be provided to the room (Figure A—48). Increasing the air change rate from 6 ach⁻¹ (base case) to 8 ach⁻¹ reduces the annual overheating hours by 18.1% and reduces T_{res} maximum by 0.9°C. Increasing the air change rate to 10 ach⁻¹ reduces the annual overheating hours by 32.6°C and the T_{res} maximum by 1.5°C.

To look at the effect of increasing the air change rate on the core surface temperatures and the air temperature leaving the core the results for 6ach⁻¹ and 10ach⁻¹ are presented in Figure A—50. As a result of the ceiling surface temperatures in the room being much lower for the air change rate of 10ach⁻¹ (Figure A—49), the core base surface temperature and core top surface temperature are much lower.

As a result of increasing the air change rate to 10ach⁻¹ the surface temperature of the core top is reduced below that of the supply air going into the core in the late afternoon (14:30hrs to 16:30hrs). However, the core base surface temperature still remains higher. The average core surface temperature remains above the air temperature supplied into the slab, however the air temperature leaving the core is slightly lower than that going into the core at 14:30hrs, 15:30hrs and 16:30hrs.

The heat exchanger efficiency of the hollow core slab still remains close to 50% (

Table A—6).

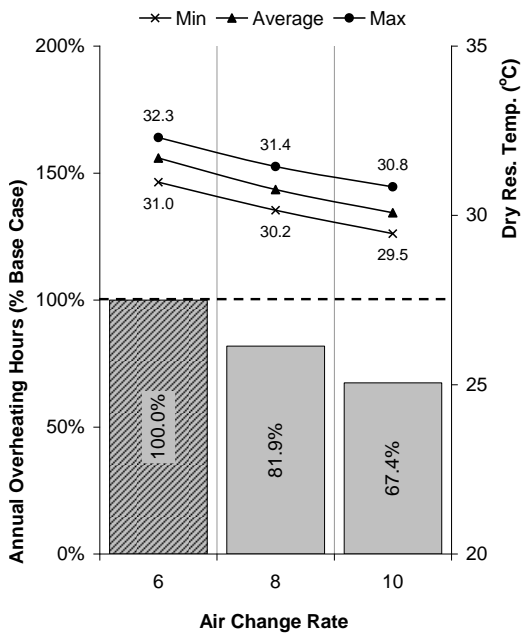


Figure A—48 HCS Strategy Annual Overheating Hours – Air Change Rate

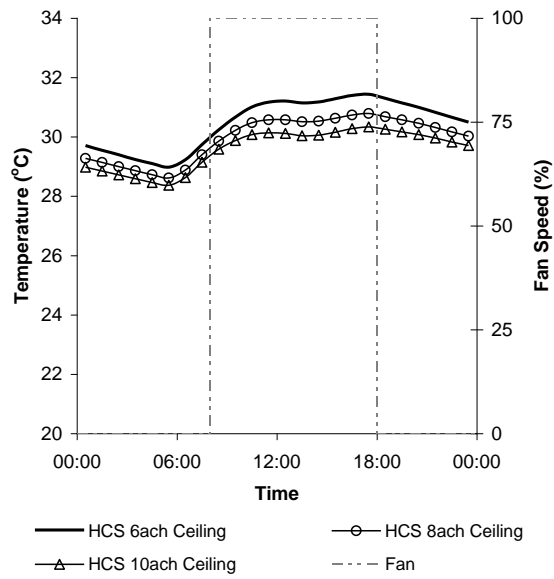


Figure A—49 HCS Strategy Ceiling Surface Temperature – Air Change Rate

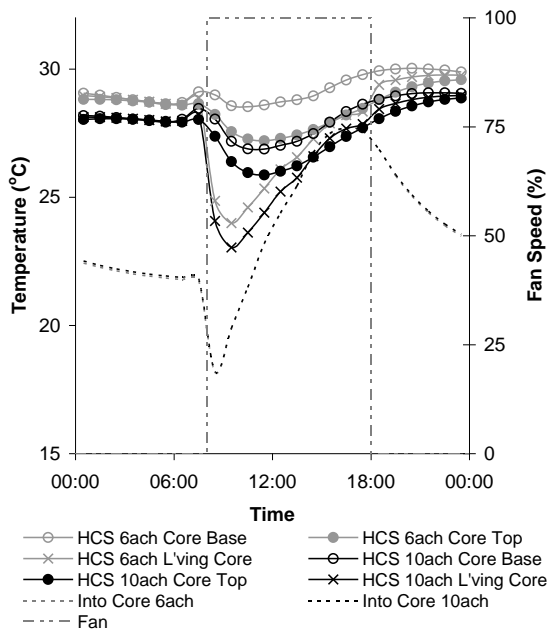


Figure A—50 HCS Strategy core and supply air temperatures – Air Change Rate

Table A—6 HCS Heat Exchange Efficiency – 10achr⁻¹

Time	Surface Temperatures (°C)			Air Temperatures (°C)		Heat Exchange Efficiency	50% Efficiency	
	Core Base	Core Top	Average Core	Into Core	Leaving Core		Leaving Core	Accuracy
08:30	28.05	27.38	27.72	18.19	24.07	38.3%	22.95	95.4%
09:30	27.18	26.39	26.79	19.89	23.04	54.3%	23.34	101.3%
10:30	26.89	25.96	26.43	21.49	23.62	56.8%	23.96	101.4%
11:30	26.88	25.87	26.38	23.19	24.40	62.0%	24.78	101.6%
12:30	27.02	26.01	26.52	24.39	25.22	60.9%	25.45	100.9%
13:30	27.18	26.22	26.70	25.44	25.76	74.6%	26.07	101.2%
14:30	27.48	26.56	27.02	26.74	26.60	150.0%	26.88	101.1%
15:30	27.93	26.97	27.45	27.49	27.30	-375.0%	27.47	100.6%
16:30	28.34	27.37	27.86	27.69	27.68	106.1%	27.77	100.3%
17:30	28.63	27.71	28.17	27.59	27.85	55.2%	27.88	100.1%

A.2.2 Annual Cooling Load

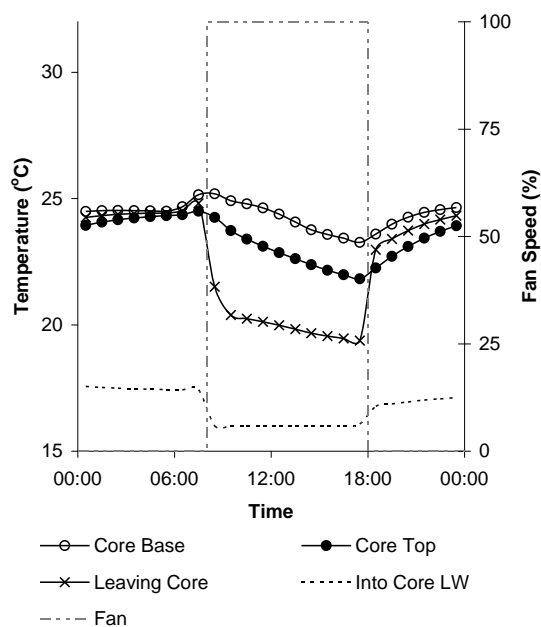


Figure A—51 HCS Strategy with Cooling core and supply air temperatures

A.2.2.1 Thermal Mass

During the peak summer day none of the levels of thermal mass can meet the comfort criteria of T_{res} of $24^{\circ}\text{C} \pm 2^{\circ}\text{C}$.

Figure A—52 and Figure A—53 show that none of the rooms can achieve the setpoint temperature in the morning period (morning period due to test room being east facing and receiving direct solar gain in the morning period). Due to the dampening effect of the HW and VHW levels of thermal mass these rooms come closer to achieving the setpoint temperature.

Increasing the amount of thermal mass in the test room from LW (base case) to HW reduces the annual cooling load by 2.7% (Figure A—52). Increasing the thermal mass further to VHW reduces the annual cooling load by 1.1%. Reducing the thermal mass from LW to VLW only results in an increase in annual cooling load of 0.3%.

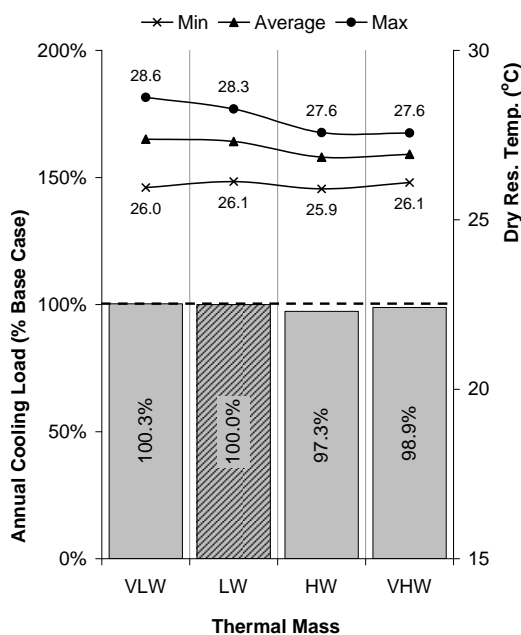


Figure A—52 HCS Strategy Annual Cooling Load – Thermal Mass

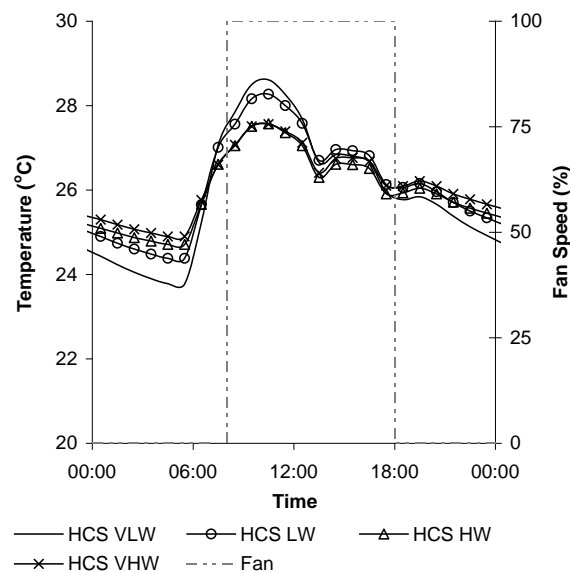


Figure A—53 HCS Strategy with cooling T_{res} on a peak summer day – Thermal Mass

The internal surface temperatures of the floor (Figure A—54), the ceiling (Figure A—55) and the internal walls (Figure A—56) on a peak summer day demonstrate the effect of the different levels of thermal mass.

The surface temperatures of the floor closely follows the temperatures of the room, however the surface temperatures of the HW and VHW internal walls and all of the ceiling surface temperatures show a dampening effect, demonstrating the thermal mass of these surfaces. All of the levels of thermal mass have an exposed concrete soffit as part of the hollow core slab strategy. The surface temperatures of the ceiling for all levels of thermal mass follow the same profile, and due to the cooling all remain at a similar temperature.

To look at the effect of increasing the level of thermal mass in the room on the core surface temperatures and the air temperature leaving the core the results for the LW and HW levels of thermal mass are presented in Figure A—57. As a result of the ceiling surface temperature in the room being very similar the difference between the air temperature leaving the core for the LW and HW levels of thermal mass is minimal.

The heat exchanger efficiency of the hollow core slab remains close to 50% (Table A—7).

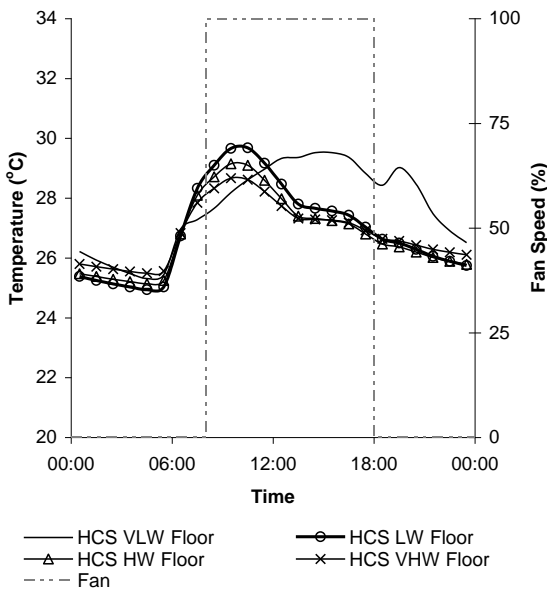


Figure A—54 HCS Strategy with Cooling Floor Surface Temperature – Thermal Mass

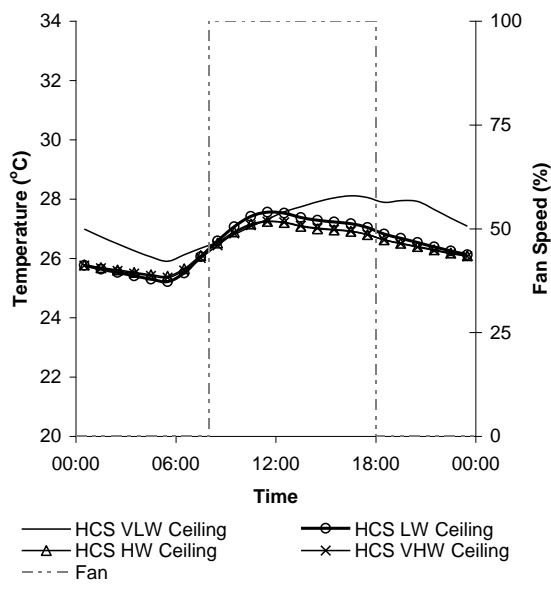


Figure A—55 HCS Strategy with Cooling Ceiling Surface Temperature – Thermal Mass

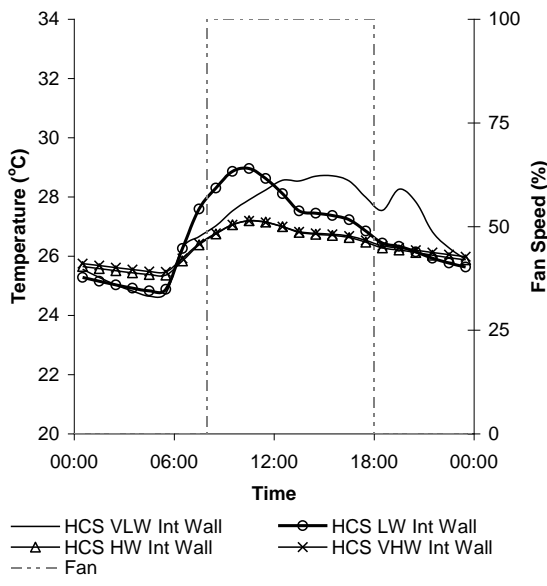


Figure A—56 HCS Strategy with Cooling Internal Wall Surface Temperature – Thermal Mass

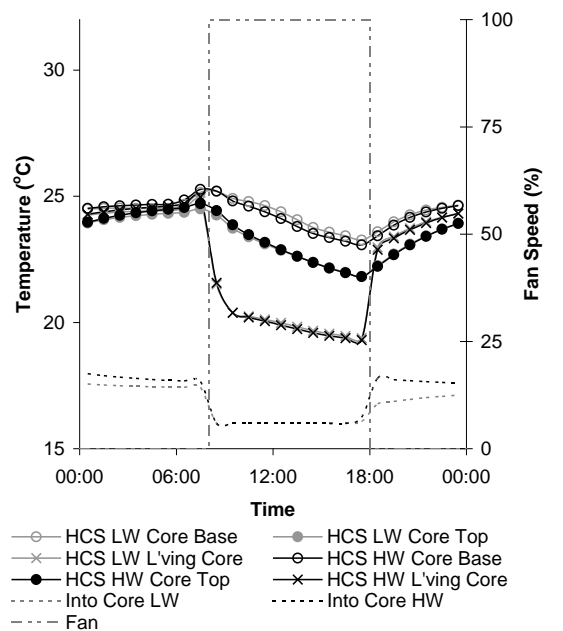


Figure A—57 HCS Strategy with Cooling core and supply air temperatures – Thermal Mass

Table A—7 HCS with Cooling Heat Exchange Efficiency – HW Thermal Mass

Time	Surface Temperatures (°C)			Air Temperatures (°C)		Heat Exchanger Efficiency	50% SE	
	Core Base	Core Top	Average Core	Into Core	Leaving Core		Leaving Core	Accuracy
08:30	25.20	24.43	24.82	16.00	21.57	36.8%	20.41	94.6%
09:30	24.81	23.87	24.34	16.00	20.38	47.5%	20.17	99.0%
10:30	24.60	23.48	24.04	16.00	20.20	47.8%	20.02	99.1%
11:30	24.38	23.17	23.78	16.00	20.05	47.9%	19.89	99.2%
12:30	24.11	22.88	23.50	16.00	19.89	48.1%	19.75	99.3%
13:30	23.80	22.62	23.21	16.00	19.74	48.1%	19.61	99.3%
14:30	23.52	22.37	22.95	16.00	19.58	48.5%	19.47	99.5%
15:30	23.36	22.15	22.76	16.00	19.47	48.6%	19.38	99.5%
16:30	23.22	21.97	22.60	16.00	19.38	48.7%	19.30	99.6%
17:30	23.07	21.81	22.44	16.24	19.30	50.6%	19.34	100.2%

A.2.2.2 Thermal Mass with Night Cooling

Night cooling reduces the temperature of the test room during the unoccupied period for all levels of thermal mass (Figure A—59). The T_{res} in the VLW and LW rooms reach a low of around 21°C and 22°C and the HW and VHW reach a low of around 23°C.

Again none of the levels of thermal mass can meet the comfort criteria of T_{res} of $24^{\circ}\text{C} \pm 2^{\circ}\text{C}$ in the morning period on the peak summer day (Figure A—58 and Figure A—59). Due to the dampening effect of the HW and VHW levels of thermal mass these rooms come closer to achieving the setpoint temperature.

Introducing night cooling reduces the annual cooling load for the VLW room by 11.5%, the LW room by 13.4%, the HW room by 14.0% and the VHW room by 11.5% (Figure A—58).

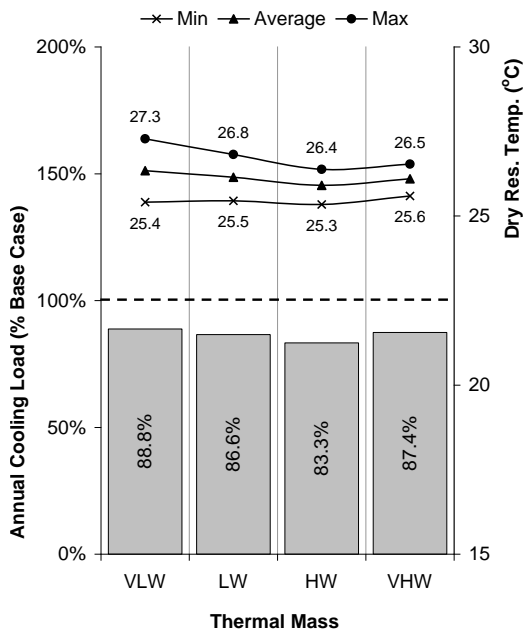


Figure A—58 HCS Strategy Annual Cooling Load— Thermal Mass with Night Cooling

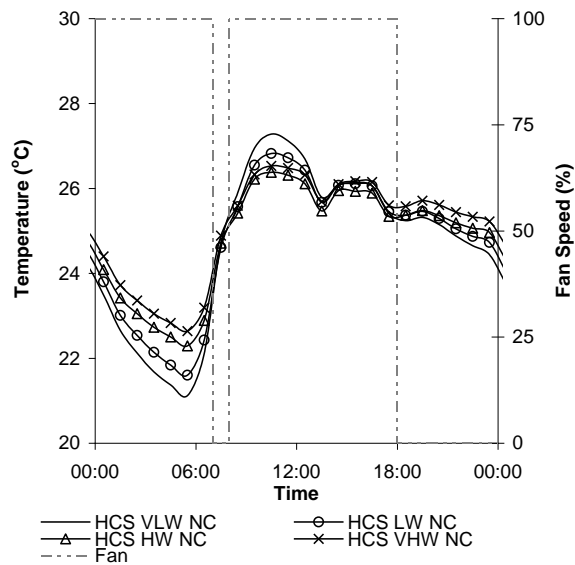


Figure A—59 HCS Strategy with cooling T_{res} on a peak summer day – Thermal Mass with Night Cooling

The surface temperatures of the ceiling (Figure A—60) is around 1°C lower for all levels of thermal mass. The difference between the various levels of thermal mass is now reduced.

To look at the effect of adding night cooling on the core surface temperatures and the air temperature leaving the core the results for the LW and HW levels of thermal mass with night cooling are presented in Figure A—61. As a result of the ceiling surface temperatures in the room being similar, the core base surface temperature are also similar. Again the core top surface temperature is also similar. The difference between the air temperature leaving the core for the LW and HW levels of thermal mass with night cooling is therefore minimal. The heat exchanger efficiency of the hollow core slab still remains close to 50% (Table A—3).

As a result of adding night cooling to both the LW and HW levels of thermal mass the surface temperature of the core top and core base are reduced by up to 3.0°C. This results in the supply air leaving the core being heated less.

The heat exchanger efficiency of the hollow core slab remains close to 50% (

Table A—8).

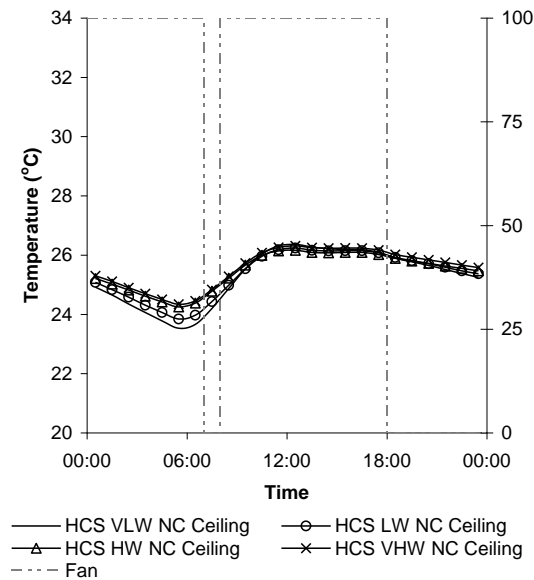


Figure A—60 HCS Strategy with Cooling Ceiling Surface Temperature – Thermal

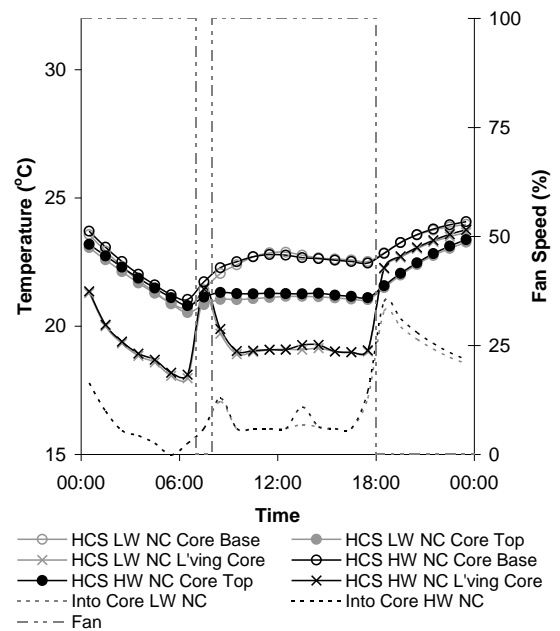


Figure A—61 HCS Strategy with Cooling core and supply air temperatures – Thermal

Mass with Night Cooling**Mass with Night Cooling****Table A—8 HCS with Cooling Heat Exchange Efficiency – HW Thermal Mass with Night Cooling**

Time	Surface Temperatures (°C)			Air Temperatures (°C)		Heat Exchanger Efficiency	50% SE	
	Core Base	Core Top	Average Core	Into Core	Leaving Core		Leaving Core	Accuracy
00:30	23.70	23.19	23.45	17.78	21.36	36.8%	20.61	96.5%
01:30	23.08	22.74	22.91	16.68	20.05	45.9%	19.80	98.7%
02:30	22.52	22.30	22.41	15.93	19.40	46.5%	19.17	98.8%
03:30	22.02	21.87	21.95	15.73	18.93	48.5%	18.84	99.5%
04:30	21.61	21.49	21.55	15.43	18.69	46.7%	18.49	98.9%
05:30	21.22	21.11	21.17	14.98	18.18	48.3%	18.07	99.4%
06:30	21.04	20.80	20.92	15.43	18.11	51.2%	18.18	100.4%
08:30	22.28	21.31	21.80	17.19	19.89	41.4%	19.49	98.0%
09:30	22.51	21.27	21.89	16.00	19.03	48.6%	18.95	99.6%
10:30	22.71	21.26	21.99	16.00	19.04	49.2%	18.99	99.8%
11:30	22.79	21.28	22.04	16.00	19.08	49.0%	19.02	99.7%
12:30	22.77	21.27	22.02	16.00	19.08	48.8%	19.01	99.6%
13:30	22.67	21.26	21.97	16.85	19.26	52.9%	19.41	100.8%
14:30	22.63	21.28	21.96	16.07	19.27	45.6%	19.01	98.7%
15:30	22.57	21.21	21.89	16.00	19.01	48.9%	18.95	99.7%
16:30	22.52	21.16	21.84	16.00	18.98	49.0%	18.92	99.7%

17:30	22.46	21.11	21.79	17.47	19.06	63.2%	19.63	103.0%
-------	-------	-------	-------	-------	-------	-------	-------	--------

A.2.2.3 Solar Gains

Reducing the solar gains from high (base case) to medium reduces the annual cooling load by 6.0% (Figure A—62). Reducing the solar gains to low reduces the annual cooling load by 14.5%.

To look at the effect of reducing the level on solar gain on the core surface temperatures and the air temperature leaving the core the results for the High and Low levels of solar gain are presented in Figure A—64. As a result of the ceiling surface temperatures in the room being much lower for the Low level of solar gain (Figure A—63), the core base surface temperature and core top surface temperature are much lower. This results in the supply air leaving the slab being heated less.

The heat exchanger efficiency of the hollow core slab remains close to 50% (

Table A—9).

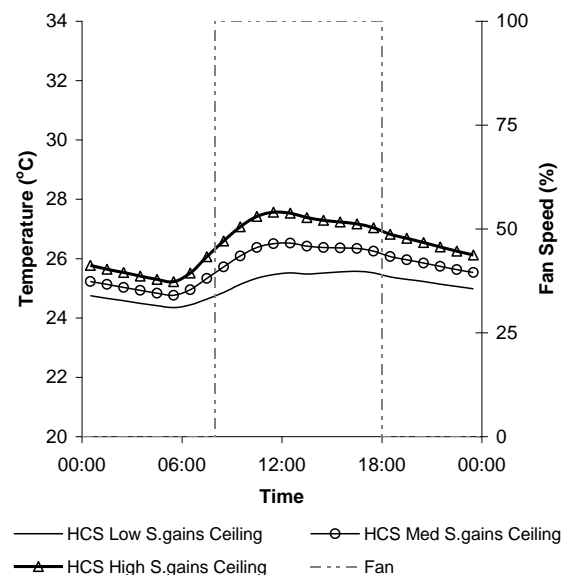
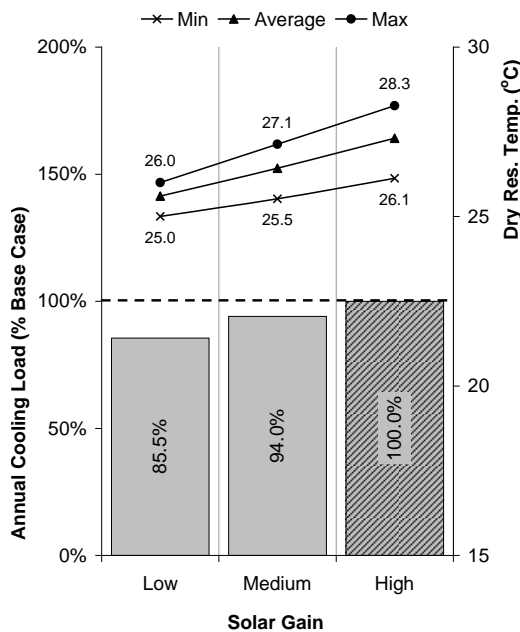


Figure A—62 HCS Strategy Annual Cooling

Figure A—63 HCS Strategy with Cooling

Load– Solar Gain

Ceiling Surface Temperature – Solar Gain

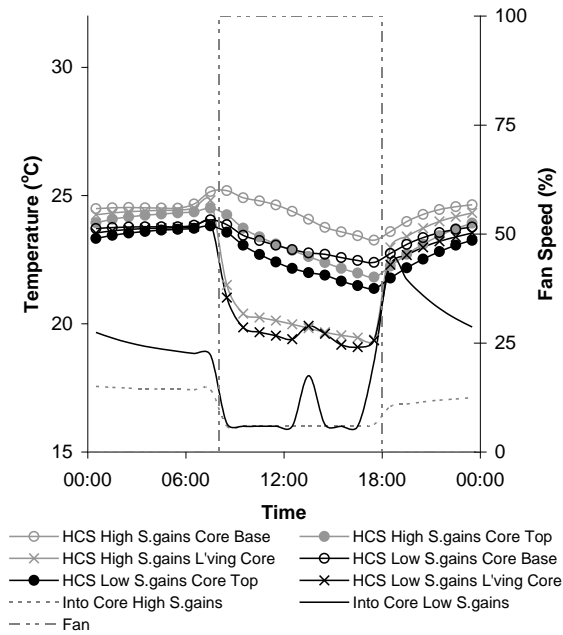


Figure A—64 HCS Strategy with Cooling core and supply air temperatures – Solar Gain

Table A—9 HCS with Cooling Heat Exchange Efficiency – Low Solar Gain

Time	Surface Temperatures (°C)			Air Temperatures (°C)		Heat Exchange Efficiency	50% Efficiency	
	Core Base	Core Top	Average Core	Into Core	Leaving Core		Leaving Core	Accuracy
08:30	23.86	23.57	23.72	16.12	21.02	35.5%	19.92	94.8%
09:30	23.45	23.06	23.26	16.00	19.86	46.8%	19.63	98.8%
10:30	23.24	22.70	22.97	16.00	19.67	47.3%	19.49	99.1%
11:30	23.06	22.41	22.74	16.00	19.53	47.6%	19.37	99.2%
12:30	22.89	22.16	22.53	16.00	19.40	47.9%	19.26	99.3%
13:30	22.76	21.99	22.38	17.97	19.92	55.7%	20.17	101.3%
14:30	22.71	21.89	22.30	16.07	19.61	43.2%	19.19	97.8%
15:30	22.58	21.66	22.12	16.00	19.18	48.0%	19.06	99.4%
16:30	22.47	21.49	21.98	16.00	19.09	48.3%	18.99	99.5%
17:30	22.39	21.37	21.88	18.52	19.35	75.3%	20.20	104.4%

A.2.2.4 Internal Gains

Reducing the internal gains from medium (base case) to low reduces the annual cooling load by 18.2% (Figure A—65). Increasing the solar gains to high increase the annual cooling load by 9.6%.

To look at the effect of reducing the level on internal gain on the core surface temperatures and the air temperature leaving the core the results for the Medium and Low levels of internal gain are presented in Figure A—67. As a result of the ceiling surface temperatures in the room being lower for the Low level of internal gain (Figure A—66), the core base surface temperature is lower, however there the core top surface temperature is only slightly lower. The supply air leaving the slab is therefore only heated slightly less for the Low level of internal gain.

The heat exchanger efficiency of the hollow core slab remains close to 50% (Table A—10).

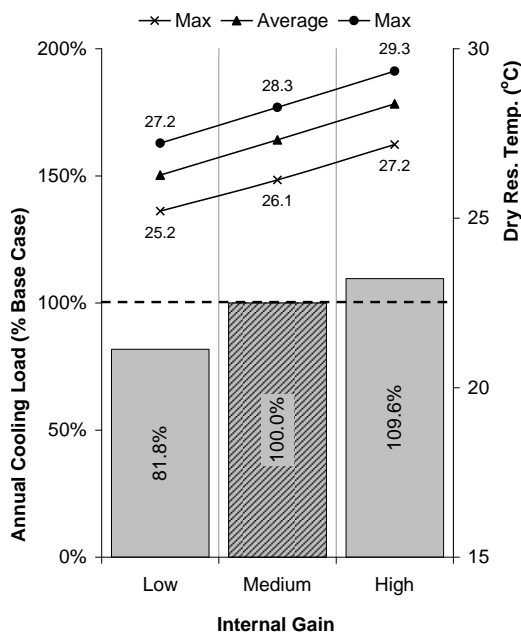


Figure A—65 HCS Strategy Annual Cooling Load – Internal Gain

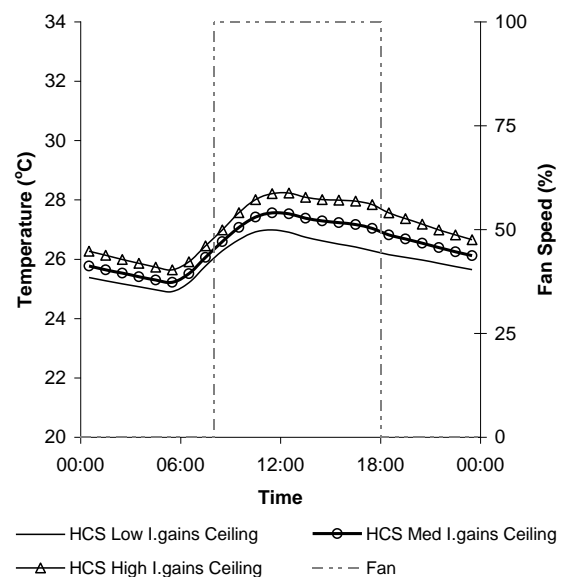


Figure A—66 HCS Strategy with Cooling Ceiling Surface Temperature – Internal Gain

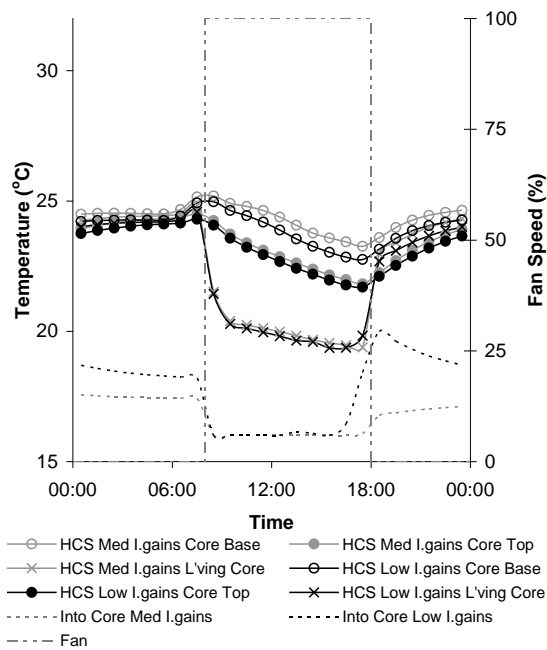


Figure A—67 HCS Strategy with Cooling core and supply air temperatures – Internal Gain

Table A—10 HCS with Cooling Heat Exchange Efficiency – Low Internal Gains

Time	Surface Temperatures (°C)			Air Temperatures (°C)		Heat Exchange Efficiency	50% SE	
	Core Base	Core Top	Average Core	Into Core	Leaving Core		Leaving Core	Accuracy
08:30	24.97	24.07	24.52	16.00	21.43	36.3%	20.26	94.5%
09:30	24.63	23.57	24.10	16.00	20.28	47.2%	20.05	98.9%
10:30	24.43	23.22	23.83	16.00	20.11	47.5%	19.91	99.0%
11:30	24.19	22.94	23.57	16.00	19.96	47.7%	19.78	99.1%
12:30	23.88	22.67	23.28	16.00	19.81	47.6%	19.64	99.1%
13:30	23.54	22.41	22.98	16.14	19.64	48.8%	19.56	99.6%
14:30	23.26	22.19	22.73	16.08	19.59	47.2%	19.40	99.0%
15:30	23.03	21.96	22.50	16.00	19.36	48.3%	19.25	99.4%
16:30	22.84	21.77	22.31	16.43	19.37	50.0%	19.37	100.0%
17:30	22.75	21.69	22.22	18.41	19.83	62.7%	20.32	102.4%

A.2.2.5 Air Change Rate

Increasing the air change rate increases the amount of free cooling that can be provided when the ambient air temperature is below that of the required supply air temperature, but also increases the amount of air that needs to be cooled when the ambient air is above that of the required supply air temperature.

Increasing the air change rate from 6ach^{-1} (base case) to 8ach^{-1} increases the annual cooling load by 11.6% (Figure A—68). Increasing the air change rate to 10ach^{-1} increases the annual cooling load by 16.3%.

To look at the effect of increasing the air change rate on the core surface temperatures and the air temperature leaving the core the results for the 6ach^{-1} and 10ach^{-1} are presented in Figure A—70. As a result of the ceiling surface temperatures in the room being lower for the 10ach^{-1} (Figure A—66), the core base and core top surface temperatures are lower. The supply air leaving the slab is therefore only heated less.

The heat exchanger efficiency of the hollow core slab remains close to 50% (Table A—10).

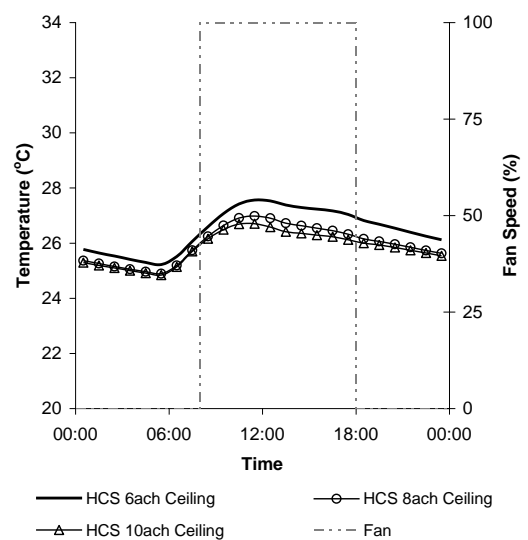
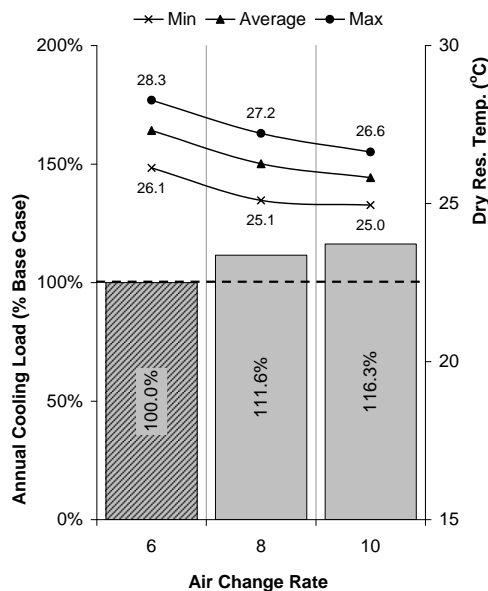


Figure A—68 HCS Strategy Annual Cooling Load— Air Change Rate

Figure A—69 HCS Strategy with Cooling Ceiling Surface Temperature – Air Change Rate

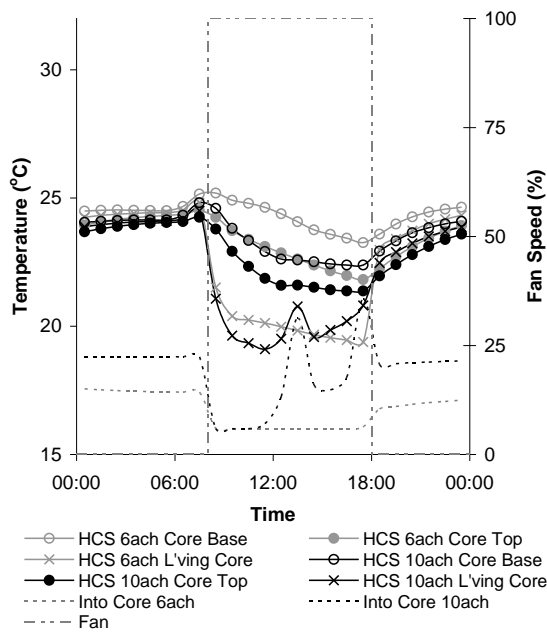


Figure A—70 HCS Strategy with Cooling core and supply air temperatures – Air Change Rate

Table A—11 HCS with Cooling Heat Exchange Efficiency – 10ach⁻¹

Time	Surface Temperatures (°C)			Air Temperatures (°C)		Heat Exchange Efficiency	50% SE	
	Core Base	Core Top	Average Core	Into Core	Leaving Core		Leaving Core	Accuracy
08:30	24.59	23.79	24.19	16.00	21.07	38.1%	20.10	95.4%
09:30	23.82	22.92	23.37	16.00	19.63	50.7%	19.69	100.3%
10:30	23.34	22.33	22.84	16.00	19.34	51.1%	19.42	100.4%
11:30	22.91	21.86	22.39	16.20	19.10	53.1%	19.29	101.0%
12:30	22.62	21.59	22.11	17.25	19.51	53.5%	19.68	100.9%
13:30	22.58	21.60	22.09	20.32	20.77	74.6%	21.21	102.1%
14:30	22.51	21.52	22.02	17.71	19.58	56.6%	19.86	101.4%
15:30	22.43	21.42	21.93	17.52	19.85	47.1%	19.72	99.4%
16:30	22.38	21.37	21.88	18.00	20.20	43.2%	19.94	98.7%
17:30	22.38	21.37	21.88	21.07	20.81	132.3%	21.47	103.2%

A.2.3 Annual Heating Load

A.2.3.1 Thermal Mass

Increasing the thermal mass from LW (base case) to HW reduces the annual heating load by 1.9% (Figure A—71), increasing the thermal mass to VHW reduces the annual heating load by 2.7%. Reducing the thermal mass to VLW also reduces the annual heating load by 0.3%.

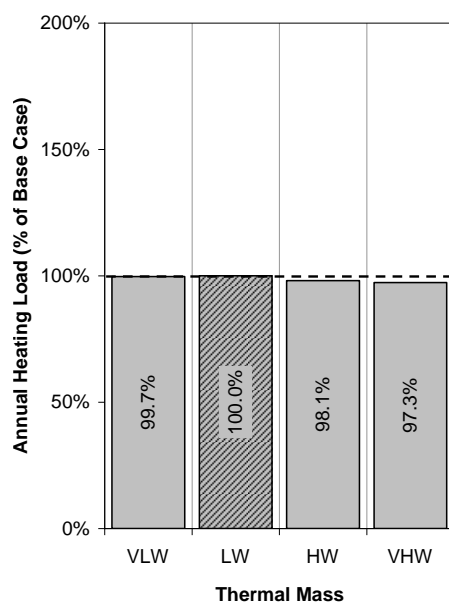


Figure A—71 HCS Strategy Annual Heating Load – Thermal Mass

A.2.3.2 Solar Gains

Reducing the solar gains from high (base case) to medium increases the annual heating load by 3.0% (Figure A—72). Reducing the solar gains to low increases the annual heating load by 6.2%.

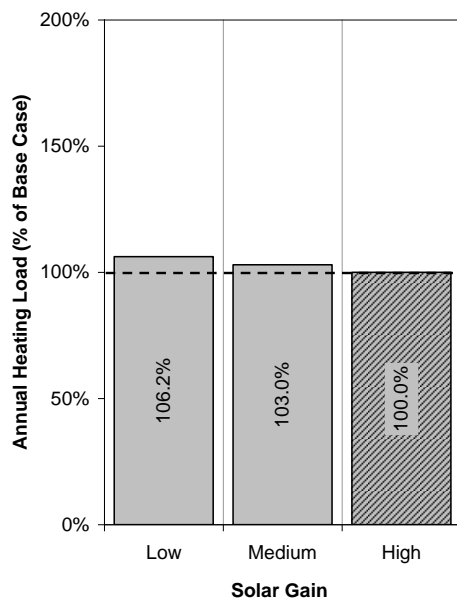


Figure A—72 HCS Strategy Annual Heating Load – Solar Gain

A.2.3.3 Internal Gain

Reducing the internal gains from medium (base case) to low increases the annual heating load by 22.3% (Figure A—73). Increasing the internal gains to high reduces the annual heating load by 16.5%.

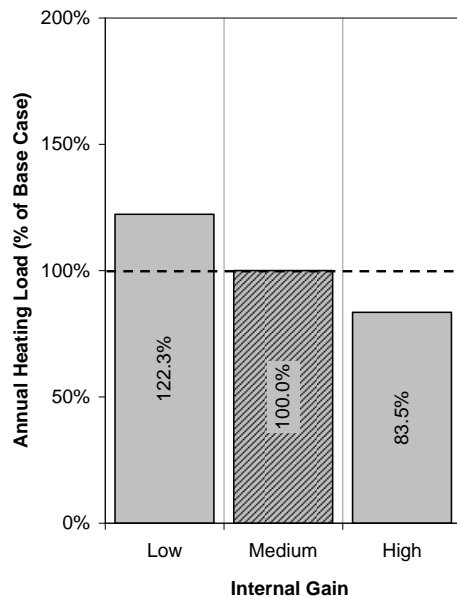


Figure A—73 HCS Strategy Annual Heating Load – Internal Gain

A.2.3.4 Air Change Rate

Increasing the air change rate from 6ach^{-1} (base case) to 8ach^{-1} increases the annual heating load by 42.1% (Figure A—74). Increasing the air change rate to 10ach^{-1} increases the annual heating load by 84.6%.

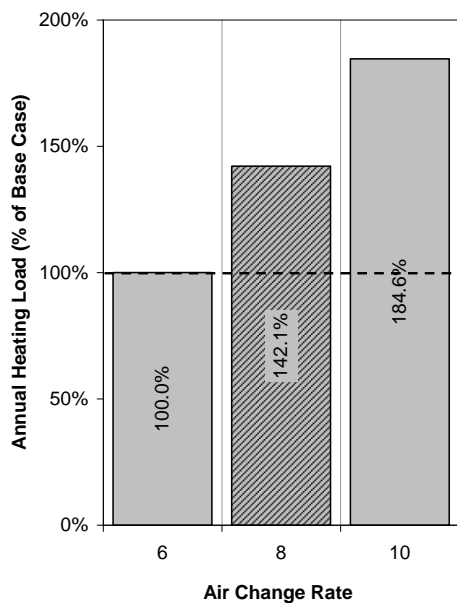


Figure A—74 HCS Strategy Annual Heating Load – Air Change Rate

A.3 Floor Void With Mass (FVWM)

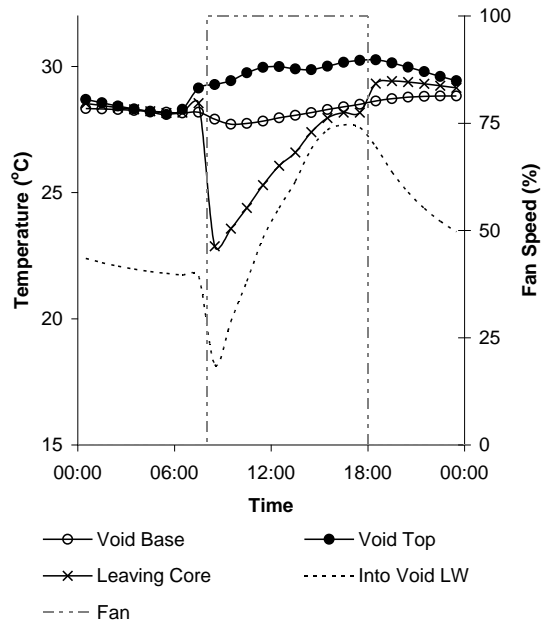


Figure A—75 FVWM Strategy void and supply air temperatures

A.3.1 Overheating Hours

Passing the supply air through the Floor Void dampens the fluctuations in the air entering into the core. Figure A—76 shows the effect that passing the air through the core has on a peak summer day.

For the base case model the surface temperatures of the core base and the core top are relatively constant. Due to this temperature being higher than that of the air entering into the core the strategy has the unwanted effect of heating the air.

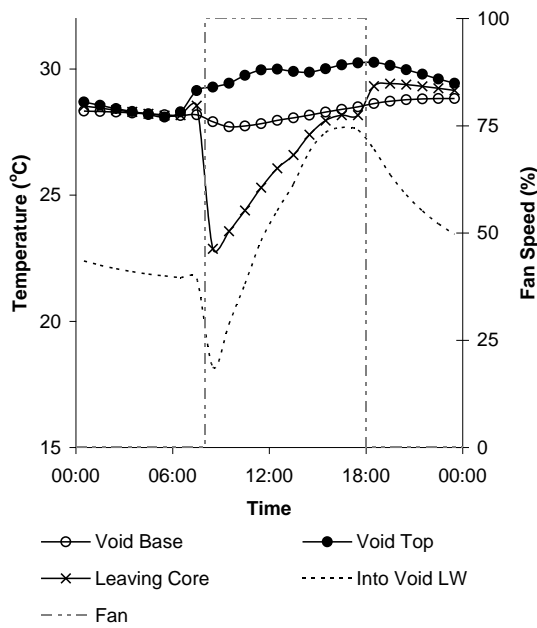


Figure A—76 FVWM Strategy void and supply air temperatures

A.3.1.1 Thermal Mass

Increasing the thermal mass from LW (base case) to HW reduces the overheating hours by 10.2% and decreases T_{res} maximum by 0.8°C (Figure A—77). Increasing the thermal mass further to VHW results in a 0.1% increase in annual overheating hours with and a further reduction T_{res} maximum of 0.1°C . Decreasing the thermal mass from LW to VLW increases the annual overheating hours by 0.2% and increases the T_{res} maximum by 0.2°C .

The dampening effect of the thermal mass on the fluctuation in the temperature can be seen in Figure A—78.

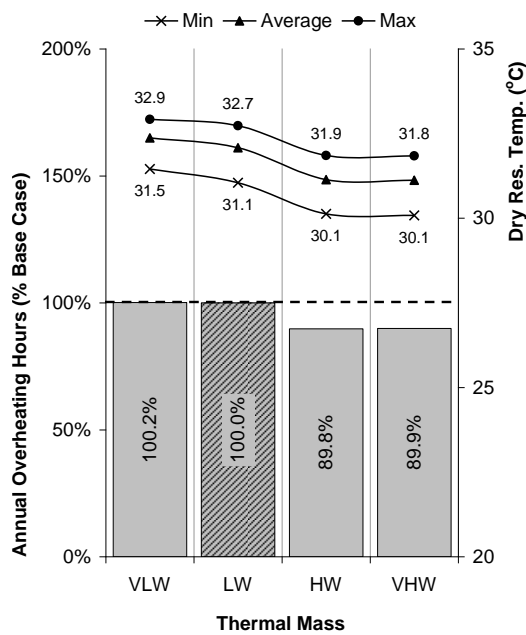


Figure A—77 FVWM Strategy Annual Overheating Hours – Thermal Mass

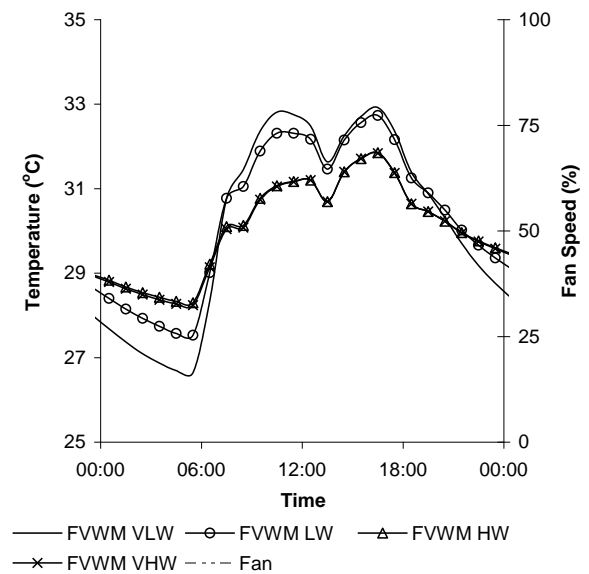


Figure A—78 FVWM Strategy T_{res} on a peak summer day – Thermal Mass

The internal surface temperatures of the floor (Figure A—79), the ceiling (Figure A—80) and the internal walls (Figure A—81) on a peak summer day demonstrate the effect of the different levels of thermal mass.

The surface temperatures of the floor and ceiling closely follows the temperatures of the room, however the surface temperatures of the HW and VHW internal walls surface temperatures show a dampening effect, demonstrating the thermal mass of these surfaces.

All of the levels of thermal mass have a raised floor as part of the FVWM strategy. The surface temperatures of the floor for all levels of thermal mass therefore follow the same profile, however the VLW and LW remain higher than the HW and VHW due to the higher temperatures in the room above.

To look at the effect of increasing the level of thermal mass in the room on the void surface temperatures and the air temperature leaving the floor void the results for the LW and HW levels of thermal mass are presented in Figure A—82.

As a result of the floor surface temperature in the room being lower in the HW room, the void top surface temperature is lower. However there is minimal effect on the void base surface temperature. The difference between the air temperature leaving the void for the LW and HW levels of thermal mass is therefore minimal.

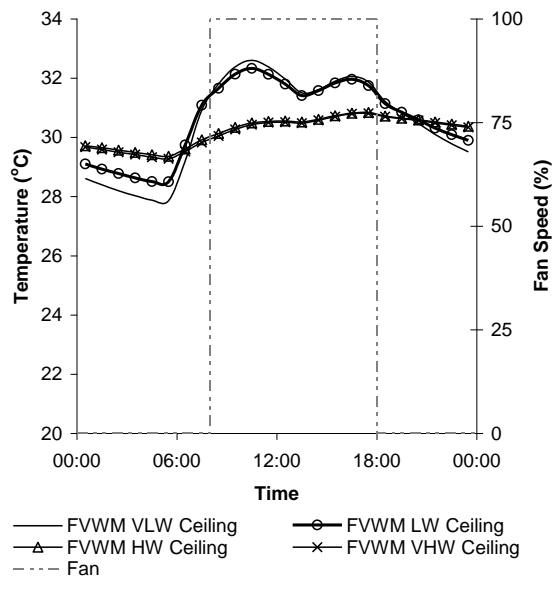
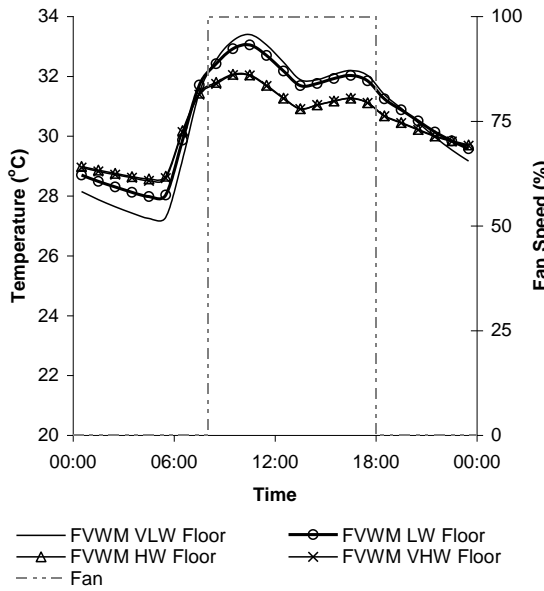


Figure A—79 FVWM Strategy Floor Surface Temperature – Thermal Mass

Figure A—80 FVWM Strategy Ceiling Surface Temperature – Thermal Mass

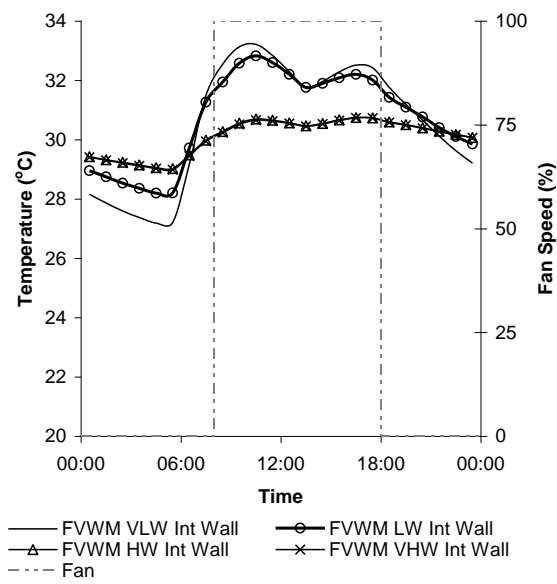


Figure A—81 FVWM Strategy Internal Wall Surface Temperature – Thermal Mass

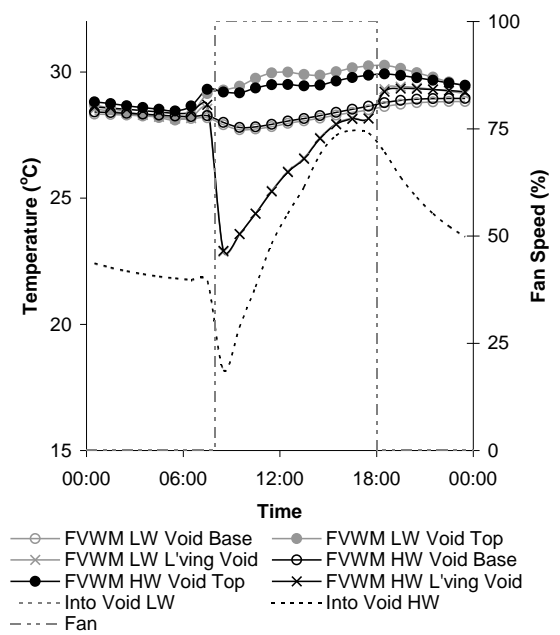


Figure A—82 FVWM Strategy void and supply air temperatures – Thermal Mass

A.3.1.2 Thermal Mass with Night Cooling

Night cooling reduces the temperature of the test room during the unoccupied period for all of the levels of thermal mass (Figure A—84). The T_{res} in the VLW and LW rooms reach a low of around 23°C and 24°C and the HW and VHW reach a low of around 25°C.

Night cooling reduces the annual overheating hours by 20.3% for the LW (base case) reducing the maximum T_{res} on a peak summer day by 1.0°C (Figure A—83).

Introducing night cooling to the HW room reduces the annual overheating hours by 23.4%, and the maximum T_{res} by 1.0°C. For the VHW room the annual overheating hours are reduced by 22.8%, reducing the maximum T_{res} by 0.9°C. There is still little difference between the HW and VHW rooms in terms of both annual overheating hours or T_{res} .

A greater difference is now found between the VLW and LW rooms. Adding night cooling to the VLW room reduces the annual overheating hours by 14.9% and the T_{res} maximum by 0.7°C.

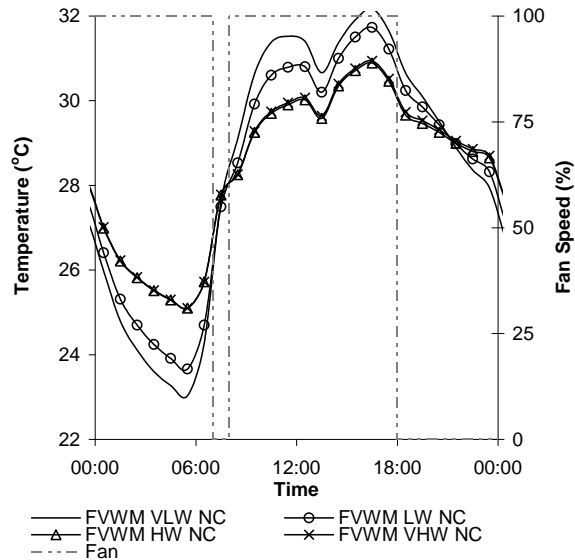
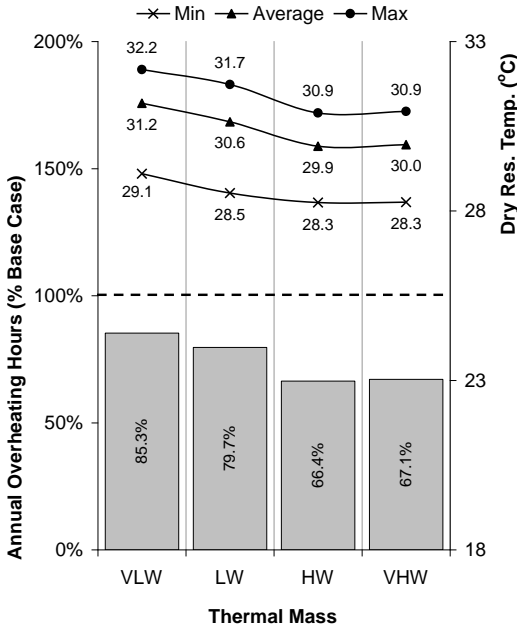


Figure A—83 FVWM Strategy Annual Overheating Hours – Thermal Mass with Night Cooling

Figure A—84 FVWM Strategy T_{res} on a peak summer day – Thermal Mass with Night Cooling

The surface temperatures of the floor (Figure A—85) is around 1°C lower for all levels of thermal mass. The difference between the various levels of thermal mass is now reduced.

To look at the effect of adding night cooling on the core surface temperatures and the air temperature leaving the core the results for the LW and HW levels of thermal mass with night cooling are presented in Figure A—86. As a result of the ceiling surface temperatures in the room being similar, the void top surface temperature are also similar. A small difference is created in void base surface temperature is now shown, however the difference between the air temperature leaving the void for the LW and HW levels of thermal mass with night cooling is minimal.

As a result of adding night cooling to both the LW and HW levels of thermal mass the surface temperature of the void base is reduced below that of the supply air going into the

core in the afternoon. The void top surface temperature still remains higher resulting in the average void surface temperature always being higher than that of the supply air going into the void, resulting in the supply air being heated for the full day except for 15:30hrs where it is slightly cooled.

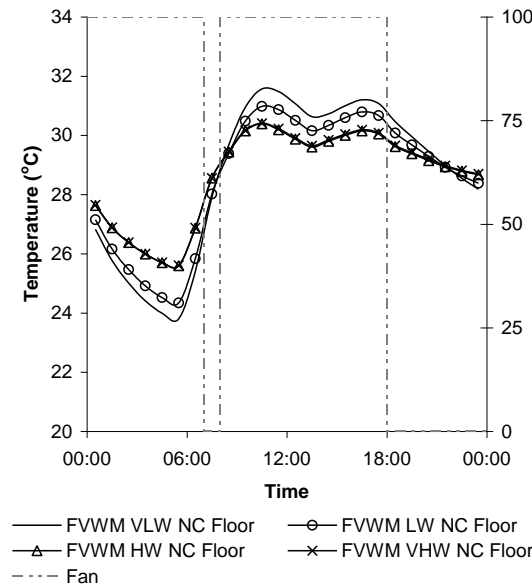


Figure A—85 FVWM Strategy Floor Surface Temperature – Thermal Mass with Night Cooling

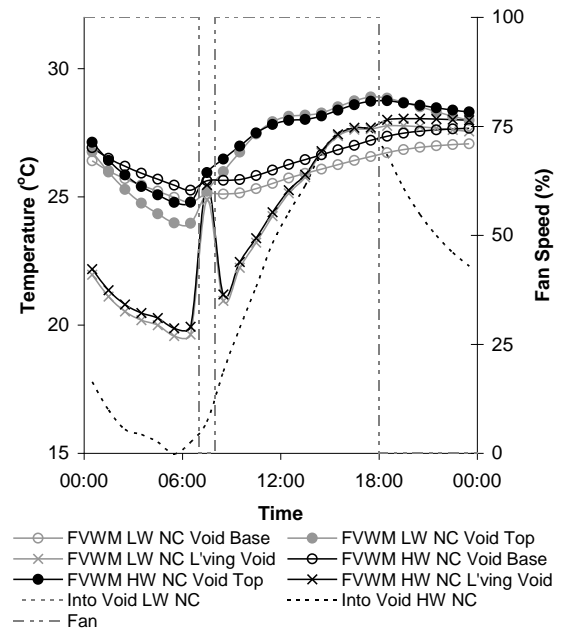


Figure A—86 FVWM Strategy void and supply air temperatures – Thermal Mass with Night Cooling

A.3.1.3 Solar Gains

Reducing the solar gain reduces the heat gain experienced by the room and therefore reduces the temperature (Figure A—87). Reducing the solar gains to medium reduces the annual overheating hours by 13.8% and the T_{res} maximum by 0.7°C . Reducing the solar gains to low reduces the annual overheating hours by 34.0% and the T_{res} maximum by 1.4°C .

To look at the effect of reducing the level on solar gain on the core surface temperatures and the air temperature leaving the core the results for the High and Low levels of solar

gain are presented in Figure A—89. As a result of the floor surface temperatures in the room being much lower for the Low level of solar gain (Figure A—88), the void top surface temperature and void base surface temperature are much lower.

As a result of reducing the solar gain to Low the surface temperature of the void base is reduced below that of the supply air going into the core in the late afternoon (15:30hrs and 16:30hrs). However, the void top surface temperature still remains higher. The average core surface temperature remains above the air temperature supplied into the slab and the air temperature leaving the void is always higher than that going into the void.

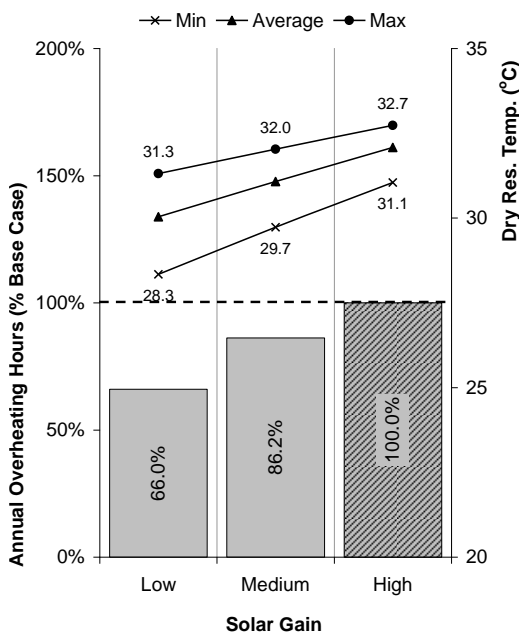


Figure A—87 FVWM Strategy Annual Overheating Hours – Solar Gain

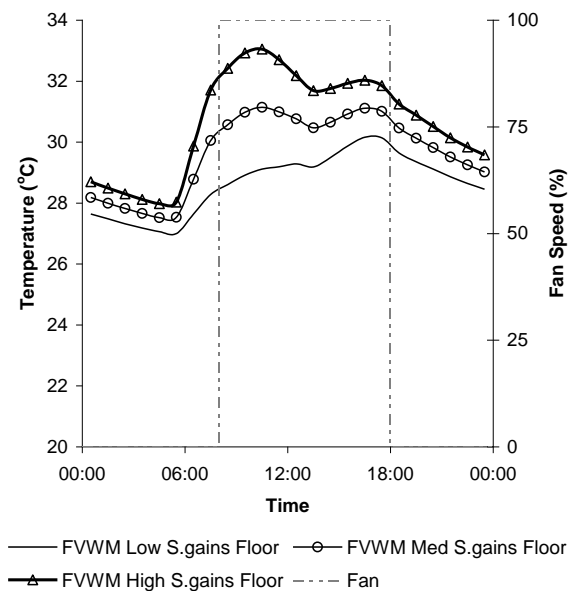


Figure A—88 FVWM Strategy Floor Surface Temperature – Solar Gain

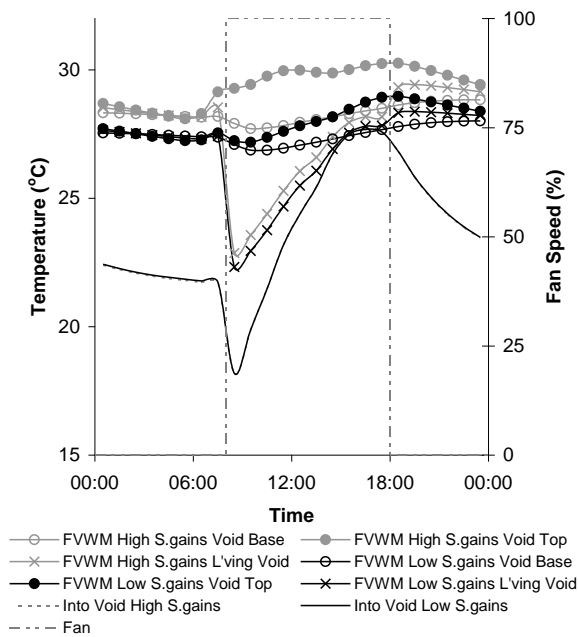


Figure A—89 FVWM Strategy void and supply air temperatures – Solar Gain

A.3.1.4 Internal Gains

Reducing the internal gain again reduces the heat gain experienced by the room and again reduces the temperature (Figure A—90). Reducing the internal gains to low reduces the annual overheating hours by 22.9% and the T_{res} maximum by 1.4°C. Increasing the internal gains to high increases the annual overheating hours by 17.7% and the T_{res} maximum by 1.4°C.

To look at the effect of reducing the level on internal gain on the void surface temperatures and the air temperature leaving the void the results for the Medium and Low levels of internal gain are presented in Figure A—92. Again as a result of the floor surface temperatures (Figure A—91) in the room being much lower for the Low level of internal gain, the void top surface temperature and void base surface temperature are lower.

As a result of reducing the internal gain to Low the surface temperatures of the void base and void top always remains above that of the supply air going into the void. The supply is therefore heated during the full occupied period.

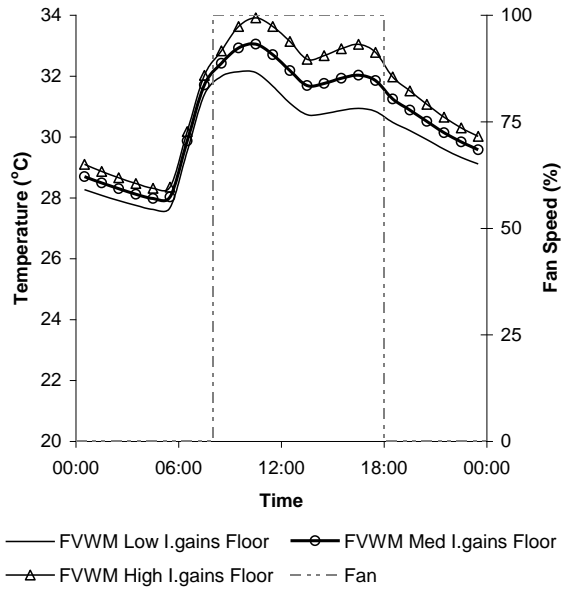
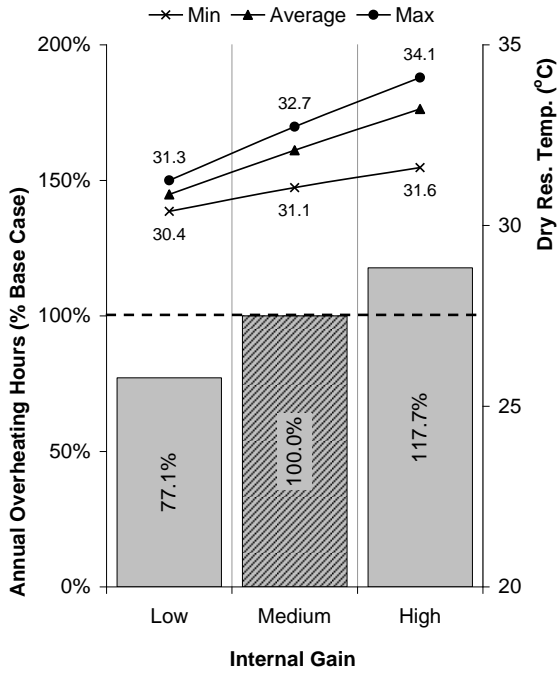


Figure A—90 FVWM Strategy Annual Overheating Hours – Internal Gain

Figure A—91 FVWM Strategy Floor Surface Temperature – Internal Gain

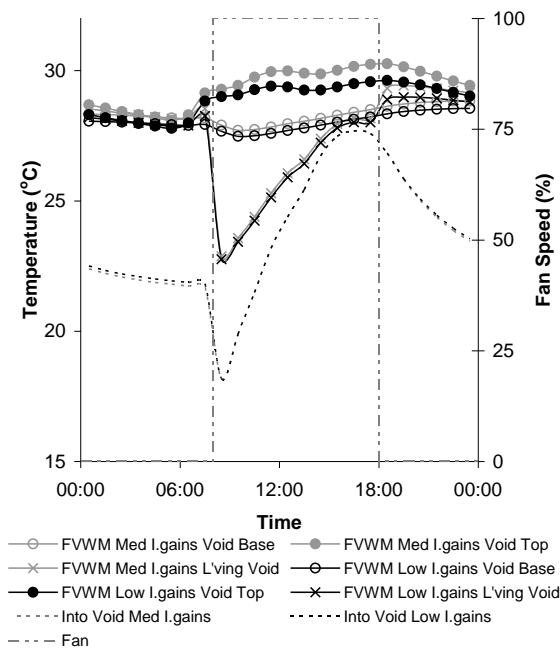


Figure A—92 FVWM Strategy void and supply air temperatures – Internal Gain

A.3.1.5 Air Change Rate

Increasing the air change rate increases the amount of free cooling that can be provided to the room (Figure A—93). Increasing the air change rate from 6 ach^{-1} (base case) to 8 ach^{-1} reduces the annual overheating hours by 17.6% and reduces T_{res} maximum by 0.8°C . Increasing the air change rate to 10 ach^{-1} reduces the annual overheating hours by 31.4% and the T_{res} maximum by 1.4°C .

To look at the effect of increasing the air change rate on the void surface temperatures and the air temperature leaving the void the results for 6 ach^{-1} and 10 ach^{-1} are presented in Figure A—95. As a result of the floor surface temperatures in the room being much lower for the air change rate of 10 ach^{-1} (Figure A—94), the void top surface temperature and void base surface temperatures are lower.

As a result of increasing the air change rate to 10ach⁻¹ the surface temperatures of the void base and void top always remains above that of the supply air going into the void. The supply is therefore heated during the full occupied period.

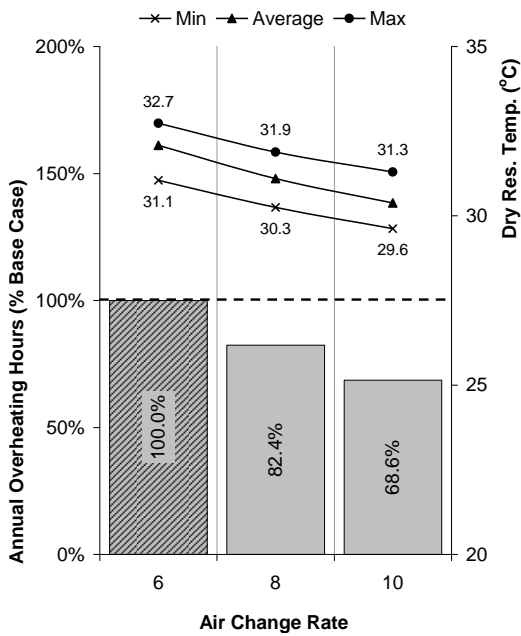


Figure A—93 FVWM Strategy Annual Overheating Hours – Air Change Rate

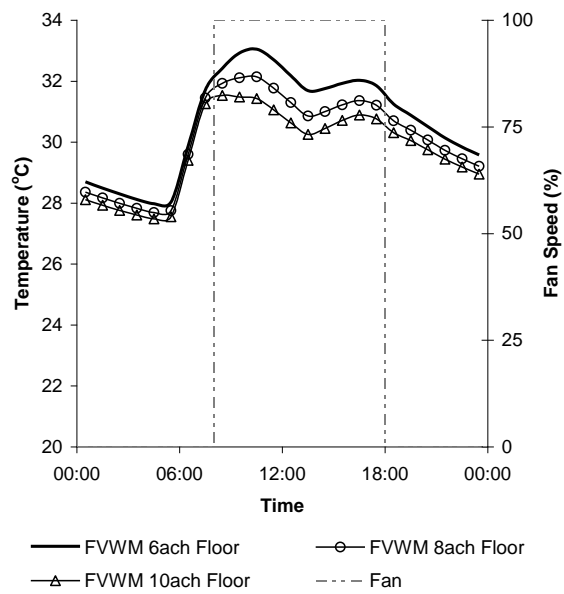


Figure A—94 FVWM Strategy Floor Surface Temperature – Air Change Rate

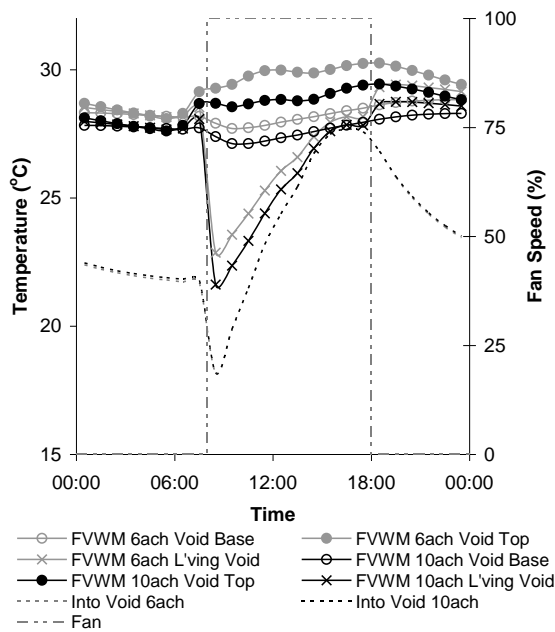


Figure A—95 FVWM Strategy void and supply air temperatures – Air Change Rate

A.3.2 Annual Cooling Load

To prevent occupant discomfort as a result of drafts caused by the supply air being too cold the cooling for the FVWM strategy is controlled to limit the air temperature of the supply air being supplied into the floor void being limited to 16°C.

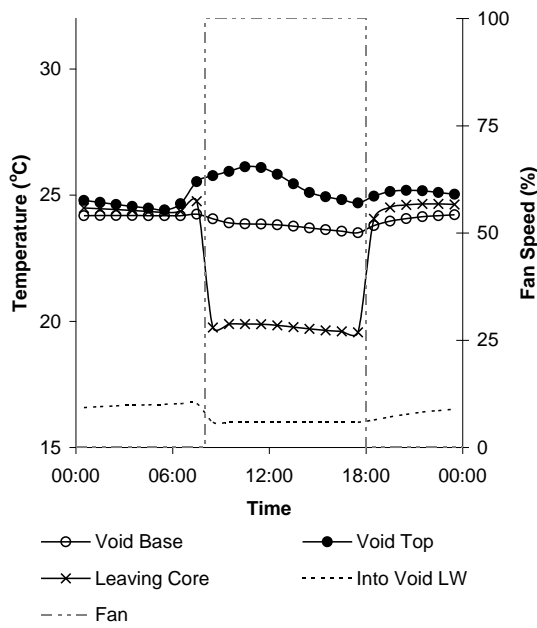


Figure A—96 FVWM Strategy with Cooling void and supply air temperatures

A.3.2.1 Thermal Mass

Increasing the amount of thermal mass in the test room from LW (base case) to HW reduces the annual cooling load by 3.5% (Figure A—97). Increasing the thermal mass further to VHW reduces the annual cooling load further by 0.1%. Reducing the thermal mass from LW to VLW only results in an increase in annual cooling load of 0.6%.

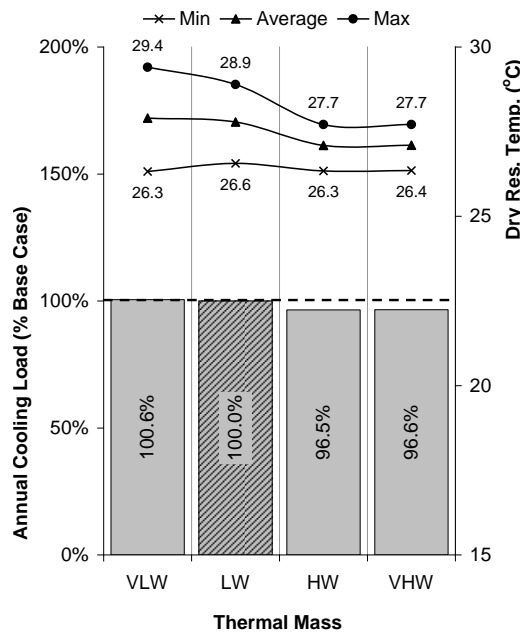


Figure A—97 FVWM Strategy Annual Cooling Load– Thermal Mass

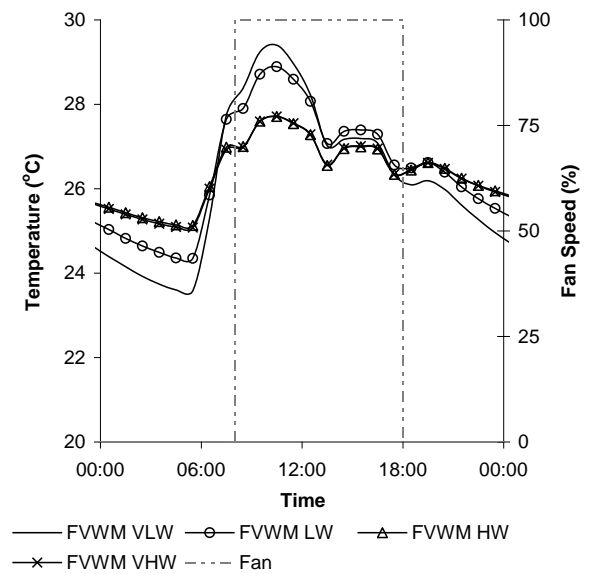


Figure A—98 FVWM Strategy with cooling Tres on a peak summer day – Thermal Mass

The surface temperatures of the floor (Figure A—99) closely follows the temperatures of the room, however the surface temperatures of the HW and VHW internal walls and all of the ceiling surface temperatures show a dampening effect, demonstrating the thermal mass of these surfaces.

To look at the effect of increasing the level of thermal mass in the room on the void surface temperatures and the air temperature leaving the void the results for the LW and HW levels of thermal mass are presented in Figure A—100. As a result of the floor surface temperature in the room being very similar the difference between the air temperature leaving the void for the LW and HW levels of thermal mass is minimal.

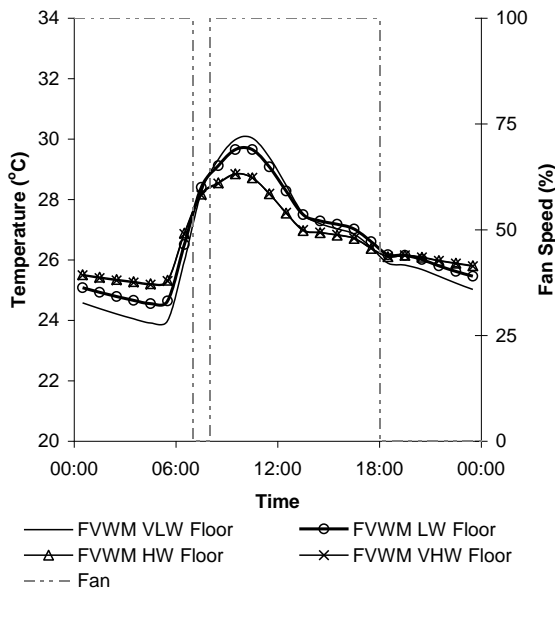


Figure A—99 FVWM Strategy with Cooling Floor Surface Temperature – Thermal Mass

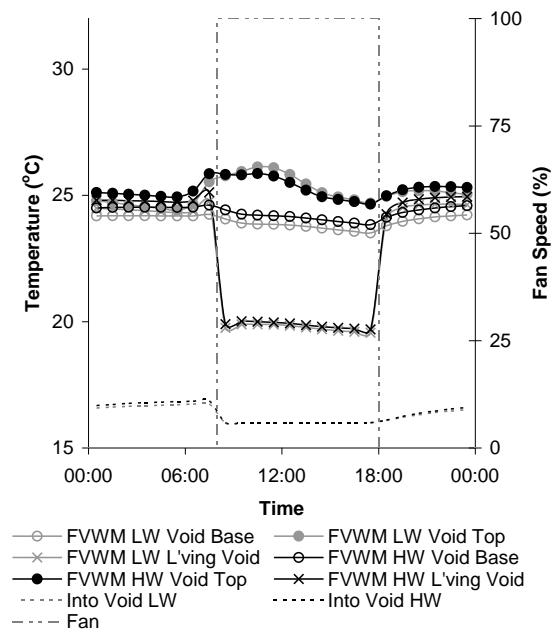


Figure A—100 FVWM Strategy with Cooling void and supply air temperatures – Thermal Mass

A.3.2.2 Thermal Mass with Night Cooling

Night cooling reduces the temperature of the test room during the unoccupied period for all levels of thermal mass (Figure A—101). The T_{res} in the VLW and LW rooms reach a low of around 21°C and 22°C and the HW and VHW reach a low of around 23°C.

Introducing night cooling reduces the annual cooling load for the VLW room by 5.3%, the LW room by 6.7%, the HW room by 7.3% and the VHW room by 6.8% (Figure A—101).

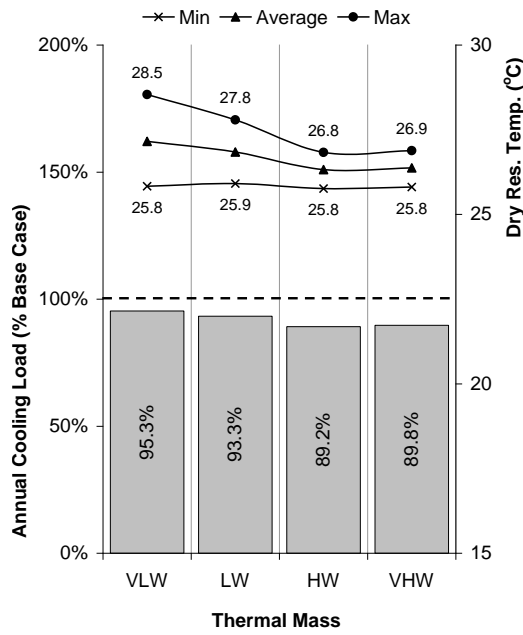


Figure A—101 FVWM Strategy Annual Cooling Load– Thermal Mass with Night Cooling

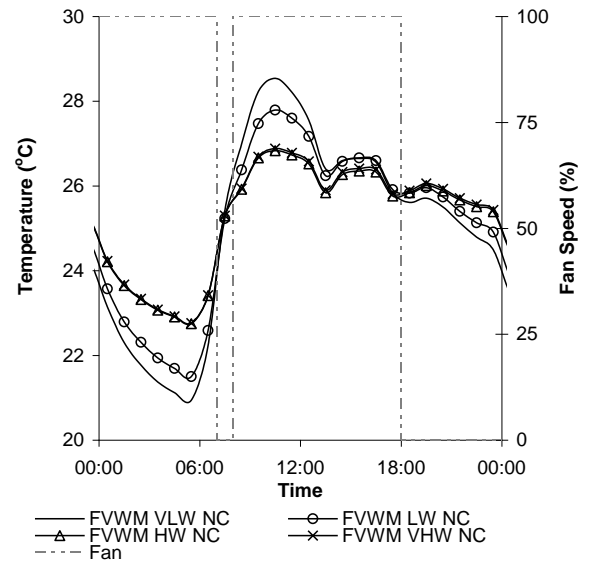


Figure A—102 FVWM Strategy with cooling T_{res} on a peak summer day – Thermal Mass with Night Cooling

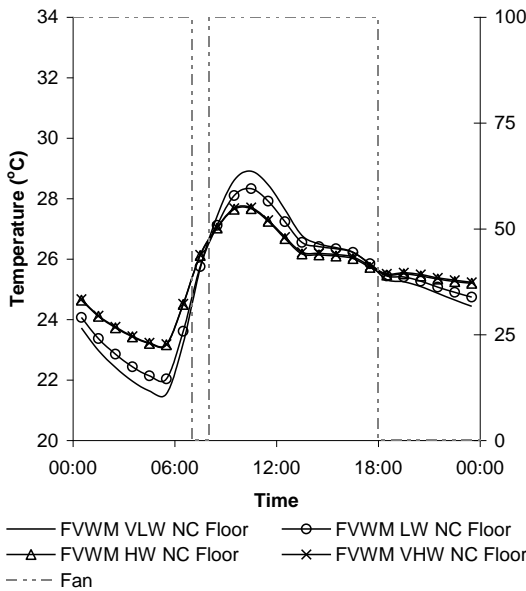


Figure A—103 FVWM Strategy with Cooling Floor Surface Temperature – Thermal Mass with Night Cooling

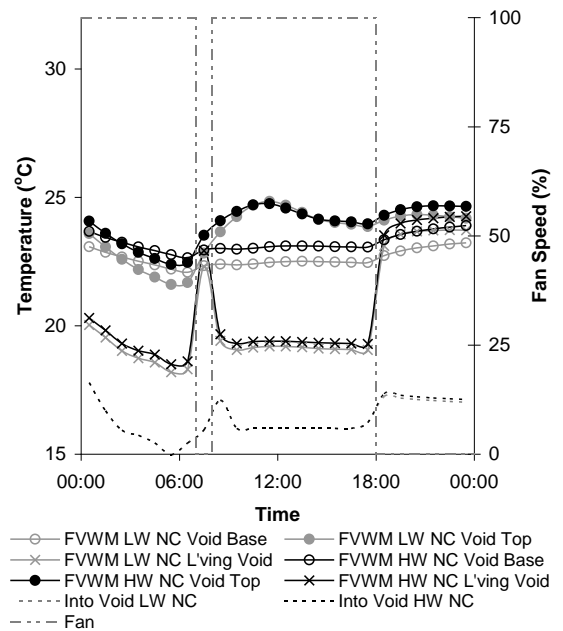


Figure A—104 FVWM Strategy with Cooling void and supply air temperatures – Thermal Mass with Night Cooling

A.3.2.3 Solar Gains

Reducing the solar gains from high (base case) to medium reduces the annual cooling load by 5.6% (Figure A—105). Reducing the solar gains to low reduces the annual cooling load by 14.1%.

To look at the effect of reducing the level on solar gain on the void surface temperatures and the air temperature leaving the void the results for the High and Low levels of solar gain are presented in Figure A—107. As a result of the floor surface temperatures in the room being much lower for the Low level of solar gain (Figure A—106), the void top surface temperature and void base surface temperatures are lower. This results in the supply air leaving the slab being heated less.

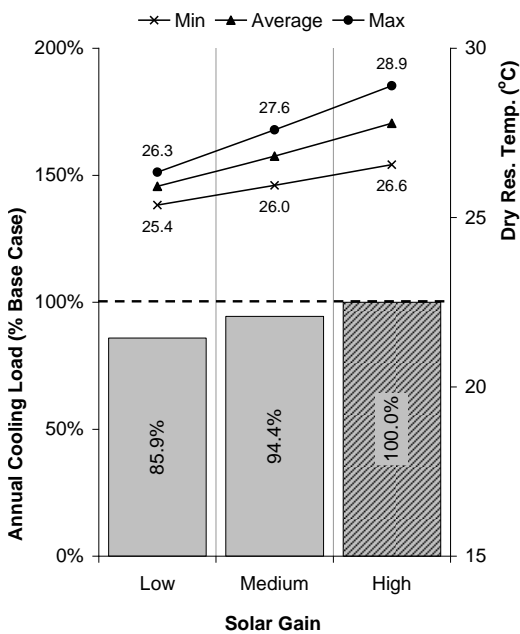


Figure A—105 FVWM Strategy Annual Cooling Load– Solar Gain

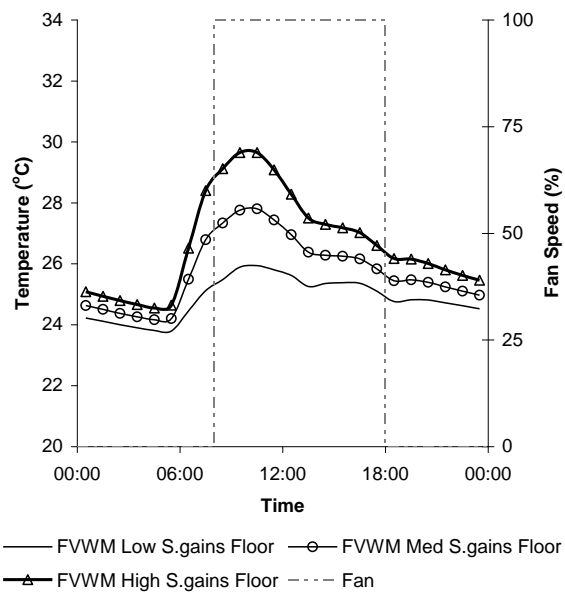


Figure A—106 FVWM Strategy with Cooling Floor Surface Temperature – Solar Gain

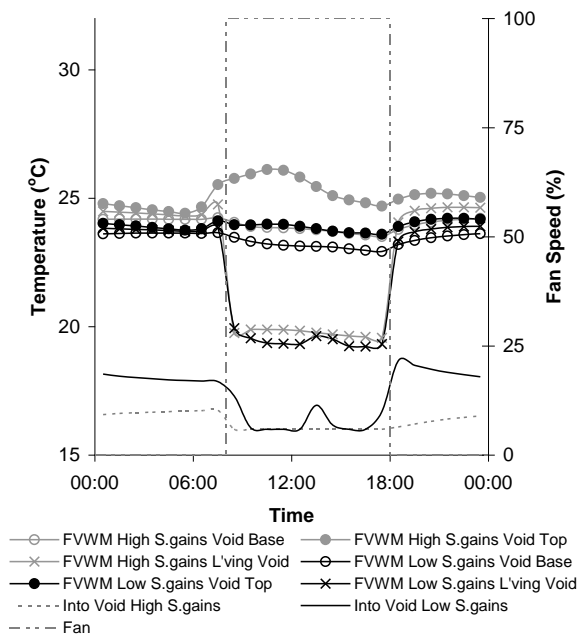


Figure A—107 FVWM Strategy with Cooling void and supply air temperatures – Solar Gain

A.3.2.4 Internal Gains

Reducing the internal gains from medium (base case) to low reduces the annual cooling load by 17.8% (Figure A—108). Increasing the solar gains to high increase the annual cooling load by 8.4%.

To look at the effect of reducing the level on internal gain on the void surface temperatures and the air temperature leaving the void the results for the Medium and Low levels of internal gain are presented in Figure A—110. As a result of the floor surface temperatures in the room being lower for the Low level of internal gain (Figure A—109), the void top surface temperature is lower, however there the void base surface temperature is only slightly lower. The supply air leaving the slab is therefore only heated slightly less for the Low level of internal gain.

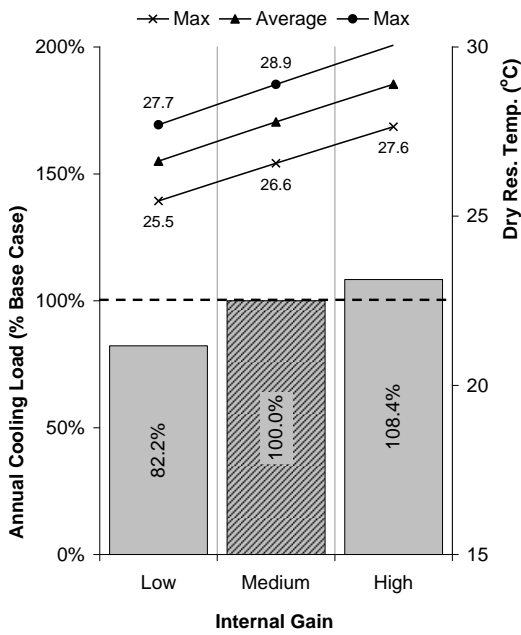


Figure A—108 FVWM Strategy Annual Cooling Load– Internal Gain

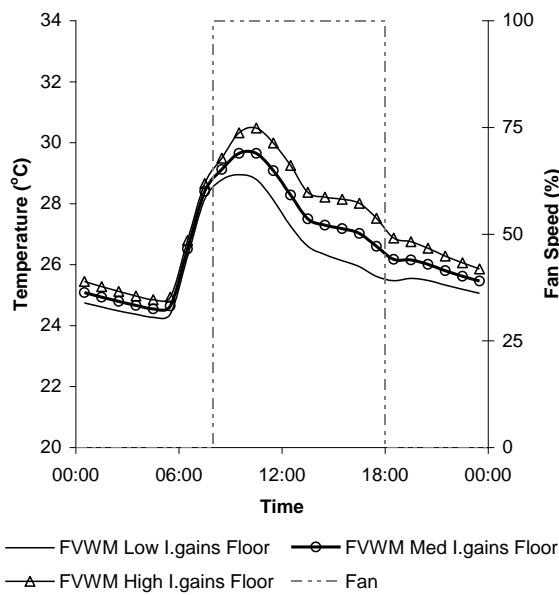


Figure A—109 FVWM Strategy with Cooling Floor Surface Temperature – Internal Gain

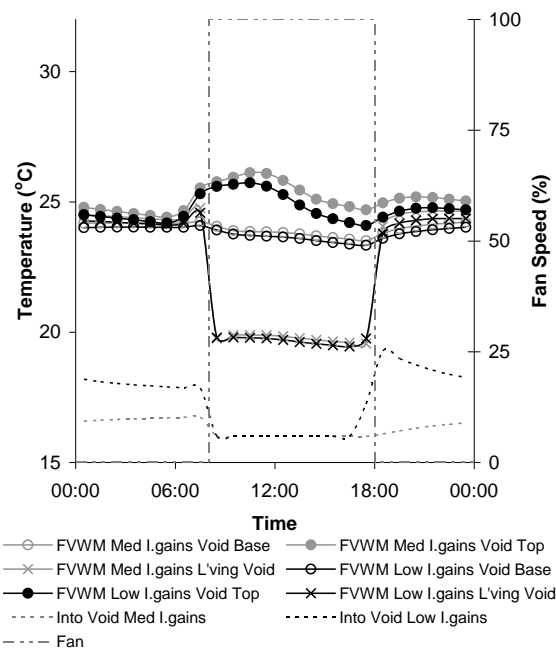


Figure A—110 FVWM Strategy with Cooling void and supply air temperatures – Internal Gain

A.3.2.5 Air Change Rate

Increasing the air change rate increases the amount of free cooling that can be provided when the ambient air temperature is below that of the required supply air temperature, but also increases the amount of air that needs to be cooled when the ambient air is above that of the required supply air temperature.

Increasing the air change rate from 6ach^{-1} (base case) to 8ach^{-1} increases the annual cooling load by 11.5% (Figure A—111). Increasing the air change rate to 10ach^{-1} increases the annual cooling load by 13.5%.

To look at the effect of increasing the air change rate on the void surface temperatures and the air temperature leaving the void the results for the 6ach^{-1} and 10ach^{-1} are presented in Figure A—113. As a result of the floor surface temperatures in the room being lower for the 10ach^{-1} (Figure A—112), the void top and void base surface temperatures are lower. The supply air leaving the slab is therefore only heated less.

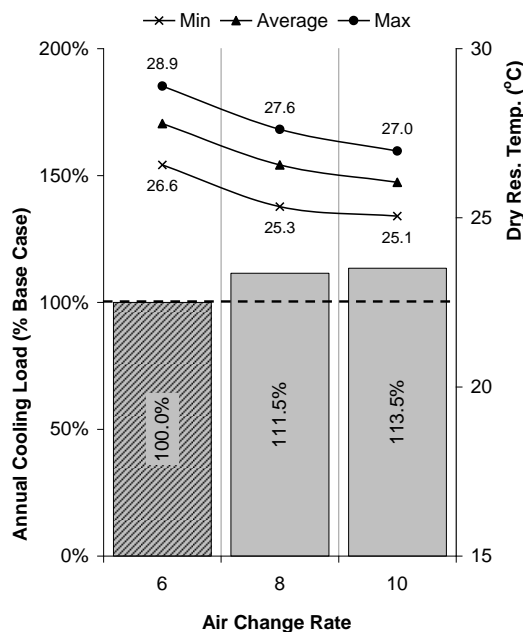


Figure A—111 FVWM Strategy Annual Cooling Load– Air Change Rate

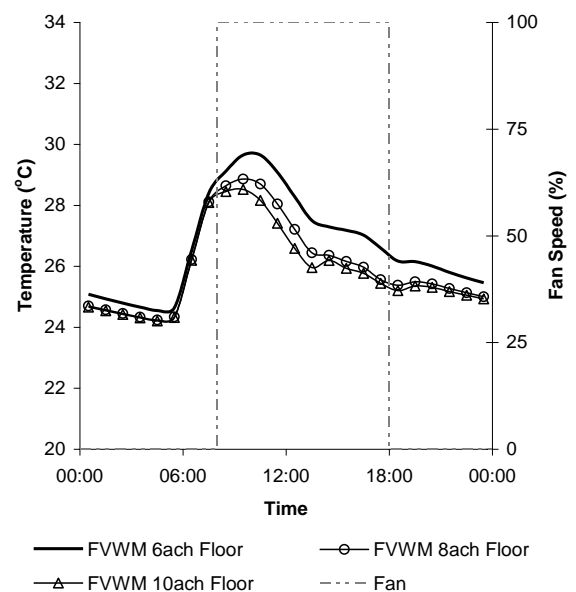
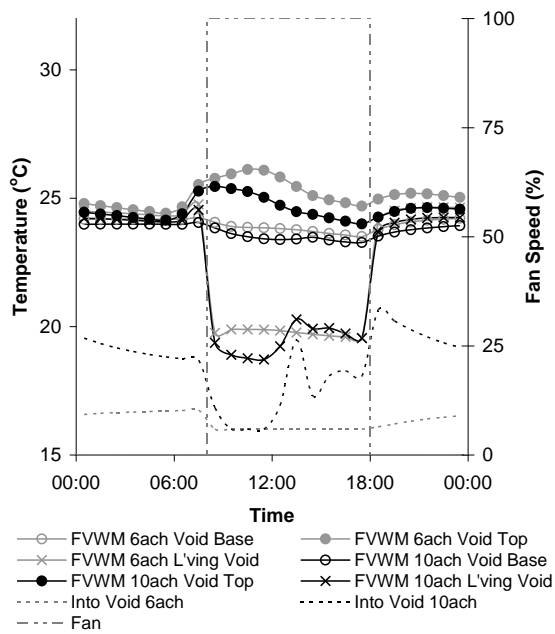


Figure A—112 FVWM Strategy with Cooling Floor Surface Temperature – Air Change Rate



**Figure A—113 FVWM Strategy with Cooling
void and supply air temperatures – Air
Change Rate**

A.3.3 Annual Heating Load

A.3.3.1 Thermal Mass

Increasing the thermal mass from LW (base case) to HW increases the annual heating load by 2.0% (Figure A—114), increasing the thermal mass to VHW increases the annual heating load by 1.6%. Reducing the thermal mass to VLW reduces the annual heating load by 0.6%.

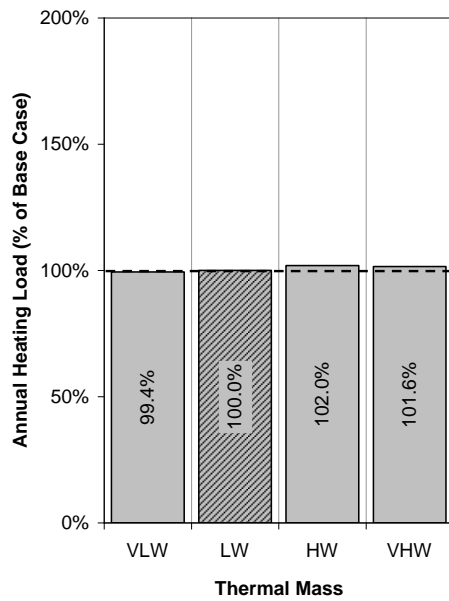


Figure A—114 FVWM Strategy Annual Heating Load – Thermal Mass

A.3.3.2 Solar Gain

Reducing the solar gains from high (base case) to medium increases the annual heating load by 2.8% (Figure A—115). Reducing the solar gains to low increases the annual heating load by 5.8%.

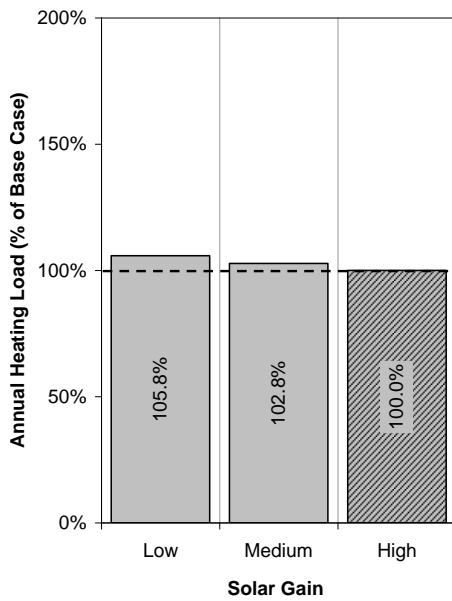


Figure A—115 FVWM Strategy Annual Heating Load – Solar Gain

A.3.3.3 Internal Gain

Reducing the internal gains from medium (base case) to low increases the annual heating load by 22.1% (Figure A—116). Increasing the internal gains to high reduces the annual heating load by 14.3%.

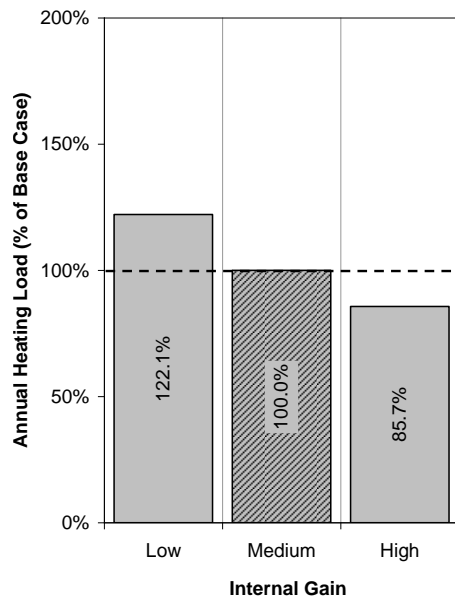


Figure A—116 FVWM Strategy Annual Heating Load – Internal Gain

A.3.3.4 Air Change Rate

Increasing the air change rate from 6ach^{-1} (base case) to 8ach^{-1} increases the annual heating load by 43.7% (Figure A—117). Increasing the air change rate to 10ach^{-1} increases the annual heating load by 88.4%.

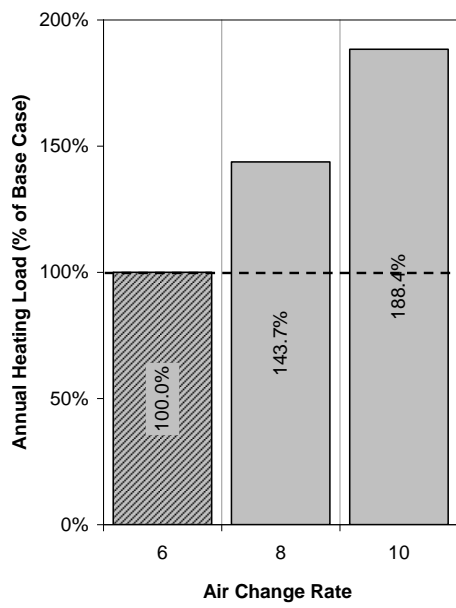


Figure A—117 FVWM Strategy Annual Heating Load – Air Change Rate

A.4 Earth-to-Air-Heat-Exchanger (ETAHE)

A.4.1 Overheating Hours

Passing the supply air through the ETAHE provides free cooling to the supply air. Figure A—118 shows the effect that passing the air through the ETAHE has on a peak summer day.

For the base case model the surface temperatures of the core base and the core top are relatively constant. Due to this temperature being higher than that of the air entering into the core the strategy has the unwanted effect of heating the air.

Table A—1 shows the temperatures of the core surfaces together with the air temperature into the core and leaving the core. The heat exchange efficiency of the core has also been calculated. The efficiency ranges between 35.9% at the start of the day to 64.4% in the early afternoon, however a 50% efficiency provides a good agreement with all but the beginning of the day with an accuracy of between 99.9% and 100.8%.

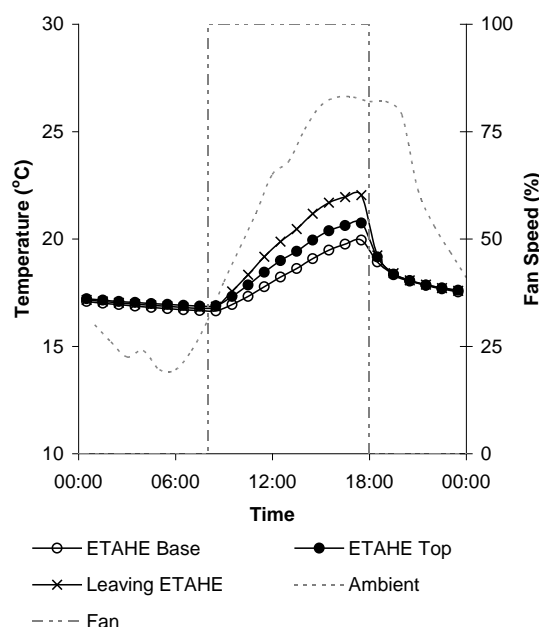


Figure A—118 ETAHE Strategy surface and supply air temperatures

A.4.1.1 Thermal Mass

Increasing the thermal mass from LW (base case) to HW reduces the overheating hours by 18.0% and decreases T_{res} maximum by 0.5°C (Figure A—119). Increasing the thermal mass further to VHW only results in a further 4.2% reduction in annual overheating hours with and a further reduction in T_{res} maximum of 0.1°C . Alternatively, decreasing the thermal mass from LW to VLW only increases the annual overheating hours by 2.8% and an increase in T_{res} maximum of 0.5°C .

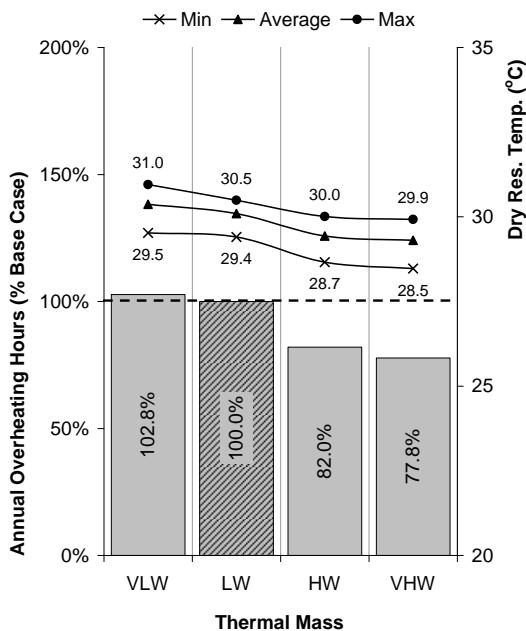


Figure A—119 ETAHE Strategy Annual Overheating Hours – Thermal Mass

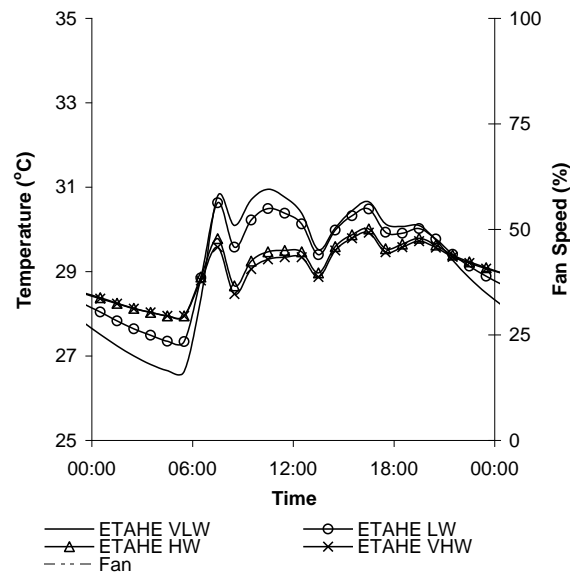


Figure A—120 ETAHE Strategy T_{res} on a peak summer day – Thermal Mass

A.4.1.2 Thermal Mass with Night Cooling

The night cooling reduces the temperature of the test room during the unoccupied period for all of the levels of thermal mass (Figure A—122). The T_{res} in the VLW and LW rooms reach a low of around 22°C and the HW and VHW reach a low of around 24°C . This then

results in T_{res} at the start of the occupied period being 1.4°C lower in the VLW room, 2.0°C lower in the LW room, 1.7°C lower in the HW room and 1.5°C lower in the VHW room.

Introducing night cooling reduces the annual overheating hours by 33.0% for the LW room (base case) reducing the maximum T_{res} on a peak summer day by 0.7°C (Figure A—121).

Introducing night cooling to the HW room reduces the annual overheating hours by 39.7%, and the maximum T_{res} by 0.7°C. For the VHW room the annual overheating hours are reduced by 36.8%, reducing the maximum T_{res} by 0.7°C. There is still little difference between the HW and VHW rooms in terms of both annual overheating hours or T_{res} .

A greater difference is now found between the VLW and LW rooms. Adding night cooling to the VLW room reduces the annual overheating hours by 18.0% and the T_{res} maximum by 0.8°C.

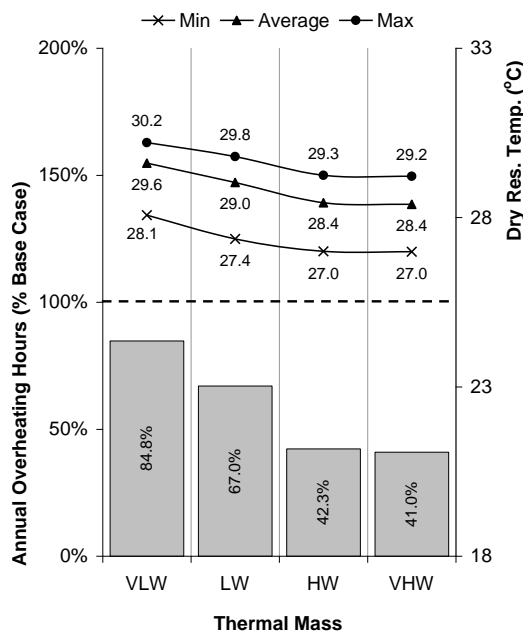


Figure A—121 ETAHE Strategy Annual Overheating Hours – Thermal Mass with Night Cooling

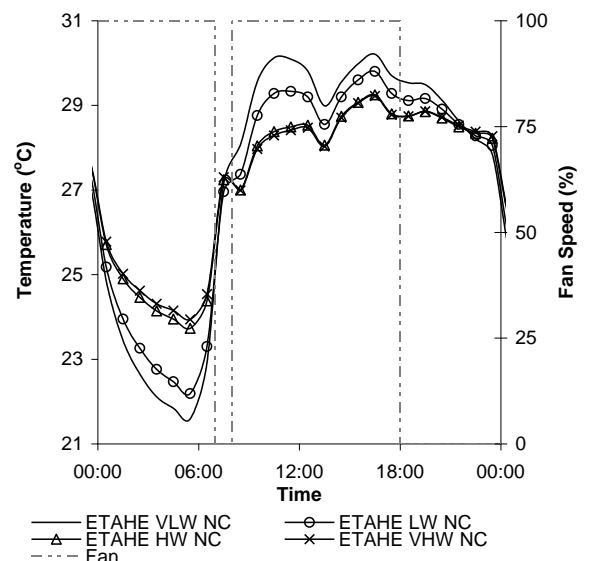


Figure A—122 ETAHE Strategy T_{res} on a peak summer day – Thermal Mass with Night Cooling

A.4.1.3 Solar Gains

Reducing the solar gain reduces the heat gain experienced by the room and therefore reduces the temperature (Figure A—123). Reducing the solar gains to medium reduces the annual overheating hours by 36.0% and the T_{res} maximum by 0.6°C. Reducing the solar gains to low reduces the annual overheating hours by 64.5% and the T_{res} maximum by 1.3°C.

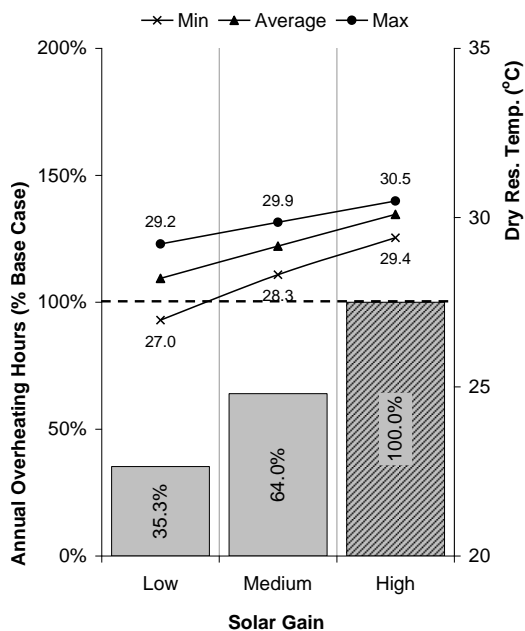


Figure A—123 ETAHE Strategy Annual Overheating Hours – Solar Gain

A.4.1.4 Internal Gains

Reducing the internal gain again reduces the heat gain experienced by the room and again reduces the temperature (Figure A—124). Reducing the internal gains to low reduces the annual overheating hours by 45.7% and the T_{res} maximum by 1.2°C. Increasing the internal gains to high increases the annual overheating hours by 30.0% and the T_{res} maximum by 1.3°C.

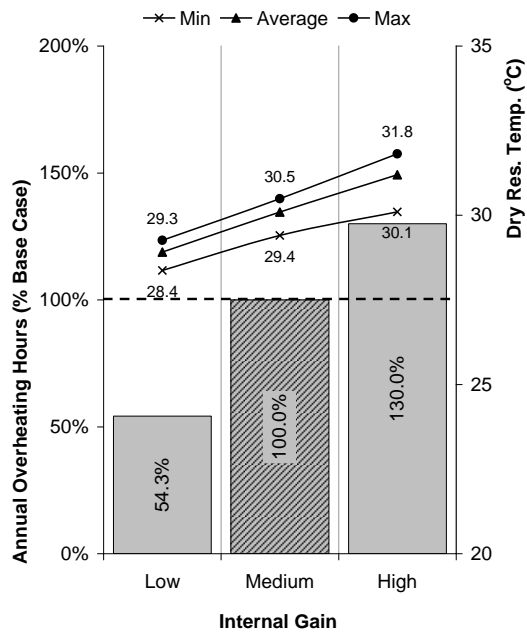


Figure A—124 ETAHE Strategy Annual Overheating Hours – Internal Gain

A.4.1.5 Air Change Rate

Increasing the air change rate increases the amount of free cooling that can be provided to the room (Figure A—125). Increasing the air change rate from 6 ach⁻¹ (base case) to 8 ach⁻¹ reduces the annual overheating hours by 40.7% and reduces T_{res} maximum by 1.0°C. Increasing the air change rate to 10 ach⁻¹ reduces the annual overheating hours by 65.5% and the T_{res} maximum by 1.8°C.

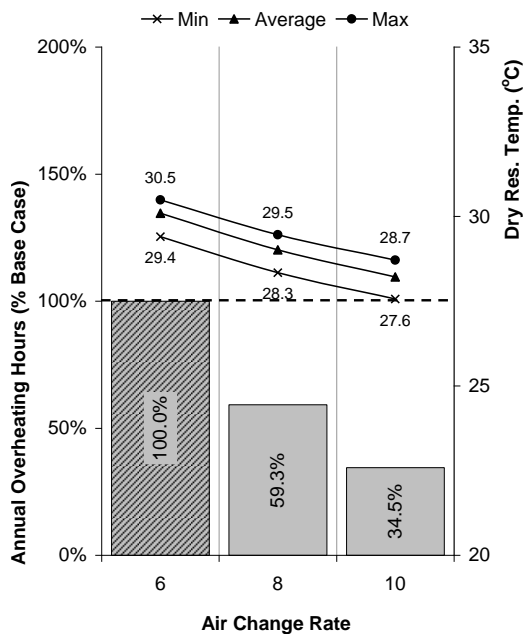


Figure A—125 ETAHE Strategy Annual Overheating Hours – Air Change Rate

A.4.2 Annual Cooling Load

A.4.2.1 Thermal Mass

Increasing the amount of thermal mass in the test room from LW (base case) to HW reduces the annual cooling load by 10.3% (Figure A—126). Increasing the thermal mass further to VHW only reduces this by a further 2.5%. Reducing the thermal mass from LW to VLW only results in an increase in annual cooling load of 0.3%.

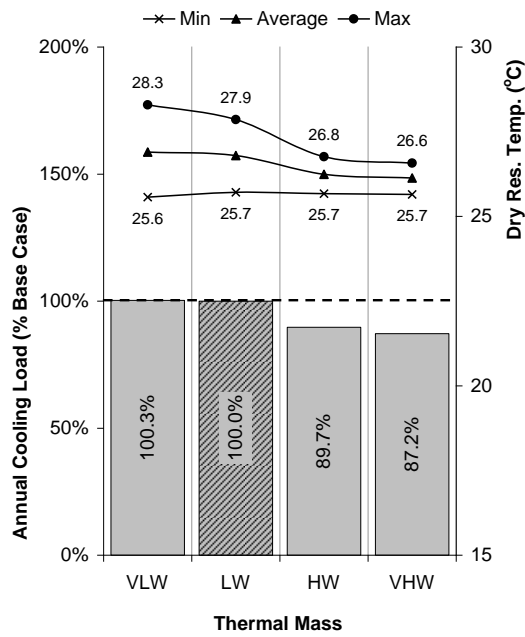


Figure A—126 ETAHE Strategy Annual Cooling Load– Thermal Mass

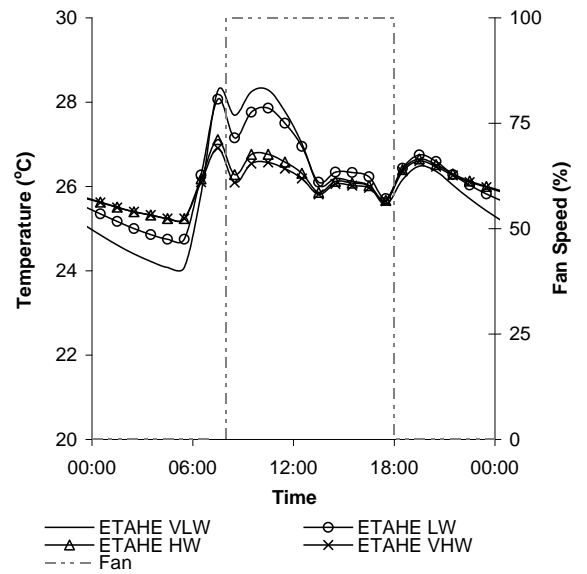


Figure A—127 ETAHE Strategy with cooling T_{res} on a peak summer day – Thermal Mass

A.1.1.1 Thermal Mass with Night Cooling

Introducing night cooling reduces the annual cooling load for the VLW room by 7.3%, the LW room by 11.7%, the HW room by 14.3% and the VHW room by 13.5% (Figure A—128).

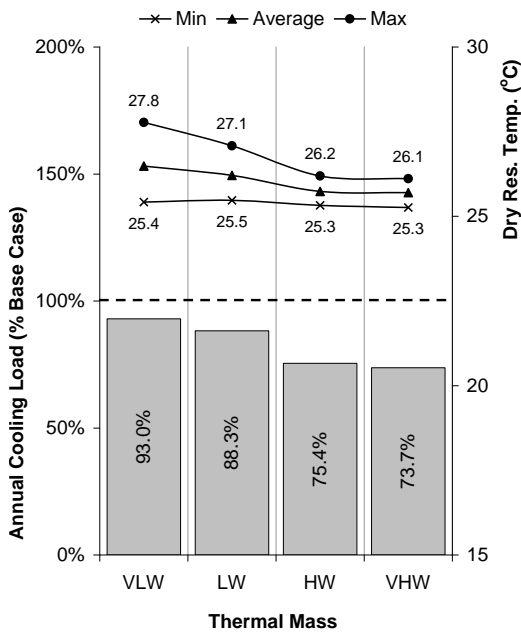


Figure A—128 ETAHE Strategy Annual Cooling Load– Thermal Mass with Night Cooling

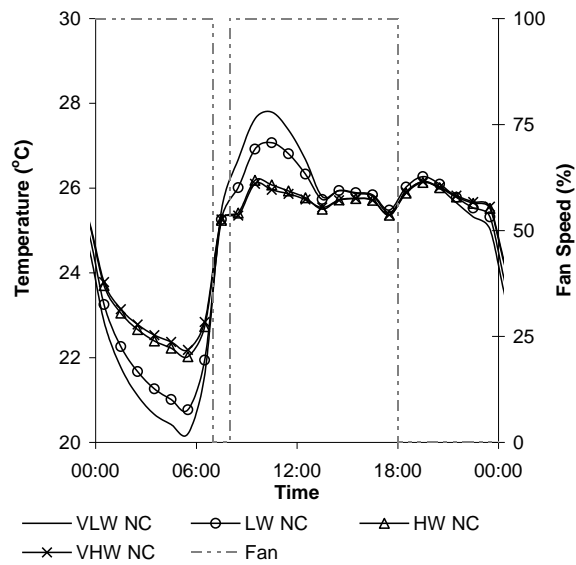


Figure A—129 ETAHE Strategy with cooling Tres on a peak summer day – Thermal Mass with Night Cooling

A.1.1.2 Solar Gains

Reducing the solar gains from high (base case) to medium reduces the annual cooling load by 14.4% (Figure A—130). Reducing the solar gains to low reduces the annual cooling load by 31.9%.

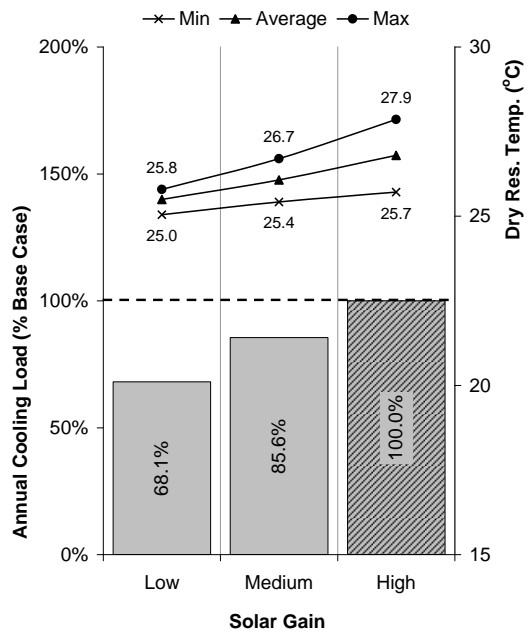


Figure A—130 ETAHE Strategy Annual Cooling Load– Solar Gain

A.1.1.3 Internal Gains

Reducing the internal gains from medium (base case) to low reduces the annual cooling load by 37.4% (Figure A—131). Increasing the solar gains to high increase the annual cooling load by 25.3%.

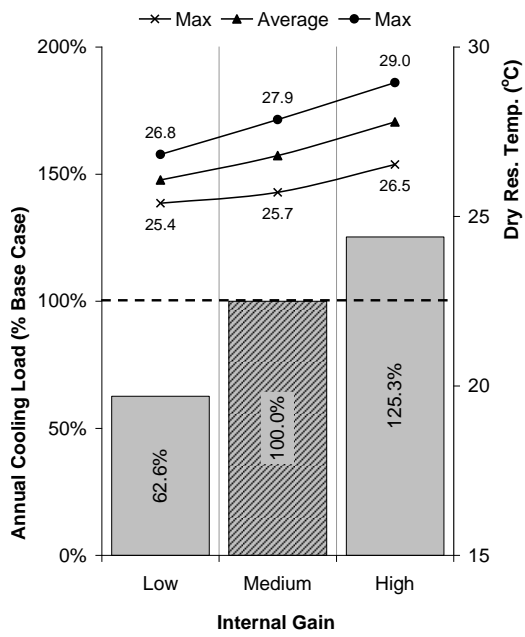


Figure A—131 ETAHE Strategy Annual Cooling Load– Internal Gain

A.1.1.4 Air Change Rate

Increasing the air change rate from 6ach^{-1} (base case) to 8ach^{-1} increases the annual cooling load by 11.8% (Figure A—132). Increasing the air change rate to 10ach^{-1} increases the annual cooling load by 23.3%.

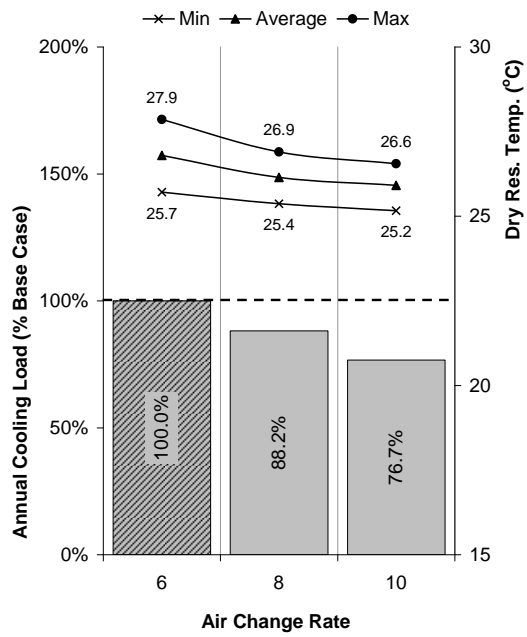


Figure A—132 ETAHE Strategy Annual Cooling Load– Air Change Rate

A.4.3 Annual Heating Load

A.4.3.1 Thermal Mass

Increasing the thermal mass from LW (base case) to HW increases the annual heating load by 2.8% (Figure A—133), increasing the thermal mass to VHW increases the annual heating load by 3.3%. Reducing the thermal mass reduces the annual heating load by 1.8%.

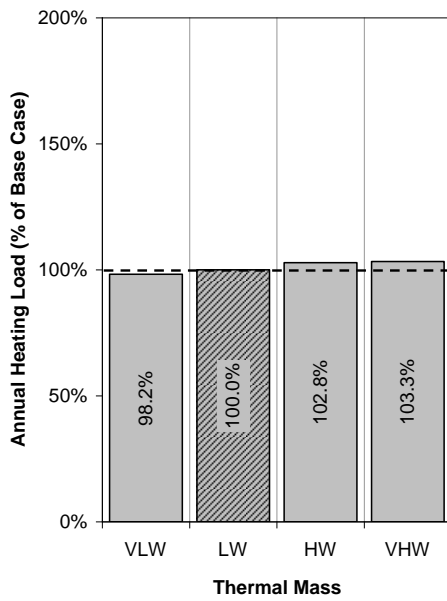


Figure A—133 ETAHE Strategy Annual Heating Load – Thermal Mass

A.4.3.2 Solar Gain

Reducing the solar gains from high (base case) to medium increases the annual heating load by 2.2% (Figure A—134). Reducing the solar gains to low increases the annual heating load by 4.8%.

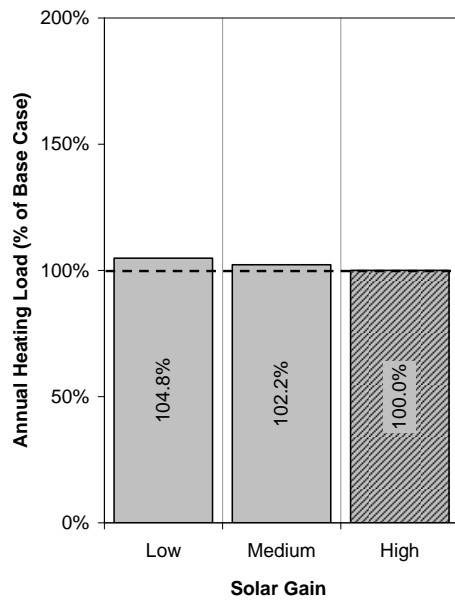


Figure A—134 ETAHE Strategy Annual Heating Load – Solar Gain

A.4.3.3 Internal Gain

Reducing the internal gains from medium (base case) to low increases the annual heating load by 19.3% (Figure A—135). Increasing the internal gains to high reduces the annual heating load by 12.6%.

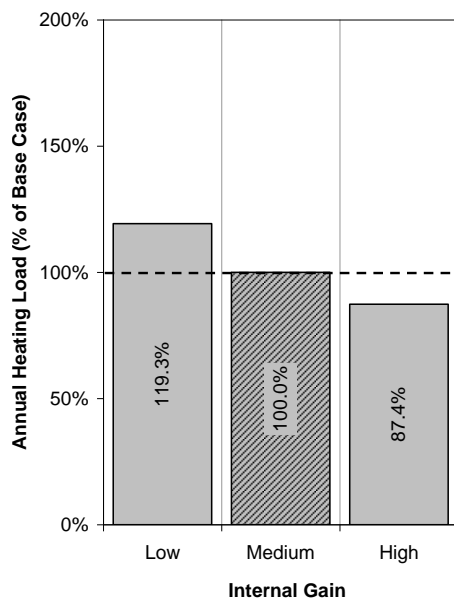


Figure A—135 ETAHE Strategy Annual Heating Load – Internal Gain

A.4.3.4 Air Change Rate

Increasing the air change rate from 6ach^{-1} (base case) to 8ach^{-1} increases the annual heating load by 41.9% (Figure A—136). Increasing the air change rate to 10ach^{-1} increases the annual heating load by 85.7%.

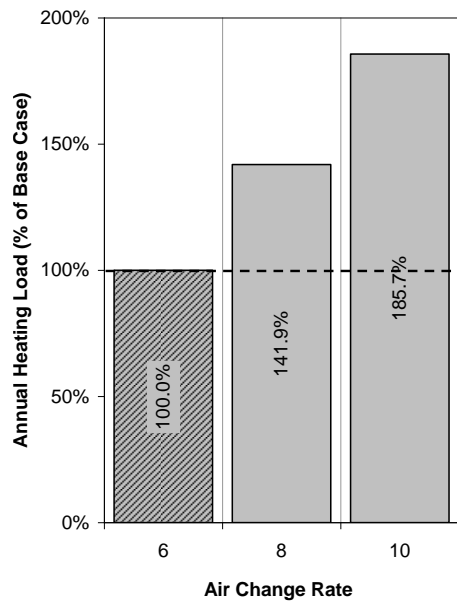


Figure A—136 ETAHE Strategy Annual Heating Load – Air Change Rate

A.5 Thermal Labyrinth

A.5.1 Overheating Hours

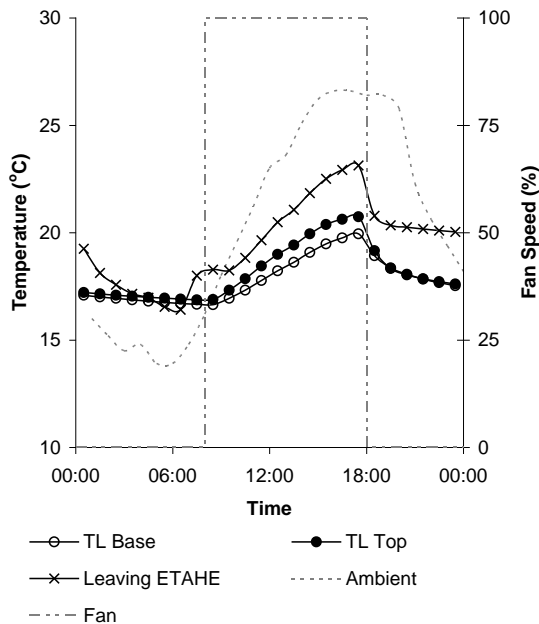


Figure A—137 TL Strategy surface and supply air temperatures

A.5.1.1 Thermal Mass

Increasing the thermal mass from LW (base case) to HW reduces the overheating hours by 17.6% and decreases T_{res} maximum by 0.5°C (Figure A—138). Increasing the thermal mass further to VHW only results in a further 2.4% reduction in annual overheating hours with and a further reduction T_{res} maximum of 0.1°C. Alternatively, decreasing the thermal mass from LW to VLW only increases the annual overheating hours by 2.0% and an increase in T_{res} maximum of 0.3°C.

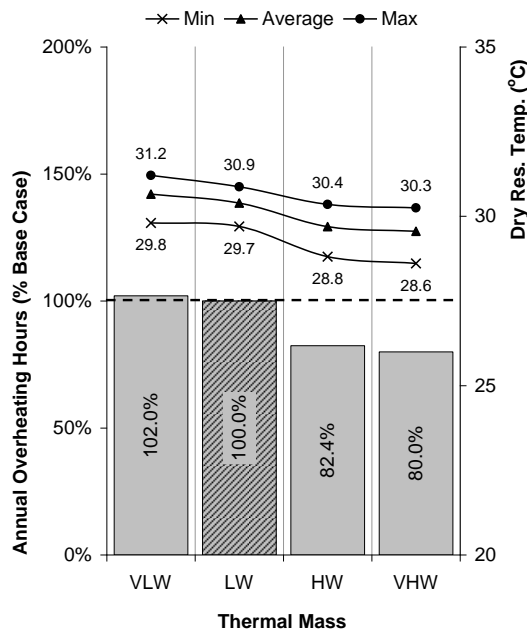


Figure A—138 TL Strategy Annual Overheating Hours – Thermal Mass

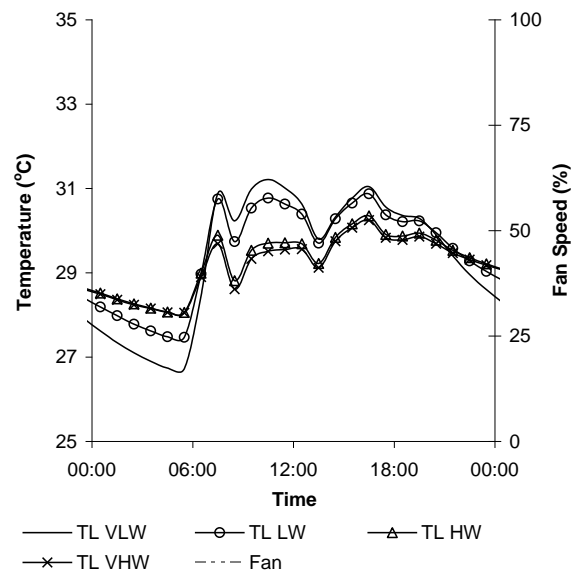


Figure A—139 TL Strategy T_{res} on a peak summer day – Thermal Mass

A.5.1.2 Thermal Mass with Night Cooling

The night cooling reduces the temperature of the test room during the unoccupied period for all of the levels of thermal mass (Figure A—141). The T_{res} in the VLW and LW rooms reach a low of around 23°C and the HW and VHW reach a low of around 25°C. This then results in T_{res} at the start of the occupied period being 1.1°C lower in the VLW room, 1.7°C lower in the LW room, 1.3°C lower in the HW room and 1.1°C lower in the VHW room.

Introducing night cooling reduces the annual overheating hours by 21.2% for the LW (base case) reducing the maximum T_{res} on a peak summer day by 0.6°C.

Introducing night cooling to the HW room reduces the annual overheating hours by 26.8%, and the maximum T_{res} by 0.7°C. For the VHW room the annual overheating hours are reduced by 26.2%, reducing the maximum T_{res} by 0.6°C. There is still little difference between the HW and VHW rooms in terms of both annual overheating hours or T_{res}.

A greater difference is now found between the VLW and LW rooms. Adding night cooling to the VLW room reduces the annual overheating hours by 11.9% and the T_{res} maximum by 0.5°C.

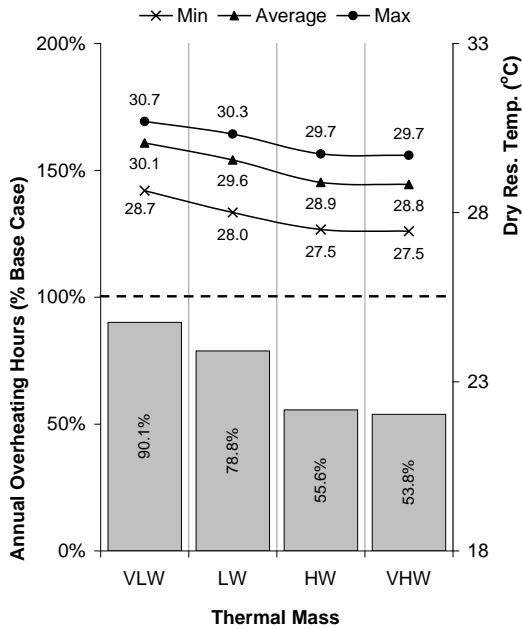


Figure A—140 TL Strategy Annual Overheating Hours – Thermal Mass with Night Cooling

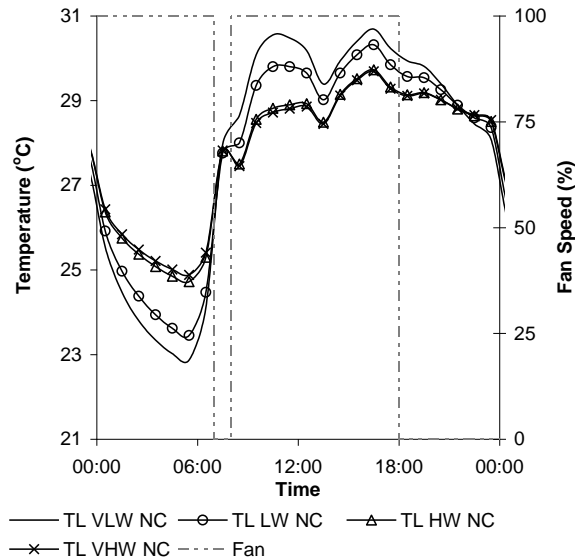


Figure A—141 TL Strategy T_{res} on a peak summer day – Thermal Mass with Night Cooling

A.5.1.3 Solar Gains

Reducing the solar gain reduces the heat gain experienced by the room and therefore reduces the temperature (Figure A—142). Reducing the solar gains to medium reduces the annual overheating hours by 26.6% and the T_{res} maximum by 0.6°C. Reducing the solar gains to low reduces the annual overheating hours by 56.8% and the T_{res} maximum by 1.3°C.

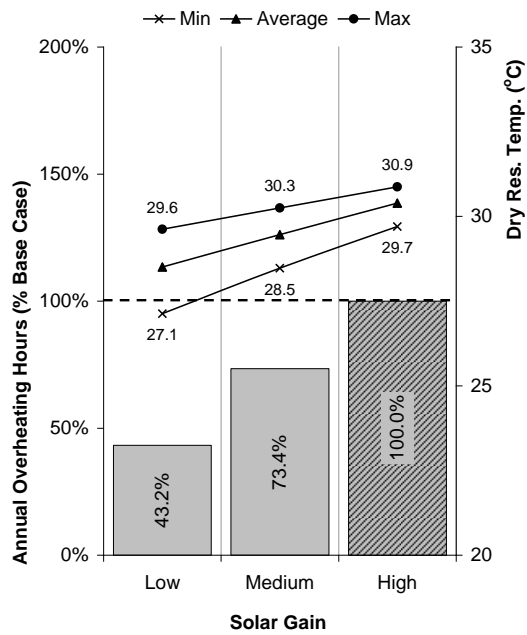


Figure A—142 TL Strategy Annual Overheating Hours – Solar Gain

A.5.1.4 Internal Gains

Reducing the internal gain again reduces the heat gain experienced by the room and again reduces the temperature (Figure A—143). Reducing the internal gains to low reduces the annual overheating hours by 41.4% and the T_{res} maximum by 1.4°C. Increasing the internal gains to high increases the annual overheating hours by 25.5% and the T_{res} maximum by 1.3°C.

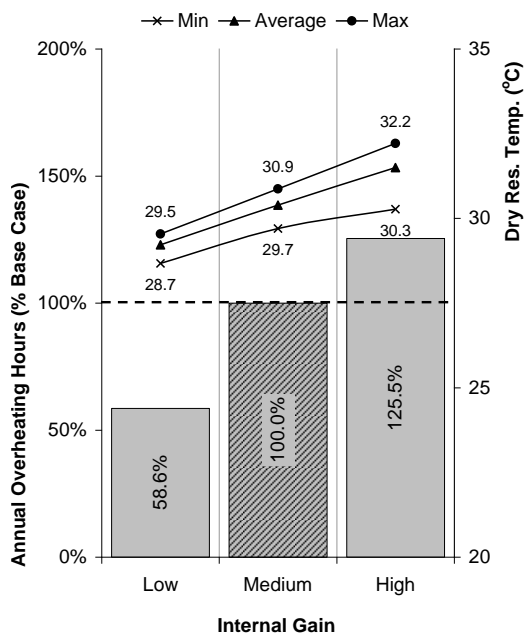


Figure A—143 TL Strategy Annual Overheating Hours – Internal Gain

A.5.1.5 Air Change Rate

Increasing the air change rate increases the amount of free cooling that can be provided to the room (Figure A—144). Increasing the air change rate from 6 ach⁻¹ (base case) to 8 ach⁻¹ reduces the annual overheating hours by 31.5% and reduces T_{res} maximum by 1.0°C. Increasing the air change rate to 10 ach⁻¹ reduces the annual overheating hours by 55.6% and the T_{res} maximum by 1.7°C.

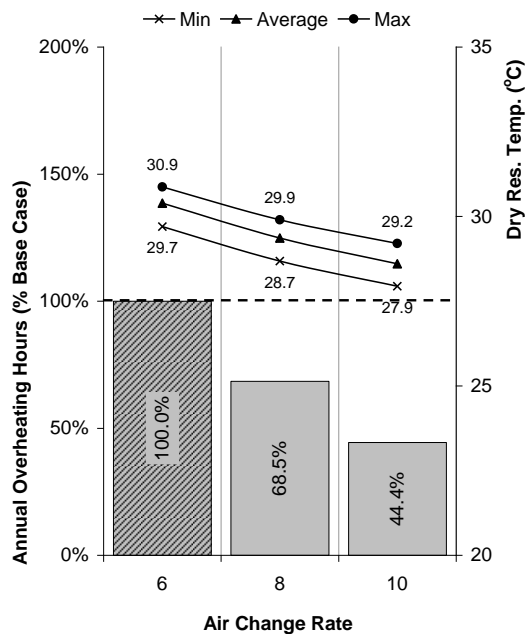


Figure A—144 TL Strategy Annual Overheating Hours – Air Change Rate

A.5.2 Annual Cooling Load

A.5.2.1 Thermal Mass

Increasing the amount of thermal mass in the test room from LW (base case) to HW reduces the annual cooling load by 9.7% (Figure A—145). Increasing the thermal mass further to VHW only reduces this by a further 2.0%. Reducing the thermal mass from LW to VLW also results in an reduction in annual cooling load of 0.2%.

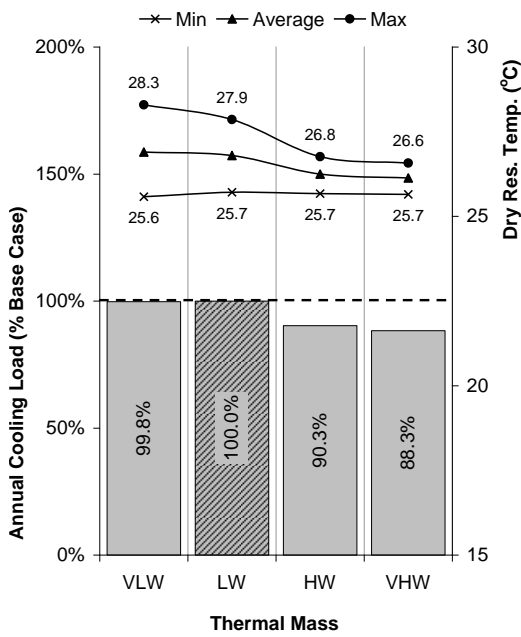


Figure A—145 TL Strategy Annual Cooling Load– Thermal Mass

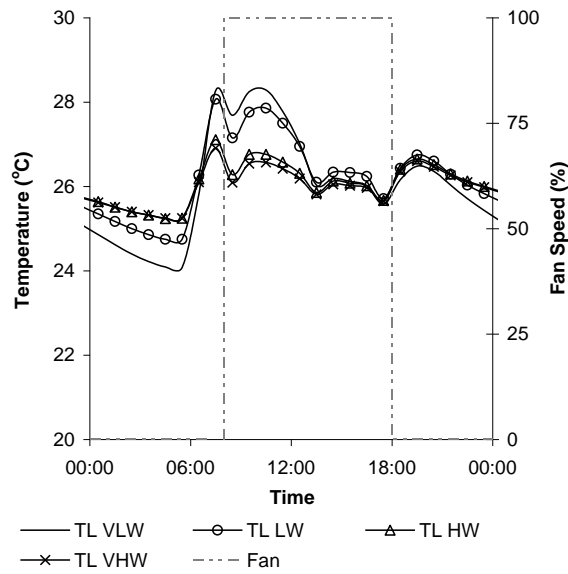


Figure A—146 TL Strategy with cooling T_{res} on a peak summer day – Thermal Mass

A.5.2.2 Thermal Mass with Night Cooling

Introducing night cooling reduces the annual cooling load for the VLW room by 5.1%, the LW room by 8.3%, the HW room by 9.8% and the VHW room by 9.2% (Figure A—147).

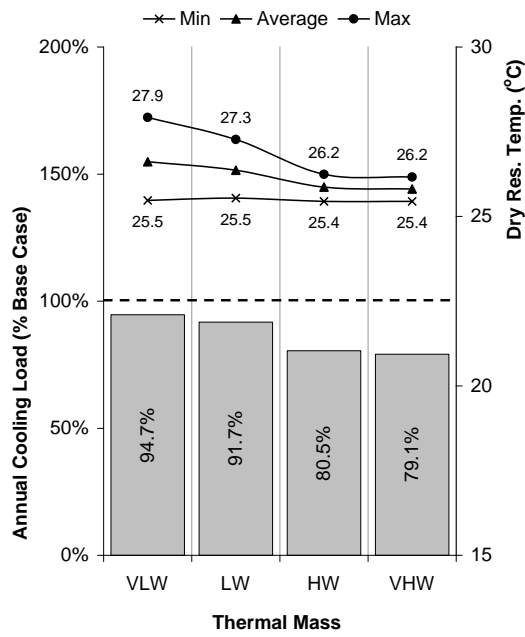


Figure A—147 TL Strategy Annual Cooling Load— Thermal Mass with Night Cooling

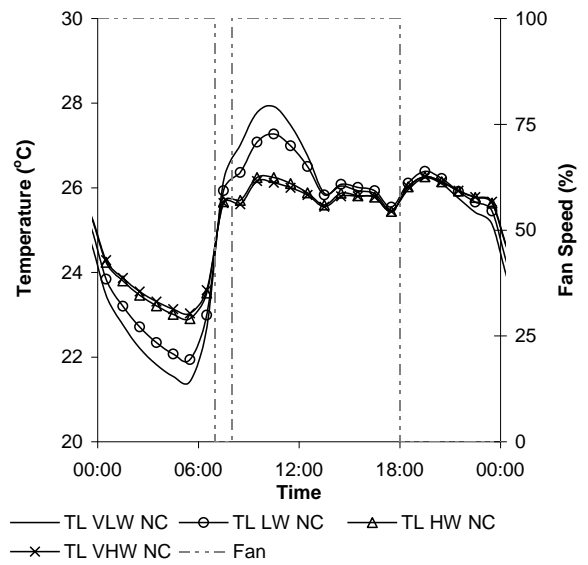


Figure A—148 TL Strategy with cooling T_{res} on a peak summer day – Thermal Mass with Night Cooling

A.5.2.3 Solar Gains

Reducing the solar gains from high (base case) to medium reduces the annual cooling load by 13.6%. Reducing the solar gains to low reduces the annual cooling load by 30.0% (Figure A—149).

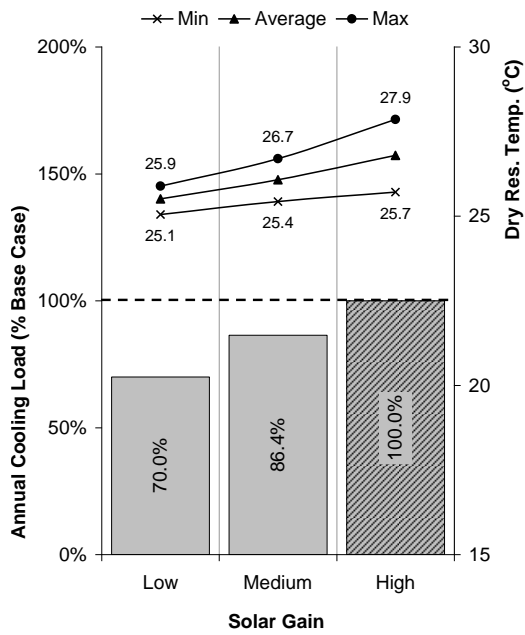


Figure A—149 TL Strategy Annual Cooling Load– Solar Gain

A.5.2.4 Internal Gains

Reducing the internal gains from medium (base case) to low reduces the annual cooling load by 33.3%. Increasing the solar gains to high increase the annual cooling load by 22.7% (Figure A—150).

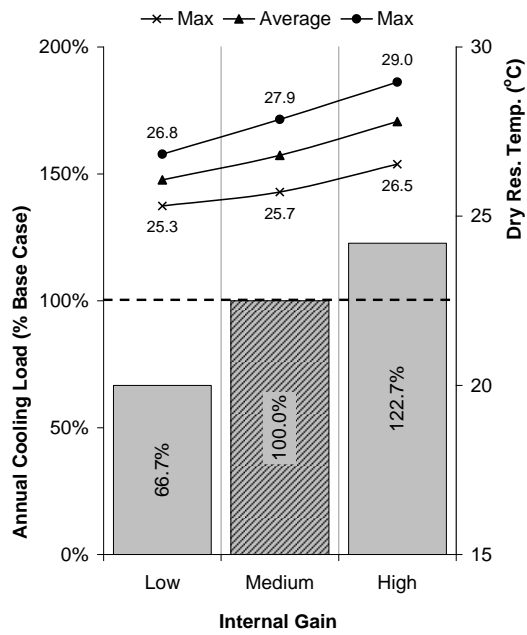


Figure A—150 TL Strategy Annual Cooling Load– Internal Gain

A.5.2.5 Air Change Rate

Increasing the air change rate from 6ach^{-1} (base case) to 8ach^{-1} increases the annual cooling load by 7.6% (Figure A—151). Increasing the air change rate to 10ach^{-1} increases the annual cooling load by 17.3%.

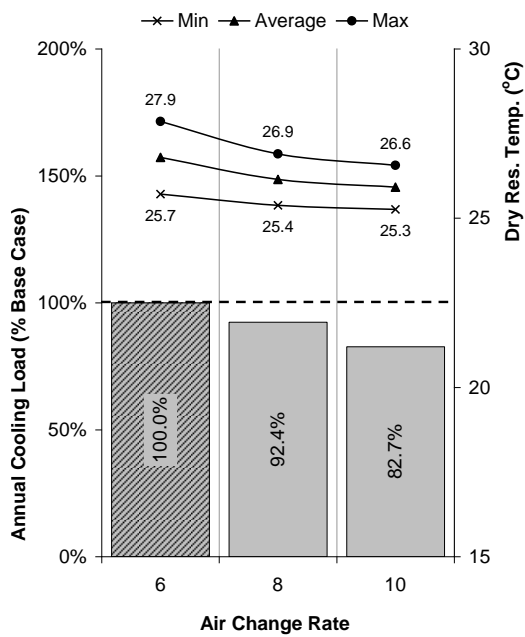


Figure A—151 TL Strategy Annual Cooling Load– Air Change Rate

A.5.3 Annual Heating Load

A.5.3.1 Thermal Mass

Increasing the thermal mass from LW (base case) to HW increases the annual heating load by 2.7% (Figure A—152), increasing the thermal mass to VHW increases the annual heating load by 3.0%. Reducing the thermal mass reduces the annual heating load by 1.7%.

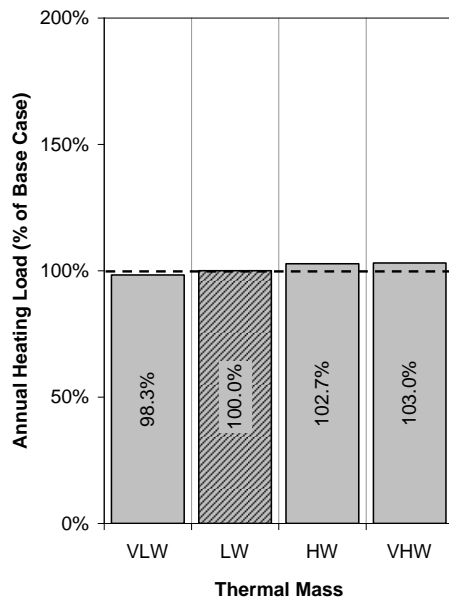


Figure A—152 TL Strategy Annual Heating Load – Thermal Mass

A.5.3.2 Solar Gain

Reducing the solar gains from high (base case) to medium increases the annual heating load by 2.4% (Figure A—153). Reducing the solar gains to low increases the annual heating load by 5.3%.

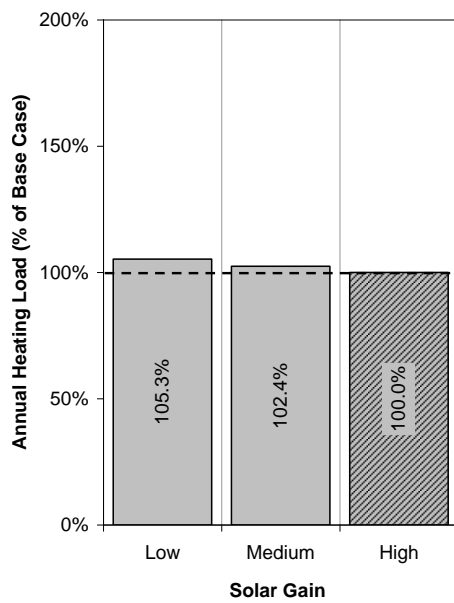


Figure A—153 TL Strategy Annual Heating Load – Solar Gain

A.5.3.3 Internal Gain

Reducing the internal gains from medium (base case) to low increases the annual heating load by 20.2% (Figure A—154). Increasing the internal gains to high reduces the annual heating load by 14.5%.

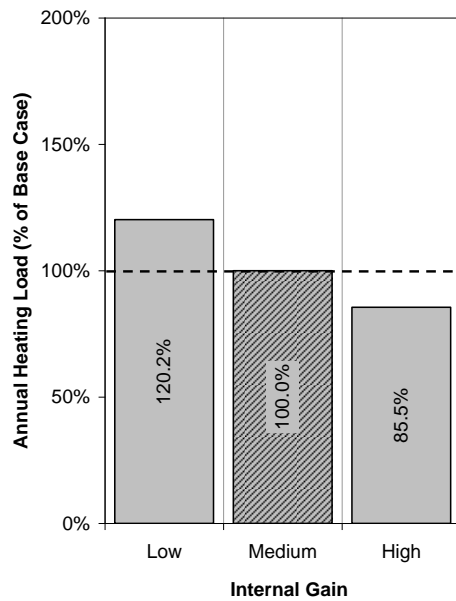


Figure A—154 TL Strategy Annual Heating Load – Internal Gain

A.5.3.4 Air Change Rate

Increasing the air change rate from 6ach^{-1} (base case) to 8ach^{-1} increases the annual heating load by 41.9% (Figure A—155). Increasing the air change rate to 10ach^{-1} increases the annual heating load by 85.7%.

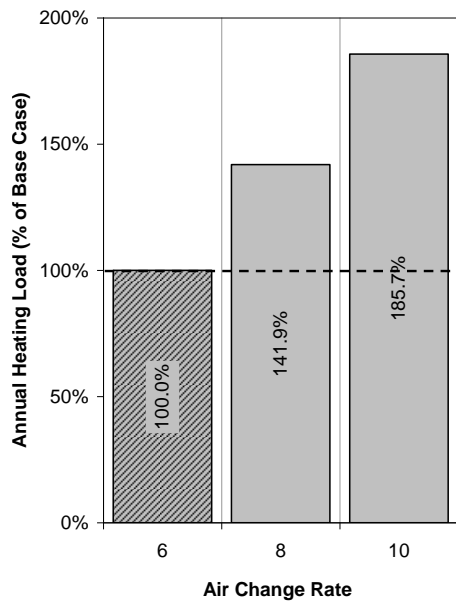


Figure A—155 TL Strategy Annual Heating Load – Air Change Rate

Appendices B, C and D have been removed from the thesis due to publisher's copyright restrictions.
